POLYORGANOSILOXANES AS ELECTRONIC DEVICE ENCAPSULANTS

By

Gregory John Gibbons B.Sc.

For submission to the degree
of Doctor of Philosophy

University of Warwick

Department of Physics

February 1996

LIST OF CONTENTS.

LIST OF FIGURES.

LIST OF TABLES.

ACKNOWLEDGEMENTS

I would like to thank Dr Diane Holland for her support and guidance during the course of my study. I also wish to acknowledge the EPSRC and BNR for the finantial support during the study. I would like to offer my thanks to the MSL group at Warwick, in particular to Prof Ray Dupree for granting me access to his spectrometer and to Dr Andy Howes for setting up the spectrometer and his assisting me with all my experiments. I wish to thank the NMR group of the chemistry department at Warwick for taking my solution NMR spectra and in particular Dr Oliver Howarth for his helpful advice. I wish to thank Dr Dave Haddleton and his group, also of the chemistry department at Warwick, for granting me access to the GPC apparatus. I wish to thank Martin Coleman, Ed Knight and Tony Hillman of the Materials Evaluation Centre at BNR for their kind assistance in obtaining my THB measurements and for their hospitality during my visits. Finally, could I thank anybody else who has helped me over the last three years, including all the glass ceramics technicians, past and present and everybody in glass ceramics.

DECLARATION.

The material in this thesis is my own work except where specifically stated as otherwise. This work was carried out in the Department of Physics, the University of Warwick, in the period from October 1992 to December 1995. No part of this work has been submitted previously to the University of Warwick, nor any other academic institution, for admission to a higher degree. Some of the work has already appeared in the form of publication which is given in the bibliography section.

SUMMARY

Heat curable polysiloxane inorganic - organic hybrid materials, prepared from the hydrolysis and condensation of chloro - or alkoxysilanes, have been investigated as possible electric device encapsulants. Preparation - structure - property relationships have been determined for a simple difunctional system prepared by the direct hydrolysis of chlorosilanes. The system cyclisation was found to be highly dependent upon the system concentration, and most sensitive at low dilution. Due to the dilution associated with the addition of an aqueous base, even a solventless preparation was found to result in a large cyclic content, a result independent of the organic nature of the precursor employed.

The copolymerisation of inorganic monofunctional end - blocking units with difunctional species was found to be beneficial in reducing the level of cyclisation within the system. However, high levels of end blocker with unreactive organic functionalities are to be avoided as the resulting high levels of oligomeric species are deleterious to the material's thermal and dielectric properties. The introduction of thermally reactive organics at much higher levels are possible without property degradation although high levels of reactive groups such as vinyl (-$CHCH_2$) or allyl (-$CH_2CH{=}CH_2$) are deleterious to the hermetic properties of the material.

Introduction of tri - and tetrafunctional inorganic units into the difunctional systems, to prepare inorganically cross - linked materials, was easily achievable by the cohydrolysis of the precursors. The inorganic cross - linking afforded control over the system viscosity which was found to be particularly sensitive to the distribution of the di - and trifunctional species throughout the network, which in turn was a function of both the preparation pH and temperature. Useable materials were obtained for T group levels of less than 20%. Levels up to 50% were possible for more homogeneous T group distributions.

Interpenetrating networks employing short and long chain components were successfully prepared. Their mechanical properties were assessed and correlated to their composition and structure. The role of the inorganic cross - links was found to be a larger determinant of the mechanical properties than the inorganic network. Extreme values of Young's moduli of 288kPa and 16.6 MPa were obtained for low and high vinyl containing materials respectively. Their dielectric properties were comparable to conventional encapsulation materials, with ε' and $\tan\delta$ being in the range 3.36 ± 0.06 to 3.9 ± 0.1 and 0.001 ± 0.005 to 0.0370 ± 0.0002 respectively. A number of IPN materials, exposed to environmental testing (85°C / 85% RH), all afforded protection over the entire 1000hrs test period, with no failure resulting from sample limitations.

Dedicated
To

Mum, Dad
&
Philip

To begin at the beginning...

CHAPTER 1: INTRODUCTION

The massive growth in the semiconductor electronics industry over the last 30 years has only been realised via a concomitant expansion in device packaging technology.

The growth of Plated Through Hole (PTH) technology, in which the input / output (I/O) connections are passed through the printed wire board (PWB) and soldered on the reverse side, has been limited to applications requiring only low I/O densities, due primarily to the area requirements of the through holes (vias). PTH devices tend to be single chip units, encapsulated in hard plastic, this forming the physical perimeter of the device. Developments in PTH technology, nominally through pin grid arrays, where the I/Os are not restricted to the device perimeter but cover the whole area of the package, have allowed higher I/O count devices to develop. A large growth in the I/O and chip packing densities has been realised by the introduction of Surface Mount Technology (SMT), where the I/O connections are made directly to bond pads mounted on the substrate surface. The configuration of PTH and SMT packaging is highlighted in Figure 1.1. SMT has served the industry well since the late 1970s [1] and is expected to

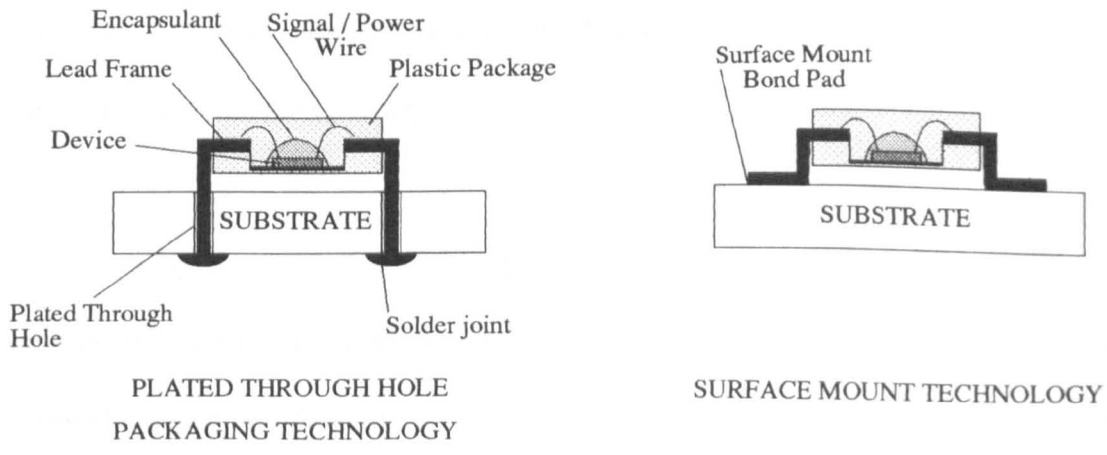

Figure 1.1. The configuration of PTH and SMT packaging technologies.

remain an important technology at least up to the end of the 1990s but demand for lower costs and improved performance has directed the development towards smaller devices with higher I/O densities, encouraging the growth of Chip On Board (COB) technology. In COB, the chip is directly attached to the substrate, eliminating the requirement for plastic packaging, as illustrated in Figure 1.2. This has large savings on the area required by a device, thus allowing packages with 200 I/Os (the limit for SMT) to be easily obtained at reasonable cost and with package sizes only 1/3 those of a comparable SMT package [2]. COB technology is very cost effective for low (<200) I/Os and in applications where low weight is a premium, such as in the telecommunications and auto - motive industries. For higher performance applications, laminated substrate Multi Chip Module (MCM-L) technology is preferred, offering multilayered I/Os (>400) [2] and a 85% [3] component density compared to 60% [4] for both SMT and COB. Both COB and MCM-L technologies are expected to lead the market well into the next century.

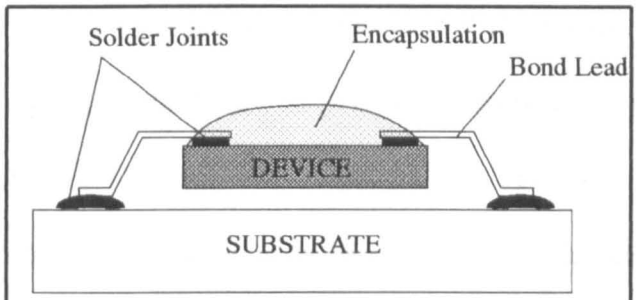

Figure 1.2. A typical COB configuration (tape automated bonded - outer lead bonded).

It is generally accepted that device packaging serves two main purposes; firstly it provides the most economic and expedient interface between the device and the surroundings and secondly, but no less importantly, it affords the device environmental protection, this being achieved via encapsulation. Encapsulation materials range from

metals, glasses and ceramics (also glass - ceramics are becoming more important) to a whole range of polymeric materials, these being both organic and inorganic. The choice of material used depends on the degree of hermeticity that is required. Subdivision of encapsulation processes into hermetic and non - hermetic is generally made.

Totally hermetic packages utilise highly water impermeable materials such as metals, glasses and ceramics to form hermetically sealed units around the device. Examples of hermetic packaging are the CERDIP package, based on a KOVAR / Alloy42 lead frame, encapsulated in low temperature glass between a ceramic lid and base[5] (see Figure 1.3) and, more recently, the Integral Substrate Package (ISP) [5] which allows hermetic encapsulation of a number of devices in one module and to some degree realises affordable hermetic packaging (see Figure 1.3). Totally hermetic packaging is only used where reliability is paramount such as in military applications. Their use in lower level devices is ruled out by their high cost. Also, with the likely increased use of larger area MCMs, this type of packaging may become more difficult to achieve.

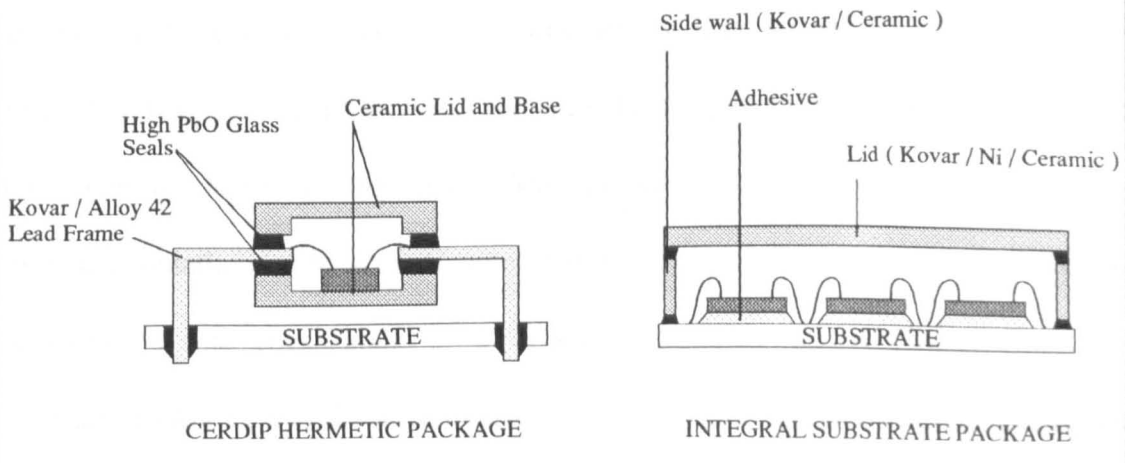

Figure 1.3. Examples of some hermetic packaging configurations.

Non - hermetic packaging utilises polymeric materials which, despite in many cases having a high percentage of hydrophobic groupings within the structure, are water permeable. The mechanism by which protection from corrosion is afforded relies on the ability of the encapsulant to prevent the accumulation and migration of ionic species at the device interface.

Plastic moulded packages, the first industrially accepted non - hermetic packages, were introduced in the 1960s and heralded the birth of low cost mass production of ICs. Plastic encapsulated devices (PEDs) comprise a chip that is bonded to a metal lead frame and encapsulated in a plastic via a transfer moulding process (see Figure 1.1) . Typical encapsulation materials are epoxy novalac resins, silicones, polyurethanes and polyimides, the epoxy novolac resins having the majority share of the market primarily as a result of their superior chemical resistance, thermal and adhesive properties[6]. It is estimated that 95% of all devices produced utilise plastic encapsulation [6].

Moulding is not the sole PED processing route. A second configuration exists in which the device is bonded to a conventional substrate, be it polymeric or ceramic, and the encapsulant is applied in a 'blob' over the chip. This is generally referred to as glob or blob top encapsulation (see Figure 1.2). Materials used are those employed in moulding processes, sometimes with some degree of modification being necessary to assist the application of the encapsulant or to modify its curing characteristics. Glob top encapsulation has a particular advantage over moulded packaging in that the dimensions of the encapsulated device are little larger than the bare device. This suggests a good future for glob top technology in applications where space is a premium such as in COB

and MCM packaging. Glob topping of MCM packages may be in fact the only viable encapsulation technology as the quest for improved performance and greater levels of integration pushes the size of MCMs upwards and forces the I/O pitch downwards, soon making it technically impossible to produce PEDs using moulding techniques.

This introduction has highlighted the principal packaging technologies that are currently in use today and has introduced the materials that are generally employed. The following section examines more closely the need for encapsulation and the properties required by a good encapsulant. Also an overview of the materials presently used is given, with a view to what extent each material fulfils these requirements.

CHAPTER 2: BACKGROUND - ENCAPSULATION.

2.1 The Need For Encapsulation

The role of encapsulation is twofold, firstly it provides mechanical support to the device metallization, minimising the risk of damage occurring as a result of mechanical shock received during chip handling at both the fabrication stage and during use in the field. Secondly, it affords protection to the delicate metallization on the device surface from airborne contamination. Typical contaminants are dust, gas, moisture and ionic species, the latter three posing the most serious threat to the reliability of the device due to their ability to cause corrosion of the metallization (the former are eliminated to the sub micron level by working in clean room conditions).

Failure mechanisms may be classified as either chemically or electrochemically initiated processes. Corrosion of the metallization via chemical processes include [7] oxidation at elevated temperatures, tarnishing in the presence of sulphur, and corrosion in the presence of chlorinated solvents, aluminium being particularly sensitive to the latter. The direct corrosion of aluminium in the presence of Cl^- is a frequently documented process, the equation for this reaction is given in equation 1.

$$\begin{aligned} &Al + 4\,Cl^- \longrightarrow AlCl_4^- + 3e \\ &AlCl_4^- + 3H_2O \longrightarrow Al(OH)_3 + 3H^+ + 4Cl^- \\ &Al + 3Cl^- \longrightarrow AlCl_3 + 3e \\ &AlCl_3 + 3H_2O \longrightarrow Al(OH)_3 + 3H^+ + 3Cl^- \end{aligned} \qquad (1.)$$

Electrochemical processes are operative only in the presence of moisture in the form of a layer at the device surface. Three possible failure mechanisms may operate, these being charge separation in MOS devices, direct galvanic corrosion of the metallization and electrolytic conduction.

***Charge Separation*:** This process relies on the increased mobility of surface charges on insulating materials. Only under severely damp conditions does this lead to device failure, unless accelerated by contaminant ions.

***Corrosion of Metallization*:** Dissimilar metals in contact with each other, as are found at wire - bond pad interfaces (Al - Au, Al - Ag etc) in the presence of a electrolyte (water with dissolved ionics) will set up galvanic currents leading to the corrosion of the more electropositive metal. This process is not necessarily observed in real devices due to the presence of applied d.c voltages. In this case the corrosion mechanism is that of electrolytic conduction.

Electrolytic Conduction : The dissolution of Cl- or Na^+ in a condensed water layer forms an effective electrolyte and, when spanned between two conductors of similar or dissimilar metals at different potentials, an electrochemical corrosion cell is set up. A schematic diagram of a typical corrosion cell is given in Figure 2.1. A number of reactions may occur at the anode, these being, the reduction of Cl^- to Cl_2, the reduction of OH^- to H_2O and O_2 and, more seriously, the electrolytic current may encourage the anode to dissolve in the electrolyte, transfer through the electrolyte, and be deposited at the cathode. Plating at the cathode results in a dendritic growth formation. The

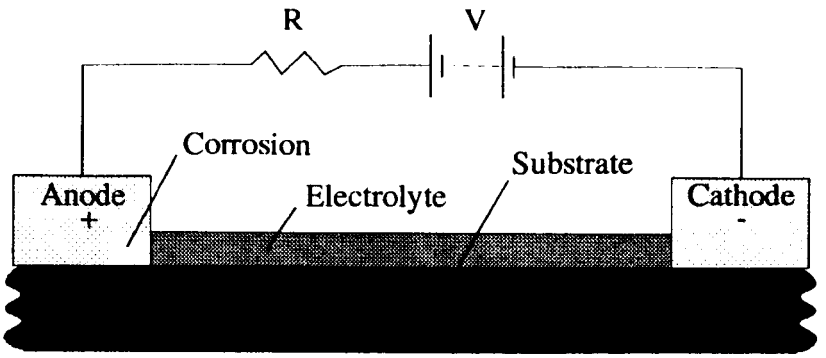

Figure 2.1. A typical electrochemical cell between two conducting electrodes at different potential.

developing dendrite grows back towards the anode thus increasing the field gradient between the conductors and accelerating the corrosion. Device failure occurs when the dendrite creates a short across the conductors.

2.2 The Properties Required of A Good Encapsulation Material.

2.2.1 Mechanical Properties.

***Excellent Adhesion*:** It is quite clear from the above discussion of failure mechanisms that the prevention of formation of an ion laden moisture layer at the surface of the device is crucial to its reliability. The principal function of an encapsulant is to prevent this layer forming. Since all polymers are permeable to moisture their ability to do this relies on their having excellent adhesion to the device and the substrate. The adhesion of the polymer molecules to the substrate reduces the free surface area over which the contaminants may move, thus limiting their mobility. The adhesion should be

unimpaired in field use under conditions of variable temperature and humidity.

***Good Compliance*:** The encapsulant is in intimate contact with the metallization and die and thus is capable of exerting stress upon them, particularly under conditions of varying temperature. Any encapsulant should thus be as flexible as possible, possessing a low elastic modulus.

***Resistance to Thermal Shock*:** The field use environment is one of a constantly changing temperature, with rapid changes occurring at power on / off. Stresses will be developed within the material as a result of thermal coefficient of expansion (TCE) mismatch between it and the device. Since TCE matching is not feasible with the materials under consideration the material should have sufficient flexibility to be able to withstand these stresses without rupturing.

2.2.2 Electrical Properties.

Ultimately, the electrical properties of a semiconducting device are limited by the materials chosen for the device metallization, substrate and encaspulant. The parameters of fundamental importance are signal bandwidth, attenuation, propagation velocity, distortion and noise. All these are directly influenced by the dielectric constant ε', of the encapsulant, where ε' is more fully expressed in terms of the complex dielectric permittivity, ε^*, as given in equation 2 [8]. Where ε'' is the complex, loss component of the complex permittivity. Generally a low ε' is required to optimise the performance of a system. A lowering of ε' results in a reduction in the capacities

$$\varepsilon' = \varepsilon^* + i\varepsilon'' \qquad (2.)$$

associated with any signal line discontinuities (non impedance matched components), which leads to an improvement in signal bandwidth [9]. Signal attenuation along a transmission line, as defined by the ratio of the output voltage over the input voltage is given by equation 3 [9]. where α is the transmission line attenuation factor and L is the

$$\frac{Vout}{Vin} = e^{-\alpha L} \qquad (3.)$$

line length. α is a compound function of three loss functions, one being skin effect dependent, one being resistive and one being associated with the dielectric loss of the encapsulant. The latter loss term, α_D, is frequency dependent and is related to the loss tangent, $\tan\delta$ ($= \varepsilon''/\varepsilon'$), of the encapsulant by equation 4 [9], where f is the signal frequency and v is the signal propagation velocity. Encapsulation materials must therefore possess a low loss tangent.

$$\alpha_D = \pi \tan \delta \frac{f}{v} \qquad (4.)$$

A dielectric constant that is invariant to frequency is particularly important for transmission of short pulses which will be composed of series of high frequency waves whose propagation velocities, Vp, are given by equation 5 [9]. Thus to avoid both pulse delay and pulse distortion, ε' must be low and constant over the range of frequencies within the pulse.

$$V_p = (\varepsilon')^{-1/2} \quad (5.)$$

Finally, signal noise, primarily due to cross - talk between channels, is minimised by the use of low dielectric material. This has the effect of decreasing both the mutual capacitance and characteristic impedance of the channels.

2.2.3 Chemical Properties.

***Good Solvent Resistance*:** It is generally accepted that a good degree of solvent resistance is required by an encapsulant to ensure that it is not degraded by atmospheric pollutants. In some applications though, such as encapsulation of MCMs, a removable encapsulant is sometimes advantageous as it allows access to failed ICs (integrated circuits) within a MCM, thus lowering repair costs and increasing the effective lifetime of the unit.

***High Degree of Hermeticity*:** As previously mentioned, no polymeric materials are completely hermetic but careful consideration of the encapsulant's constituents and control over its structure may allow minimisation of its permeability.

***High Degree of Thermal Tolerance*:** Due to ever increasing levels of integration, devices are consuming more power and are consequently running at higher temperatures. Encapsulants are required to withstand these temperatures for long periods of time without degradation of their properties. Also, they may be expected to tolerate much higher temperatures for short periods of time, as may be experienced in subsequent processing routines.

2.3 Encapsulation Materials

2.3.1Epoxy Resins

Early epoxy materials were prepared from the reaction between epichlorohydrin and bisphenol - A to form diglycidylethers of bisphenol - A (DGEBA) [10]. The preparation route of DGEBA is given in Figure 2.1 Control of n, the number of repeat units within the structure, allows control of the resin viscosity from liquids to hard solids. The materials prepared from DGEBA have a relatively low glass transition temperature, T_g, of around 100 - 120°C [11]. The low T_g of bisphenol - A materials was responsible for their discontinuation as encapsulation materials. Devices coated with these materials were subject to a mode of failure known as 'windowing'. As a result of passing through T_g, the increased rate of expansion caused the wirebonds of the device to be detached from their bond pads and subsequently be reconnected during cooling.

A more suitable moulding material came in the form of Novolac resin. The Novolac resin is prepared by reaction between phenol and formaldehyde. Further reaction of the resin with epichlorohydrin yields the epoxy - novolac resin [10] (see Figure 2.2). The principle advantage of Novolac resin over bisphenol - A is the increased T_g which may be as high as 150°C [11] or even 160°C [12] and a good thermal stability, with little sign of thermal degradation being seen at prolonged exposure to temperatures of 200°C [13]. Both properties are conferred on the material as a result of the higher level of functionality of the phenyl groups. It is also common practice to increase T_g under post - mould temperature excursions [14]. Also, as a result of the increased degree of phenyl - phenyl cross - linking, they possess a lower degree of water absorption. Prior to

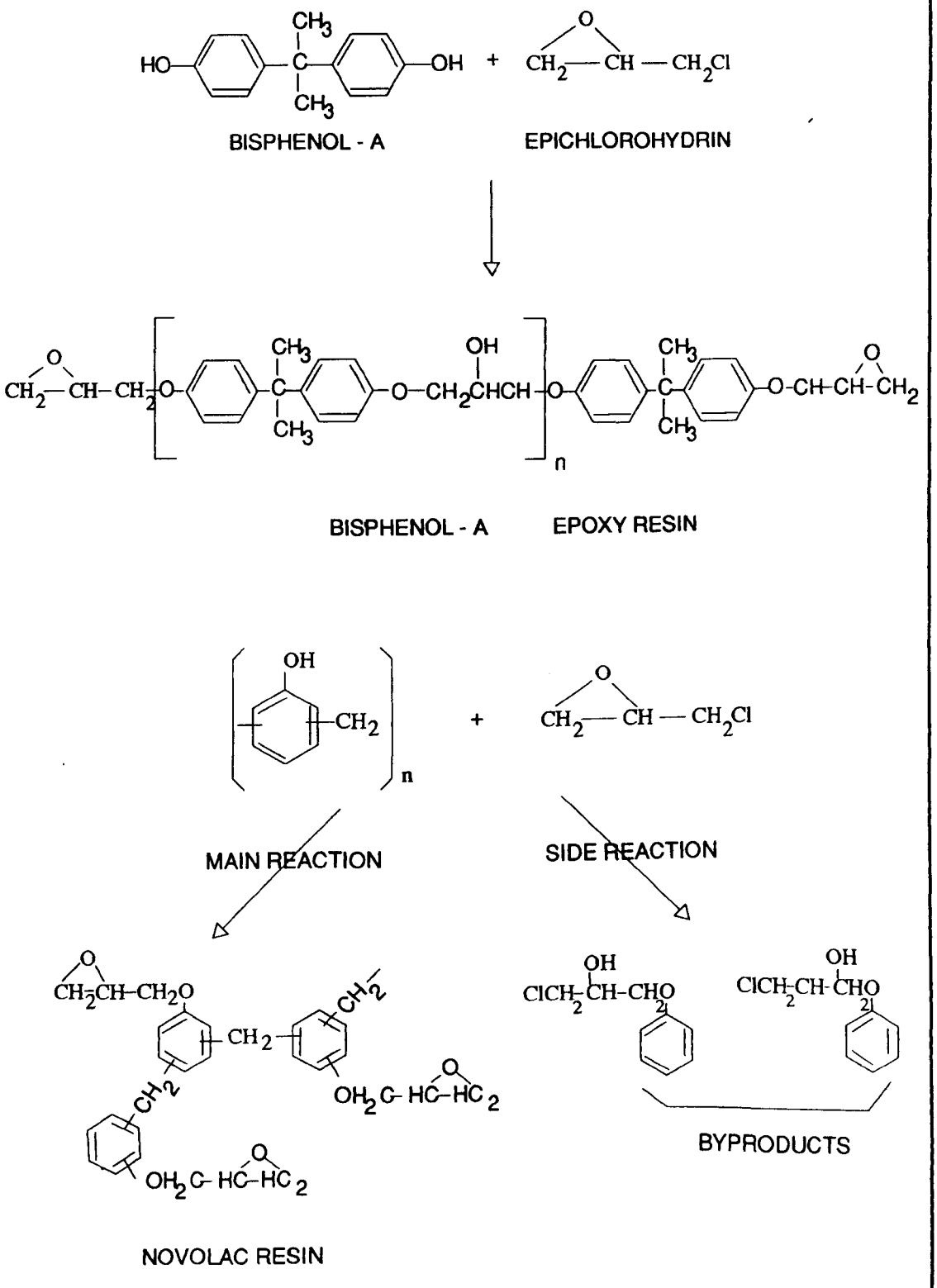

Figure 2.2.The preparation route of DGEBA from bisphenol -A and epichlorohydrin and the preparation of Novoalc resin from DGEBA and epichlorohydrin.

transfer to the mould, the resin is blended with accelerators and hardeners. These control the direction and rate of the cure processes, ultimately controlling the final viscosity and hardness of the cured resin. Aliphatic and cyclic amines or acid anhydrides are most often used as hardeners with liquid cyclic amines yielding the most highly cross - linked, water impermeable structures [11].

The above properties make Novolac resins the principal PED encapsulation material. Despite their positive attributes, epoxy resins have a number of less attractive characteristics. The aforementioned properties, in particular the high T_g and the high degree of water impermeability, are achieved at the expense of the material's mechanical compliance. Epoxies are inherently brittle, having Young's moduli, E, of between 7 and 35×10^9 Nm^{-2} [15]. The high values of E result in the production of large stresses when an epoxy encased device is subjected to a temperature excursion . The stress is related to E by equation 6 [12], where K_1, K_2 are constants, α_1, α_2 are the material's temperature coefficients of expansion (TCE) below and above T_g respectively, E_1, E_2 are the material's Young's moduli below and above T_g respectively and T_1, T_2 are the lower and upper temperature limits of the excursion. The stress is limited to some extent by the low TCE of 40 - 80 MK^{-1} for the resin [15].

$$\text{Stress} = K_1 \int_{T_1}^{T_g} E_1 \, \alpha_1 \, dT \quad + \quad K_2 \int_{T_g}^{T_2} E_2 \, \alpha_2 \, dT \qquad (6.)$$

To limit the stresses even more, filler materials are added to the base resin. SiO_2 is generally used for this purpose. For a typical resin with 68 -72% SiO_2 filler the TCE is effectively halved [16]. Added advantages of using a filler are an improved thermal

conductivity and enhanced thermal shock resistance. It is usual practice to use only 1 - 2% filler in association with a resin flexibiliser [16]. since too high a filler content decreases the tensile strength of the resin, making it more prone to cracking.

These modifications can only partially alleviate the problems of stress. With the increasingly widespread use of ULSI and MCMs in low level consumer products, an area dominated by transfer moulded plastic packaging, increased package sizes exacerbate the problem of stress. Using conventional plastic packaging materials under these conditions has led to the identification of new chip failure mechanisms [17]. including cracks from the die mounting, metal deformation, passivation cracking and multilayer oxide cracks. The stresses result from the TCE mismatch between the epoxy resin, silicon and its passivation layers and lead frame materials. Thermal excursions resulting from initial material curing and post - mould curing processes set up stress gradients within the die and resin. Shrinkage of the epoxy during cooling generates restrained shrinkage stresses [18]. The stress is generated by the presence of the device restricting the contraction of the resin [19] since the TCE of the resins is at least an order of magnitude larger than that of passivation / die materials. Shear stresses of up to 14 MNm^{-2} [19] have been measured for epoxy coated circular inclusions using photoelastic techniques. As a result of these stresses, temperature cycling of transfer moulded packages leads to the creation of crevices between the epoxy and the device [20]. It was proposed by R. E. Thomas [18] that the chip edges act as stress concentrators which initiate microcracks during thermal cycling, the degree of cracking being proportional to the stress gradient across the die [17]. S. Sasaki et al [21] have suggested that post - cure stresses lead to partial delamination at the epoxy - device interface, this possibly

being exaggerated by degradation of the epoxy's adhesive properties by contamination from mould release agents [20]. These crevices may create moisture traps at the interface, thus accelerating the corrosion processes, possibly at rates above those for an exposed device.

Low stress resins have been developed using a silicone modified base resin [12] which show a lowered E without a lowering of T_g. These materials may be suitable for MCM applications. Commercial liquid epoxy resins have been developed for COB/ MCM applications where glob top encapsulation is required. Developments in these materials have led to UV curable systems. These have the advantage of a very rapid cure with no requirement to heat. The cured material's properties [22], (hard with a high T_g, low TCE and ε') suggest a very high filler content, possibly conferring poor mechanical properties.

2.3.2 Silicones.

Silicones are organic - inorganic hybrid materials based on a Si-O-Si siloxane network with organic functionalities (methyl, phenyl, vinyl etc) pendant to the silicon atoms. 'Silicone' was initially adopted to describe these materials as the R_2SiO repeat unit (where R is an organic group) , characteristic of a silicone, was compared to that of a ketone (R_2CO). Silicones belong to the generic group of materials known as organopolysiloxanes, but the name silicone is generally reserved for technical materials that are used commercially. Silicones have been widely used as electronic device encapsulation materials for over a quarter of a century [15]. Their success as

encapsulants has been as a result of their superior properties over other polymeric materials. In particular, their resilience to thermal degradation is excellent, with long term exposure at temperatures in excess of 250°C having no detrimental effects. Their thermal properties are inherited from the inorganic network, this also being responsible for the low dielectric constant and loss tangent characteristic of silicones. Due to their low water absorption [23] these properties are retained under conditions of high humidity. Silicones also exhibit superior adhesive properties, these being attributed to their ability to interact chemically with hydroxyls on the die / substrate surface [23]. As a consequence of this interaction silicone rubbers exhibit excellent protection from corrosion under conditions of high temperature and humidity [24,25] . Finally, silicones can be manufactured with a very high level of purity, with mobile ion concentrations as low as 1ppm [26].

The advent of silicone encapsulation was seen by the introduction of room temperature vulcanising (RTV) silicone rubber, classified as RTV-I. The highly cross - linked structure of silicone rubber is produced by the catalyst initiated cross - linking of hydroxy - end - blocked (HEB) siloxane chains via suitable species, these most commonly being an alkoxy silane such as tetraethoxysilane (TEOS). Its reaction with the HEB siloxane can be seen in Figure 2.3. The reaction is usually catalysed by organotitanium or organotin compounds [27]. Although the hydroxy - alkoxy condensation route is most often employed, other functionalities such as acyloxy, amine and oxime are also available [28]. This type of RTV material is generally found as a two component system, with one component being a mixture of the siloxanol with the cross - linker and the other being the catalyst. One component materials are also available

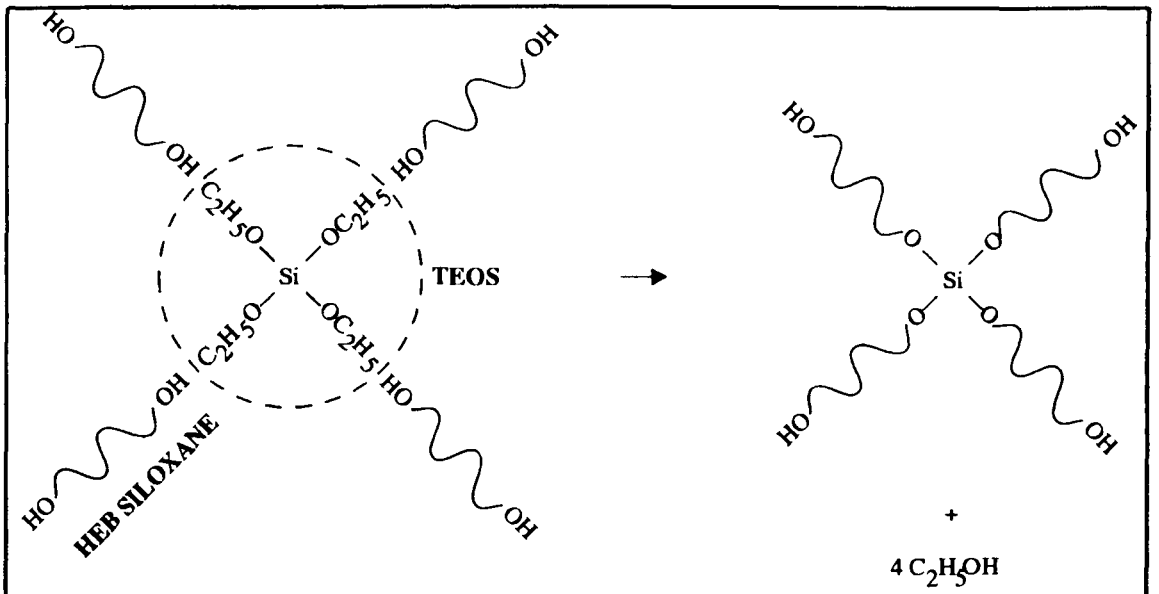

Figure 2.3. The RTV cross - linking between hydroxy - end - blocked siloxane and TEOS in RTV silicone rubber.

which only react in the presence of moisture. The majority of one component systems vulcanize through the interaction between α - ω polydimethylsiloxane diols and acetoxy (CH_3COO -) substituted silanes or siloxanes.

Due to the highly cross - linked nature of silicone rubber elastomers they tend to be rather stiff, this stiffness has been shown [20] to result in device failures due to the stresses imparted to the device by the RTV during thermal cycling [20]. This inflexibility has resulted in the decline in the use of RTV silicone as a moulding compound due to bond delamination being common after temperature cycling tests and its subsequent poor performance in salt spray tests [11]. A further problem associated with RTV silicones is colloidal particle formation resulting from local catalyst concentrations. Problems associated with this phenomenon are nozzle clogging during application to

the substrate and inadequate surface coverage leading to uneven surfaces with voids and pinholes which are reliability concerns [26]. To alleviate this problem it has been suggested that the addition of alcohol to the RTV system improves the material's properties [27].

The problems associated with RTV silicone rubbers have led to the development of RTV-II rubbers, commonly referred to as silicone gels. Gels have been used as an encapsulation material for at least a decade [27]. Gels are based on linear chains with hydro and vinyl substitution. Curing of the gels is achieved through the platinum catalysed, thermally initiated addition of the vinyl through the hydro group [15], as seen in Figure 2.4. The level of catalyst used is generally of the order of 1 - 2 ppm [15]. Gels tend to be two component materials due to the cross - linking reaction occurring at room temperature. RTV-II materials with a thermally activated catalyst have allowed the development of single component encapsulants.

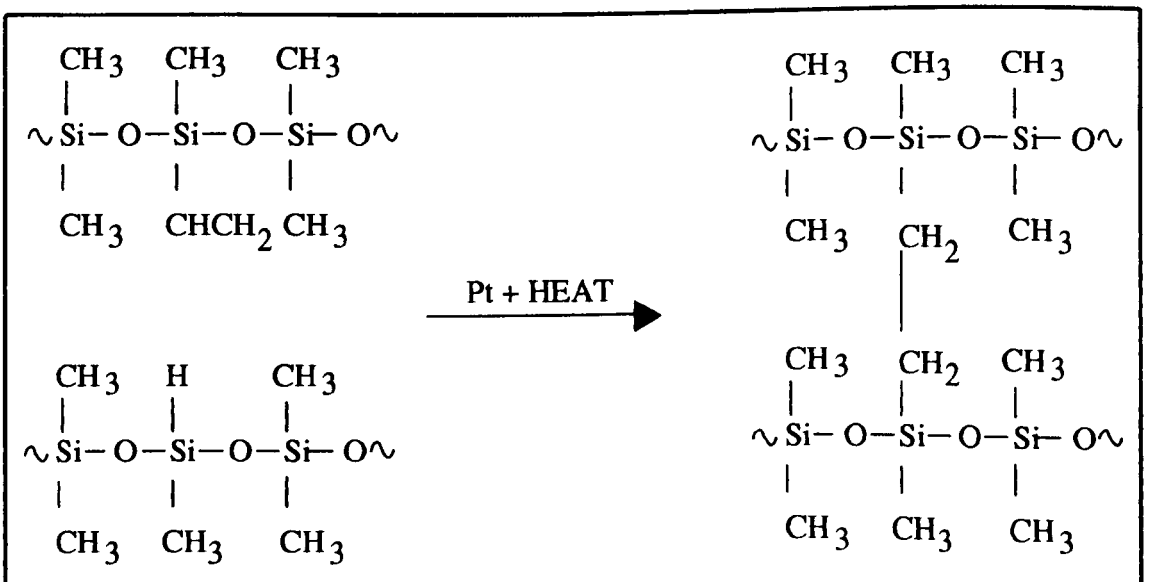

Figure 2.4. The platinum catalysed hydro - vinyl addition cure mechanism operative in silicone gel materials.

The effectiveness of silicone gels in preventing moisture absorption onto the device has been thoroughly tested [29] and all results indicate that their performance is superior to that of all other coatings. In a paper by White [25], he states that any material that is able to interact chemically with the surface hydroxyls will afford good moisture protection. In silicone gels, this interaction may be envisaged as either being between the methyl and hydroxyl groups or between residual hydroxy groups in the gel and surface hydroxyls.

The principal advantage of gels over RTV silicones is their very much lower elastic modulus, making them less damaging to bond wires which are then less liable to debond from the die / substrate during temperature cycling. The low values of E are disadvantageous in that the materials are inherently mechanically weak, thus providing little mechanical support to the device metallization. Also, due to the low level of cure associated with the gels, necessary to impart the high level of flexibility, they have a poor degree of solvent resistance. Attempts have been made to modify the gels via the addition of fused silica, with the aim of improving their mechanical and chemical properties [33]. Although this has the effect of reducing the TCE, improving the solvent resistance and raising the mechanical strength of the silicone, it also has the disadvantage of increasing its viscosity. It has been indicated [29] that device passivation layers, particularly nitride type, are not flawless and may contain pinhole defects. Any reasonable level of viscosity may encourage the gel to tent over the pinholes, resulting in localised corrosion sites, thus compromising the reliability of the device.

The future of silicone encapsulation materials lies in two areas, MCMs and single chip

packaging (SCPa):

MCM application: From both a cost and technological standpoint, the viability of hermetic packaging of large size (>100 mm sq) MCMs seems less likely. The savings in cost from utilising silicone encapsulation comes not only from the lower material costs, with the need for expensive ceramic substrates and sealing methods being avoided, but also from the high level of accessibility to the chips afforded by silicones, allowing replacement of faulty devices and upgrading of system units without recourse to whole module replacement. Other advantages are a saving in weight, and volume. The reliability of gels in MCMs has been assessed [26] and they have shown excellent reliability under temperature - bias - humidity (THB) and temperature cycling testing although a sensitivity to the method of application has been highlighted, specifically the requirement for a low viscosity to avoid tenting and void generation. The performance of RTV rubber on MCMs has not fared as well as the gels, primarily due to wire bond damage although the use of thinner coatings has been suggested to alleviate this problem. The use of silicone rubber as a lid sealing medium has also been proposed [15].

SCP Application: SCP is not to be dismissed as a viable packaging technology for the future, a number of large computer product producers, namely Fujitsu and Hitachi apply a SCP design approach to their high performance devices [1]. The use of both RTV rubber and silicone gel in SCP can greatly improve the device reliability by insulating it from the deleterious effects of the brittle epoxy. The plastic overcoat may also enhance the properties of the silicone by constraining its expansion. Device failure in plastic - RTV coated SCPs has been attributed to the stiffness of the RTV [20] but these fails are controllable by the application of thin coatings [26], indeed, RTV has been employed by AT&T with epoxy post mould coatings for a number of years.

2.3.3 Polyimides / poly (amide - imide)s

Polyimides, PIs, are a class of thermoplastic polymer characterised by the repeat unit of Figure 2.5[30]. Ar and Ar' are generally aromatic with the form Ar  , 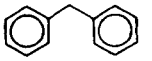 etc Ar': 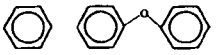 , etc.

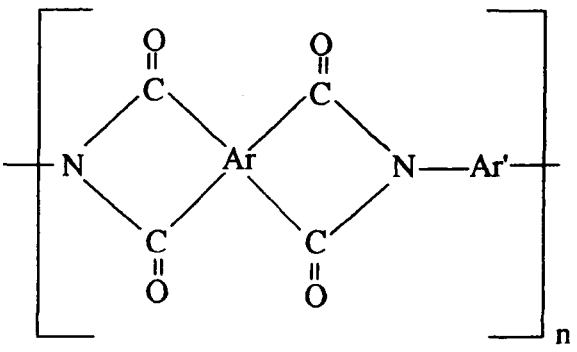

Figure 2.5. The repeat unit of polyimide.

Application of polyimides to the device / substrate may be by two methods, firstly, by conventional spray or dip coating of the device in a reactive precursor followed by a thermal cure procedure, and secondly, by applying a preimidized (pre - cured) solution of polyimide, with subsequent desolvation [32]. The former method usually consists of the application of a solution of poly(amic) acid, desolvation at between 120 - 250°C [31], followed by final imidization at 300 - 450°C under N_2 [31]. The cure reaction is given in Figure 2.6 [32]. It can be seen from Figure 2.6 that the cure reaction liberates water, this may have the effect of reducing the average molecular weight of the polymer unless removed using anhydrides and pyridine in a 'chemical cure' [30]. The use of polyimide as an encapsulant is limited by the high cure temperature, restricting it to ceramic substrates. Preimidized systems eliminate the requirement for a high temp - erature cure but the coat is soluble in polar solvents, which is undesirable.

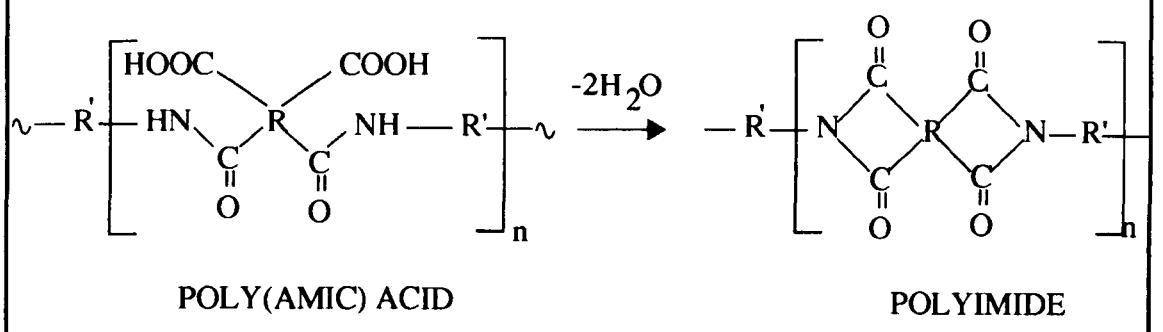

Figure 2.6. The imidization reaction for the preparation of a polyimide from poly (amic) acid.

Poly (amide - imide)s, PA-Is, are polymers containing both imide and amide groups and are prepared from the reaction of a triacid derivative with a diamine [30] .The repeat unit of a PA-I is given in Figure 2.7.

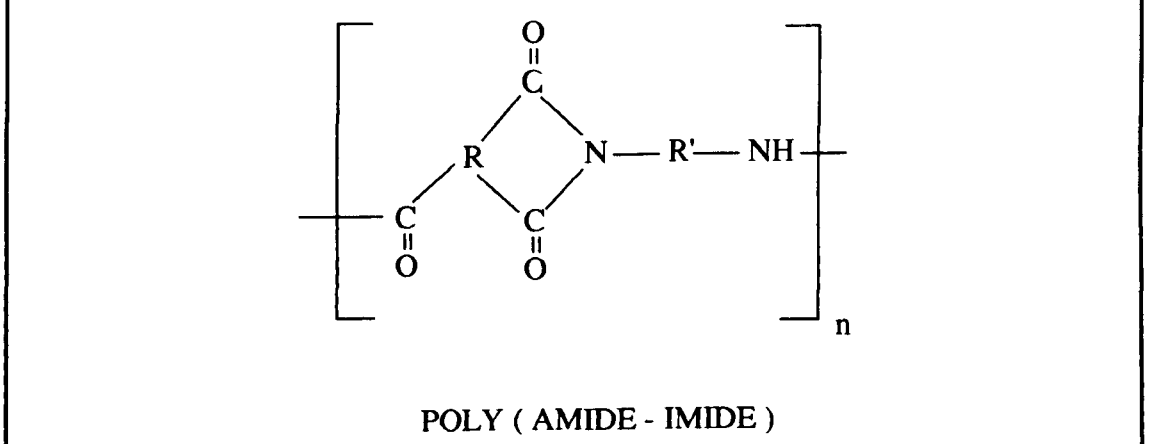

Figure 2.7. The repeat unit of poly (amide - imide).

Both PI and PA-I films demonstrate excellent thermal stability due to their mainly aromatic structure. PI coatings are non - degraded at temperatures up to 500°C [31] but

PA-I materials have a lower thermal tolerance, and are only useable up to approximately 250°C [30]. PI materials are generally rather brittle with elastic moduli in the range 3 - 12 GPa [10]. The TCE of PIs range from 3 to 80 MK^{-1} [15] but the low TCE materials tend to be the most brittle and have lower tensile strength [31]. PIs are thus not a compliant encapsulant and will cause severe damage to the device metallization, and possibly be prone to cracking. Aromatic PIs exhibit excellent adhesion to aluminium but they offer only poor adhesion to oxides such as SiO_2, Al_2O_3 [31], which are common passivation and substrate materials. The electrical properties favour their use as encapsulants over epoxies, with ε_r values in the range 3.1 - 3.7 [31] at 1kHz, just slightly higher than those of silicones. A tanδ of 0.001 - 0.003 [31], also at 1kHz, is on a par with that of silicones and epoxies. Unlike silicones, PIs have high water absorption values [32]. This not only results in severe degradation of their electrical properties [31], but also their adhesion is dramatically reduced [32].

Developments in PIs must be focussed on developing lower cure temperature materials, with lower elastic moduli and TCEs and a lower level of moisture absorption. One development has been the application of Langmuir - Blodgett (LB) film technology to PI film preparation. LB films are highly ordered, densely packed ultra - thin layers. LB PI films have been successfully prepared from amphiphilic modified poly(amic) acids [32]. These layers have been shown to be more resilient to water permeation than standard PI. Used as an overcoat layer over a thicker PI coating, the deterioration of the bulk PI material by water hydrolysis is prevented, improving the reliability of devices protected in this manner. Copolymers of PI and silicone have been developed and are commercially available. Advantages over PI are improved adhesion on SiO_2 and other

substrate materials [31] and a lower cure temperature [26]. Their performance as encapsulants has been proven in reliability testing [31] but a reliability concern may be their poor solvent resistance.

2.3.4 Poly - p - Xylylene (Parylene©)

Poly - p - Xylylene is prepared from the high temperature vaporisation of p - Xylene (**I**) to form the reactive intermediate monomer p - Xylylene (**II**). Upon cooling to below 30°C this monomer polymerizes to form the high molecular weight polymer, poly - p - Xylyene (**III**) (see Figure 2.8) [33] . The device is coated directly in a chamber containing the monomer vapour. The resulting conformal coatings are smooth and pinhole free which, due to the low temperature deposition, are virtually stress free. This

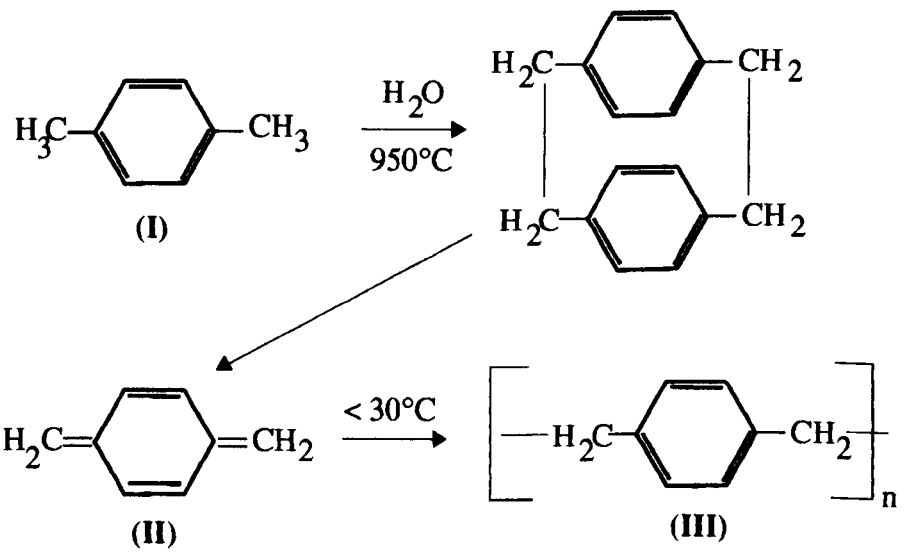

Figure 2.8. The Preparation of Poly - p - Xylylene Conformal Coating.

bodes well for high reliability, indeed, Parylene© is used as a conformal total area printed circuit board (PCB) coating in military applications [26]. The principal advantages of Parylene are its ease of application, low residual stress, purity, thermal

stability and good electrical properties. The main disadvantage is the slow deposition rate, although chlorine substitution on the benzene ring has been shown to increase this. A further disadvantage is the need for an adhesion promoter such as an aminosilane [26].

CHAPTER 3: BACKGROUND - POLYORGANOSILOXANES.

3.1 Introduction

As indicated in section 2.1.3, silicones are commercially available technical products, generally possessing a highly cross - linked structure, obtained through either RTV-I HEB technology or through hydro - vinyl addition reactions (RTV-II type silicone gel). Silicones belong to the group of organic - inorganic hybrid materials generically known as polyorganosiloxanes. These are based on an inorganic siloxane (Si-O-Si) network, with at least one Si-C bonded organic group per molecule. The fundamental properties of polysiloxane based materials are determined by the Si-O and Si-C bond characteristics and the interaction between the two, thus, a brief introduction to the siloxane and Si-C bonds is now given.

Siloxane bond. The strength of the Si-O single bond is subject to conjecture, the value seemingly being dependent upon both the method by which it was obtained and the material studied. Pauling's value of 369kJmol^{-1} [34], obtained from thermochemical data is the lowest estimate, the upper level of 423 - 427 kJmol^{-1} being set by Thompson [35] using data from the heat of combustion of siloxanes. Despite these variations it is consistently found that the Si-O single bond strength is higher than both C-C and Si-C bonds. Associated with this high bond strength there is found an anomalously short bond length of only 1.64Å [36] which cannot be explained in terms of the atomic or ionic radii of the respective elements. It has been postulated [37] that the short distance is as a result of the Si-O bond not being solely of single bond character but in fact being a resonance structure of three bond types: covalent, polar and double. The double bond

component is thought to be possible as a result of the involvement of unoccupied 3d orbitals in bonding. The Si-O bond is thus not only formed from the interaction of the sp^3 orbitals of the silicon with the p orbitals of the oxygen but also from the partial overlap of the oxygen's p orbital electrons with the 3d orbitals of the silicon, creating a d_π-p_π interaction, thus forming the Si=O bond. Note that this is a **component** of a bond **resonance**, the existence of an isolated Si=O bond has not yet been proved. It is this component of the bond that is responsible for the observed short bond length and the high bond strength. The resistance of the siloxane bond to cleavage by electrophilic species such as protic (e.g HCl, H_2SO_4) and Lewis (e.g BF_3) acids is determined by the availability of the lone pair of electrons on the oxygen atom [36] . Thus the strength of the siloxane bond can be considered to be determined by its polarity, which is in turn controlled by the electronegativity of the substituents attached to the silicon. More electronegative substituents such as phenyl (C_6H_5) will depolarise the bond (and increase the d_π-p_π component), making it less susceptible to cleavage. On the other hand, long alkyl groups which exert a +I (electron donating) effect on the silicon atom will increase the bond polarity, thus weakening it.

The Si-C bond. The sensitivity of the bond strength to the type of substituent is also reflected in the strength of the Si-C bond. More electronegative groups will increase the polarisation of the essentially covalent bond, thus weakening it to attack by electrophilic species. This bond, as for the siloxane bond, is subject to a d_π-p_π interaction although the extent of the interaction is less due to the longer Si-C bond length of 1.88 - 1.92Å [36]

From the above discussion it can be seen that the properties of Si-O and Si-C bonds are dependent upon each other. Thus the physical properties of any particular siloxane will be dependent upon the nature of the organic substituents within it, not only through their chemical reactivity, physical properties and mutual interactions but also through their effect on the nature of the siloxane bond. It should be noted that the properties of the organic substituents will not in general be identical to those within an analogous organic polymer. This is due to both the small (12%) [36] polar character of the Si-C bond and the existence of a certain level of d_{π}-p_{π} interaction . The level of the interaction will be dependent upon the type of substituent involved but it can be said that it will always be lower than for the Si-O bond as a result of the longer Si-C bond length. The degree of modification of a functionality, for example a C=C bond, within an organic substituent is reduced by an increase in the number of carbon atoms separating it from the silicon atom and is assumed to be unmodified when separated by a propyl ($-(CH_2)_3-$) group.

3.2 The Inorganic network

3.2.1 Introduction.

The inorganic network of polysiloxanes can be thought of as being composed of a number of building blocks. The fundamental monomeric repeat unit is given in equation 7. R is an organic grouping and can be alkyl, aryl, reactive or inert. Since the

$$R_nSi(O_{1/2})_{4-n} \qquad n = 0 \text{ to } 4 \qquad (7.)$$

network is extended through Si-O-Si linkages, the number of R groups bonded to the

silicon atom determines the functionality of the unit, ie, to how many other silicon atoms it is capable of making bonds. Five basic units are thus identified: SiR_4, $R_3SiO_{½}$, $R_2Si(O_{½})_2$, $RSi(O_{½})_3$ and $Si(O_{½})_4$. The non-functional tetraorganosilane unit, SiR_4, has limited application in polysiloxane technology due to its inability to form anything other than an isolated unit, unless the organic groups are themselves reactive and are able to extend the network via interaction with other neighbouring reactive R groups. At the other extreme, the $Si(O_{½})_4$ unit represents the fundamental structural unit of all silicate materials and is only rarely employed in the preparation of polysiloxane materials. The species corresponding to n=0 to 3 (see equation 7) are defined in Figure 3.1. The overall dimensionality of the structure thus formed will be dependent upon the type and relative proportions of the monomeric structural units within the material. Also, the units employed in the siloxane can be considered to control the degree of organic modification of the structure, allowing control over the extent of ceramic or organic character.

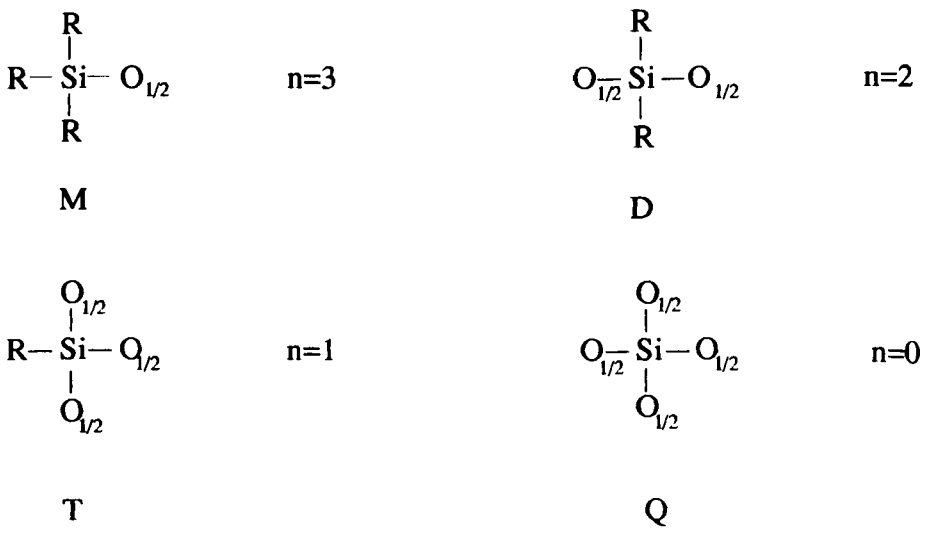

Figure 3.1. The fundamental repeat units of the polysiloxane inorganic network.

3.2.2 Inorganic network formation- reactions and mechanisms

Polyorganosiloxanes may be prepared via either hydrolytic or non-hydrolytic processes. The former process involves the reaction of a suitable organofunctional silane with water with the formation of silanols (SiOH) and the subsequent condensation of the silanols to form the siloxane network. The latter process does not involve the reaction with water, and the siloxane bond is formed by the direct condensation between suitable precursor substituents. The two processes are discussed separately below.

Hydrolytic process

Hydrolytic preparation is most often employed due to its simplicity. The precursors to the process must have at least one hydrolysable (removable by the reaction with water) group and thus have the general formula $R_{4-n}SiX_n$, where X can be OR', OCH_2COOH, NR'_2, H, Cl [38] etc (R' is alkyl / aryl and may be different to R). Reaction of these with water yields silanol species. The formation of the inorganic network proceeds via a condensation reaction. Depending on the degree of hydrolysis of the precursors, and on the reaction conditions, the condensation reaction that occurs may either be between two silanols or two X groups (homocondensation) or between a silanol and an X group, the latter being a heterocondensation process.

Non-hydrolytic Processes.

As previously mentioned, non-hydrolytic preparation of polyorganosiloxanes allows the creation of the siloxane bond directly from the reaction of silicon functional groups,

side stepping the hydrolysis stage. Due to the wide selection of silicon functional groups available for reaction, there exists an equally wide range of possible reactions, each with their own particular conditions. An excellent treatise on these can be found in Noll [38] and further discussion of non-hydrolytic processes will be reserved for reactions pertinent to this study.

In the following discussion, the processes of hydrolysis and condensation are dealt with separately although, in a real system, which may contain a number of different precursors with individual reactivities, the two processes may occur simultaneously.

3.2.2.1 Hydrolysis

The general outline for an hydrolysis reaction is given in equation 8. Before examining the reaction in any detail, a few general comments should be made. The mechanism of

$$X_n SiR_{4-n} + mH_2O \rightleftharpoons (HO)_m X_{n-m} SiR_{4-n} + mHX \qquad (8.)$$

hydrolysis is via nucleophilic attack on the silicon atom by the H_2O molecule, thus, the rate of the reaction is determined by the electron density around the silicon atom. The consequence of this is that the rate of hydrolysis is highly dependent upon the polarity of the Si-X bond[38] and thus chlorosilanes, which possess a strongly polar Si-X bond[39] are much more readily hydrolysed than alkoxysilanes which have a more covalent Si-OR bond. This also implies that the rate of hydrolysis increases with the number of hydrolysable groups attached. The rate of hydrolysis will also be controlled by the nature and number of organic substituents on the silicon. These will affect the

reactivity of the silane via both inductive and steric effects. Inductively, groups with a proficient electron withdrawing capability such as phenyl will draw electrons away from the silicon which will in turn withdraw electrons from X, thus reducing the polarity of the bond and reducing its reactivity[38]. Allyl group substitiution increases the electron density around the silicon atom, increasing the rate of hydrolysis under acid catalysis and vice versa under base catalysis [40], an effect that is understood by consideration of the stability of the transition states (see 3.2.2.1.a and 3.2.2.1.b). Sterically, large groupings can physically hinder or prevent the water molecule from attacking the Si-X bond [41], and according to Voronkov[42], this can be a more important effect than the inductive effects. The pH of the reaction solution is of prime importance in determining the rate of the hydrolysis reaction. Both acid and base catalysis may be used, the proposed mechanisms for each are now given.

3.2.2.1.a Acid Catalysis.

The actual mechanism for the hydrolysis is argued to proceed via either a pentacoordinated intermediate [40, 43, 44] or via a trivalent siliconium (X_3Si+) intermediate, although a number of researchers [45, 46] present evidence against the likelihood of the siliconium species being formed.

The pentavalent state mechanism: The mechanism for acid catalysis relies on the protonation of X. This induces a partial positive charge,δ^+,on the silicon atom, leaving it open to attack by the water molecule, attack leads to the generation of a pentavalent transition state which decays with the elimination of HX and H^+ to form the silanol. Two models have been suggested for the generation of the transition state. The first

model, suggested by Pohl and Osterholtz [43] can be seen in Figure 3.2. This model suggests that the attack by the H_2O molecule is made to the rear of the silicon - functional molecule. This leads to the generation of the transition state I. The water molecule acquires a partial positive charge which reduces the positive charge of the

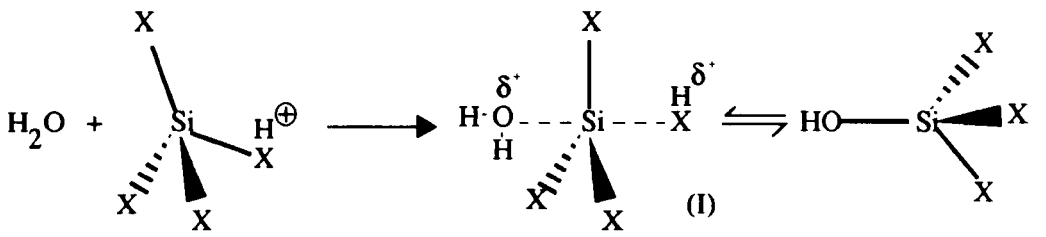

Figure 3.2. The Pohl - Osterholtz acid catalysed hydrolysis mechanism.

protonated X ligand, leaving it more likely to be ejected. Upon elimination of HX and H^+ the transition state decays to an inverted tetrahedron. Inversion occurs in displacement reactions with good leaving groups e.g Cl^-, OC(O)R whose conjugate acids have pKa values less than 5. For poorer leaving groups e.g H, OR whose conjugate acids have pKa values greater than 5, inversion may occur depending on the solvent and catalyst counter ion used [47]. This may be considered to be a S_N2 - Si reaction (bimolecular nucleophilic substitution). Substituents that reduce the steric crowding around the silicon atom would increase the reaction rate; electron donating groups would increase the rate by stabilising the positive charges.This effect is not too important though as the charge on the silicon atom is small.

A second model, suggested by Keefer [44] does not require tetrahedron inversion and involves the flank - side attack of the silicon atom by the H_2O molecule, as is indicated in Figure 3.3. In this model, the protonated X withdraws electrons from the silicon

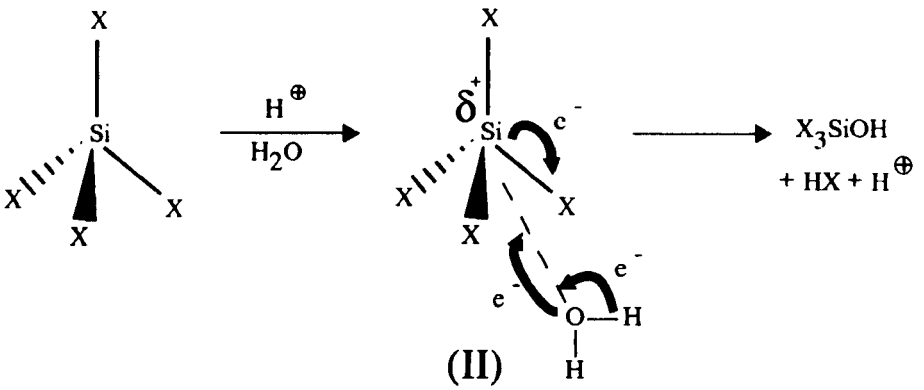

Figure 3.3. The Keefer acid catalysed hydrolysis mechanism.

atom, increasing its positive charge. The water molecule then attacks the silicon from the side, forming a covalent bond between the O and Si. The oxygen atom withdraws electrons from the hydrogen atom which is subsequently released as a proton. Transition state II decays upon the elimination of HX and no tetrahedron inversion results. An hydrolysis reaction proceeding via the Keefer model would be very susceptible to the inductive effects of X and from those of R directly bonded to the silicon atom since the δ^+ on the silicon atom would be strongly influenced. The occurance of inversion in hydrolysis reactions is seen to be dependent upon both the type of leaving group [47] and also on the polarity of the solvent [40].

Common to all acid catalysed hydrolysis reactions is a positively charged transition state (TS). The stability of the TS will be a function of the electron density at the silicon atom [40], decreasing with a decrease in electron density. Since a high reaction rate is dependent upon a stable TS any loss of electron density at the silicon atom will result in a lowering of the rate of reaction. The degree to which silicon substituents withdraw electrons from the silicon atom increases in the order [40] R, OR, OH, OSi, Cl, thus, for

the hydrolysis of alkoxysilanes, an increased degree of hydrolysis results in a reduced hydrolysis rate, and vice versa for the hydrolysis of chlorosilanes.

3.2.2.1.b Base Catalysis

As for the acid catalysed system, various models for the base catalysed reaction have been suggested. Pohl and Osterholz [43] suggest a model in which the OH^- (from the dissociated water molecule) attaches to the silicon atom forming a pentavalent state, as

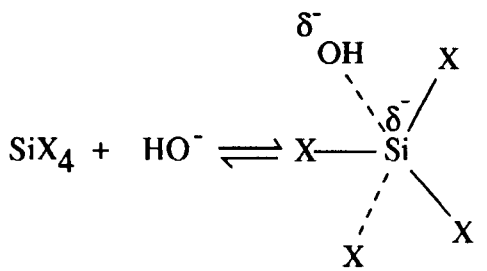

Figure 3.4. The Pohl - Osterholz mechanism for base catalysed hydrolysis, generation of the pentavalent state.

shown in Figure 3.4. A redistribution of charge around the pentavalent state then occurs, resulting in a formal negative charge appearing on the silicon atom. This state then rapidly decays to a second pentavalent transition state in which the formal negative charge is reduced by one of the X ligands accepting a partial negative charge, as in Figure 3.5. $X^{\delta-}$ then leaves the second transition state and combines with a proton from the water. This reaction mechanism is classified as an S_N2^{**}-Si [40] type, reflecting the creation of the pentacoordinated transition state. The rate of this reaction would be very sensitive to the inductive effects of the X and R groupings due to the development of the formal negative charge on the silicon atom. A second mechanism, also involving the production of a pentavalent transition state, was suggested by Schmidt et al [47] . This

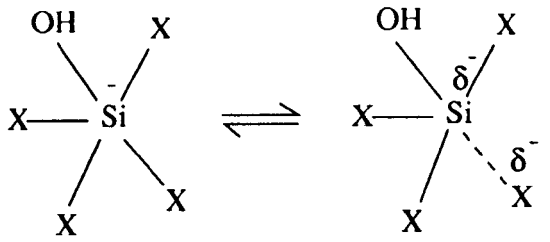

Figure 3.5. The redistribution of charge and the formation of the second pentavalent state in the Pohl - Osterholtz mechanism.

reaction is initiated by the attack on the silicon atom by OH^-, resulting in the creation of a pentavalent transition state as in Figure 3.6 (I). The water molecule attacks $X^{\delta-}$ electrophilically and associates with it, as in Figure 3.6 (II). This state then rapidly decays by elimination of the XH and OH^- molecules.

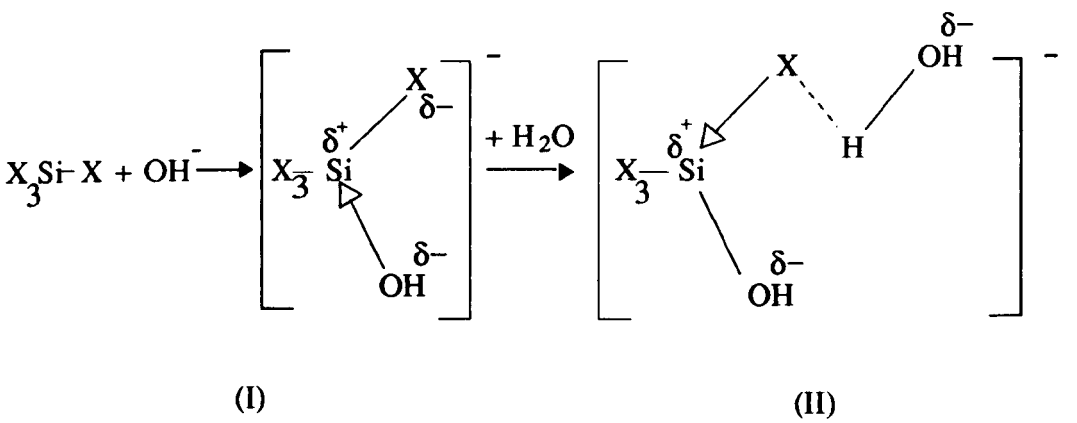

Figure 3.6. The Schmidt mechanism for base catalysed hydrolysis.

A mechanism has been suggested by Keefer [44] which suggests the direct substitution of the OR group by the hydroxyl without the creation of the intermediate pentacoord -inated transition state but does involve tetrahedral inversion.

Analogous to the acid catalysed hydrolysis mechanisms, all base catalysed mechanisms involve the generation of a transition state (here negative), and thus for the hydrolysis of alkoxysilanes, the rate of reaction increases with the degree of hydrolysis and vice versa for the reaction of chlorosilanes.

3.2.3 Condensation

Condensation reactions are those reactions involving the joining of two larger molecules with the subsequent elimination of a smaller molecule. In a large number of condensation reactions the ejected molecule is H_2O but, as will be seen later, these reactions do not result exclusively in the release of water.

For a condensation reaction to occur the 'monomeric' units from which the polymer is formed are required to have suitable reactive functional groups that are able to react with each other to create the siloxane bond. Condensation reactions may be classified as either homofunctional or heterofunctional, the former resulting from reaction between identical functional groups and the latter from reaction between different groups.

3.2.3.1 Homocondensation

The reaction between silanols (produced via the reaction of equation 8), is illustrated in equation 9. This forms the most common of the homocondensation reactions. In general it can be said that the rate of condensation increases with the number of silanols [40] and decreases with both the size [49] and number of substituent groups directly

$$\equiv Si-OH \quad HO-Si\equiv \rightleftharpoons \equiv Si-O-Si\equiv \quad + \quad H_2O \qquad (9.)$$

bonded to the silicon atom. No evidence for the reaction occurring spontaneously is observed but the formation of the siloxane bond proceeds very rapidly in the presence of small concentrations of catalyst [48] . Dehydrating agents such as H_2SO_4, P_2O_5, trifluoroacetic acid and many more [38] encourage the generation of the siloxane bond by the removal of the condensed water thus resulting in a shift in the equilibrium position of equation 9 to the right. As in the case of the hydrolysis reaction, the reaction is also catalysed by both acids and bases. The generally accepted mechanism for acid catalysed condensation is the nucleophilic attack on the silicon atom of a protonated silanol by a neutral silanol, as seen in Figure 3.7. [40] The initial first step of silanol protonation is observed to occur very rapidly [43], with the rate determining step of the reaction being the attack by the non-protonated silanol. The role of the protonated silanol in the reaction is suggested by the observation that the condensation rate increases below the isoelectric point of silica (≅ pH2) [40], in a region where silanols

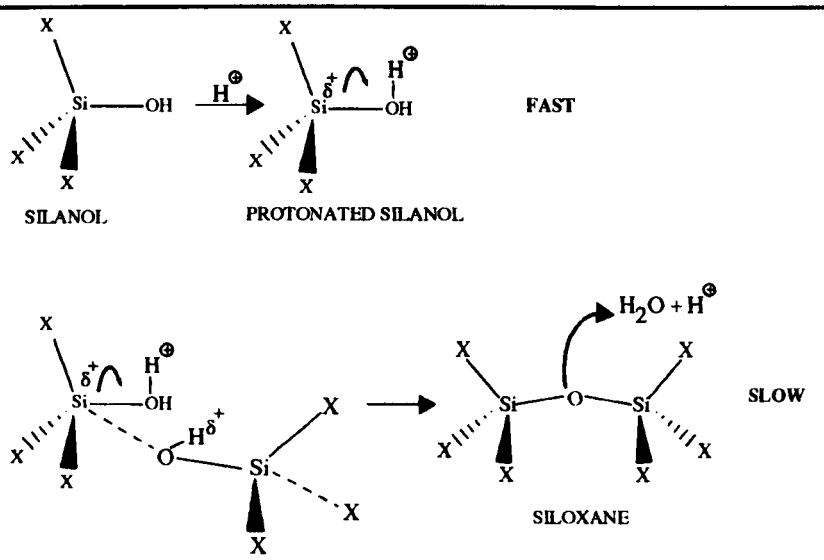

Figure 3.7. The acid catalysed condensation reaction mechanism.

would be expected to be protonated [40]. This mechanism is supported by Pohl and Osterholtz [43] but no specific information can be identified concerning the existence or type of transition state (S_N*2-Si, S_N**2-Si) involved in the reaction.

The base catalysed reaction occurs above the isoelectric point for silica where silanols would be expected to be deprotonated, depending upon the acidity of the silanol, which is in turn dependent upon the other substituents on the silicon atom. With this in mind, the mechanism of base catalysed condensation has been suggested by Brinker [40] to involve the nucleophilic attack on neutral silanols by siliconium - like deprotonated silanols ($\equiv$ Si O–), as given in equation 10. As the reaction is dependent upon both the concentration of neutral and deprotonated silanols its rate is found to be a maximum at around pH7 where the concentrations of the two species are at a maximum.

$$X_3SiOH + OH^- \longrightarrow X_3SiO^- + H_2O \qquad \textbf{FAST}$$
$$X_3SiO^- + X_3SiOH \longrightarrow X_3SiOSiX_3 + OH^- \qquad \textbf{SLOW} \qquad (10.)$$

As for the acid catalysed reaction, Pohl and Osterholtz [43] suggest a two stage mechanism with a rapid first stage involving the deprotonation of the silanol, and a second, slower, rate determining step, involving the deprotonated silanols attack on the neutral silanol. The rate of the deprotonation stage is determined by the acidity of the proton and thus the reaction is faster for silicon species that have already condensed to some degree. In other words, the greater the extent of inorganic cross - linking of a silanol species, the more likely is the silanol to take part in the condensation reaction.

Swain and coworkers [46] have proposed the involvement of transition states with silicon in a coordination state greater than 4, involving S_N^*2-Si or $S_N^{**}2$-Si type reactions.

Homocondensation reactions are not restricted to silanol condensation, alkoxy - alkoxy condensation is also possible although severe reaction conditions (high T, catalysts) [38] are required to achieve condensation.

3.2.3.2 Heterofunctional Condensation.

In a reacting system of hydrolysable silanes, depending on the relative rates of the hydrolysis and condensation reactions, it is not unlikely that conditions for heterofunctional condensation may exist. The most important of these, with respect to this study, is the alcohol producing condensation between a silanol and an alkoxy group, as given in equation 11. This reaction will be particularly relevant in systems

$$\equiv Si\text{-}OH + RO\text{-}Si\equiv \rightleftharpoons \underset{\text{SILOXANE}}{\equiv Si-O-Si\equiv} + \underset{\text{ALCOHOL}}{ROH} \qquad (11.)$$

involving sub - stoichiometric volumes of water and where the homocondensation rate is low, thus leading to a large population of both silanols and alkoxysilanes. If chlorosilane precursors are employed it would be necessary to isolate the silanol groups from the action of the HCl produced via equation 8 so as to discourage the homocondensation of the silanols.

It has been shown that, with the employment of an uncharged Lewis base such as triethylamine (Et_3N) in conjunction with a supernucleophile such as 4-dimethylaminopyridine (DMAP), promotion of the heterofunctional condensation reaction occurs at the expense of the homocondensation reaction and other side reactions (eg. disproportionation) [50]. These catalysts have been used by Rubinsztajn et al [50] for the heterofunctional condensation of chlorosilyl terminated siloxane oligomer. Cypryk et al [51] used identical catalysts for the condensation of acetoxysilyl terminated siloxane with oligomeric diols. Both authors report the same mechanism for these reactions. From kinetic studies they conclude that, with only the Lewis base used, the base forms an hydrogen bonded complex with the silanol terminated siloxane in a fast reversible step, as given in equation 12. This proton acceptance characteristic shows the base to be acting as a Brönsted base, creating the transition state (I). The nucleophilic powers of the oxygen atom in (I) are increased and this encourages it to attack the

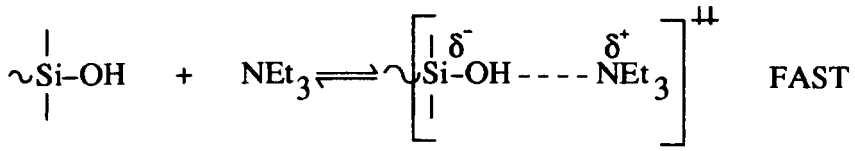

(12.)

(I)

silicon atom of a silyl functional siloxane, as in Figure 3.8. In the presence of the

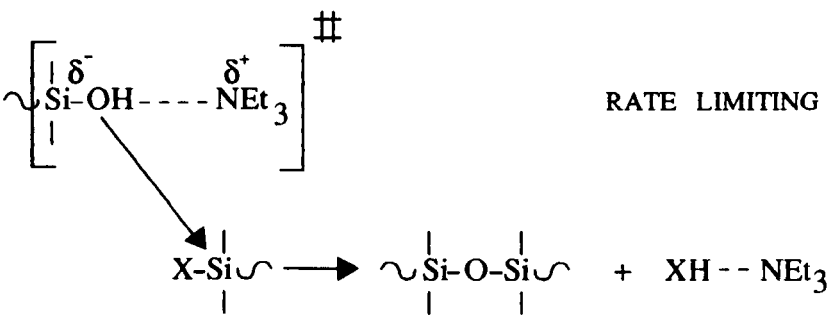

Figure 3.8. Action of uncharged Lewis base in heterocondensation - decay of transition state.

supernucleophile (DMAP), the catalytic properties of Et_3N can be ignored and it can be seen to act only as an acid acceptor. The role of the DMAP is most probably that of forming an ionic complex with the silyl functional siloxane, as in Figure 3.9.

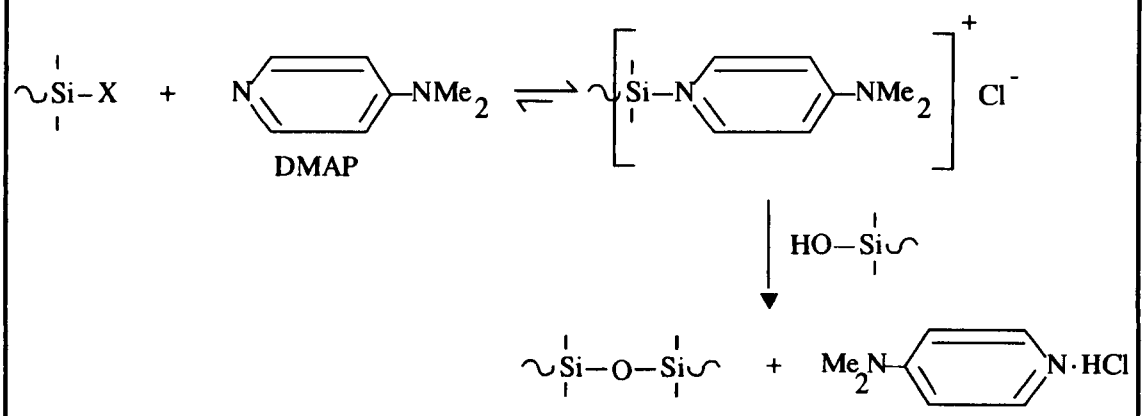

Figure 3.9. The role of a supernucleophile (DMAP) as an heterofunctional condensation catalyst (adapted from Rubinsztajn [50]).

3.2.4 Hydrolysis and Condensation of Difunctional Silanes: Species Prepared.

Initially, the monomeric silanes, whether they contain alkoxy or chloro groups, will hydrolyse to some degree to form reactive silanols (see equation 8). These, via either homofunctional condensation (equation 9) or heterofunctional condensation (equation 11) processes will undergo chain extension leading to the development of oligomeric (short) linear species. Depending on the thermodynamics of the system, a preparation of these will form cyclic species via the intramolecular condensation of the chain ends, as shown in Figure 3.10, where 'X' are condensible units. Non cyclizing oligomeric species will, providing that there is a supply of monomeric units, continue to grow. As the polymer grows there is a decrease in the probability that it will cyclize, simply as a result of the decreased probability that two chain ends on the same chain will meet.

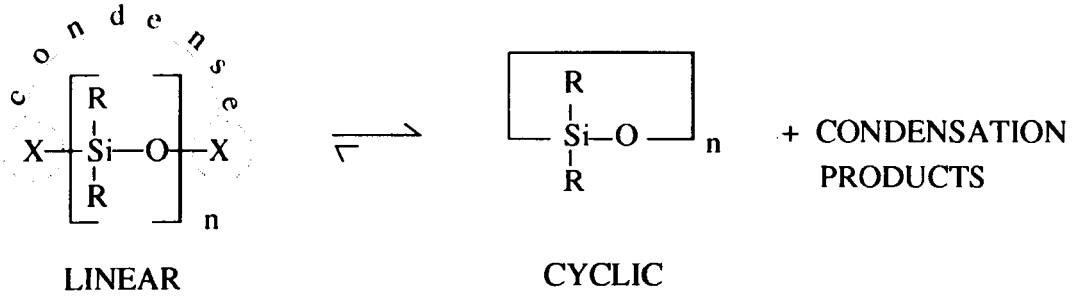

Figure 3.10. A schematic representation of the process of cyclisation.

Thus, at equilibrium, a condensed system can be thought of as two separate populations, the linears and the cyclics; these groups will be in thermal equilibrium with each other and also all species within each group will be in equilibrium with all other species of that group. The species prepared from a polycondensation reaction of this type will be strongly dependent upon the environment, in that the competition between the linear condensation and cyclisation reactions usually depends upon the reaction conditions such as pH, T, solvent type and monomer concentration. Fundamentally the competition is between the processes of intramolecular condensation (cyclisation) and intermolecular condensation (linear extension). Attempts have been made to model these reactions and to predict the molecular size distribution obtained from them. Flory [52] obtained relations for the weight fraction of linears in terms of the fraction of reacted end groups in an equilibrium system. The model is rather abstract from a real system since it assumes a completely linear system with each species in the system having equal reactivity regardless of length (whereas longer chain siloxanes are more stable than shorter ones). A more comprehensive theory was offered by Jacobson and Stockmeyer [53]. In this theory (the J-S theory), the coproduction of cyclics and linears proceeds from a monomer reservoir. The influence of the concentration of the

polymerising mass and that of the chain stiffness upon the molecular distribution is also considered. A limitation of this model is, as in the Flory model [52], that the reactivity of all species is considered equal, regardless of chain length. This is untrue for both linear and cyclic species, the stability of cyclic species being particularly dependent upon the ring size as has been previously shown [54,55]. The level of complexity of the Stockmeyer - Jacobson theory increases as the diversity of the monomer species expands. In particular, the inclusion of non - identical monomer species in the model leads to a very complex analysis which is only viable for certain limiting situations. Application of the J-S theory [53] to the condensation of α - ω - siloxane diols indicates that the equilibrium between open chains and cyclics, is given by equation 13. This suggests that the concentration of the total cyclic population is independent of the initial monomer concentration. A further consequence of this is that dilution of the

$$K_n \cong \left[\left[R_2SiO \right]_n \right]_{eq} \qquad (13.)$$

system would result in a lowering of the total yield of linear species and a concomitant increase in the cyclic yield so as to maintain the equality of equation 13. This would indicate a critical concentration, below which, no linear fraction exists. Jacobson and Stockmeyer presented the case of a condensing siloxane α - ω diol and developed a set of equations to describe both the linear and cyclic population distributions. The theory is rather involved and the reader should refer to reference 53 for the revelant details, although a number of important points may be stated. The linear and cyclic distributions, C_n and R_n, may be described by equations of the form of equation 14a and 14b respectively, where n is the number of units within the species and x is the

fraction of reacted end groups within the cyclic fraction. This suggests that chains are prepared up to much higher degrees of polymerisation than the cyclics, with the latter generally having number average degrees of polymerisations less than 4.

$$C_n = Ax^n \qquad A = \text{constant} \tag{14a.}$$

$$R_n = Cx^n\, n^{-5/2} \qquad C = \text{constant} \tag{14b.}$$

The yield of the linear polymer may be controlled by the addition of a non - reactive end stopper such as trimethylsiloxy. These prevent the subsequent intramolecular condensation of the chain from occurring, thus increasing its thermal and chemical stability. It can be assumed that the Flory distribution is still valid for end blocked materials as long the degree of polymerisation is high enough for the end groups to be insignificant relative to the chain. It is known that the driving force for the conversion of a cyclic species into a linear chain is the associated gain in conformational entropy [48]. For bulky substituents, the chain flexibility is reduced, thus, the gain in entropy is diminished and the linear is less likely to form.

Classically, intramolecular condensation is seen as first order with respect to the monomer, whereas, intermolecular condensation is second order with respect to the monomer. It has been indicated by Chojnowski [48] that, in certain solvent systems, assistance by a third functional group may result in second order kinetics for both processes. This effect is thought to occur via intra -inter catalysis, involving the third 'assisting group' catalysing both the intra and inter condensation processes, as seen in Figure 3.11. The mechanism of the assistance is acid - base in character. The silanol

group (being more basic than the chain [56]), withdraws H^+ from the OH^- group attached to the silicon atom. This leaves the oxygen with an increased nucleophilic character and thus more likely to attack the silicon atom of a second chain.

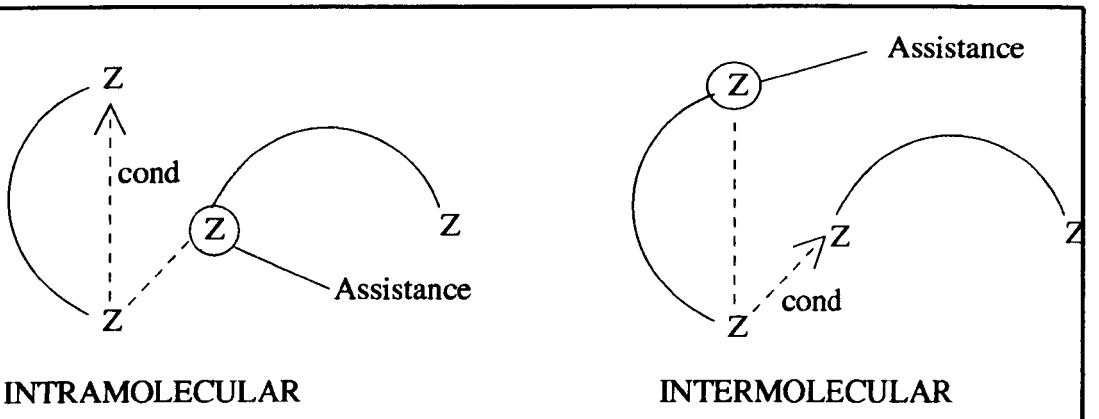

Figure 3.11. Intra - inter molecular catalysis.

The cyclics prepared via polycondensation reactions generally result in the preparation of low weight cyclics, with cyclics higher than the hexamer being in very low abundance [56]. The tetramer is often used in ring opening equilibriation reactions to prepare higher polymers. Equilibriation reactions are initiated with strong acids or bases, such as CF_3SO_3H, alkali metal complexes, sodium or potassium mirrors (2Na ,2K) etc [56] . Such ring opening reactions are thermodynamically controlled and as such, the populations are independent of the catalyst.

3.2.5 Polymerisation of inorganic network

For many applications the molecular weight of the species, both linear and cyclic, prepared by the hydrolysis and condensation of difunctional silanes is not sufficient. A further process, that of polymerisation, may be introduced into the preparation route. This enables the low molecular weight materials (having a low degree of

polymerisation) to be converted into high molecular weight materials (having a high degree of polymerisation). A number of significant advantages are achieved with this process. Firstly it affords a degree of control over the viscosity of the material which is desirable in many applications, particularly for employment as a glob topping material (see Chapter 1). Secondly, since the low molecular weight cyclic and linear materials are easily volatilised [36], their conversion into higher molecular weight molecules enhances the thermal tolerance of the material.

Polymerisation of siloxanes may be achieved both thermally and by the use of catalysts. Processes involving the thermal polymerisation of siloxanes are only operative under extreme conditions (200°C - 300°C / high pressure) [38]. Due to the required conditions, and the possibility of degradation of the organics, catalytic routes are generally preferred.

Catalytic polymerisation may be achieved both by acid (protic or Lewis) and by bases. For details concerning the reactions the reader is referred to the discussions by Noll [38] and Chojnowski [48], only important results will be discussed in this work.

Acid catalysed polymerization: is operative in the presence of protic acids, particularly H_2SO_4 [58] and CF_3SO_3H [59]. The action of Lewis acids is less clear but they are not thought to be as efficient as protic acids and in fact their inclusion as catalysts may be via their conversion into protic acids in the presence of protic contaminants.

Two different mechanisms have been proposed for the acid catalysed polymerisation of

siloxanes. The first, suggested by Patnode and Wilcock [58] suggests that the acid dissociates and adds across the siloxane bond as in equation 15, forming a linear

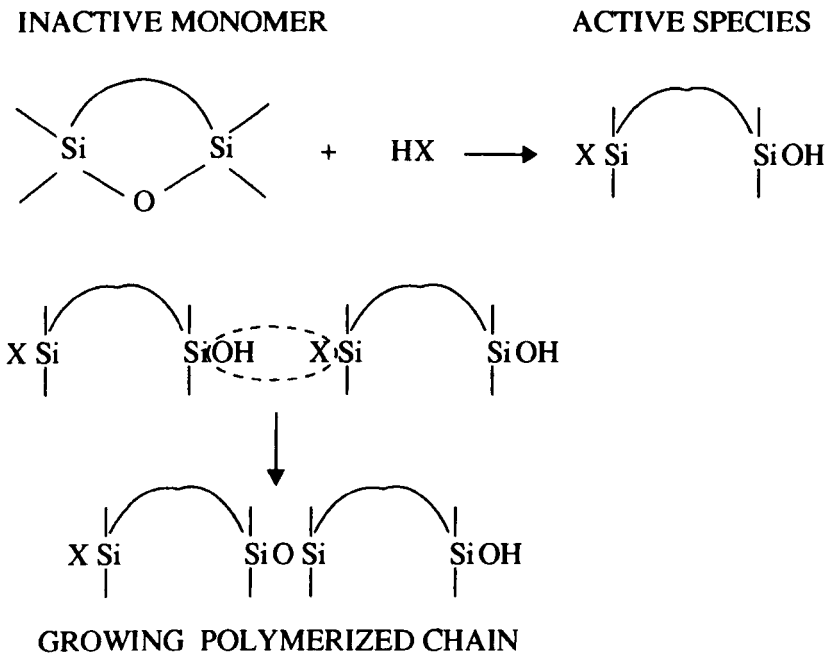

(15.)

species with reactive end species, which, upon subsequent condensation (heterofunctional), form the new siloxane bond. A second mechanism has been proposed by Andrianov and Yakushkina [60] in which active, 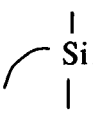 , groups add directly to a growing chain. The mechanisms operative in a real system are not known exactly but are thought to be a combination of the two mentioned above. A drawback of the acid catalysed reaction is the generation of a large number of cyclics with the number of units per ring being integer multiples of the inactive cyclic monomer [48].

***Base catalysed (anionic) polymerization*:** is usually achieved with alkali metal hydroxides. Initiation of the process involves the interaction of the siloxane bond of the monomer (cyclic or linear) with the catalyst leading to the formation of a silanolate end

group, $\equiv SiO^{-}Mt^{+}$, as in equation 16a. These then form the reactive species which, via interaction with further siloxane groups, lead to the propagation of the chain (equation 16b). Chain scrambling reactions may also occur (equation 16c) that do not in themselves introduce any further degree of polymerization.

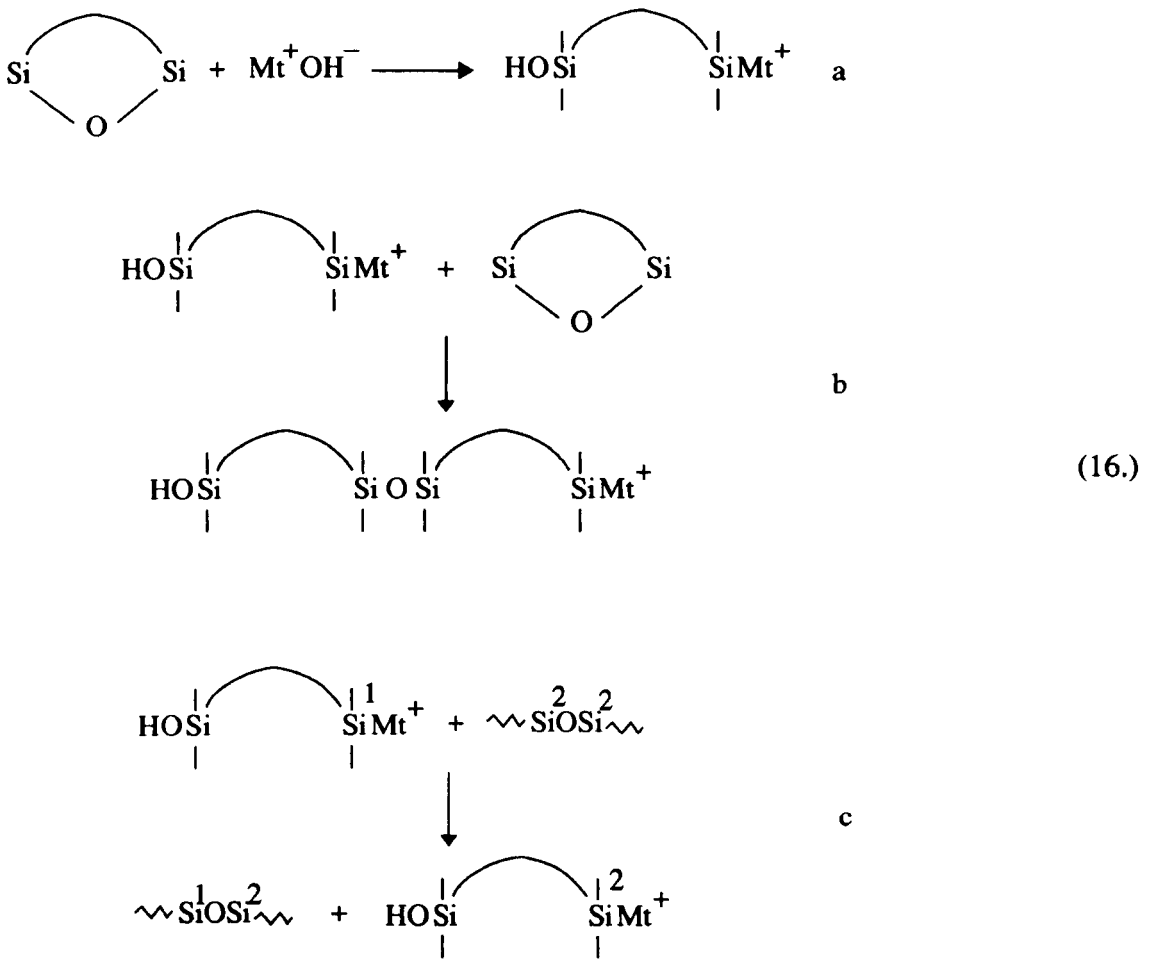

A number of interactions may occur both between the silanolate end groups and between the end groups and the siloxane bonds of the same chain. Both these interactions lead to a reduction in the degree of polymerisation of the polymer. The addition of a 'promoter' such as 2-methoxymethylether (diglyme) limits the degree of aggregation, thus maximising the yield of high polymer. Anionic polymerization is also very sensitive to water and alcohol contamination [38] . Both these are very effective at reducing the molecular weight of the polymer and should be excluded from the system.

3.3.1 Introduction to the organic network.

Previous sections have detailed the development of and growth of the inorganic component of polyorganosiloxanes (see sections 3.1, 3.2). The introduction of certain reactive organic groups, directly attached to the silicon atom, afford the opportunity to increase the connectivity of the polymer via extension of its organic component. Such 'extension' is achievable via cross - linking reactions that are well characterised in organic chemistry texts.

The intention of modification is primarily to obtain a useable rubbery or elastomeric coating, obtained with a level of organic modification that is sufficient to procure the desired level of mechanical resilience. An excess of organic modification is in general to be avoided as this would compromise the advantageous properties associated with the inorganic component (good thermal tolerance and dielectric properties). Due to the well known β effect [61] , for an organic functionality to maintain its 'normal' organic nature it must be attached to at least the carbon γ to the silicon atom. As this would result in a large degree of organic modification, the chemistry utilised in the development of the organic network in polysiloxanes is an adaptation of normal organic chemistry.

3.3.2 Peroxide induced free radical reactions.

The initiating species for such reactions are free radicals, created by the homolysis of a peroxide material (containing a weak -OO- bond). The radicals are short lived, highly

reactive species with unpaired electrons [62]. Their interaction with saturated or unsaturated C-C bonds results in bond cleavage. The first of such reactions was employed for polydimethylsiloxane (PDMS) with a diaryloxy peroxide (benzoyl peroxide) in large concentrations [63], with the cross - linking mechanism being hydrogen extraction from the CH_3, as indicated below in equation 17. The maximum efficiency of this reaction is only one cross - link per molecule of peroxide and in real systems it is generally a lot

$$\begin{aligned} &ArOOAr \xrightarrow{\Delta T} 2Ar\dot{O} \\ &\equiv Si-CH_3 + Ar\dot{O} \longrightarrow \equiv Si-\dot{C}H_2 + HOAr \\ &\equiv Si-\dot{C}H_2 + \dot{C}H_2-Si\equiv \longrightarrow \equiv Si-CH_2CH_2-Si\equiv \end{aligned} \qquad (17.)$$

lower [63,64] due to initiator side reactions [63] and the low probability that the $\bullet CH_2$ radicals will be in a position to unite, particularly in a viscous system [64].

A system more suited to peroxide cross - linking is one with a small amount of vinyl substitution. The process becomes a chain reaction and is thus more efficient, with efficiencies (number of cross - links per peroxide molecule) in excess of 100% [65]. The most likely reaction is that proposed by Bork and Rousch [66] as given in equation 18.

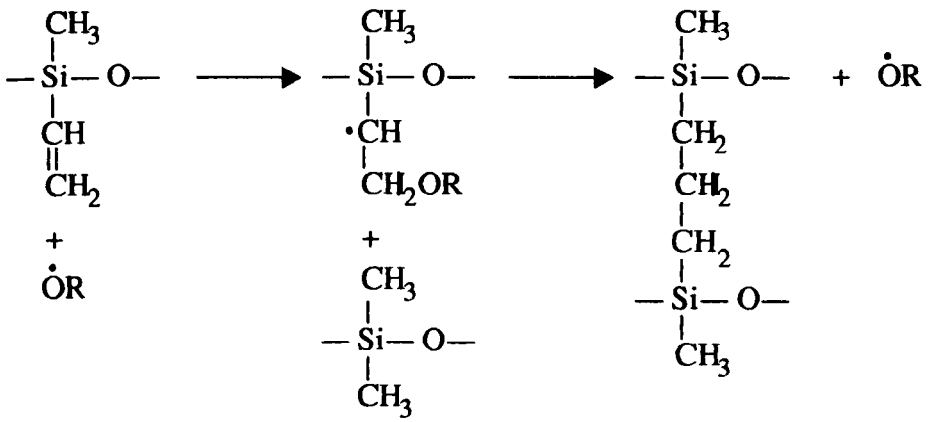

(18.)

3.3.3 Photo - initiated hydrosilylation reaction.

The platinum catalysed cross - linking reaction between a vinyl and a hydro group pendant to a silicon atom is well known, this reaction is also observed with exposure to UV radiation. The cure rates are slow for the systems solely cured with UV exposure but when used in conjunction with Pt catalysts, utilising the heat from the UV source, appreciably faster cure rates are obtained.

3.3.4 Acrylate polymerised systems.

Cross - linking of the polysiloxane system is achieved by UV irradiation of a blend of multi-acrylate functional species (diluents) such as ethoxylated pentacrylthritol tetraacrylate (PPTTA) with acrylate functional siloxane species. The choice of diluent is carefully considered so as to obtain a low viscosity system, allowing thorough mixing of initiator and complete reaction. Initiation of the photopolymerisation has generally been effected using benzophenone or diethoxyacetophenone. Recent work by Burrows [66], in which a range of initiators and diluents have been assessed for the curing of polyorganosiloxane glob top material, has found that, to obtain a through cure using the above initiators, a high loading of initiator is required. Two systems were developed employing a low level of initiator, of a type other than those mentioned above, whilst maintaining a suitable through cure.

3.4 Multicomponent Polymers: Interpenetrating Networks (IPNs).

One of the fastest growing segments of polymer technology is the development of multicomponent polymer materials. This has been driven by the ever increasing

demand for materials possessing properties superior to the parent polymers. The technology covering multicomponent polymer systems encompasses polymer blends, in which the components rely solely on physical mixing to form the material, graft and block polymers, where the polymer components are covalently bonded together and interpenetrating network materials (IPNs), where one or both of the polymer components are cross - linked into a network. Of these three techniques, only the IPN is of relevance to this study although the reader is referred to the texts [68] and [69, 70, 71, 72] for details of polymer blend and graft / block copolymer technologies respectively.

An IPN material is defined as a two component system in which one or both of the phases is cross - linked and in which there exists the opportunity for the phases to become mutually entangled. Nomenclature of IPNs is usually of the form cross-(POLYMER 1) - inter - cross-(POLYMER 2) or, more simply POLYMER 1 / POLYMER 2. IPN materials may be subdivided according to the method of preparation. IPNs may be made sequentially or simultaneously. In the former case, component A is formed and cross - linked into a network. The monomer of component B then infiltrates the network and is either cross - linked (to make the full IPN) or is left linear (to form a semi IPN). Simultaneous preparation of the two polymers, using different polymerisation chemistries for each phase, followed by cross - linking of one or both of the prepared polymers also permits preparation of both full and semi IPNs.

Work on homo IPNs, where both phases have the same chemical structure, has mostly been restricted to polyethylene - polyethylene (PE / PE) systems [74, 75, 76]. Research has mainly concentrated on hetero IPNs where the components have different chemical

structures. A large number of polymer pairs have been investigated and many have realised commercial success, particularly those of EPDM/PP (EPDM is a polypropylene (PP) / polyethylene / ethylene - propene - diene monomer), rubber - PE and acrylic - urethane - polystyrene [75].

The incorporation of siloxane as a component in organic - inorganic (O-I) IPN materials has also received much attention and has resulted in the development of a number of thermoplastic materials. A moulding / extrusion grade silicone - aromatic polyester urethane IPN is commercially available as Rimplast© produced by Petrarche Systems, this incorporates 10% silicone with either aliphatic urethane, nylon 12 or nylon 6/6 [77]. Siloxane has either been incorporated directly into the IPN as one of the components or has been used to modify one of the organic components. In the former case the siloxane system generally used is polydimethylsiloxane (PDMS) and has been employed in conjunction with a host of organic materials including polyimide [78] , EPDM [79], polymethylmethacrylate [80 , 81], poly(2,6 - dimethyl,11,4 phenylene oxide [81] and PTFE [82]. Tetrafunctional siloxane species have also been employed to form the inorganic network [84]. In the latter case of siloxane modified organic polymers, modification of epoxy - urethane - acrylic [85], urethane [86] and polyimide [87] have been investigated.

Research into homo IPN of type cross -siloxane - inter - cross- siloxane has been very limited. Hamurcu and Baysal [89] have investigated the mechanical properties of full IPNs prepared from the catalysed condensation of α -ω polydimethyldiols. The prepared IPNs were composed of a short chain network and a long chain network with interpentration between the two. It was found that the mechanical properties were

governed by the long chain network. Kang et al [89] investigated poly(1 - trimethylsilyl - 1 -propyne) (PTMSP) / PDMS IPNs for application as semi - permeable membranes.

CHAPTER4: EXPERIMENTAL METHODS - THEORY AND PRACTICE

4.1 Structure analytical techniques

4.1.1 Nuclear Magnetic resonance (NMR)

4.1.1.1 General Introduction

In the following discussion a basic knowledge of the fundamentals of NMR is assumed. A good introduction to the theory of NMR can be found in Harris [89]. NMR was first used experimentally in 1945 by Purcell , Torrey and Pound [89] , and, in the same year, by Bloch, Hansen and Packard [90]. Since then the technique has grown into possibly the most valuable spectroscopic tool for obtaining detailed information on chemical structure at the molecular level.

In this study, NMR of both the ^{13}C and ^{29}Si nuclei has been employed. Both these are spin ½ nuclei and thus are not subject to any quadrupolar interactions. ^{13}C has a higher sensitivity than ^{29}Si for equal numbers of nuclei but silicon's greater natural abundance of 4.70% [93] (relative to ^{1}H), compared to 1.11% [93] for ^{13}C results in silicon being twice as sensitive as carbon, although, relative to ^{1}H they only have receptivities of 3.69×10^{-4} and 1.76×10^{-4} respectively [95]. Despite these low receptivities, usable spectra for both nuclei are easily obtained using Fourier transform (FT) NMR techniques. Since the techniques employed to obtain the spectra are very dependent upon the nature of the sample, particularly on its viscosity (and associated degree of cross - linking), crystallinity etc, the method used will be discussed separately for each class of sample and for each nucleus.

4.1.1.2 Solution NMR Techniques

Due to the isotropic tumbling of the molecules within a good solution, ie, one in which the molecules are well separated, with little interaction between them, spatially dependent effects such as the chemical shift anisotropy [95] and dipole - dipole coupling [95] will be averaged to zero. Thus, all samples, regardless of the nucleus under scrutiny, were prepared as dilute solutions in $CDCl_3$. The deuterated solvent also provided a ^2H signal for field / frequency locking purposes. In all cases a small volume of tetramethylsilane (TMS) was added so as to provide an internal reference. All samples were placed in 10mm outside diameter tubes, filled to approximately 30mm and sealed. These were rotated at approximately 30Hz to ensure proper mixing and adequate molecular motion, and to average inhomogeneities of the magnetic field.

To avoid the complications of scalar J coupling [90, 96] the spectra were obtained under proton decoupled conditions [90]. Under these conditions, nuclear Overhauser enhancement (NOE) [97] occurs for both the ^{13}C and ^{29}Si spectra. For ^{13}C, positively enhanced signal intensities would be observed, with the level of enhancement being dependent upon both the balance between the various relaxation mechanisms operative [97] and on the number of directly attached protons [97]. In the case of ^{29}Si the NOE results in a negative enhancement and , more seriously, a possibility of a null signal occurrence (zero signal intensity). To eliminate these deleterious effects all spectra, unless otherwise stated, were run under inverse gated proton decoupled conditions [98], allowing proton decoupled, non NOE enhanced, spectra to be obtained. All solution spectra were run on a 400MHz Bruker spectrometer with $^{13}C\{^1H\}$ spectra being obtained at 100.614MHz and $^{29}Si\{^1H\}$ spectra being obtained at 79.495 MHz. A

relaxation delay of 10 seconds was used for both the ^{13}C and ^{29}Si experiments as this was found to be sufficient to prevent signal saturation. In a number of spectra $Fe(acac)_3$ was employed in a 0.03M concentration as a shiftless paramagnetic relaxation agent. The $Fe(acac)_3$, a powder at room temperature, was readily dissolved in the solution. The number of free induction decays (FIDs) required to obtain a suitable signal to noise ratio (S/N) varied depending on the sample type, specifically its chemical composition and its viscosity. For ^{13}C , spectra were obtained with between 100 and 1000 FIDs, the range for ^{29}Si being larger, with between 100 and 6000 FIDs collected.

An investigation was performed into the possible effect of the solvent used on the chemical shift positions of a simple siloxane. For this study, two samples were prepared. One sample was prepared for NMR using the usual technique, dissolved only in $CDCl_3$ (30% v/v). The second sample was solvated in a mixture of 5% C_6D_{12}, 25% C_6H_{12} (v/v). The $^{29}Si\{^1H\}$ spectra were obtained in the usual manner.

4.1.1.3 Solid State NMR Techniques.

All solid state NMR was performed on a Bruker 360MHz MSL spectrometer with ^{13}C spectra being obtained at 90.555MHz and ^{29}Si spectra being obtained at 71.535MHz. All experiments utilized magic angle spinning (MAS) [98] so as to eliminate dipolar broadening. The samples were spun at rates of between 3.3 and 3.6kHz using a Bruker double bearing probe Z 33.6 DR MAS. 7DB (^{13}C) and HP WB73A MAS. 7DB (^{29}Si). Referencing in all cases was made to TMS, the signal reference (SR) being obtained from a sample of TMS spun at approximately 1kHz (to obtain proper mixing) using 2-3 thousand FIDs (collected using a 1 second pulse delay).

The ^{13}C samples were packed into zirconia (ZrO_2) rotors and the ^{29}Si samples were packed into either ZrO_2 or silicon nitride (Si_3N_4) rotors, both were sealed with either kel-F (ambient temperature) or Delrin (high temperature) caps. Care has to be taken to avoid including resonances in the spectra from extraneous sources, in particular, ^{13}C resonances from the polymeric caps. Kel - F (poly(chlorotrifluoroethylene)) is transparent in ^{13}C spectra due the a strong C-F spin coupling resulting in a very broad resonance [100]. Delrin (polyoxymethylene) on the other hand has a strong resonance at 89ppm [10]. The method of rotor packing depends greatly on the nature of the sample.

Sample preparation for solid state NMR - general

All solid samples were obtained by thermally heating the siloxanes in air on PTFE sheets, the samples prepared and the cure conditions used are given in Table 4.1. Depending on the level of 'cure' received and on the composition of the polymer, the samples obtained are, at room temperature (RT), either below T_g and brittle in nature or above T_g and elastomeric. The high T_g materials were prepared into a powder by crushing at RT using a pestle and mortar, followed by packing of the rotor, also at RT. The method of preparation for the low T_g materials varied from sample to sample depending on the level of cure of the material. Highly elastomeric materials were powdered under liquid N_2 and packed at room temperature whereas materials with a very low degree of cure, and thus 'sticky' to the touch, were both powdered and packed under liquid N_2 . All samples above T_g were difficult to spin due to the 'powder' having poor flow properties at RT.

The possibility of in situ curing of the siloxanes was assessed as this would have a

Sample	Composition	Cure temp °C / time hrs
80D'20T/1	80mol% DCMVS:20mol% MTMOS	200/2
80D'20T/2	" "	220/2
80D20T/1	80mol% DCDMS:20mol% MTMOS	220/4
100D'/1	100mol% DCMVS	200/4
100D'/2	"	200/8
100D'/3	"	220/4
100D/1	100mol% DCDMS	200/4
100D/2	"	240/4
IPN9010D'D	SHORT CHAIN PHASE	
	15mol% DCMVS:75mol% DCDMS: 10mol% MTMOS	
	LONG CHAIN PHASE	200/24 + 220/2
	81mol% DCMVS:9DCDMS: 10mol% MTMOS	
	SCP:LCP 1:1	

DCDMS= dichlorodimethylsilane DCMVS= dichloromethylvinylsilane

DCDPS = dichlorodiphenylsilane MTMOS = methyltrimethoxysilane

Table 4.1. Preparation conditions for the ^{13}C Cross - polarisation (CP) MAS NMR

number of possible advantages over powder samples, namely, a higher packing density, resulting in a stronger signal intensity and the rotors may have been easier to spin. All in situ cured materials were heated in ZrO_2 rotors. The test material had a composition of 32.5 $-(C_6H_5)_2SiO-$: 65.0 $-(CHCH_2)(CH_3)SiO-$: 2.5 SiO_2. Samples were prepared using two different techniques:

i) Heating the siloxane in air at a) 200°C with controlled ramp rate of 60°C hr^{-1} heating, 30°C hr^{-1} cooling with a 3hr dwell and b) 180°C with a ramp rates of 10°C hr^{-1} on both heating and cooling.

ii) Heating the siloxane under vacuum. This was achieved by placing the siloxane filled zirconia rotor in a holder made from refractory material. This was then inserted into a silica tube, sealed at the one end. The open end was fed to a vacuum pump (maximum vacuum of 20kPa). Heating was achieved by inserting the silica tube into a top loading Heraeus furnace. A number of heating profiles were employed, as given in Table 4.2.

Heating rate °C hr^{-1}	Dwell temperature °C / time hrs	Cooling rate °C hr^{-1}
30	180/4	10
60	180/5	60
120	190/4	60
120	170/4	60
10	190/5	60

Table 4.2. The heating profiles employed for the in situ, NMR samples cured under vacuum.

Neither of the above methods (i and ii) were successful in preparing solid samples suitable for MAS. The principal problems were i) the entrapment of gas bubbles within the samples, thus destabling the rotor, and ii) the development of a cure gradient through the length of the sample.

Cross - polarization (CP) MAS NMR of ^{13}C

A requirement to obtain quantitative ^{13}C NMR under normal conditions is that the relaxation delay is greater than $5T_1$ [100], where T_1 is the spin - lattice relaxation time, which for ^{13}C is usually of the order of 1 - 30 seconds. Thus, to obtain a reasonable number of FIDs, and hence a good S/N ratio, excessively long experimental times are required . This problem is circumvented by the employment of cross - polarization [98, 99,102]. CP is a double resonance experiment whereby the ^{13}C obtains its magnetisation from the protons, thus dramatically increasing its signal intensity and also, since the relaxation of the ^{13}C is determined by that of the protons, high pulse repetition rates are possible. A schematic of the CP pulse sequence is given in Figure 4.1. During the period τ_c it is necessary to match the precessional rates of ^{13}C and ^{1}H. This implies that the Hartmann - Hahn condition (equation 19) is satisfied. This was achieved practically by setting the low power ^{13}C transmitter to a predetermined power level and adjustment of the high power ^{1}H transmitter power level until match was reached. Indication of the degree of match is given by performing a 'set up' experiment

$$\gamma_H H_{1H} = \gamma_C H_{1C} \qquad (19.)$$

using adamantane $C_{10}H_{16}$ and adjustment to provide maximum signal intensity. To ensure that no resonances were being suppressed due to too short a τ_c (resulting in an incomplete polarization transfer) spectra were obtained for a range of τ_c (1 - 10μs). All spectra were obtained with a pulse delay of 1 - 2 seconds. The number of acquisitions required for each spectrum varied depending on the sample type, with most spectra requiring 1K - 30K FIDs, with up to 60K FIDs required in certain cases to obtain a

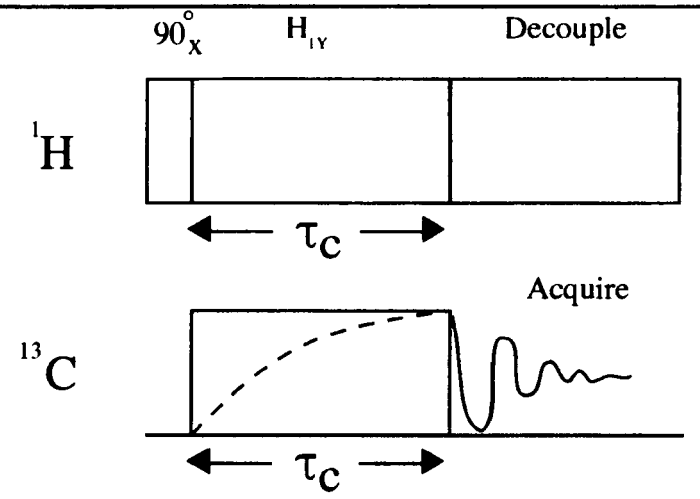

Figure 4.1. The pulse program used to perform ^{13}C cross - polarization MAS NMR.

suitable S/N ratio.

***Variable temperature ^{13}C CP MAS NMR*:**

Variable temperature ^{13}C CP MAS NMR was performed on a sample of 80D'20T/3 (see Table 4.1. for composition and cure conditions). Samples were run in a zirconia rotor, sealed with a Delrin cap. The standard Z 33.6 DR MAS 7DB probe was used. Heating was supplied via a Bruker variable temperature unit which allowed direct heating of the stator. The CP condition was set up using the standard method discussed in the previous section. Broad band dipolar decoupling was applied during acquisition. All spectra were obtained using a pulse repetition rate of 1Hz and a τ_c of 10ms and a pulse width of 1μs. Spectra were obtained within the temperature range 295K to 400K. After each temperature adjustment the sample was allowed to equilibrate for 20 minutes prior to acquisition. Also, due to the changing air density around the rotor it was necessary to adjust the spin speed to maintain a rate of 3.6kHz.

Proton coupled spectra:

Proton coupled ^{13}C solid state NMR spectra were obtained for siloxane with the composition 100D'. Samples were prepared for analysis by heating to a solid at 200°C for 4 hrs in air and then prepared as a powder by powdering under liquid N_2 (see previous section). The standard NMR conditions as discussed above were employed. This sample was employed under proton decoupled conditions using pulse parameters as those used for a CP MAS NMR (see next section) study of the sample . Spectra were collected using a pulse repetition rate of 500ms and a pulse width of 1μs. 100Hz line broadening was applied to the spectrum to obtain an identifiable signal. A spectrum of this sample was also obtained under normal dipolar - proton decoupled conditions, again using a 500ms pulse repetition rate and a 1μs pulse width.

***Spectral editing of ^{13}C polymeric material MAS NMR*:**

Techniques that allow spectral editing of ^{13}C nuclei in rigid solids are not widely available. Dipolar dephasing [103] is commonly applied to solids to distinguish between quarternary and methyl carbon species. Many techniques have been developed based on the C-H heteronuclear J - coupling although these are only effective for elastomeric materials with high mobility [103]. Cross - polarization - depolarization (CPD) has been applied to rigid solids with considerable success [104, 105] although this technique is very sensitive to the accuracy of the Hartmann - Hahn match and requires calibration of the field strengths [103, 105]. Wu and Zilm [106] suggest a simple method by which completely edited spectra of CH and CH_2 are obtained using a slightly modified CP pulse program. The polarization inversion pulse program is given in Figure 4.2. The simultaneous inversion of the polarisation of the nuclei after the normal CP contact

time allows separation of the CH and CH_2 resonances. The period $\tau_{PI1}+\tau_{PI2}$ was varied between 1μs and 700μs. The CP match condition was set up in the usual manner.

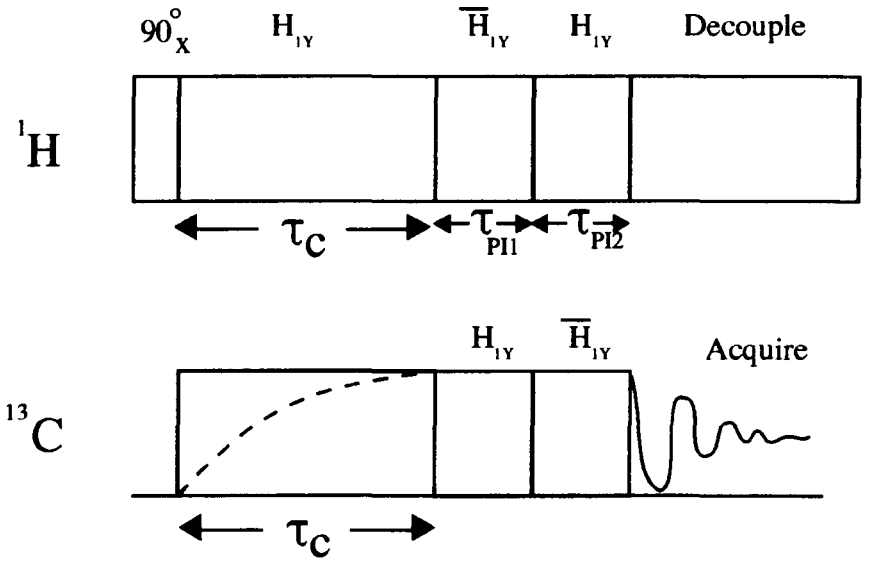

Figure 4.2. The pulse program for ^{13}C polarization inversion CP (CPPI).

4.1.2. Infrared Spectroscopy

All IR spectra were obtained using a Perkin Elmer 983 double beam dispersive infrared spectrophotometer with a wavenumber range of 180 - 4000cm^{-1} (55.6μm - 2.5μm.) All spectra were recorded at room temperature.

***Solution sample analysis*:**

The liquid samples were contained in a cell consisting of two AgCl plates held within a PTFE case. Rubber 'o' rings formed a seal between the plates and the case. AgCl is transparent to IR over the range used and thus does not contribute to the spectra. Unless otherwise stated, all spectra were obtained with a resolution of 11.5cm^{-1}. Prior to measurement, the AgCl plates were thoroughly cleaned in isopropylalcohol (IPA). To prepare the samples a small volume of sample was placed between the plates which were placed together to form a thin film of sample trapped between them. The plates

were then inserted into the PTFE case which was hand tightened. After placing the sample into the sample beam of the spectrometer the transmitted intensity was observed. If the intensity was less than 10% at 4000cm^{-1} then the cell was removed and some of the sample was removed. The procedure was then repeated until the transmitted intensity at 4000cm^{-1} exceeded 10%. This procedure was necessary to ensure that less than 100% absorption occurred.

***Solid sample analysis*:**

Attenuated total reflection IR spectroscopy was used to obtain IR spectra of solid samples. The technique relies on total internal reflection. The degree to which this occurs at an interface between high and low refractive index materials depends on the difference in refractive index of the former material. Thus, a low refractive index sample material coating a high refractive index material, when absorbing, causes a change in the intensity of the light internally reflected and thus the absorption is recorded. In practice, the high refractive index material was a KRS-5 thallium doped iodide / bromide crystal from Graseby - Specac Ltd. The samples were crushed to a fine powder and applied to both faces of the crystal (see Figure 4.3) which was previously cleaned in IPA. The crystal was held within a metal holder which also allowed pressure to be applied to plates placed over the crystal faces, used to keep the sample in optical contact with the crystal. The sample holder was mounted on a Perkin Elmer TR - 9 total reflection unit, which was subsequently placed in the sample beam of the spectrometer. Due to the attenuation of the sample beam it was necessary to place an attenuator in the reference beam. Before each experiment three independent adjustments were necessary; the orientation of the two mirrors and that of the crystal (see figure 4.3). Adjustment of

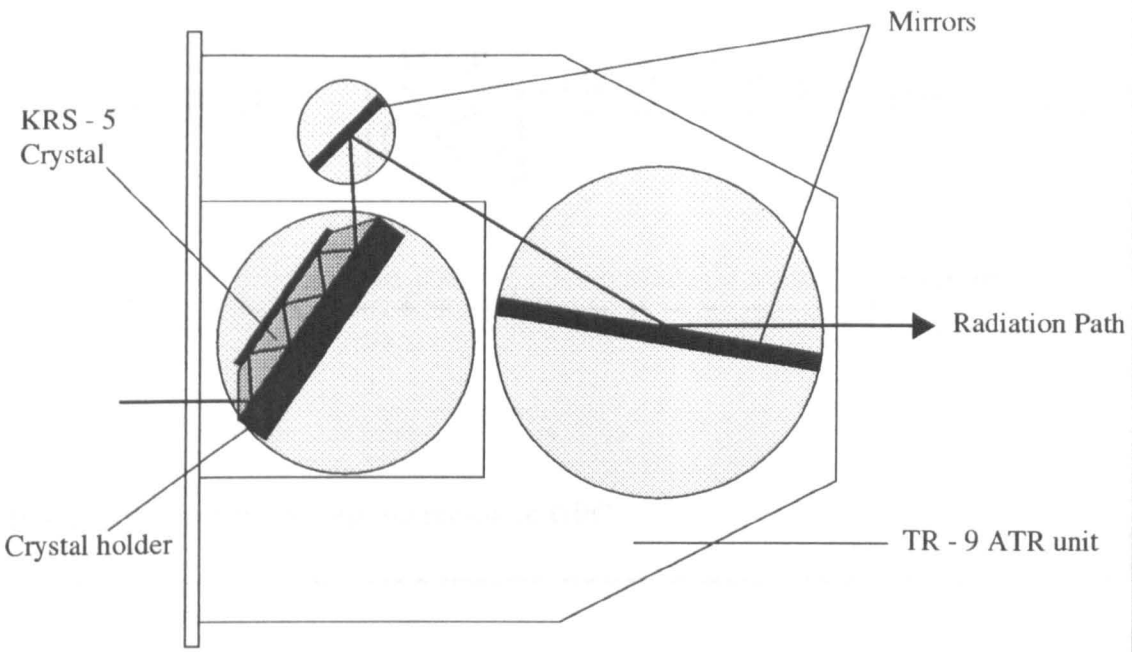

Figure 4.3. The ATR unit with KRS-5 crystal, for IR analysis of solid materials.

the attenuator to obtain less than 100% absorption at 300cm^{-1} was required to maintain the spectra within the transmission range of the spectrometer.

4.1.3 Gel Permeation Chromatography.

The technique: Gel permeation chromatography (GPC) is a size exclusion chromatographic technique whereby the sample, having an unknown molecular size distribution, is prepared in a solvent solution and passed through a column containing a separating medium, and is thus separated out. The separating column used was a polystyrene sphere packed 'mixed E-gel' from Polymer Labs Ltd, this separates the molecules by entrapping smaller molecules inside the spheres whilst letting the larger molecules pass through. The GPC apparatus is shown diagramatically in Figure 4.4. The samples were prepared for GPC by diluting a few drops with approximately 5ml of tetrahydrofuran (THF). The THF was doped with 0.1molar toluene to allow monitoring

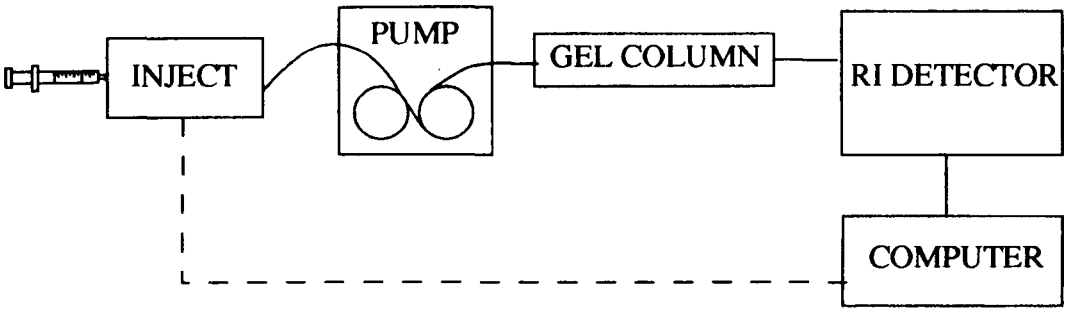

Figure 4.4. A schematic representation of GPC.

of the solvent stream flow rate. The mobile phase was pumped at a pressure of 100MPa and at a rate of 1 ml min^{-1}. Detection of the sample elution was accomplished via an ICI LC1240RI detector which detects the refractive index change of the solvent stream. The gel columns have an upper useable mass limit, above which all the species, regardless of size, are eluted together. Two GPC systems were available, one suitable for low mass and one for high mass samples. The choice of system used for each sample was made to allow optimum resolution without exceeding the upper limit. The GPCs were routinely used to separate polymethylmethacrylates (PMMA) and thus they were calibrated using narrow PMMA standards. Since the calibration was not universal it was necessary to calibrate the systems using appropriate siloxane materials. Four materials were used, three linear α, ω - polydimethylsiloxanes with number average molecular masses of 770, 5970 and 17250 and one cyclic compound, octaphenyltetrasiloxane, Mn = 793. The three former were obtained from ACBR and the latter was obtained from Aldrich Chemical Co Inc. Molecular weights were obtained from the calibration curves but obtaining molecular weight averages required

a more involved process which is described in Appendix II.

4.2 Mechanical techniques

4.2.1 Young modulus determination

The Youngs modulus of a material ,Y, is defined in equation 20, where F is the

$$Y = \frac{\text{STRESS}}{\text{STRAIN}} = \frac{F/A}{\Delta l / lo} \qquad (20.)$$

applied tensile force, A is the cross - sectional area of the test sample, Δl is the resulting extension and lo is the original sample length. Thus, in practice, to obtain Y, a constantly increasing extension is applied to the sample and the resulting force is measured. Y is obtained from the gradient of the linear section of the stress - strain plot.

Sample preparation:

A PTFE mould was manufactured having the dimensions as in Figure 4.5. The design of the mould was developed following a number of preliminary designs. a problem was found that upon cooling, the ends of the samples were prone to being ripped off due to the mismatch in the temperature coefficient of expansion between the PTFE ($174MK^{-1}$ (25 - 250°C)) [108] and the siloxanes (>200 MK^{-1}). The final design employed smooth radii at the transition point between the spade ends and the central linear area.

The mould was held flat onto a sturdy stainless steel plate via bolts passed through the mounting holes. This was necessary to prevent the substrate from warping at the cure temperature. The metal plate was designed for it to be possible to level it in the curing

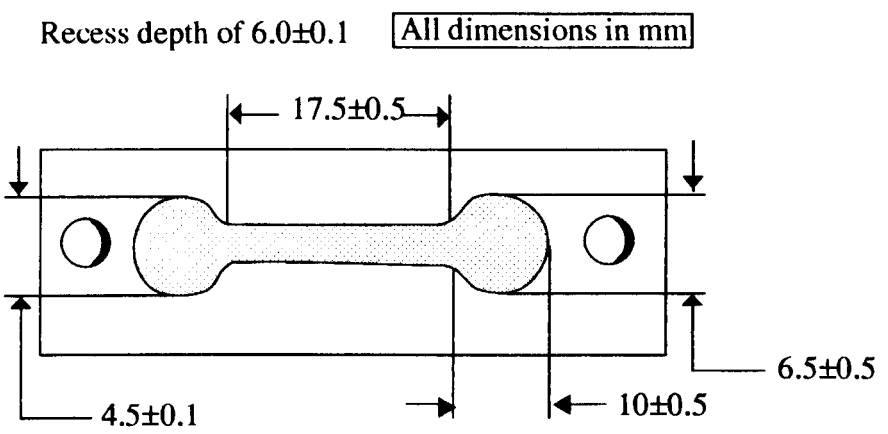

Figure 4.5. Geometry of the PTFE mould used to produce the tensile test samples.

oven.

***Testing procedure*:**

Due to the small size of the samples it was necessary to manufacture a pair of jaws with which to grip the samples. Abrasive emery cloth was bonded to the inside of the jaws to afford better grip. Tensile testing was performed on a JJ T22K tensile testing apparatus using a 100N load cell with a measuring range of 1-100N FSD. The method of sample clamping was dependent upon the material characteristics. Highly cured, brittle materials, were clamped directly into the jaws, taking care to maintain the two jaws parallel so as to not pinch the sample. For testing of more fragile, elastomeric materials, it was necessary to bond aluminium lead tabs to the samples using a cyanoacrylate adhesive. The tabs were constructed so as to allow the tensile force to be pulled through the centre of the sample and not to exert a couple on it. All samples were pull tested using a cross - head speed of 1mm min^{-1}.

4.2.2 Adhesion testing

4.2.2.1 Lap shear test

The lap shear test is commonly used as a test for the bonding strength of adhesives. The principle of the test is to strain a single or double lap joint (see Figure 4.6) until rupture

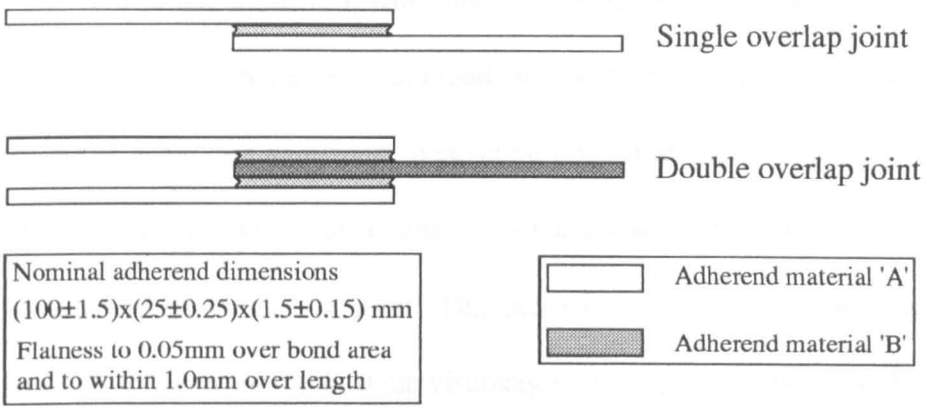

Figure 4.6. The lap shear test, sample geometry.

of the adhesive - adherend bond occurs. The breaking load, for a particular adhesive, is a function of the dimensions of the bond area (although not simply related) and is also dependent upon a host of other parameters, such as the bond line thickness, the rate of change of the applied force and the properties of the adherend. To obtain reproducible results, referral to BS 5350, part C5, 1976 [109], is often made. This offers a standardised test procedure with the above parameters defined.

Adherends suggested in BS5350 were either metallic (aluminium coated aluminium alloy (BS 1152 standard) or rolled mild steel), or polymeric (PVC sheet (BS3757:1 standard) or phenolic composite (BS2572)). Since exposure by the adherend to temperatures possibly exceeding 200°C was likely during the siloxane cure procedure,

only the metals were considered usable. Aluminium was chosen on the grounds that bonding properties to a commonly used microelectronic metallization material would be more useful than bonding to other materials. In this vein, alumina, Al_2O_3 was also selected as a possible adherend as this is a widely used electronic substrate material.

A typical lap joint preparation, following the BS5350 guidelines, would be application of the adhesive to a solvent cleaned adherend such as to minimise any variation in the joint. Methods of achieving a uniform, repeatable bond line thickness would be via the application of a known volume of adhesive over a known area or by the insertion of shim of a known thickness into the joint. This procedure is suited to the testing of more viscous adhesives which maintain their viscosity during the cure process. This is not true in the case of the siloxanes studied, these all being thermally cured. For this and other reasons, to be discussed shortly, it was necessary to depart from the ideal British Standards lap joint test. The developments made and their relative successes are now discussed.

***Testing procedure*:**

All tensile testing was performed on an Instron model 1114 tensile tester. This used self tightening jaws that were free to swivel about the axes in the plane of the bond line. A FSD of 500kg was employed with a constant cross - head speed of 1mm min^{-1}.

***Substrate preparation*:**

Aluminium test pieces, 25x2x100 mm were saw cut from sheet, deburred and acetone degreased. Alumina substrates, 15mm wide and 25mm long, were cut from 0.6mm

thick alumina sheet. The tensile strength of the alumina sheet was measured using the Instron tensile tester and was found to be approximately 900N. This was deemed insufficient for the bond strengths expected, therefore, the samples were strengthened by creating triple ply laminates using an epoxy resin as adhesive between the layers. Due to the brittle nature of the alumina, clamping of the test pieces in the jaws of the tensile tester was found to result in them cracking, making the application of aluminium pull tabs necessary. In both cases a high vinyl content siloxane was used as adhesive, and was chosen on account of its availability at the time of testing.

***Bonding to aluminium*:**

An initial investigation, where a small volume of siloxane was placed between two aluminium substrates and heated, highlighted a major problem associated with this technique, that of the sample flowing out from within the overlap area. This was accentuated by the lowering of viscosity associated with the cure temperature. To try to limit the flow of the siloxane a modified substrate preparation was employed. An area, 22x13 mm was masked out on the aluminium and the surrounding area was spray coated in PTFE from a PTFE / 111- trichloroethylene dispersion. The bond gap was maintained using a) 220μm and b) 30μm brass shim of 2mm width, as shown in Figure 4.7. Sample spreading was observed to a similar degree as in the unmodified case. To prevent the flow of the siloxane, a gasket sealed system was investigated. The test sample design is given in Figure 4.8. The depth of the bond line was controlled by the depth of the recess and was varied from 1.2 - 2.0 mm. The area to which the RTV silicone gasket was applied was precoated with PTFE to minimise its adhesion to the substrate. The samples were held together using a purpose built clamp whilst the

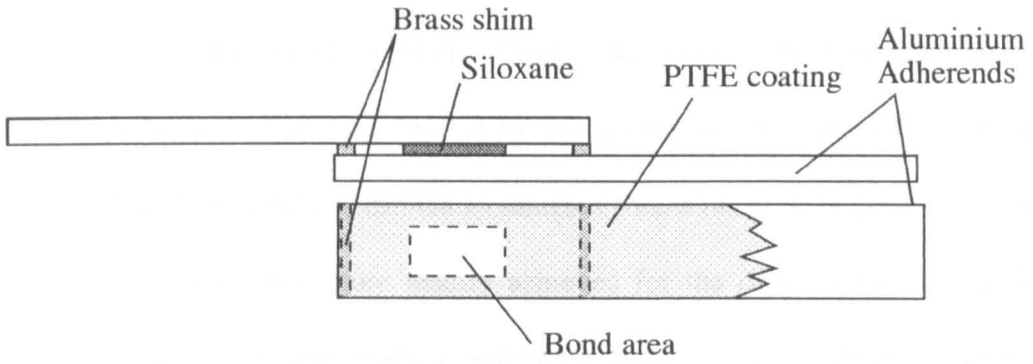

Figure 4.7. The first modifications of the lap shear test in an attempt to prevent sample spread away from the bond area.

siloxane was cured. The success of this technique was limited for a number of reasons. Firstly, great care had to be taken to apply the correct pressure to the sample during the cure procedure as too little pressure resulted in sample leakage and too high a pressure resulted in damage to the RTV seal and again sample leakage occurred. Secondly, it

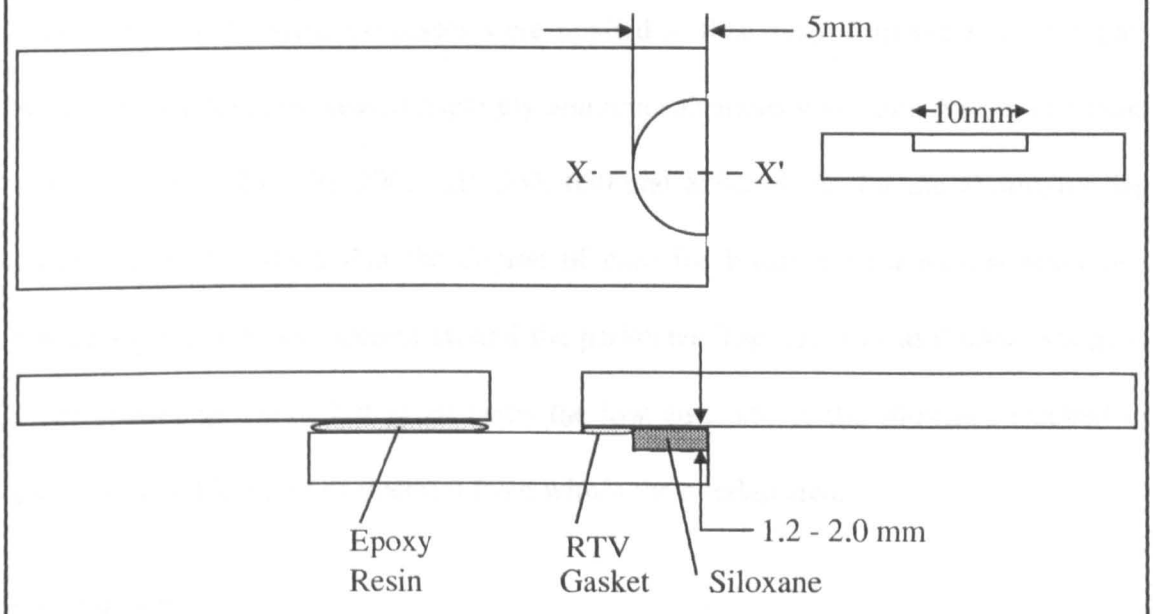

Figure 4.8. Substrate design and test sample configuration for gasket sealed shear test.

was found that despite the RTV being applied over a layer of PTFE, a reasonably high level of adhesion was formed between it and the aluminium, thus preventing determination of actual bond strengths. Thirdly, the accuracy to which the bond line thickness can be controlled to is limited by the degree to which the RTV seal can be controlled. Also, this system is limited to samples with a fairly thick bond line. Finally, curing of the siloxane was more readily achieved for the outer surface of the bond, resulting in a 'degree of cure' gradient across the bond (in the direction x-x' of Figure 4.8), with the level of cure increasing in the direction x to x'. This was also apparent for the modified lap shear test of Figure 4.7 where it was observed that the siloxane preferentially cured around the perimeter of the bond area, with areas further in from the edge not receiving a sufficient cure.

***Bonding to alumina*:**

Adhesion testing to alumina was run in parallel to the aluminium bonding work and as such, many of the same processes were applied to this study. Lap shear test samples were prepared from degreased triple ply alumina substrates with shim maintained bond gaps (45, 110, 125, 156, 200, 320, 500, 650 and 850μm). As for the aluminium lap shear test it was found that the degree of cure for bonds with a narrow bond line thickness was very poor except around the perimeter. The larger bond thicknesses gave more promising results but in all cases the low viscosity of the siloxanes resulted in partial or complete loss of material from within the overlap area.

***Conclusion*:**

Lap shear testing is not a suitable test method for the adhesion testing of siloxanes. The

low viscosity of the material, particularly at the cure temperature, prevents consistent bond area coverage being achieved. Also, it is apparent that the curing of siloxanes within a bond with a low bond line thickness is very much impeded, thus preventing the preparation of uniformly cured bonds. The reason for this lack of cure has been investigated and the results of this will be discussed later.

***Peroxide cured siloxane adhesion testing*:**

More success was achieved for siloxane materials cured via a thermally activated peroxide mechanism within a siloxane of composition 32.5 $(C_6H_5)_2SiO$: 65 $(CH_2CH)(CH_3)SiO$: 2.5 SiO_2.

***Sample preparation*:**

The test samples were prepared from 1.5mm thick aluminium sheet, saw cut into 10x25 mm pieces. These were degreased in acetone prior to coating. The test samples were prepared from a sandwich of non peroxide doped and peroxide doped siloxane. The non doped material was applied to the substrate by pipette and then thermally cured. A range of samples were thus 'precoated' at a number of temperatures between 180 and 250°C. Doped siloxane materials were prepared using dicumyl peroxide $[(C_6H_5C)(CH_3)_2]O_2$ in 1, 3 and 5 wt% concentrations. The lap shear samples were prepared by addition of a small volume of the doped siloxane onto the precoated substrates followed by a thermal cure, again at temperatures between 180 and 250°C.

A number of samples were also prepared in which the aluminium was abraded with wire wool so as to remove the top oxide layer. Samples were then prepared in the above

manner.

***Sample testing*:**

Samples were tensile tested in the usual manner. Bond areas were assessed visually with starved areas excluded from the measurements.

4.2.2.2 90° peel test for a rigid - to - rigid assembly.

The peel test, like the lap shear test, is routinely used to assess the performance of adhesives, details of the technique can be found in the British Standards BS5350: Part C14: 1976. In particular, the 90° peel test for a rigid - to - rigid assembly allows peel testing from a wide range of substrates. The principle of the technique is covered in the British Standard BS 5350: Part C14: 1979. The technique determines the force required to pull apart two bonded adherends. So as to not exert a lever force on the bond, at all times the force remains at 90° to the plane of the adherend , as is shown in Figure 4.9.The adherends are separated at a steady rate so that separation occurs progressively along the length of the sample. A necessary requirement is that the adherends are of a uniform width and thickness over the whole length, they should be rigid in as much as the forces required to delaminate the samples are insignificant relative to their yield points, they should be flexible to a degree that they are defomable to the desired curvature and finally, they must be tolerant of the cure temperatures.

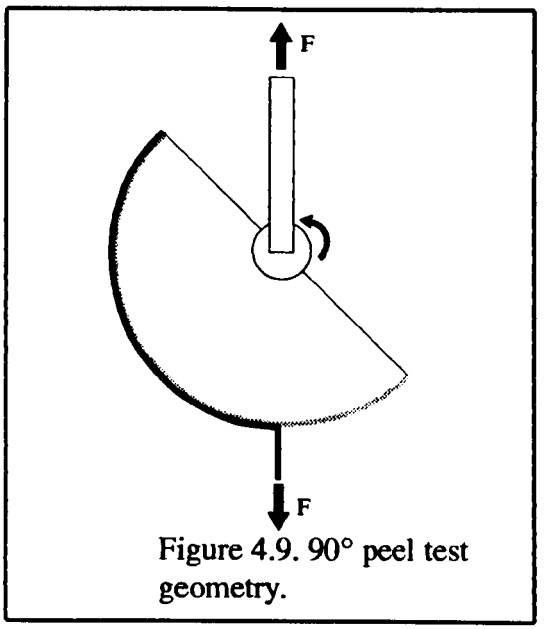

Figure 4.9. 90° peel test geometry.

***Test jig design*:**

A test jig was manufactured based on the BS5350: C14 [109] design, as is given in Figure 32 and had a diameter of 150mm, this allowing a sample of length 180mm to be easily accommodated around the perimeter. The jig was constructed from brass, using a silver steel axle. The sample clamp and upper support were both aluminium.

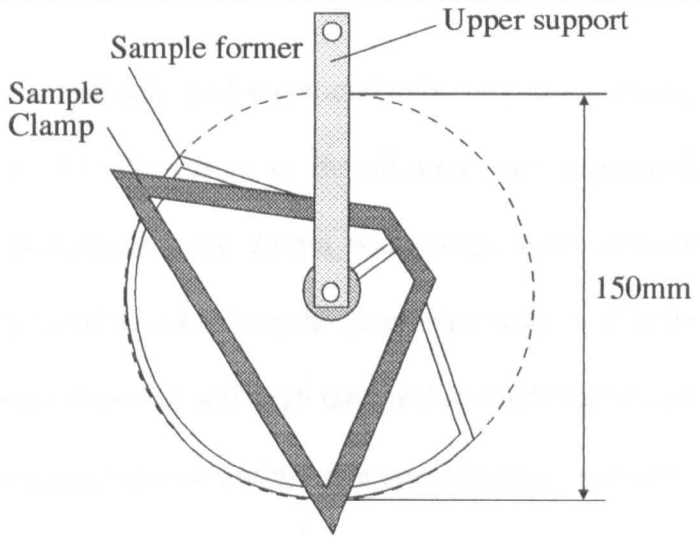

Figure 4.10. Construction of the jig used for the peel testing of adhesives

***Sample preparation*:**

For all peel tests performed, the substrate used was aluminium sheet or foil. The length of the sample strips was within the range 150-180 mm. All samples were passed through a degrease in 1,1,1-trichloroethylene followed by an abrasion process (P1200 emery cloth) so as to obtain a consistent surface texture. A number of parameters were adjusted during the development of this test for its application to siloxane materials. These are now discussed:

***Adherend thickness and width*:**

Due to the bond strength characteristics of the siloxanes, it was required that the

thickness of the adherend to be stripped be of the order of 100μm. Thicknesses greater than this resulted in the adherend not being flexible enough to maintain a 90° bend at all times during the testing, thus creating a lever effect, rendering the results void. The thickness of the non stripped adherend was less critical, with aluminium between 0.5 and 1.0 mm typically used.

The width of the stripped adherend was found to be very important as, in the case of the lap shear tests (4.2.2.1) the curing of the siloxane was impeded in a narrow bond thickness. Tests performed using 25mm wide strips were unsuccessful in that the samples were only found to cure along the outer edge; tests employing 8mm wide strips allowed more complete curing, although the bond strength was found to be much more sensitive to variations in the width of the area covered by the siloxane.

***Bond line thickness and method of maintaining a constant value*:**

Due to the required flexibility of the stripped adherend it was found that a large number of shim strips (120μm) were required along the length of the sample to maintain an even bond thickness. This has the undesirable effect of reducing the area of siloxane bonded and thus creating irregularities in the bond force. The use of longitudinal shim, in the form of 80μm wire run parallel to the edge of the samples, along their length, was assessed but this was found to impede the siloxane cure to an even greater extent.

***Most successful design*:**

The most successful design was found to be that as shown in Figure 4.11. During the curing period the sample was held together using paper clips. A PTFE tape coated

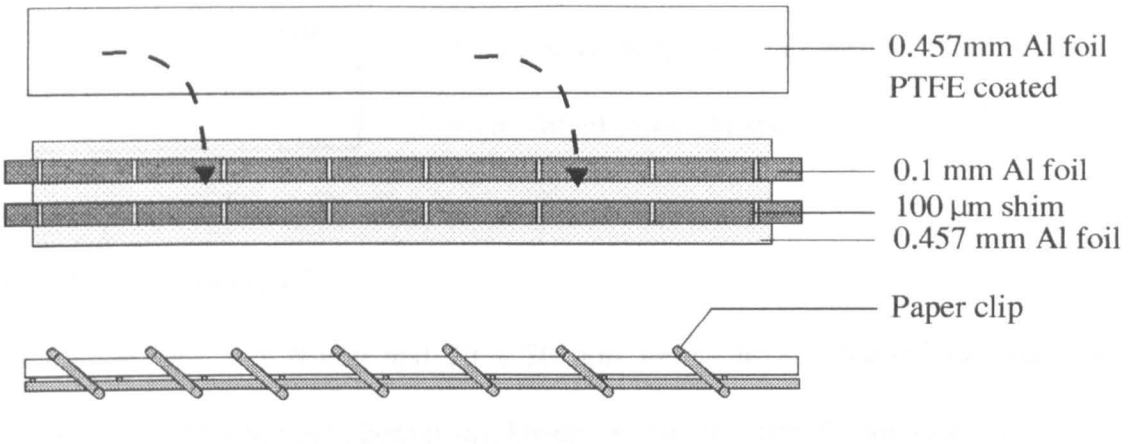

Figure 4.11. The optimum peel test configuration

strip of 1.0mm thick aluminium was required between the clips and the foil so as to allow an even pressure to be applied. The narrow width of the test strips resulted in the bond strengths being very low, as a result, the asymmetry in the test jig (see Figure 4.10) was evident in the results.

***Testing procedure*:**

The samples were clamped to the perimeter of the test jig , which was suspended from the tensile tester (JJ Instruments T22K) via the upper support. A section of the bond was delaminated and the stripped adherend was clamped into the lower jaws of the tensile tester. A constant extension of 1mm min^{-1} was applied until total delamination occurred.

4.2.2.3 Butt joint testing under direct tension.

British standards BS 5350: Part C3: 1989 [110] suggests a method of determining the bond strength of adhesives by application of direct tension to a butt joint between two rods, as in Figure 4.12. Due to the problems encountered in curing siloxanes in

Figure 4.12. Butt joint.

confined geometries (4.2.2.1, 4.2.2.2), a butt joint bonded directly using siloxanes was discarded in favour of two modified test methods.

***Modified butt joint test 1*:**

Aluminium tabs, 6 x 6 mm and 20 x 20 mm were siloxane bonded to aluminium substrates (0.457 mm thick, 20mm sq). Using the 36 mm^2 tabs the substrate was PTFE coated apart from a 6mm sq area in the centre. A bond line thickness of 200 μm was maintained using brass shim. Aluminium rod, 6mm diameter, 15 mm in length, was epoxy bonded to both the substrate and the tabs, these rods allowing clamping of the samples in the tensile testing rig. Care was taken to position both rods directly over each other and both normal to the plane of the substrate, as shown in Figure 4.13a.

***Modified butt joint test 2*:**

Siloxane coatings were cured in air onto 20 mm sq, 0.457 mm thick, aluminium substrate. As above, aluminium rod was epoxy bonded to both the substrate and the siloxane coating, as shown in Figure 4.13b. The samples prepared using both methods were were pull tested using a JJ T22K testing rig, at a cross - head speed of 1 mm min^{-1}

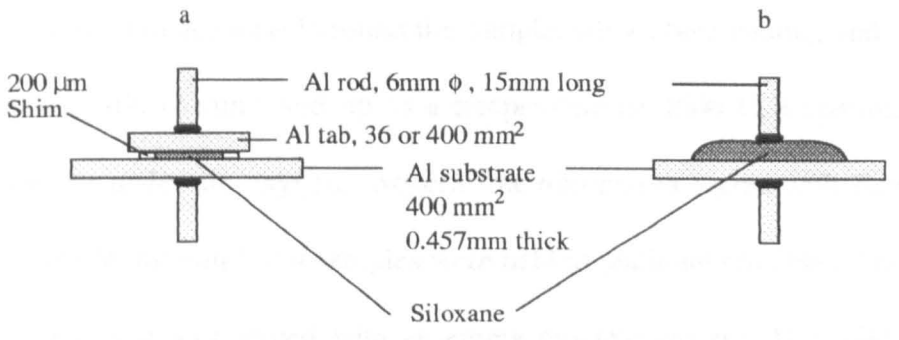

Figure 4.13. Sample configuration for modified butt pull tests

4.3 Thermal techniques.

4.3.1 Thermogravimetric analysis (TGA).

TGA is a technique that allows investigation of thermally activated processes that occur with a concomitant weight change. Such processes may be physical (vaporisation, sublimation, absorption - desorption) or chemical (decomposition, oxidation, solid state reactions, solid - gas reactions (e.g, oxidation, reduction)). The weight changes are measured using a thermobalance. The thermobalance consists of a balance arm with a sample and a balance weight holder at opposite ends. The tilt of the arm is controlled via a moving coil which supplies a torque to an axle mounted to the arm. A change in mass of the sample causes an offset of the balance. The offset is detected optically and a feedback circuit adjusts the current fed to the coil so as to maintain the balance. The current required to do this forms the output signal. A schematic of the system is given in Figure 4.14. Many of the above mentioned processes are sensitive to both the nature and flow rate of the surrounding atmosphere, thus it is usual to perform TGA under a known atmosphere, at a known flow rate. The gas also acts as a carrier for any evolved products.

TGA experiments were performed using a Stanton Redcroft TG-750 Thermobalance which, via a microfurnace raised around the sample, allows both heating and cooling at rates from 1 to 100°C min^{-1} and up to a temperature of 1000°C. Experiments were performed either under air, oxygen, oxygen free nitrogen or argon, with flow rates of between 20 and 50 ml min^{-1}. All samples were held in platinum crucibles. Prior to each TGA run, the output was zeroed with an empty crucible present. The solid or liquid samples were then weighed out into the crucible with between 6 - 10 mg routinely used.

Unless otherwise stated, the solid samples were prepared as a powder. Isothermal TGA was also performed using this equipment. Differential TGA (DTG) was applied to some samples, the differential output (dm/dt) being obtained from a Stanton Redcroft DTG unit (see Figure 4.14).

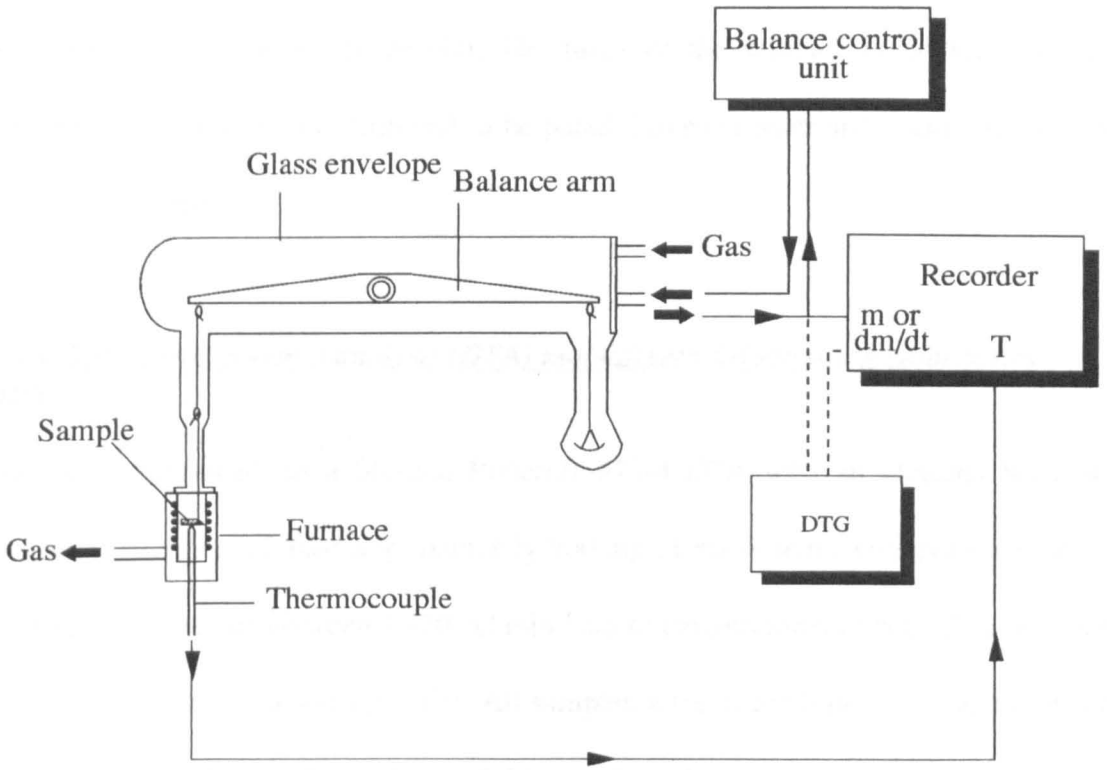

Figure 4.14. Schematic representation of apparatus for thermogravimetric analysis

4.3.2 Dilatometry.

Dilatometry was used to determine the thermal coefficient of expansion of a number of siloxanes. All measurements were performed on a Netzsch 402E dilatometer. The TCE values were calculated using a subtraction routine, allowing the expansion of the alumina sample holder to be removed from the results. The measurements were made over the temperature range RT - 250°C.

***Sample preparation*:**

Samples were cured in air, at the appropriate temperature, in a PTFE mould, having

dimensions 30x6x6 mm. Due to the variability in the curing characteristics of each sample (evaporation of solvent or volatiles, final cured density) the cross - sectional area of the cured samples was typically 30±6 mm^2. As the upper surface formed a meniscus, it was necessary to remove it, either by gentle abrasion (brittle materials) or by trimming (elastomeric materials). The faces of the samples in contact with the dilatometer push rods were trimmed to be parallel to each other and normal to the long side of the sample.

4.3.3 Differential thermal analysis (DTA) and differential scanning calorimetry (DSC).

DTA was performed on a Stanton Redcroft 673-4 DTA with an alumina head and platinum crucibles (of mass approximately 900 mg). Experiments were peformed in air, with heating rates of between 1 -10 °C min^{-1} up to temperatures of 600°C. In all cases reference was made to silica powder. All samples were in the liquid state and typically of mass 100 - 150 mg. The masses of the sample and reference were matched so as to obtain equivalent thermal masses. DSC was performed using a Netzsch 404 heat flux DSC with a high sensitivity head. Conditions used were as for the DTA experiments. The crucibles used were either platinum or alumina and the sample masses were approximately 20mg. Again reference was made to silica using matched sample and reference weights.

4.4 Electrical measurements

4.4.1 Dielectrics: an introduction

A dielectric is any material that provides electrical insulation. As such, an ideal

dielectric is completely non conducting to dc fields. In the simplest case, a dielectric sheet, of thickness d, placed between two conducting plates, each of area A, forms a parallel plate capacitor, as shown in Figure 4.15. Under dc conditions the dielectric prevents conduction and polarisation of the device occurs, resulting in equal and opposite charge being developed on the plates. The charge stored, Q (Coulombs), is related to the capacitance, C (Farads), and the applied potential,V (Volts), via Q=VC, where C is defined as in equation 21, where ε_o and ε_r are the permitivity of free space

$$C = \frac{\varepsilon_o \, \varepsilon_r \, A}{d} \qquad (21.)$$

and the relative permittivity of the dielectric respectively. For a perfect dielectric R_{dc} is thus ∞. Under ac conditions, the 'resistance' is a function of the frequency, f, of the applied voltage, and thus the impedance, Z (Ω), is defined as in equation 22.

$$Z = 1/(2\pi f C) \qquad (22.)$$

A non ideal dielectric will allow current to flow and thus may be represented as an ideal capacitor in parallel with a pure resistive element, R, as shown in Figure 4.15. In this case, under ac conditions, the induced current waveform and the applied voltage waveform will be out of phase with each other by a value Θ. It is usual to show this graphically via an Argand diagram[111], as in Figure 4.16 . The permittivity of a material may be generalised to contain both the real and

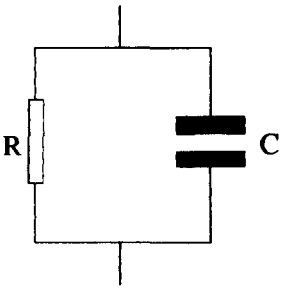

Figure 4.15.Representation of a non ideal dielectric non ideal dielectric

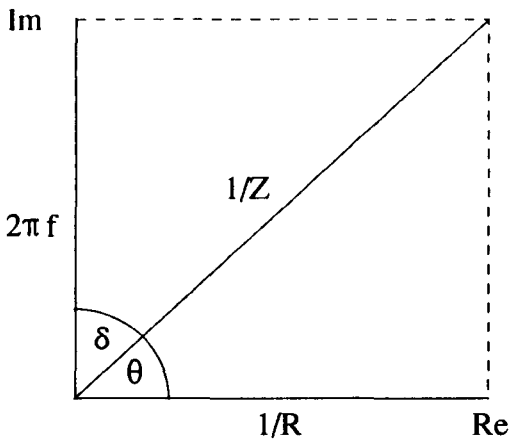

Figure 4.16. The Argand diagram representation of complex impedance.

imaginary parts indicated in Figure 4.16. The resulting complex permitivity ε^*, is defined as in equation 23[111]. ε' is the relative permittivity of the material and ε'' is related to the resistive element, as given in equation 24 [111]. Co is a constant

$$\varepsilon^* = \varepsilon' - j\varepsilon'' \qquad (23.)$$

depending on the geometry of the capacitor and is equal to $\varepsilon_o A/d$. The ratio $\varepsilon''/\varepsilon'$ is denoted as $\tan\delta$ (see Figure 4.16) and is proportional to the heat dissipated by the

$$\varepsilon'' = \frac{1}{2\pi f \, Co \, R} \qquad (24.)$$

material (or the energy absorbed from the applied voltage). As was discussed in section 2.2.2, both ε' and $\tan\delta$ are of considerable importance, and knowledge of the dielectric properties of a siloxane material over a wide frequency range is most desirable.

4.4.2 Low frequency dielectric testing.

4.4.2.1 General introduction to the test apparatus.

All low frequency dielectric measurements were performed on a Hewlett Packard HP4192A low frequency analyser. This allowed measurement of both capacitance and tanδ over the frequency range 5Hz to 10 MHz. The samples were prepared in the form of parallel plate capacitors, thus allowing ε' to be directly obtainable from the sample capacitance via application of equation 21 and knowledge of the sample geometry. A range of test methods were investigated, the relative merits and demerits of each are discussed.

4.4.2.2 Sample preparation

Samples were cured in air on aluminium plate, previously cleaned in acetone. Initially the samples were applied directly to the aluminium but the material wastage was fairly high due to sample flow. To prevent this, the siloxane was contained within a well prepared by either epoxy bonding a nitrile 'O' ring, 25mm diameter onto the aluminium or by forming a wall using RTV silicone rubber. The former was limited to materials with a cure temperature of around 200°C whereas the RTV silicone was usuable up to 250°C. After cure, if required, Au electrodes were sputtered onto the sample using a washer with dimensions 14±0.05 mm inside diameter, 15±0.05 mm outside diameter, to create a guard ring. The edge of the sample was precoated in silicone grease to prevent the gold conducting through to the bottom aluminium plate. The thickness of the sample was limited to being less than 3mm, which, assuming an ε_r of 2 (ideal value), gives a C of greater than 0.1pF, which is the minimum measurable.

4.4.2.3 Electrode guarding

Consider a parallel plate capacitor with plane conducting electrodes, as shown in Figure 4.17a. The measurement of the capacitance of such a device would include an error due to stray electric field lines around the edge of the capacitor. This edge effect may be removed by introducing a guard ring onto one of the electrodes, as shown in Figure 4.17b. The effectiveness of the guard ring is maximised when the ratio of the width of the gap between the guard ring and the signal electrode (gap g in Figure 4.17b) and the thickness of the sample, d, is minimised.

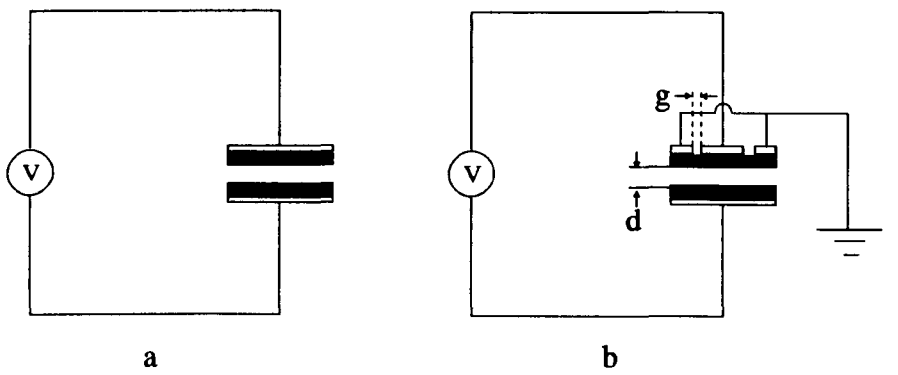

Figure 4.17. A parallel plate capacitor, without (a) and with (b) a guard ring.

4.4.2.4 Open - short correction

The measured impedance will be a combination of the sample impedance plus a number of other stray impedances from the test fixture and the connecting leads. To remove these the HP 192A supports an open - short correction routine, the details of which are given in the HP192A user manual [112]. It is important to note that the open - short correction is only valid within a certain frequency range (5Hz - 1kHz, 1kHz - 10kHz, 100kHz - 1MHz and for every spot frequency within the range 1 - 10 MHz).

4.4.2.5 Measurements using the HP16451B test fixture.

The HP1645B is a test fixture designed to allow easy measurement of both the loss factor, tanδ, and ε'. The design of the fixture is given in Figure 4.18. The electrode set comprises a lower non guarded electrode, 56mm in diameter, upon which the device under test (DUT) is placed, and a set of two interchangeable guarded electrodes, which, when attached to the fixture, are vertically adjustable via a micrometer screw. The spring loaded electrode has a spring mounted ball bearing end whereas the rigid metal electrode has a fixed position signal electrode. The orientation of the non guarded electrode is adjustable to allow the two electrodes to be made parallel (see user manual [112] for details).

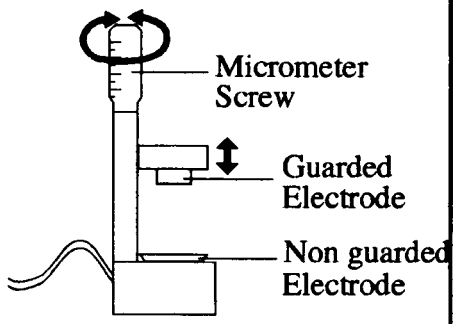

Figure 4.18. The HP16451B dielectric test fixture.

Test method 'A': the air gap method.

This method was originally investigated since, being a non - contact method, it allows measurement of soft films without causing damage to the coating. Also, the need for the application of thin film Au electrodes is removed. For these measurements the rigid metal electrode (Figure 4.19) was employed. In the measurement procedure it was necessary to maintain an accurate gap of less than 10% of the sample thickness, which, for an average sample, implied a gap of <100μm. It was found that obtaining this level of eveness over the entire area of the coating was not trivial and large errors resulted in the ε_r determination as a consequence of the inaccuracy of the gap measurement.

Test method 'B': contact method using the spring loaded electrode.

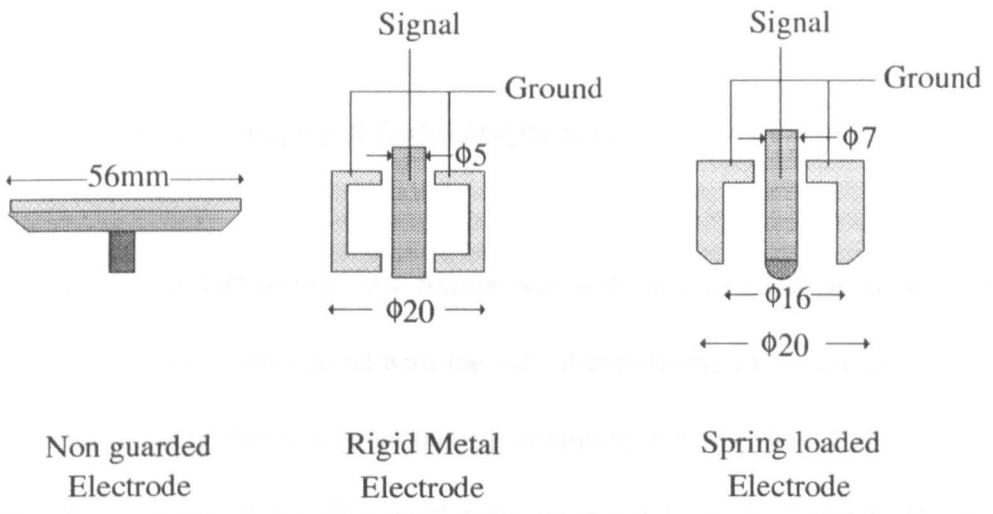

Figure 4.19. The electrode set for the HP16451B dielectric test fixture

The spring loaded electrode, SLE, was used in conjunction with Au thin film electrodes. The principal advantage of this technique is that errors due to air gaps between the sample and the electrode are minimal (although the Au film electrodes should be complete over the entire area of the sample). A problem with this technique is that, in order to bring the guard of the electrode into contact with the guard ring of the sample, a certain degree of over travel is required. In elastomeric films this has the effect of reducing the sample thickness at the point of contact, removing the thin film electrodes, thus making remeasurement difficult, and in some cases sample damage occurs.

Test method 'C': contact method using the rigid metal electrode.

As a result of the sample damage received when using the SLE, the rigid metal electrode (RME) was assessed for its suitability. Due to the uneveness associated with the siloxane coatings, it was decided to use the RME in conjunction with thin film electrodes so as to minimise air gap induced errors. As for the SLE this electrode was

found to damage the sample surface.

4.4.2.6 Measurements using a fabricated test fixture.

***Design considerations*:**

It was clear that the HP16451B test fixture was not suitable to study these siloxane coatings. A fixture was constructed with the aim of preventing excessive pressure being applied to the coating but still maintaining optimum contact. The fixture is shown schematically in Figure 4.20. The bond pads were cut from gold sheet. These were spring loaded using light coil springs. A rack and pinion system allowed vertical adjustment of the pads. The spacing of the pads was chosen so as to allow the standard sample preparation route to be used. The guard electrode consisted of an aluminium sheet 4mm thick. The fixture was connected up in a 3 terminal mode, with connections as shown in Figure 4.21b. The 3 terminal mode was chosen on the grounds of its frequency coverage (100Hz - 10MHz) [111]. Illustrated in Fig 4.21a are the possible stray capacitances that may occur with such a device. The techniques used to eliminate these are now discussed. Co, the capacitance between the connection cables, is

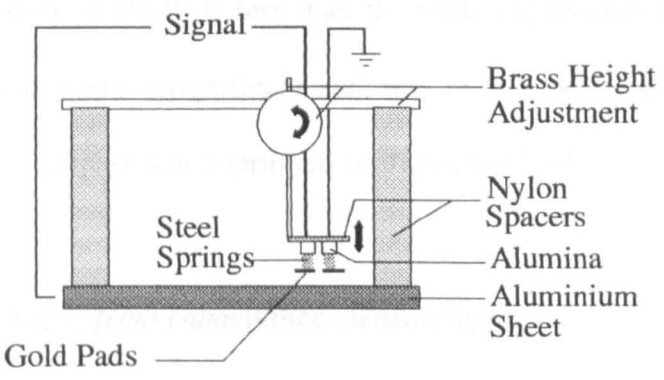

Figure 4.20. A schematic of the fabricated dielectric test fixture for measurement of soft siloxane films.

removed by connecting the outer sheath of the coaxial cables to ground (connection 1). Capacitances Ch and Cl are minimised by ensuring that the two connection ports (high and low) are shielded from each other [113], achieved by placing a grounded sheet, A, between the two connections. A further source of error, that of contact resistance, should also be assessed. Unchecked, these will give a positive error in the tanδ [113]. Contact errors are reduced by ensuring a good firm connection to the DUT, as is given

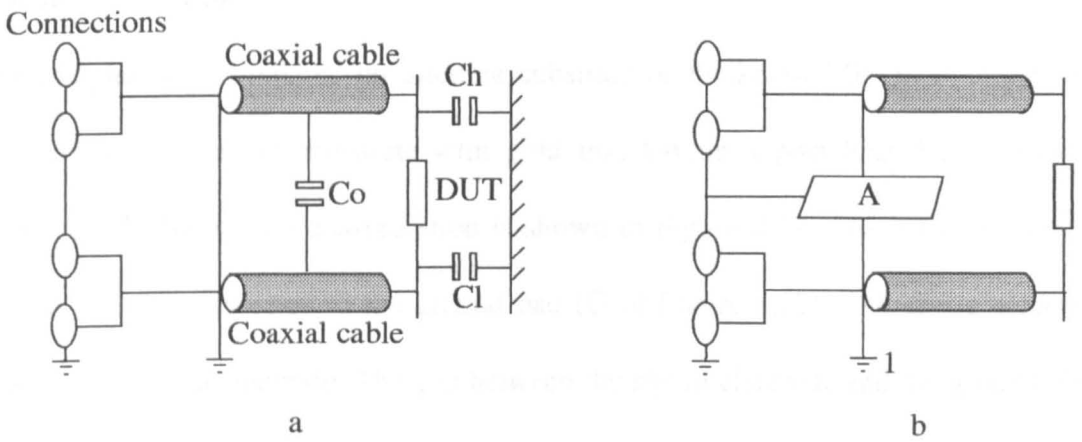

Figure 4.21. The connection configuration of the 3-terminal dielectric test fixture

by the spring loaded gold contact pads. Also, as is the case here, provided the DUT capacitance (of the order of 10pF) is less than the cable capacitance (of the order of 100pF), then these errors are insignificant and will in fact be lower than the error obtained using a more complex 4 or 5 terminal configuration [112].

4.4.2.7 Determination of ε' from capacitance measurements.

ε' was calculated from the capacitance measurements directly via equation 21. The area of the electrode was determined by the washer, placed on the coating prior to sputtering of the thin film electrodes and in all cases was $(1.54\pm0.07)\times10^{-4}$ m^2. The

sample thickness was measured using a digital micrometer with an inherent accuracy of 3μm. As the surfaces were not perfectly even the thickness was calculated from a number of measurements, with an error in the mean value of $\pm\sigma N^{-1/2}$, where σ is the standard deviation in the measurements and N is the number of measurements.

4.4.3 High frequency dielectric measurements

***Sample preparation*:**

The samples were prepared on alumina substrate of thickness 1.0mm. A circuit was screen printed onto the substrate with gold ink, having a post heated resistivity of $10.8\mu\Omega cm^{-1}$. The circuit configuration is shown in Figure 4.22. The outer two form a ground and are connected to the ground pad (G of Figure 4.22). The centre electrode acted as the signal electrode. The gap between the signal electrode and the ground plate was 50μm. The printing had a line width of 250μm and a line spacing of 50μm at the probe contact area (P of Figure 4.22). To prevent the siloxane flowing over any area of the substrate other than the ground pad, G, laser cut alumina enclosures were bonded around G using RTV silicone. After sample curing, performed in air at the appropriate temperature, the surround was removed , the sample trimmed to size and any residual RTV was removed with acetone. To complete the signal electrode the upper surface of the sample was gold sputtered, using a foil mask. In some instances the samples were too thick to allow the gold to contact

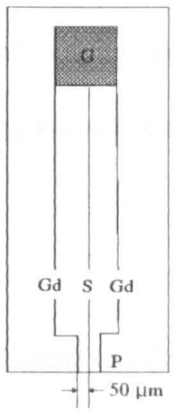

Figure 4.22. Design of the sample substrate.

down from the surface to the signal electrode. In these cases the path was completed using silver conductive paint.

***Measurement*:**

Measurements were performed on a Microtech Test Bed, fed from a HP86148-S parameter test set, driven by a HP83620A synthesized sweeper (10MHz to 20GHz capability). Analysis was performed by a HP8570B network analyser. A Microtech microprobe with a signal - ground configuration was employed (see Figure 4.23). This probe was employed rather than a ground - signal - ground (g-s-g) probe since the resolution of the screen printing was not high enough to allow a g-s-g probe to be used. The frequency range 45MHz to 3GHz was swept for all samples. Prior to measurement, the system was open, short and load corrected, with the latter two performed using known standards.

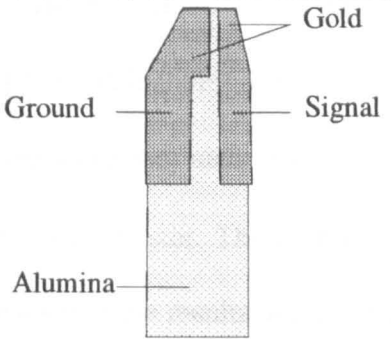

Figure 4.23. The geometry and construction of the Microtech Microprobe.

***Problems encountered*:**

After measurements had been performed it was found that the substrate exhibited a very complex characteristic, this being due to the inductances and capacitances associated with the gold lead paths to the electrode, as indicated in Figure 4.24. Also, more surprisingly, the substrate showed considerable resistive character. The tracks, having a resistivity of 10.8 μΩ cm, were approximately 5 times more resistive than pure gold [1]. The complex nature of the substrate system resulted in the appearance of many

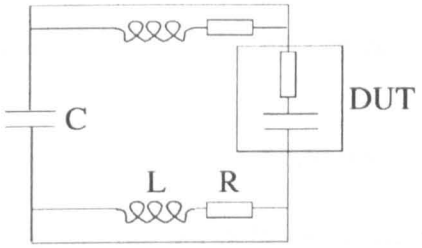

Figure 4.24. Passive component representation of the high frequency dielectric sample circuit.

resonances in the scattering parameter / frequency spectrum. The substrate was used as a calibration sample in order that the effects due to the inductance, capacitance and resistance of the leads could be subtracted. Load correction was performed by joining a 51Ω SMT resistor across the gap between the signal line to sample electrode. The resistor was bonded using Abelstick Abelbond 81 - 1 LMI conductive epoxy, cured at 160°C / 30 minutes. The calibration was not too effective since the measuring system requires a 50Ω impedance signal line up to the calibration resistor. The inability to calibrate out the complex behaviour of the substrate means that the results did not offer any clear information concerning the dielectric behaviour of the encapsulant material at high frequencies, as is illustrated in Figure 4.25, which shows the real part of the complex impedance as a function of test frequency for the 51Ω SMT resistor load and a typical sample.

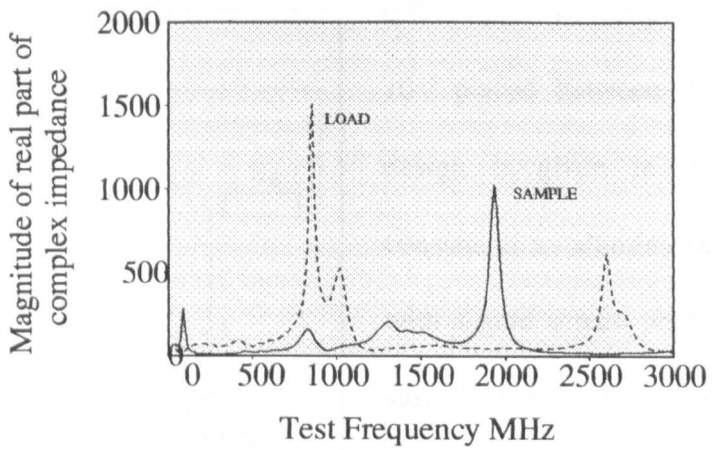

Figure 4.25. The magnitude of the real part of the complex impedance measured for the 51Ω SMT resistor load and a typical sample.

4.5 Reliability testing.

4.5.1Immersion - bias hermeticity test.

The electrolytic hermeticity test or 'salt - cell test' is a short term reliability test that focuses on the hermeticity of the coating (ie, to what degree it resists the ingress of water into the structure) which, as discussed in section 2.1, is a major factor determining the corrosion protection of the coating. Measurement of the leakage current through the coating offers an insight into the degree of water permeation, which, ultimately provides a method by which poor materials may be eliminated at an early stage of the development process.

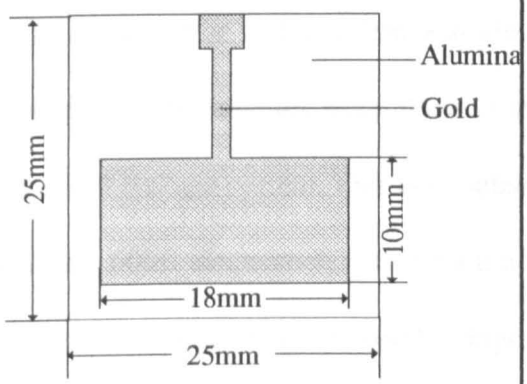

Figure 4.26. The immersion - bias test cathode substrate.

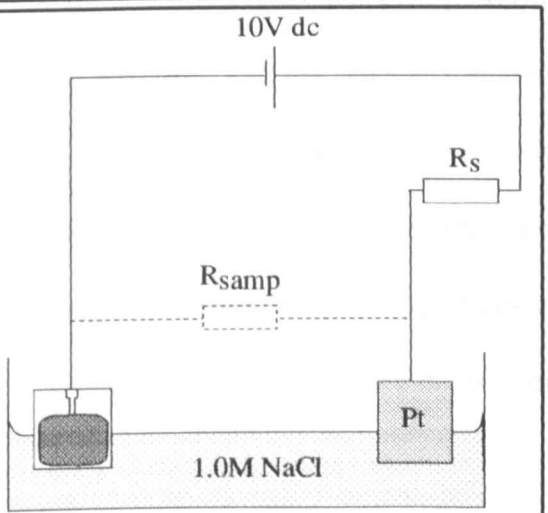

Figure 4.27. Schematic layout of the immersion - bias hermeticity test.

***Measurement of leakage current*:**

Following the method employed by Needes and Button [114] the electrochemical cell consists of an anode (platinum due to its inert behaviour) and a cathode (the test sample), immersed in a salt solution with a potential difference of 10V placed between them. The cathode design is given in Figure 4.26. This consists of an alumina sheet, 25 x 25 mm, with a gold screen printed pattern on one side. To prevent the siloxane flowing over the area of the tile it was contained in either epoxy resin or RTV silicone

enclosures. All the samples were cured in air at the required temperature. A schematic of the test system is given in Figure 4.27. The salt solution was contained in a perspex sample container which incorporated a lid to minimise water evaporation, so as to maintain a constant salt concentration. It was possible to raise and lower the samples into the salt solution. The majority of measurements were performed at room temperature although the performance of a number of coatings at elevated temperatures was investigated by immersing the sample container into a regulated temperature water bath. In this case the sample container was allowed to equilibrate to a static temperature prior to introducing the samples to the salt solution and commencement of measurement. For both ambient and elevated temperature measurements, once the pd was applied the samples were allowed to equilibrate for 5 minutes prior to measuring the initial leakage current. This and subsequent leakage currents were measured using a Keithley 600B electrometer. To obtain a continuously recordered output, the pd across the series resistor (1kΩ) was used as input to a chart recorder.

4.5.2 Environmental testing - The temperature humidity bias (THB) test.

The salt - cell test determines the performance of coating materials under conditions of 100% RH. An industry standard reliability test is the 85/85 environmental test [114]. THB assesses the reliability of a device when exposed to elevated temperatures, humidity and under bias, all essential elements for corrosion. This is a commonly used technique to assess the reliability of devices but, with a suitable choice of test device, it was also possible to investigate the performance of encapsulation materials.

The substrate:

The test vehicle substrates were supplied by the supporting company, BNR Europe Ltd, and have been used by their Materials Characterisation Centre to assess the hermeticity of a wide range of commercial coating materials. The substrates were available in a wide range of materials (polyimide, cyanate ester, alumina, laminated epoxy-glass (FR405), BT epoxy) but only those materials with a suitably high T_g were employed (polyimide, cyanate ester, alumina). The two former had dimensions (56x80x1.5 mm) and the latter had dimensions (67x80x1.6 mm). The test patterns employed are interdigitated meandering paths as shown in Figure 4.28. Each substrate contained

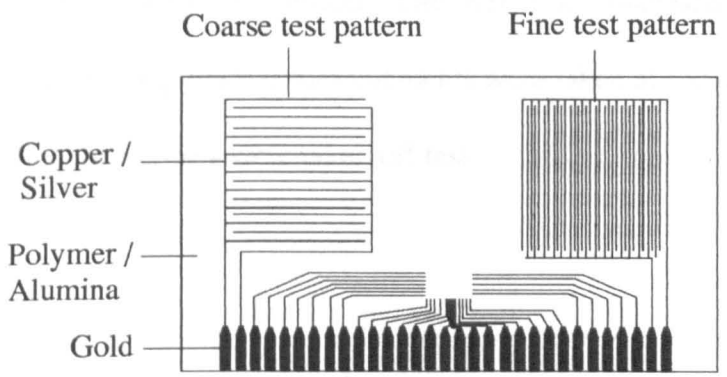

Figure 4.28. The board layout for the 85/85 environmental test

two test tracks, one fine, with a line spacing of 318μm and one coarse, with a line spacing of 635μm. The test patterns were copper in the case of the polymer boards and silver for the alumina boards. The remaining metallisation allowed incorporation of a stress measuring chip but was redundant in all 85/85 tests.

***Sample preparation*:**

Prior to coating the substrates they were cleaned in acetone. To prevent sample flow, epoxy resin enclosures were placed around the test pattern area. Samples were cured in air at the appropriate temperature.

***Test method*:**

All 85/85 testing was performed by A. W. Hillman, E. Knight and J. D. Watts in the Materials Evaluation Centre at BNR Europe Ltd. Details of the testing method can be found in a number of BNR internal reports [115, 116] and only an overview of the testing method will be presented here. The substrates were plugged into edge connectors (with gold connectors). Each test pattern was wired in series with a 1MΩ resistor and was biased with 10Vdc. Measurements of the voltage drop across the series resistor were made using a four - wire technique. Measurements were made at 25°C / 50%RH, 85°C / 50% RH and at 85°C / 85%RH. The RH was increased gradually to prevent condensation forming. Further measurements were taken at various times up to 1000hrs at which time the samples were taken off test.

4.6 Viscometry.

The viscosity of a material is directly related to the degree of intermolecular interaction. As the level of interaction is increased, for example as a result of increased entanglement or of forming cross - links, a concomitant increase in the material's viscosity would be observed. Viscometry thus offers a means by which the curing characteristics of siloxane material may be investigated. To enable this to be achieved required a system that allowed simultaneous sample heating and viscosity measurement.

***The viscometer*:**

An unmodified Brookfield LTV DV-1 rotating spindle viscometer was employed. A range of spindle rotation speeds within the range 0.5 to 60 rpm, in combination with

two interchangeable spindles permitted viscosity measurement over the range $5x10^{-4}$ to $16x10^{3}$ Pa.s. Due to the inherent inaccuracy of viscosities below 10% of FSD, the measured viscosity was generally maintained in excess of 30% FSD via suitable choice of the spindle rotation rate. Output from the viscometer was fed to a chart recorder.

The sample holder and heater:

The design requirement for the sample holder was that absolute viscosities could be measured at temperatures within the range 25 - 260°C with a minimal sample volume required for each measurement. The Brookfield small sample adaptor was used as a template for the design. This required a maximum sample volume of 28ml and, since the system was calibrated explicitly for use with it, absolute measurements were obtainable. Due to the material limitations the small sample adaptor was only useable up to 100°C thus a replica was fabricated from stainless steel. A number of design details had to be addressed to allow stable, accurate temperatures to be taken simultaneously with viscosity measurements. Since the viscometer readings were very sensitive to the relative orientation of the sample holder and the spindle, a support between the walls of the furnace and the sample holder was required to allow the sample holder to be aligned and held rigid whilst allowing thermocouple access to the sample holder. The heater employed was an Heraeus W10/1 A muffle furnace which had only simple on - off temperature regulation.

System 1:

Design: A schematic representation of system 1 is given in Figure 4.29. The sample holder was embedded within a refractory fire brick, shaped so as to fit the dimensions of the muffle. A stainless steel plate with levelling feet was attached to the furnace to

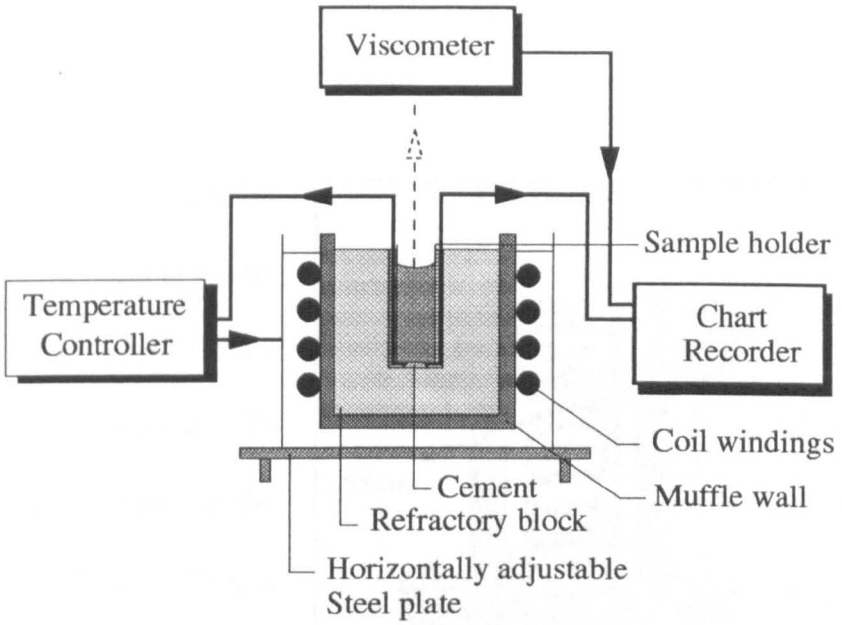

Figure 4.29. The design and configuration of the initial viscosity measuring system.

allow adjustment of the holder orientation. Temperature measurement was made using Ni/Cr - Ni/Al K-type thermocouples placed directly under the sample holder and in mechanical contact with it. Temperature control was performed using a Eurotherm controller employing phase angle switching without Proportional Integral Differential (PID) control.

Performance: The stability of the sample was found to be good, allowing easy measurement of the viscosity. The temperature control was less favourable with a large degree of overshoot (+14°C) and very poor temperature stability (±5°C) (see Figure 4.30). This effect was probably due to a combination of the large thermal mass

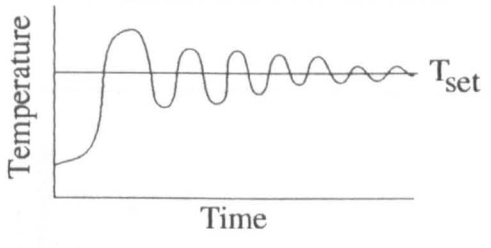

Figure 4.30. A typical temperature time profile exhibited by system 1.

of the sample holder support and to deficiencies in the power controller.

System 2:

Design: System 1 was modified by improving the sample holder design and employing a more suitable power controller. To reduce the thermal mass of the support, a light weight aluminium design was used, as given in Figure 4.31. N_2 gas cooling coil (3mm copper tubing) was incorporated into the support to allow the time over which samples were exposed to elevated temperatures to be controlled more accurately. A Eurotherm 815 PID controller was employed for power regulation, allowing the controller to be self - tuned for each set temperature.

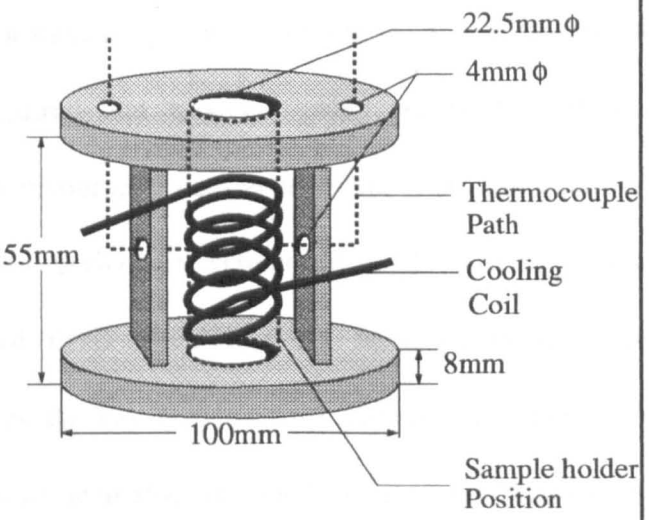

Figure 4.31. Design of the lightweight sample holder support.

Performance: This system was even more mechanically stable than system 1. Also, both the temperature overshoot and the time taken to stabilize were dramatically reduced and typically the temperature profile observed was as given in Figure 4.32. The N_2 gas cooling

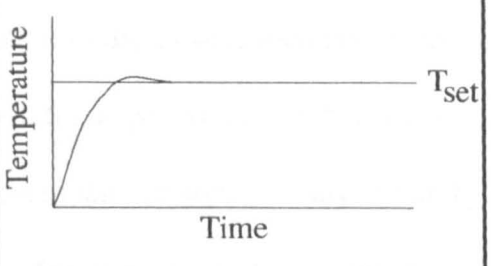

Figure 4.32. A typical temperature - time profile exhibited by system 2

coil was very effective at controlling the cooling time, with forced cooling rates of up to 15°C min^{-1} being attained.

4.7 Sample synthesis: the standard preparation route.

It is convenient at this point to define a standard preparation route. At an initial stage of the study a synthesis route was required that was reasonably simple to perform, allowing material preparation without recourse to complicated wet chemical synthesis techniques. For this purpose a process described by Schmidt et al [117] was employed. Synthesis was achieved by direct hydrolysis of chlorosilanes under either acidic or basic conditions. Figure 4.33 indicates the key stages of the preparation route, with emphasis on the processing conditions available for modification. For copolymer preparations, where more than one precursor was employed, these were added simultaneously. In such multicomponent systems the precursors were stirred together for ½ hr, sealed to the atmosphere, to ensure thorough mixing. The solvent, where used, was a 50/50 v/v mixture of toluene and ethylacetate. Hydrolysis was achieved by addition of a stoichiometric volume of water (sufficient to just hydrolyse the precursors). After a further ½ hr, neutralization of the systems was achieved by the controlled addition of KOH solution (KOH in 4 x the stoichiometric volume of water and a volume of ethanol (EtOH) equivalent to the stoichiometric volume of water - such a solution was required to allow it to be more soluble in the system solvent). Once a stable pH9 was reached the systems were reacted for a period of 3½ hrs. Finally, samples were refined by filtration of any KCl precipitate, removal of any water by phase separation and desolvation. This route, as discussed later, has a number of dismerits, and indeed, many of the samples prepared in this study employed more

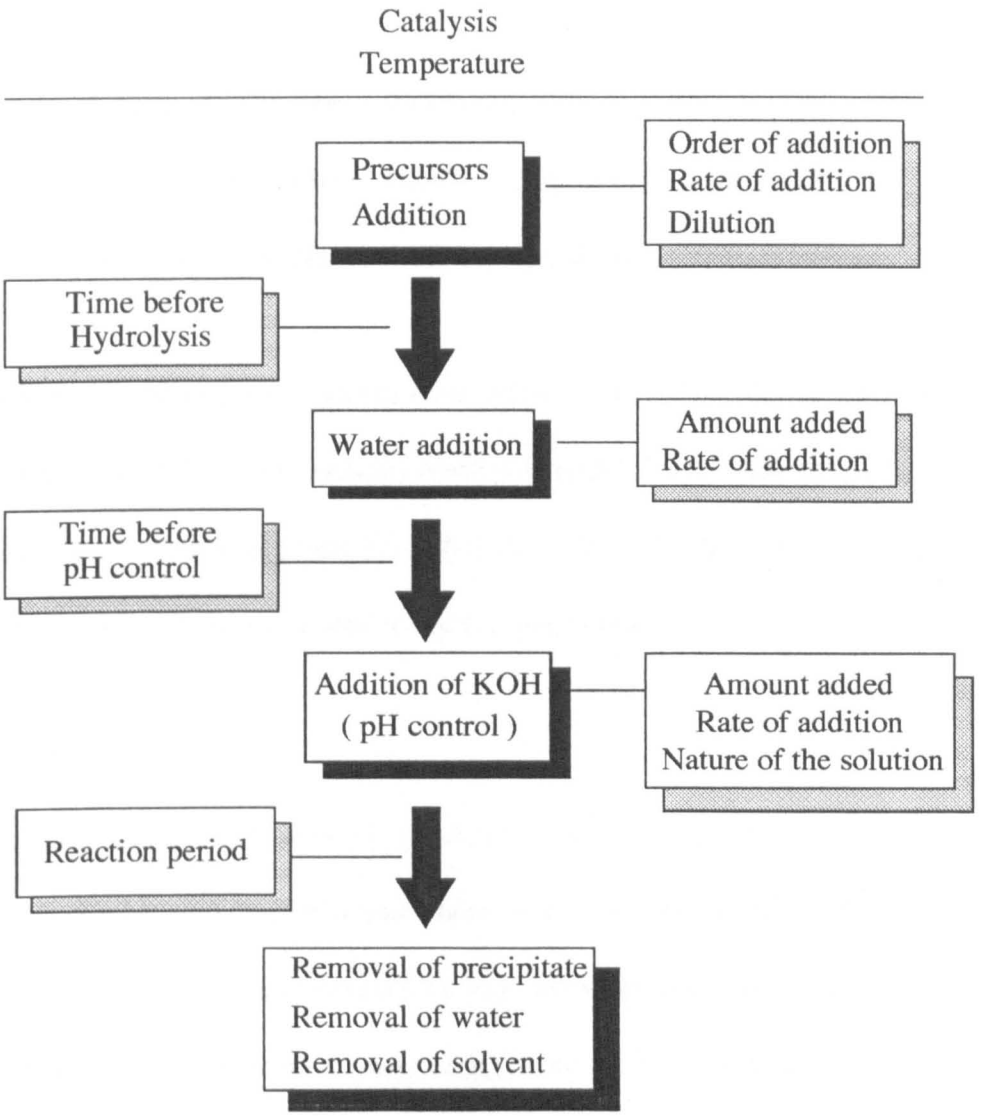

Figure 4.33. A flow diagram of the standard preparation route indicating adjustable parameters.

complex synthesis routes, the peculiarities and details of which will be described where appropriate. Many of these more involved preparation routes are derivatives of the standard route, usually involving adjustment of one or a number of the parameters highlighted in Figure 4.33; this alone justifies its validity.

CHAPTER 5: SYSTEMS CONSISTING OF DIFUNCTIONAL UNITS - RESULTS AND DISCUSSION

Owing to the absence of tri or tetra - functional siloxane units from this system there is no possibility of inorganic cross - linking. Only linear species (with reactive end groups) and cyclics will be present (see 3.2.4) after hydrolysis / condensation.

Preparation: All difunctional systems were prepared from dialkyldichlorosilanes using the standard route (4.7). Three systems were investigated, one containing only D units ($-(CH_3)_2SiO-$), one containing only D' units ($-(CH_3)(CHCH_2)SiO-$) and one containing both D and D' units. These three will be treated separately.

5.1 The D system

The samples in this system were all prepared from DCDMS and are summarised in Table 5.1. It can be seen from this that many of the samples were prepared during the development of other siloxane systems (which are to be discussed later). Since these simple materials form the basis of many other, more involved systems, an investigation into the nature and population of the structures formed using the particular basic preparation route discussed in 4.7 was deemed necessary. Of particular interest was the role of initial monomer concentration in determining the material's structure. This has been extensively investigated, both theoretically [53] and experimentally [116] but it was considered that a true feel for the sensitivity of the system to the monomer concentration could only be established by direct experimentation. The results of the NMR study were complemented by the GPC investigations.

Sample	Preparation pecularities	Reason for preparation
D1	solventless system	^{29}Si solution NMR analysis
D2	8.0 M precursor solution	" "
D3	0.9 M precursor solution	" "
D4	solventless system	GPC analysis
D5	0.9 M precursor solution	" "
D6	1.8 M precursor solution	^{29}Si solution NMR analysis to assess effect of $Fe(acac)_3$
D7	10.0 M solution in CH_2Cl_2 Triethylamine acid acceptor React with atmospheric H_2O	Used in later studies (see 8.1.2.2)
D8	0.375 M solution in CH_2Cl_2 Pyridine acid acceptor	Used in later studies (see 8.1.2.2)
D9	0.375 M solution in CH_2Cl_2 Triethylamine acid acceptor	Used in later studies (see 8.1.2.2)
D10	Precursor added to excess cold H_2O Very slow precursor addition pH 7 maintained	Used in later studies (see 7.1.1.2)
D11	1.0 M solution, DMAP catalyst	TGA analysis

Table 5.1. Samples prepared employing D units ($-(CH_3)_2SiO-$) only.

5.1.1 ^{29}Si solution NMR results for D system materials prepared via the standard route with a variable initial monomer concentration.

Samples D1, D2 and D3 were investigated using ^{29} Si solution NMR. The D system is particularly suitable for NMR analysis as the spectra are not complicated by tacticity effects [117] (extra splitting of the resonances that occur due to the spatial orientation of neighbouring stereoisomers - see Appendix I). The ^{29}Si solution NMR spectra of the D1 and D3 samples are given in Figures 5.1a, and 5.1b respectively. Considering for a moment the high concentration sample, it is evident from Figure 5.1a that there is very

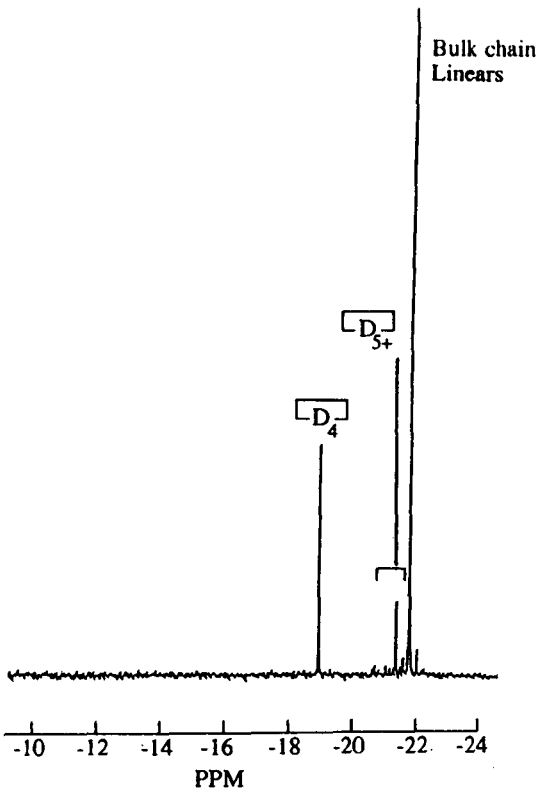

a

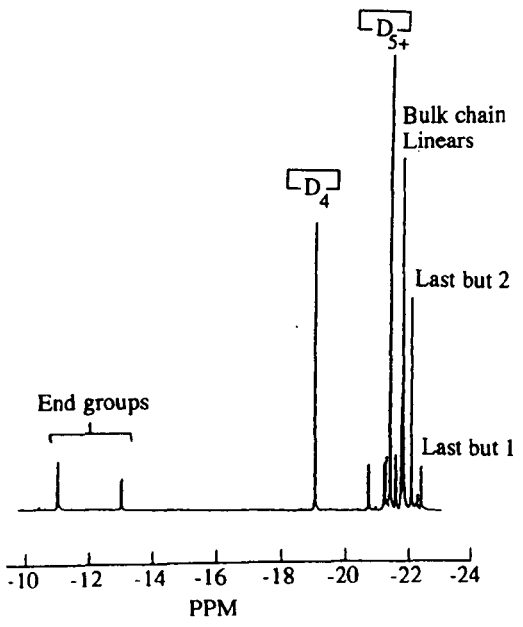

b

Figure 5.1. The ^{29}Si - $\{^{1}H\}$ solution NMR spectra for samples a) D1 (high concentration) and b) D3 (low concentration).

little evidence for the end group species (Si-OH) which, if present, would be apparent at around -12.1 ppm [118]. From this, two situations may be proposed. On the one hand, the end groups may not be visible due to the degree of polymerisation being so high as to make the end group resonance insignificant with respect to the bulk chain -D- resonances. Secondly, it may be possible that the sample is highly cyclised, when only a low level of end group species would exist. Since the sample preparation was performed under conditions of high concentration, this is considered unlikely. Further support for the former situation is given when the cyclic populations of both D1 and D3 are compared. The cyclic tetramer, $\boxed{D_4}$, is easily identifiable in both Figures 5.1a and 5.1b, being found at -19.14 ppm, -19.29 ppm and -19.12 ppm for samples D1, D2 and D3 respectively. These figures agree well with published figures of -19.51 ppm [119] and -19.6 ppm [120]. The slight discrepancy between these and the observed values is most likely due to solvent induced effects. In contrast to this, the cyclic trimer , $\boxed{D_3}$, (-9.2ppm, Engelhardt et al [121]), which is thermodynamically unstable, having between 12 - 15 kJ mol^{-1} [48] of strain energy, is not observed in any of the samples. The resonances within the D1 spectrum are therefore assigned as in Table 5.2 and in Figure 5.1a. The assignments for the bulk chain and near - chain - end groups were made by reference to work by Herbert and Clague [123] and those for the higher cyclics, with reference to Engelhardt [121], Burton and Harris [124] and Levy et al [125]. Absolute differentiation between the near end group resonances and those of the higher cyclics is difficult due to the overlap of the shift ranges reported for the higher cyclics [125] and for the linear species [123] , and thus, for the purpose of the intensity calculations given in Table 5.2, the assignments as in Figure 5.1a were used. Focussing now on sample D2, the medium dilution sample, it is clearly seen that end group

resonances are more prominent in this sample, as evidenced by the resonances at -13.00 ppm and -10.87 ppm. The former is in reasonable agreement with that suggested by Newmark [120] (-12.1 ppm) for the silanol group, particularly when it is noted that the latter data was obtained for a solventless silicone gum system. The resonances were assigned as given in Table 5.2, and were based on the previously quoted literature values. Again there is a degree of uncertainty in the assignments made for the most upfield (lowest frequency) resonances but the 'bulk linear' resonance is readily assigned on the basis of its position with respect to that observed for sample D1. The growth of the cyclic population is most striking, as indicated by the intensities given in Table 5.2. Similar resonances as for D2 were observed in D3 (Figure 5.1b) and these are also given in Table 5.2.

5.1.2 Gel permeation study of the D system materials prepared via the standard route with a variable initial monomer concentration

The GPC chromatographs of samples D4 and D5 are given in Figure 5.2. Unfortunately, shortly after the chromatographs were recorded, and prior to a calibration plot being made, a guard column was fitted to the apparatus, thus preventing the calculation of exact parameters from the chromatographs. The molecular masses presented in Table 5.3 were determined from a GPC calibration plot (Appendix II, Figure II.1) taken shortly after the addition of the guard column and will thus be prone to some error. The peak parameters are given in Table 5.3. These were calculated on the basis that the materials were 100% linear.

Sample D1		
Species	δ^{29}Si (ppm ±0.01)	Intensity (%)
Cyclics		
Tetramer	-19.14	18±1
Higher	-21.56 - -22.00	3.1±0.4
Linears		
Bulk chain	-22.24	79±2
End groups	——	

Sample D2		
Species	δ^{29}Si (ppm ±0.01)	Intensity (%)
Cyclics		
Tetramer	-19.29	12.2±0.7
Higher	-21.00 - -22.28	66±3
Linears		
Bulk chain	-22.36	10.5±0.7
Last but 1	-22.68	3.5±0.5
Last but 2	-22.57	1.2±0.4
End groups	-13.00	2.3±0.4
	-10.87	4.0±0.5

Sample D3		
Species	δ^{29}Si (ppm ±0.01)	Intensity (%)
Cyclics		
Tetramer	-19.13	46±6
Higher	-21.53 - -22.53	38±5
Linears		
Bulk chain	-22.85	12±2
End groups	-10.83	2.3±0.4

Table 5.2. The resonance position assignments for samples D1, D2 and D3.

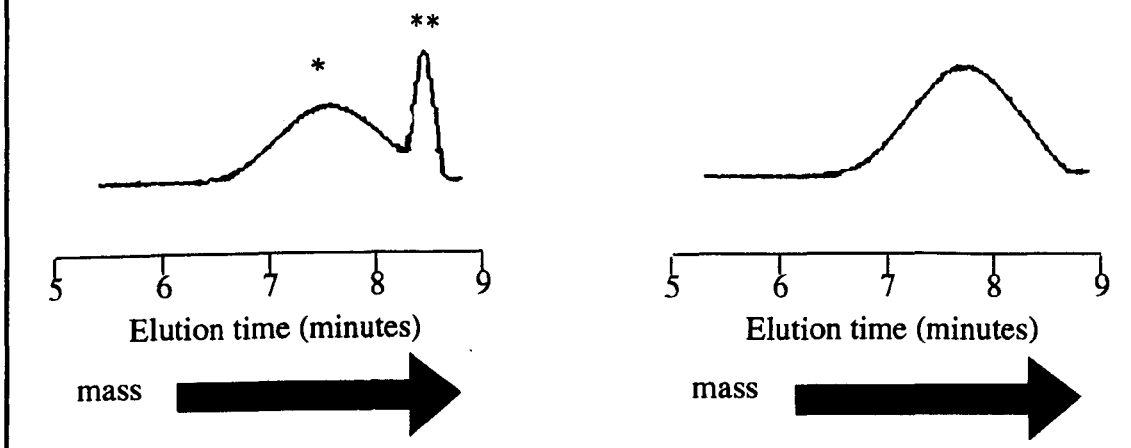

Figure 5.2. The gel permeation chromatographs for samples a) D4 (high initial precursor concentration) and b) D5 (low initial precursor concentration)

Sample	M_{min} (linear)	M_{max} (linear)
D4	429^{+108}_{-86}	8255^{+1257}_{-1481}
D5*	406^{+103}_{-82}	4912^{+944}_{-791}
D5**	300^{+50}_{-64}	406^{+103}_{-82}

Table 5.3. Parameters for the GPC peaks determined from Figure 5.2. Note '*' and '**" refer to the two GPC peaks of Figure 5.2b.

5.1.3 Thermo gravimetric analysis of the D system prepared via the standard route.

Sample D11 was prepared using the standard preparation route (4.7). A fairly high initial monomer concentration was employed, in conjunction with a heterofunctional condensation catalyst [50], DMAP (3.2.3.2), to encourage the formation of linear species with a reasonably high degree of polymerisation. TGA was performed on the sample in air (flow rate of 50cc min^{-1}) and a heating rate of 10 °C min^{-1}. The result of this is given in Figure 5.3.

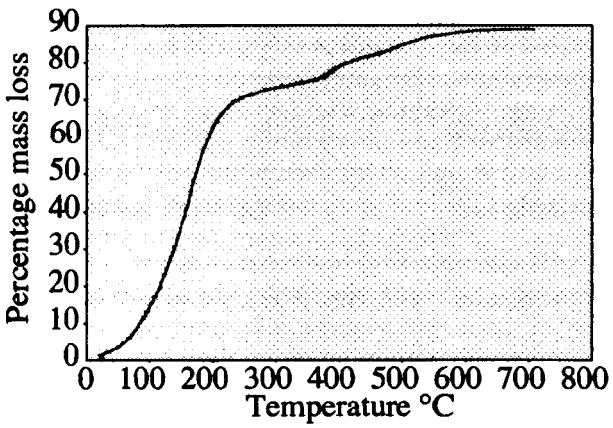

Figure 5.3. TGA of sample D11, performed in air with a heating rate of 10°C min^{-1}

5.2 The D' system.

All samples were prepared from dichloromethylvinylsilane (DCMVS). The samples prepared for this system are summarised in Table 5.4.

5.2.1 ^{29}Si solution NMR results for D' system materials prepared via the standard route, with a variable initial monomer concentration.

As can be seen from Table 5.4, samples D'2, D'3 and D'4 were prepared under essentially standard conditions (4.7) with only the volume of the solvent varied between

samples. Two samples (no dilution and 7.4 M) were duplicated so as to examine the repeatability of the preparation route. The ^{29}Si solution NMR spectra of the non diluted (D'2 and D'7), 7.4M (D'3 and D'8) and 0.825M (D'4) samples are given in Figures 5.4, 5.5 and 5.6.

Sample	Preparation pecularities	Reason for preparation
D'1	Standard conditions 1.18M	^{29}Si solution NMR ^{13}C MAS NMR (curing)
D'2	Standard conditions solventless system	^{29}Si solution NMR
D'3	Standard conditions 7.4M	^{29}Si solution NMR
D'4	Standard conditions 0.825M	^{29}Si solution NMR
D'5	Standard conditions 14.9M, O°C, pH 3-4	^{29}Si solution NMR, IR spectroscopy
D'6	Standard conditions 1.18M	Peroxide curing / adhesion tests
D'7	Standard conditions solventless system	^{29}Si solution NMR, GPC analysis
D'8	Standard conditions 7.4 M	^{29}Si solution NMR, GPC analysis
D'9	1.0 M solution, DMAP catalyst	TGA analysis

Table 5.4. Samples prepared employing D' units (-($CHCH_2$)(CH_3)SiO-) only.

Comparing the D' spectra to those for the D system it can be seen that very similar trends are observed. In particular, the resonance at -34.93 ± 0.01 ppm, which dominates in both D'2 and D'7 (solventless preparations) is seen to be considerably reduced in the diluted sample spectra (D'3, D'4, D'8) and is thus assigned to the bulk chain linear species, -D'-. It is thus assumed that the group of 5-6 resonances just downfield of this originates from the set of cyclic species D'_n (n>4). Although tacticity effects may be

observed in these materials, any such splitting of the -D'- resonance would only be, on average, of the order of 0.04ppm [119], thus it can be concluded that the resonance at -34.80 ± 0.01 ppm, which is slightly downfield of, and in close proximity to the -D'- resonance also originates from a cyclic species. The set of very low intensity resonances observed just upfield of the -D'- resonance, may, by comparison with the work of Burton et al [123], be assigned to higher cyclic species. The cyclic tetramer is prominent in all spectra at -32.49 ±0.02 ppm. In none of the samples was the cyclic trimer observed, which would be expected to be found approximately 10ppm downfield of the tetramer [126], and indeed, in sample D'5 it was observed at this position (see 5.2.3). The region between -24.20 ± 0.01 ppm and -26.56 ± 0.01 ppm is seen to exhibit between 2 and 5 resonances. These are attributed to end group species such as SiOH and SiOR. The resonance positions for all the D' samples are summarized in Table 5.5. The intensities for the resonances, which are calculated as a percentage of the total intensity of all resonances within each sample are given in Figure 5.7.

Sample	Bulk linear	End Groups	D'_4	D'_{5+}
D'2*	-34.93	-24.60 -26.53	-32.44 -32.53	-34.30 - -34.80
D'7*	-34.92	-25.00 -26.56	-32.42 -32.51	-34.15 - -34.85
D'3**	-34.92	-25.00 -26.56	-32.45 -32.54	-34.28 - -34.72
D'8**	-34.66	-25.59 -25.44 -24.84 -26.37 -25.31	-32.22 -32.30	-34.07 - -34.55
D'4***	-34.90	-24.11 -24.73 -24.55 -26.40	-32.44 -32.53	-33.05- -34.80

Table 5.5. The resonance positions for the D' system samples of Figures 5.4, 5.5 and 5.6. All values in ppm ±0.01. Samples prepared under inital precursor concentrations of: *= solventless, **= 7.4M, ***= 0.825M.

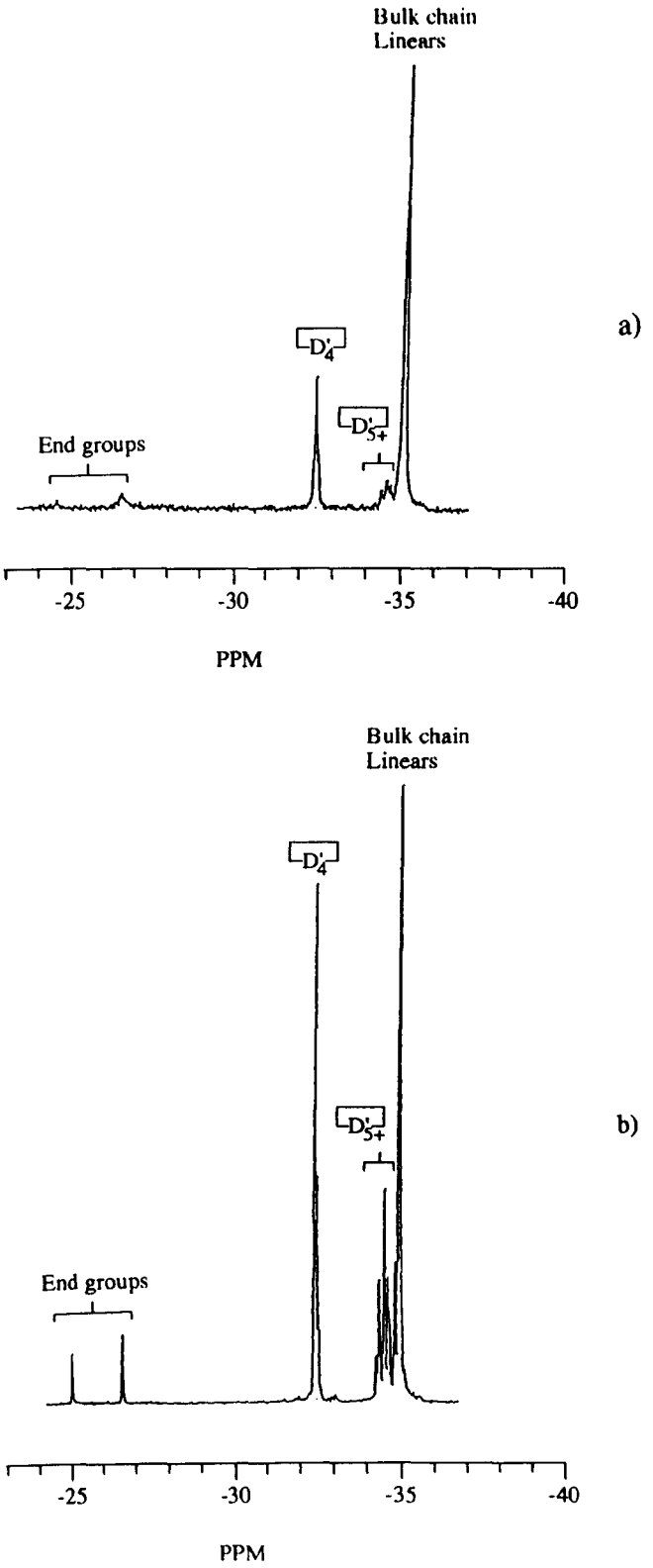

Figure 5.4. The ^{29}Si solution NMR spectra of samples a) D'2 and b) D'7, both prepared under solventless conditions.

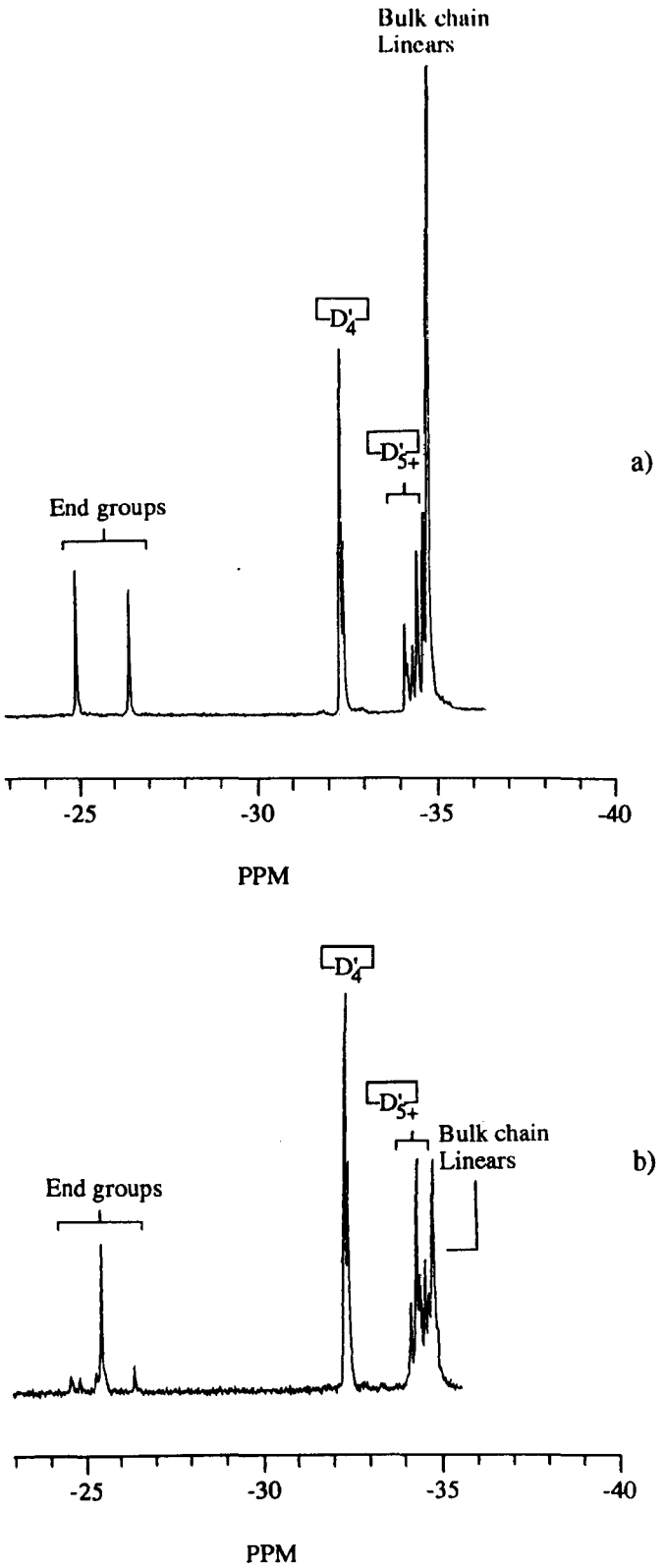

Figure 5.5. The ^{29}Si solution NMR spectra of samples a) D'3 and b) D'8, prepared with 7.4 M initial precursor concentration.

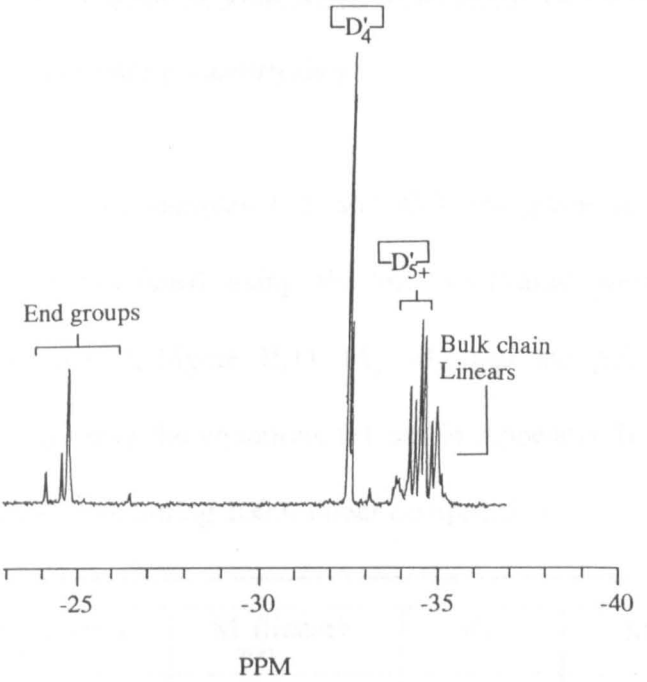

Figure 5.6. The ^{29}Si solution NMR spectra of sample D'8, prepared with a 0.825 M initial precursor concentration

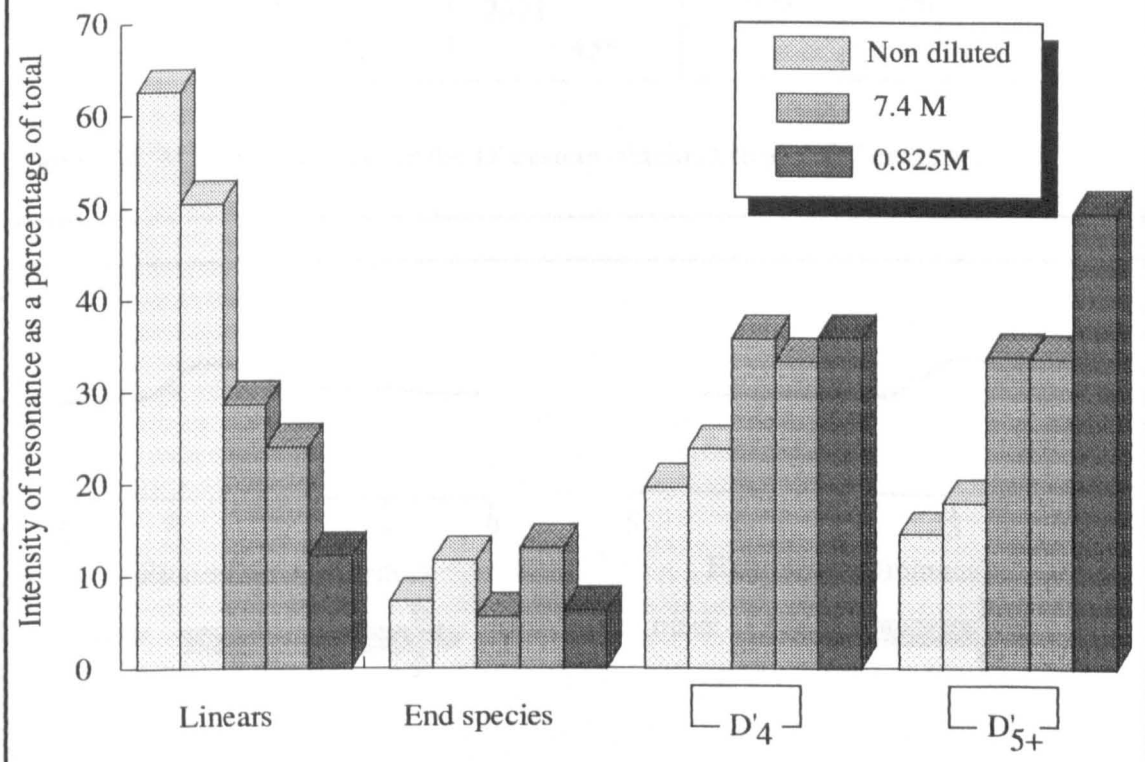

Figure 5.7.The NMR intensities within the D' system prepared under various preparation dilutions.

5.2.2 Gel permeation study of the D' system materials prepared via the standard route with a variable initial monomer concentration

The GPC chromatograms of samples D'2 and D'3 are given in Figure 5.8. The molecular masses were calculated using the low molecular weight GPC system calibration plot (Appendix II, Figure II.1). M_n, M_w and the polydispersity of the samples were calculated using the equations set out in Appendix II. Note that all the parameters were calculated assuming 100% linear composition.

Sample	M_{min} (linear)	M_{max} (linear)	M_w	M_n
D'2	351^{+110}_{-88}	16615^{+2705}_{-2326}	4680	1852
D'3	379^{+97}_{-77}	2671^{+553}_{-458}	959	790

Table 5.6. Mass parameters for the D' system obtained from GPC analysis.

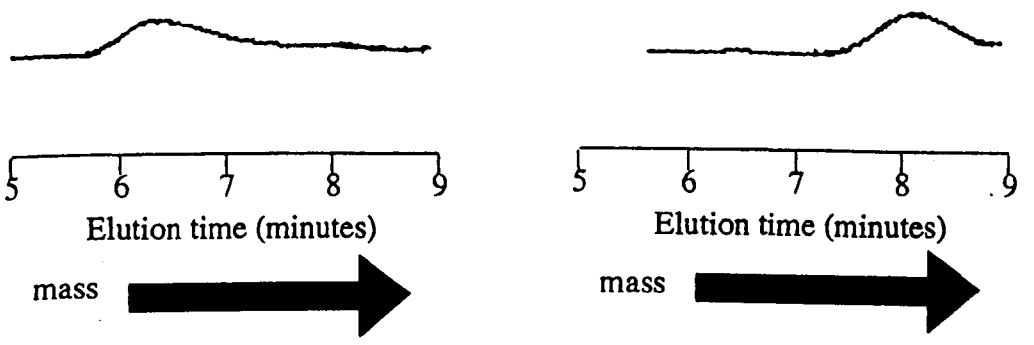

Figure 5.8. The gel permeation chromatographs for samples a) D'2 (high initial precursor concentration) and b) D'3 (7.4 M initial precursor concentration).

5.2.3 The effect of sample preparation temperature upon structure formation in the D' system.

^{29} Si solution NMR was performed on two samples of D'5, one as prepared (D'5 - 0), and one preheated at 150°C for a period of 1 hr (D'5 - 150). The spectra are given in Figure 5.9 and the peak assignments are given in Table 5.7. For these reference was made to (5.1.22), (5.2.1) and reference [125] (for the trimer position).

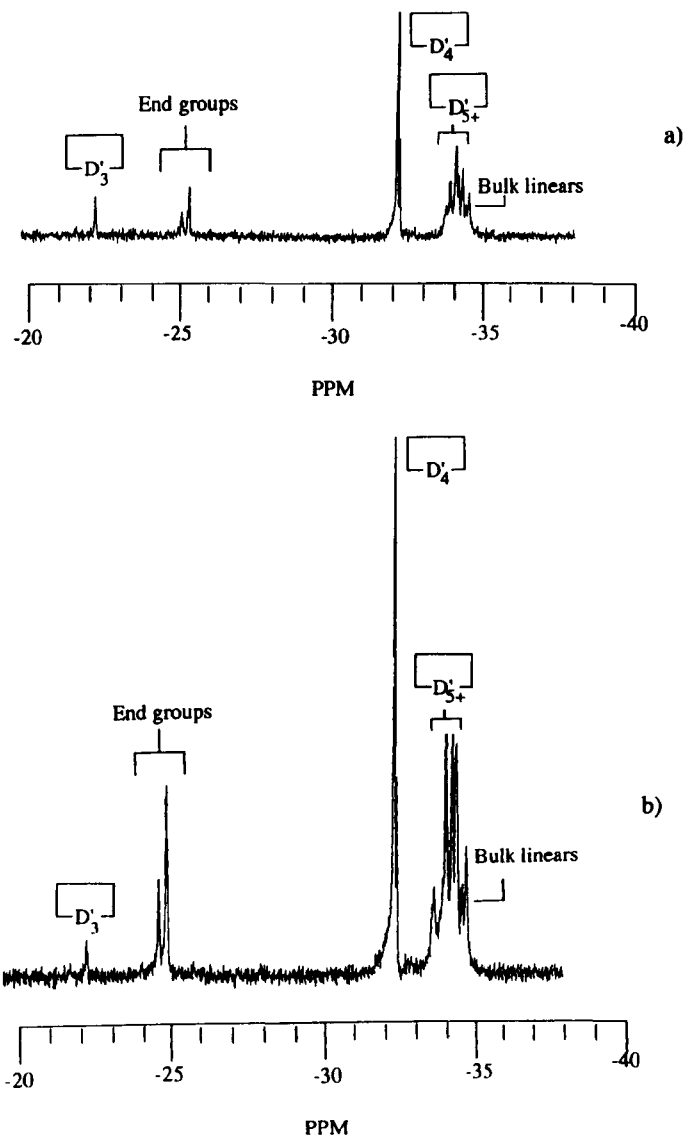

Figure 5.9. The ^{29}Si solution NMR spectra for D'5 (prepared at 0°C) for a) no heat treatment, and b) preheated at 150°C for a period of 1 hr.

Sample	Bulk linear	End groups	D'_3	D'_4	D'_{5+}
D'5 - 0	-34.54	-25.34 -25.10	-22.25	-32.14 -32.24	-33.92 - -34.44
D'5 -150	-34.75	-24.74 -24.98	-22.35	-32.33 -32.42	-33.70 - -34.62

Table 5.7. The ^{29}Si solution NMR resonance position assignments for D'5 (0°C preparation), before and after a 150°C heat. All values in ppm±0.01.

The intensities of the species were calculated from the spectra in Figure 5.9 and these are given, along with the intensity ratios between the two samples, in Table 5.8. Note that within each sample, the sum of all the intensities was normalised to 100%.

	Bulk linear	End groups	D'_3	D'_4	D'_{5+}
D'5 - 0	6.0±0.5	8.6±0.6	4.4±0.5	34±1	47±1
D'5 -150	6.3±0.3	10.7±0.4	1.3±0.3	29.4±0.6	52±0.9
$\frac{\text{D'5 -150}}{\text{D'5 - 0}} \times 100$	105±14	124±13	30±10	86±14	111±4

Table 5.8. Measured peak intensities for ^{29}Si solution NMR of sample D'5.

5.2.4 Thermogravimetric analysis of the D' system prepared from the standard route.

The preparation route for sample D'9 was identical to that employed for D11, and thus, preparation details can be found in 4.7 and 5.3. TGA was performed on the sample

under air (flow rate of 50cc min $^{-1}$) and at an heating rate of 10°C min $^{-1}$, the result of which can be seen in Figure 5.10.

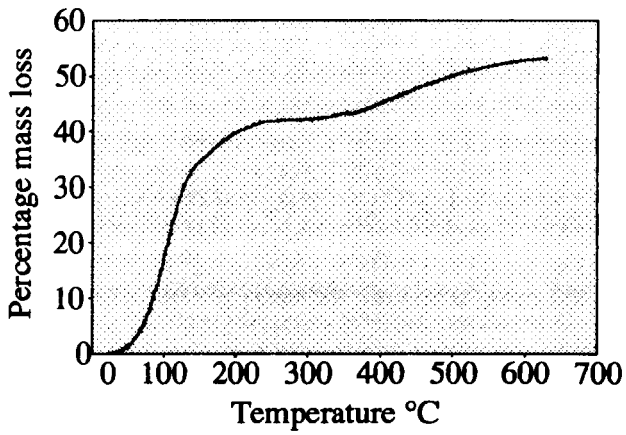

Figure 5.10. TGA of sample D'9, performed in air with a heating rate of 10° C min $^{-1}$.

5.3 The D / D' copolymer system

Copolymers of D and D' were prepared via the standard preparation route (4.7) using DCDMS and DCMVS. A summary of the samples prepared is given in Table 5.9.

Sample	Preparation pecularities	Reason for preparation
D'D1	61DCDMS / 39 DCMVS Solventless	^{29} Si solution NMR
DD'2	61DCDMS / 39 DCMVS 4.0 M solution	^{29} Si solution NMR
DD'3	61DCDMS / 39 DCMVS 0.80 M solution	^{29} Si solution NMR
DD'4	99DCDMS / 1 DCMVS 8.3 M solution	Adhesion testing
DD'5	80 DCDMS / 20 DCMVS 8.2 M solution	Adhesion testing
DD'6	50DCDMS / 50 DCMVS 7.9 M solution	Adhesion testing

Table 5.9. Samples prepared from a copolymerisation of D and D' units.

5.3.1 A ^{29}Si solution NMR investigation of the copolymerisation of D and D' units, prepared via the standard route.

^{29} Si solution NMR was performed on samples DD'1 and DD'3, the results of which are given in Figure 5.12. The origins of the resonances were deduced from the literature [118 - 127] and from the deductions made in 5.1 and 5.2.1. A summary of the assignments made is given in Table 5.10 (sample DD'1) and Table 5.11 (sample DD'3). Peaks 1-6 of Tables 5.10 and 5.11 refer to the six possible ring structures for the cyclic tetramer [127], as indicated in Figure 5.11. A further splitting of each peak is also observed and results from next neighbour tacticity effects [127, 128]. From Figure 5.11 it can be seen that a D' unit has a deshielding effect upon the D resonance and vice versa. Physically, five possible cyclic tetramer species could possibly exist, these being DDDD, DDDD', DDD'D', DD'D'D', and D'D'D'D'. The calculated probabilities for the tetrameric cyclics, assuming a 61D : 39D' initial monomer ratio are given in Table 5.12 along with the experimental intensities obtained from the spectra in Figure 5.12.

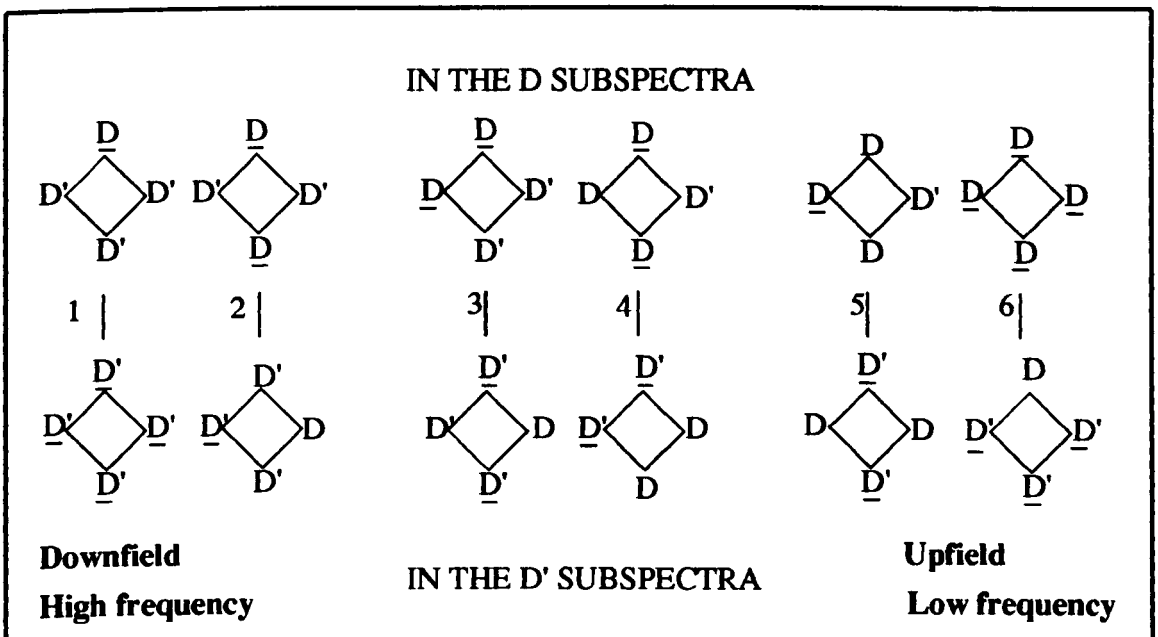

Figure 5.11. The possible cyclic tetramer structures and their assignment to the six resonances observed in both the D and D' ^{29}Si solution NMR spectra.

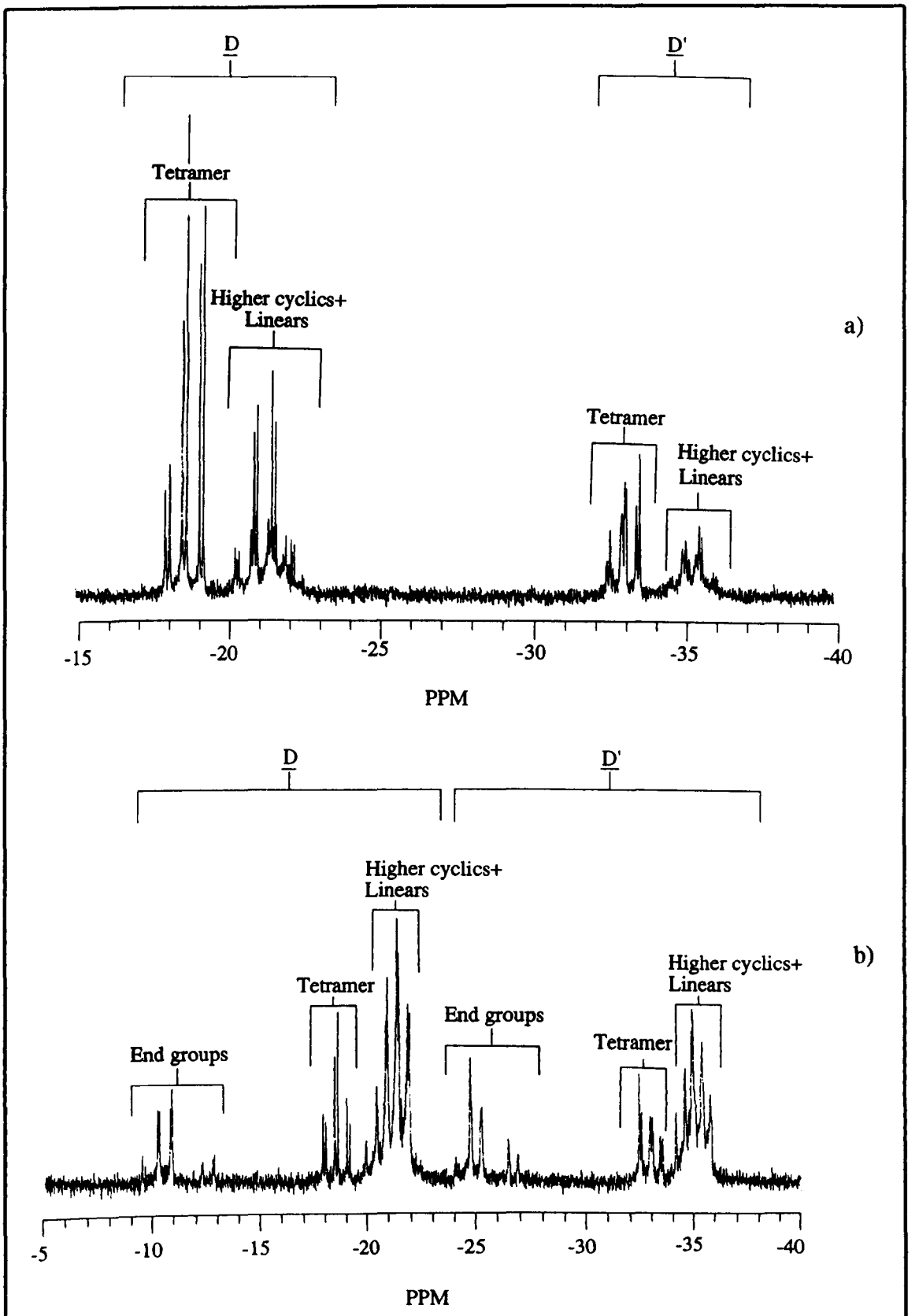

Figure 5.12. The ^{29}Si solution NMR spectra of the copolymer systems a) DD'1 (high initial monomer concentration, and b) DD'3 (low initial monomer concentration).

Resonance position *	Assignment
-9.47, -10.16, -10.24, -10.74, -10.82 -11.83, -12.20, -12.27, -12.73, -12.81	End groups : eg) HO-D-D~ HO-D-D'~ RO-D-D~ RO-D-D'~ X{DD'}$_n$X **
-17.79, -17.84 -17.98, -17.99 -18.44 -18.58 -18.99 -19.13	Peak 1 Peak2 Peak3 Peak4 Peak5 Peak6 — Cyclic tetramer D resonances
-19.89 - -22.20	Higher cyclic species + linears
-24.06, -24.65, -24.70, -25.23, -26.45, -26.88	End groups : eg) HO-D'-D~ HO-D'-D~ RO-D'-D~ RO-D'-D~ X{D'D}$_n$X **
-32.43 -32.53 -32.94 -33.03 -33.40 -33.52	Peak 1' Peak2' Peak3' Peak4' Peak5' Peak6' — Cyclic tetramer D' resonances
-34.16--35.78	Higher cyclic species + linears

Table 5.10. The ^{29}Si solution NMR resonance assignments for sample DD'1 (prepared with high initial monomer concentration). * All values in ppm ± 0.01. ** This refers to oligomeric linear species which may be individually identifiable.

The order of the D and D' units within the species is assumed to be random.

Resonance position *	Assignment
-17.97, -18.01	Peak 1
-18.12, -18.14	Peak2
-18.55, -18.56	Peak3
-18.70	Peak4
-19.11	Peak5
-19.25	Peak6
	Cyclic tetramer D resonances
-20.30 - -22.55	Higher cyclic species + linears
-32.49	Peak1'
-32.59	Peak2'
-32.98	Peak3'
-33.07, -33.11	Peak4'
-33.44	Peak5'
-33.57	Peak6'
	Cyclic tetramer D' resonances
-34.66 - -36.11	Higher cyclic species + linears

Table 5.11. The ^{29}Si solution NMR resonance assignments for sample DD'3 (prepared with low initial monomer concentration). * All values in ppm ± 0.01.

Tetramer Resonance	Calculated Probability (D subspectrum)	Calculated Probability (D' subspectrum)	Experimental Intensity (D subspectrum)	Experimental Intensity (D' subspectrum)
			* **	* **
DDDD	0.138	——	2.0±1 / 7±1	—— / ——
DDDD'	0.354	0.354	6±1 / 18±1	2±1 / 6±1
DDD'D'	0.339	0.339	7±1 / 15±1	7±1 / 13±1
DD'D'D'	0.145	0.145	3±1 / 4±1	10±1 / 10±1
D'D'D'D'	——	0.093	—— / ——	3±1 / 3±1

Table 5.12. Calculated probabilities and experimental ^{29}Si solution NMR intensities for the five cyclic tetramer species. * = sample DD'1, ** = sample DD'2.

5.3.2 Adhesion testing.

Samples DD'4, DD'5 and DD'6 were lap shear adhesion tested. Despite problems with material flow, the test geometry of Figure 4.7, with 300mm bond gap, allowed through cured samples to be prepared employing a 250°C, 4 hr heat treatment. The results obtained are given in Table 5.13.

Sample	Composition	Bond strength (KNm)
DD'4	99D 1D'	9±1
DD'5	75D 25D'	4±1
DD'6	1D 99D'	2±1

Table 5.13. Lap shear test results for DD' copolymers.

5.4 ^{13}C MAS NMR investigation of thermally cured D and D' systems -results.

Samples 100D'/1 (200°C / 4hr cure), 100'/3 (220°C / 4hr cure), 100D/1 (200°C / 8hr cure) and 100D/2 (240°C / 4 hr cure) (see Table 4.1 for composition) were investigated using a variety of solid - state NMR techniques, including MAS, DD (dipolar decoupling), CP, variable temperature CP, and CPPI (see 4.1.1.3 for a discussion of these techniques), with a view to gaining an insight into the thermally activated material curing processes. These samples were selected for discussion since their simple composition does not complicate the NMR spectra and they allow separation of curing mechanisms involving CH_3 only from those also involving $CHCH_2$. A summary of the samples investigated is presented in Table 5.14

Spectrum *	NMR technique					Pulse Rate (Hz)	τ_c ** (ms)	T (K)	$\tau_{PI1} = \tau_{PI2}$ *** (μ s)
	MAS	DD	CP	VarT-CP	CPPI				
D'/1SS1	✔					0.5		RT	
D'/1SS2	✔	✔				0.5		"	
D'/1SS3	✔	✔	✔			1.0	2	"	
D'/1SS4	✔	✔	✔			"	10	"	
D'/3SS1	✔	✔	✔			"	2	"	
D'/3SS2	✔	✔	✔			"	10	"	
D'/3SS3	✔	✔	✔	✔		"	"	295	
D'/3SS4	✔	✔	✔	✔		"	"	332	
D'/3SS5	✔	✔	✔	✔		"	"	353	
D'/3SS6	✔	✔	✔	✔		"	"	400	
D'/3SS7	✔	✔	✔		✔	"	"	RT	1
D'/3SS8	✔	✔	✔		✔	"	"	"	20
D'/3SS9	✔	✔	✔		✔	"	"	"	50
D'/3SS10	✔	✔	✔		✔	"	"	"	100
D'/3SS11	✔	✔	✔		✔	"	"	"	200
D/3SS12	✔	✔	✔		✔	"	"	"	500
D'/3SS13	✔	✔	✔		✔	"	"	"	700
D/1SS1	✔	✔	✔			"	"	"	
D/2SS1	✔	✔	✔			"	2	"	

* D'/1 = sample 100D'/1, D'/3 = sample 100D'/3 (Table 4.1)
** = CP contact time (see Figure 4.1)
*** = polarisation inversion times (see Figure 4.2)

Table 5.14. The solid - state ^{13}C NMR experiments performed.

The ^{13}C MAS, ^{13}C MAS DD and ^{13}C MAS DD CP (D'/1SS1, D'1/SS2 and D'1SS3 respectively) are presented in Figure 5.13. The ^{13}C DD CPMAS NMR spectrum of sample 100D'/1, collected by employing a CP contact time ,τ_c, of 2ms (D'/1SS3) and 10ms (D'/1SS4) (both with a pulse repetition rate of 1Hz), are presented in Figure 5.14. Spectra D'/3SS3 - D'/3SS6, obtained using variable temperature CP are presented in

Figure 5.15. This spectrum was obtained using a 10ms τ_c (Table 5.14) and is thus comparable to Figure 5.14b. Spectra D'/3SS8, D'/3SS10 and D'3SS13 (collected using the CPPI technique for a τ_{PI1}, τ_{PI2} of 1, 20, 100 and 700μs respectively) are presented in Figure 5.16. Spectra D/1SS1 and D/2SS1 (samples 100D/1 and 100D/2 respectively) are given in Figure 5.17. Finally, spectrum D'/3SS2 (of sample 100D'/3, cured at 220°C / 4hrs) is given in Figure 5.18.

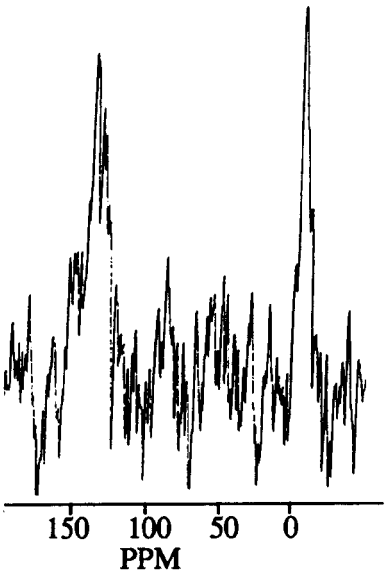

^{13}C MAS NMR

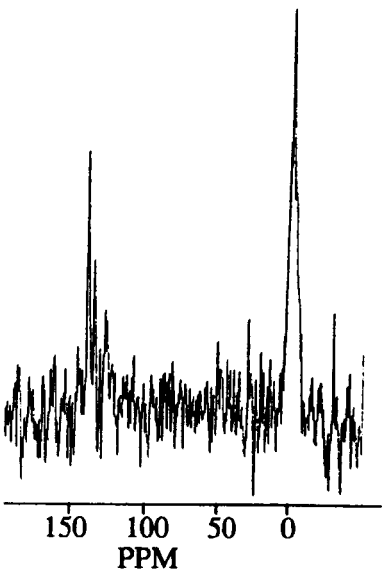

^{13}C MAS DD

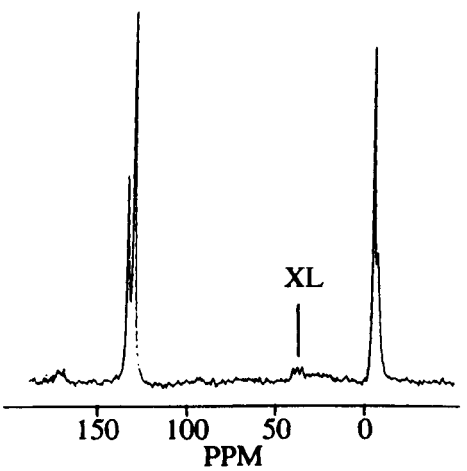

^{13}C MAS DD CP

Figure 5.13. The ^{13}C MAS, MAS DD and MAS DD CP spectra for sample 100D'/1.

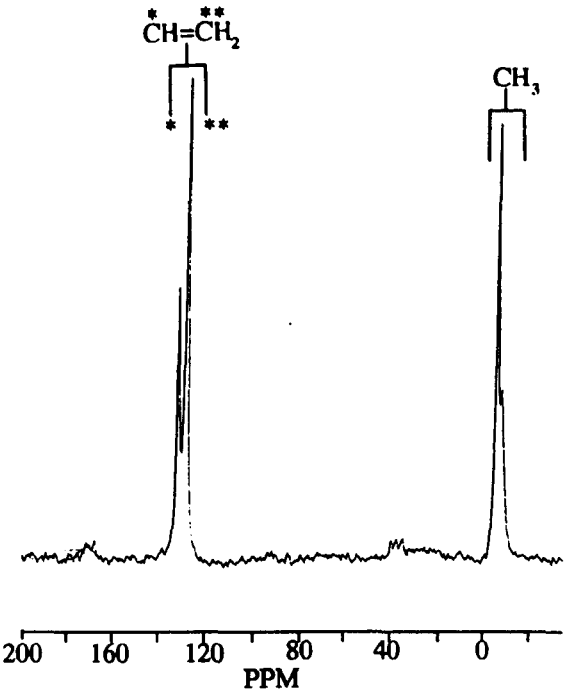

τ_c = 2ms

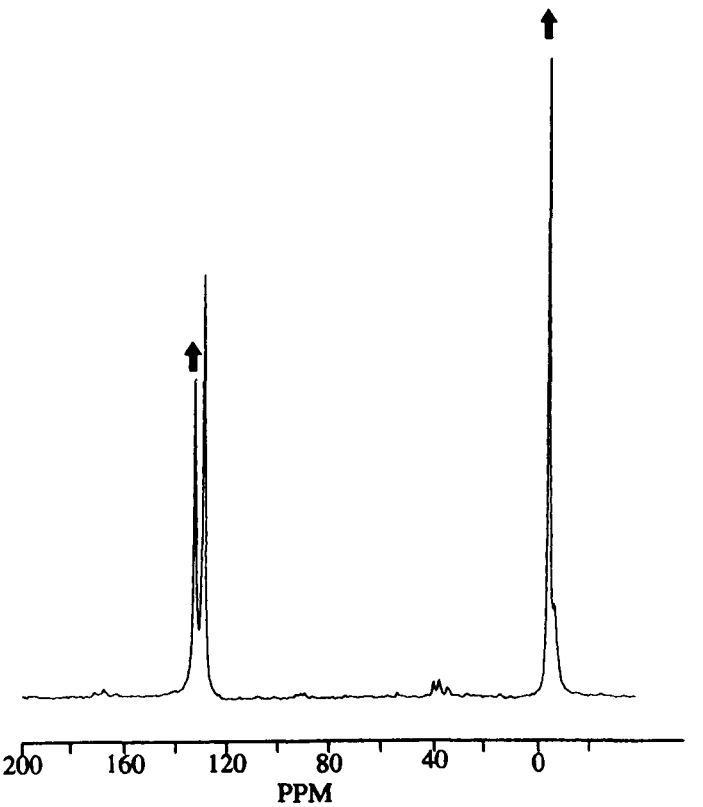

τ_c = 10ms

Figure 5.14. The ^{13}C DD CP MAS NMR spectra of sample 100D'/1, obtained using a contact time of a) 2ms (D'/1SS3) and b) 10ms (D'/3SS4).

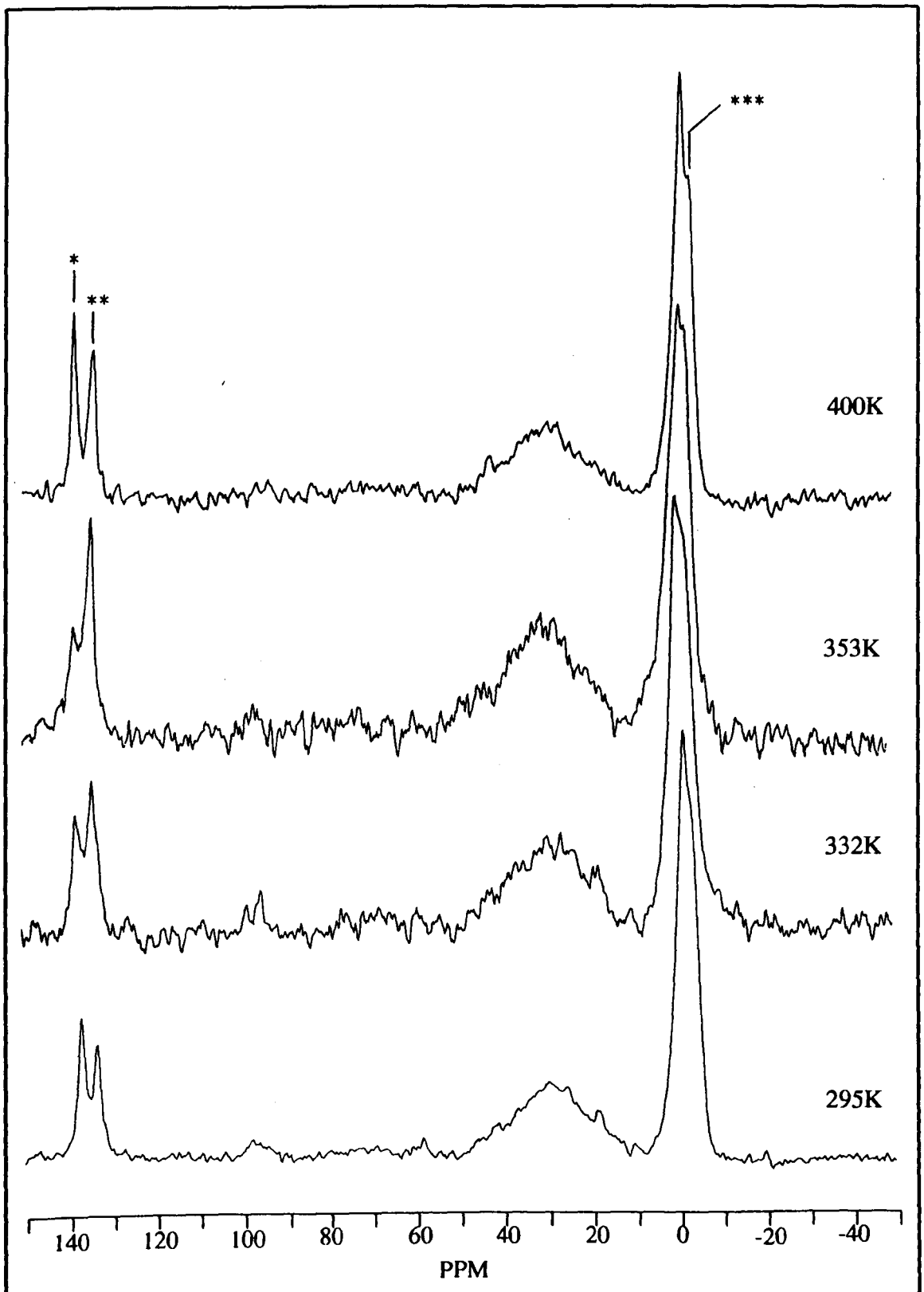

Figure 5.15. The ^{13}C MAS DD CP NMR spectra of sample 100D'/3 (220°C / 4hr) obtained at a range of temperatures between 295 and 400K.

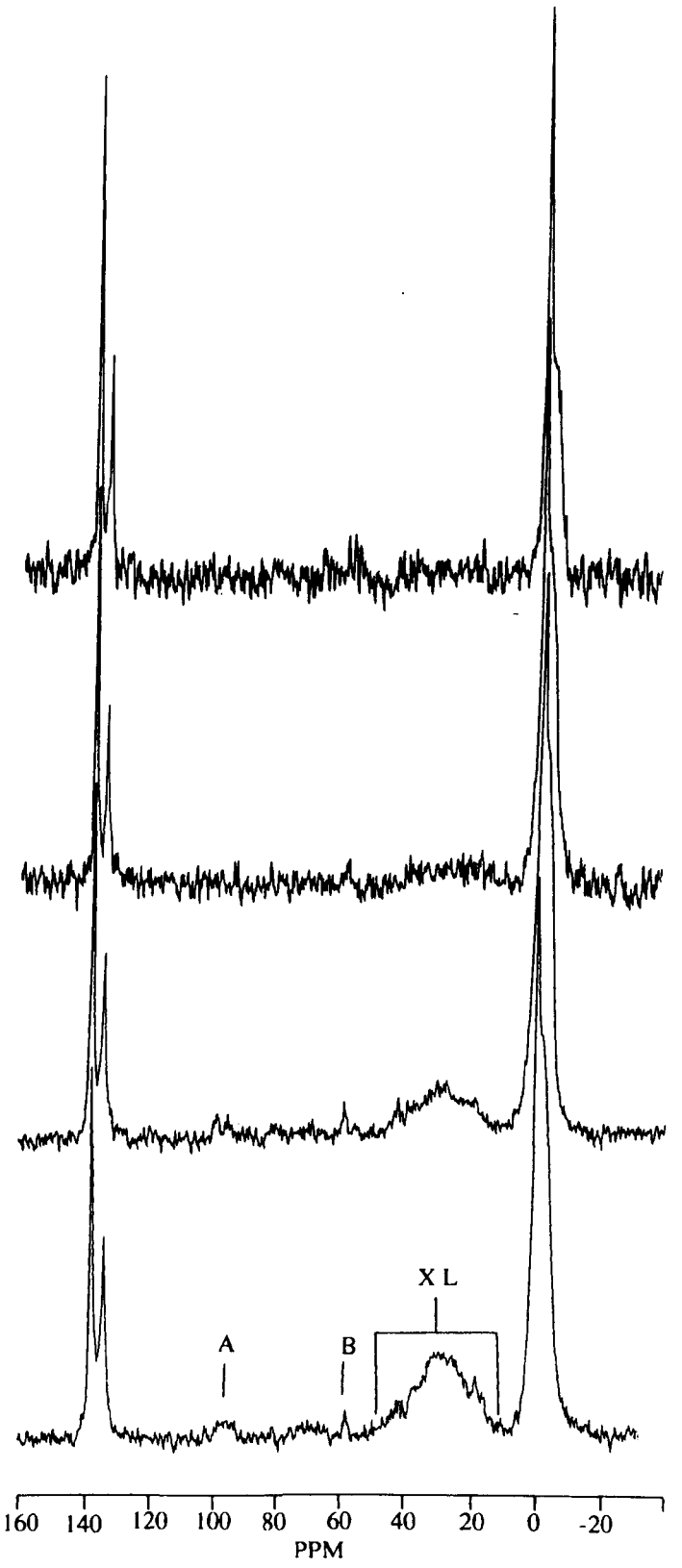

Figure 5.16. The ^{13}C MAS DD CPPI NMR spectra for sample 100D'/3 (200°C / 4hrs) obtained using a τ_{PI1} and τ_{PI2} of between 1 and 700µs.

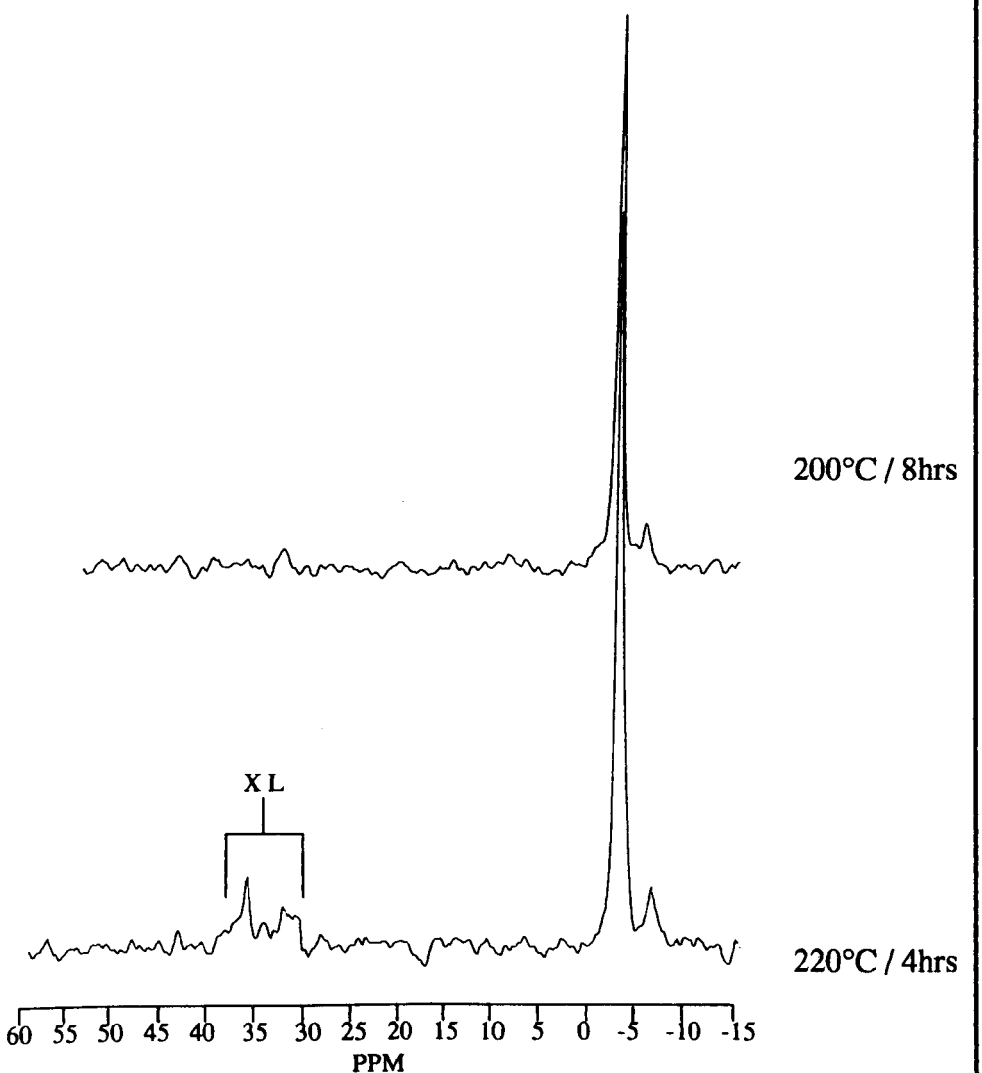

Figure 5.17. The ^{13}C MAS DD CP NMR spectra for samples a) 100D/1 (200°C / 8hrs) and b) 100D/2 (220°C / 4hrs).

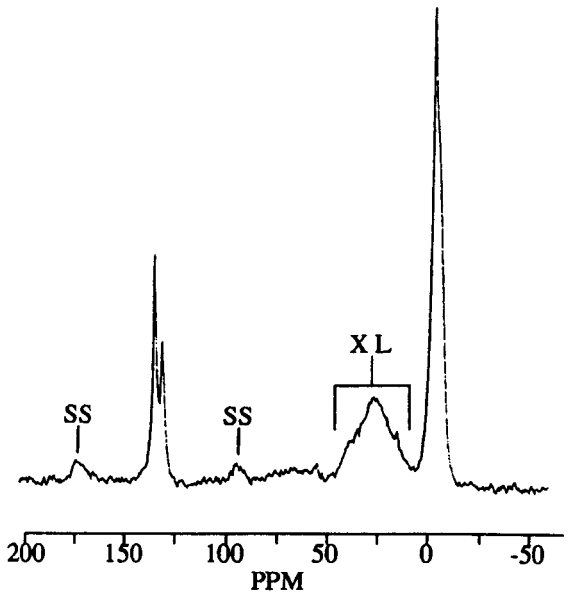

Figure 5.18. The ^{13}C MAS DD CP NMR spectrum of sample D'/3 heated 220°C / 4 hrs

5.5 Discussion

5.5.1 The D system

From the results of the NMR of samples D1, D2 and D3, as summarised in Table 5.2, it can be seen that, as prepared by the standard route (4.7), the system is strongly dependent upon the concentration of the monomer. Since NMR is a quantitative tool, the ratio of intensities of the resonances would be expected to reflect the populations of the species within the sample, provided that the conditions of the NMR do not compromise the intensity of any particular resonance. Although Si species generally have a relatively long T_1, it has been shown that there is very little difference in T_1 between species within a chain [129]. Since this work relies on quantitative NMR results, a typical PDMS sample was investigated, with spectra taken using pulse repetition rates of 10 and 60 seconds. No signal saturation was oberved (see 6.2, Table 6.4). On this basis, p_w, the fractions of cyclic D resonances within the systems were calculated and are given in Table 5.15, along with their component ratios. Under concentrated conditions, tetramers are predominantly cyclic, with 85% of the D units contained within them. Their level drops at medium dilutions but rises again at higher dilution. The lack of cyclic trimer within these systems may not be exclusively a result of strain energy excluding their production at ambient temperatures. In fact, the neutralisation stage of the preparation causes the system temperature to reach 78°C, and, as the trimers' boiling point is only 134°C at 760 mmHg [36], a loss of trimer by volatilisation is likely, although evidence against this is presented in 6.6.1. With increasing dilution it can be seen from Table 5.15 that the fraction of cyclics strongly increases, as is predicted by the J - S theory [53]. As stated above, these samples were prepared via the standard preparation route and as such, were subject to a certain degree of dilution

during the acid neutralisation stage. Thus, a more realistic concentration value would be that at the point where the system was just neutralised. This value, C_{neut}, is obviously more significant for the higher concentration samples due to the large differential between the solvent and the KOH solution volumes. C_{neut} values for the samples D1 - D3 are given in Table 5.15, and were calculated on the basis of the EtOH volume added, assuming water to be a very poor solvent. p_w is most sensitive to system dilution at low dilution (Figure 5.19). This may be accounted for by the possible local high pH in less dilute systems. As encapsulation materials, exposure to temperatures of 200°C and above during the curing procedure would possibly be routine. Cyclic siloxanes are known to have poorer thermal properties than their linear α - ω diol counterparts, as shown in Table 5.16 [36]. This is principally due to the unavailability in cyclic systems of hydrogen bonding between neighbouring species. All three samples contain a reasonably large percentage of cyclic species and thus, on the basis of the values of Table 5.15, even a material prepared under concentrated conditions would, upon heating, be expected to lose a large proportion of mass, as was observed by TGA

Sample	p_w	% Tetramer	% Higher cyclic	$1 / C_{neut} (M^{-1})$
D1	0.21±0.01	85±10	15±3	0.15±0.01
D2	0.78±0.04	16±2	85±8	0.27±0.02
D3	0.84±0.03	55±4	45±3	1.25±0.02

Table 5.15. Parameters for the cyclic species of D systems, obtained from the ^{29}Si NMR spectra (Figures 5.1a - 5.1c)

(Figure 5.3). A suitable material might be prepared by operating in the very low dilution region of Figure 5.19. This is impractical however, since dilution with both hydrolysis

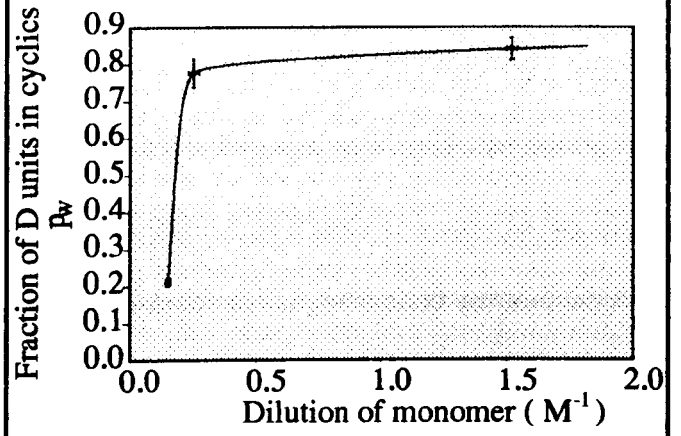

Figure 5.19. The fraction of cyclic D units within the D samples plotted as a function of the monomer dilution.

Species	Bpt (°C) (at 760 mmHg)
$HO[(CH_3)_2SiO]_3H$	268
$HO[(CH_3)_2SiO]_5H$	282
$[D_3]$	134
$[D_4]$	175
$[D_5]$	210

Table 5.16. The boiling point of a number of linear and cyclic siloxanes.

water and neutralising solution is unavoidable. The preparation route could be considered in two stages, an initial hydrolysis period under strongly acidic conditions, followed by neutralisation to pH 8 - 9 and reaction for 3 hours. Strongly acidic conditions favour cyclisation [48], thus this preparation route is unsuitable for preparation of low cyclic content materials. Alkoxysilanes, which, upon hydrolysis, only have alcohol as their by product, would be more favourable precursors for this reaction but their cost is higher than the equivalent chlorosilanes. Information about the nature of the linear species within these materials is given by both the ^{29} Si NMR and the GPC results. The average degree of polymerisation, DP_{av}, may be obtained directly from the NMR spectra using the method proposed by La Rochelle [131], with DP_{av} given by equation 25, where I_{bl} and I_{el} refer to the bulk linear and end group resonance intensities. This method is only applicable to materials in which the linear species are of a length sufficient for the end group resonances to

$$DP_{av} = 2 (I_{bl} / I_{el}) + 2 \qquad (25.)$$

be observed, and thus cannot offer information concerning the DP_{av} of the linear component of sample D1 although from intensity considerations, this must be greater than 80 (otherwise end resonances would be significant). The NMR average degree of polymerisation of samples D2 and D3 are 7±2 and 12±3 respectively. This indicates that the linears are oligomeric in nature with no significant difference in the size of the linears over the range of dilution ($1 / C_{neut}$) 0.5 to 1.5 M^{-1}. This insensitivity at higher dilution is also reflected in the observed invariance of the cyclic fraction level within this region (Figure 5.19). An interesting feature of both samples D2 and D3 is that more than one end group resonance is observed. Since the Si-Cl bond is very easily cleaved [39] (3.2.2.1) it is reasonable to assume that the contribution from Si-Cl is negligible, suggesting that the only possible species could be $-(CH_3)_2SiOH$ (M^{OH}) and $-(CH_3)_2SiOC_2H_5$ (M^{OR}). For sample D2 and D3 there are clearly two end group resonances (see Table 5.2). The position of the more downfield (higher frequency) resonance suggests this to be an $\underline{M}^{OH}$ species [132]. The upfield resonance position is comparable to the $-(CH_3)_2SiOCH_3$ resonance position of -12.00 to -12.5 ppm given by Engelhardt et al [121] (the substitution of the OCH_3 by a OC_2H_5 resulting in only a small upfield shift [133]). Resonance positions for M^{OH} are quoted as being between -11.0 ppm [131, 133] and -14.0 ppm [134], these being sensitive to both the species to which these are attached and to their environment. Less data is available for the M^{OR} resonance (Engelhardt quotes a value of -12.0 to -12.5 ppm) [121]) and this would be expected to have a similar dependency as M^{OH}.

The information obtainable from the GPC is limited due to i) no calibration curve being available with which to obtain M_n and M_w values, and ii) the peaks in the

chromatograph (Figure 5.2) will be a convolution of the linear and cyclic distributions, each having an unknown molecular mass distribution (MMD). It can be said though that there is a large relative increase in the maximum mass of the species prepared when moving to a non solvated system, as is indicated by the parameters in Table 5.3 and by the shift in the peak of the chromatograph to lower elution time. It can also be seen that the higher mass peak of D4 is much broader than that of D5, indicating a higher polydispersity and a wider spread of the degree of polymerisation of the species.

5.5.2 The D' system

Analysis of the results of the NMR of the D' samples, Figure 5.7, indicates that, as for the D system, there is a high dependency upon the system dilution. The D' preparations followed the same route as the D systems and, as such, can also be considered to be two stage (see 5.5.1 for details). D_{av}, p_w, the percentage of D' units within the cyclic tetramer, and $1 / C_{neut}$ (the system dilution at neutralisation) are presented for each sample in Table 5.17. A plot of p_w as a function of system dilution is shown in Figure 5.20. As can be seen from Table 5.17, increasing sample dilution provides a decreasing linear polymer yield and also a concomitant decrease in the average length of these species. Note that for sample D'9, the value of D_{av} is subject to a large error due to the low intensity of both the bulk chain and end group resonances. The average lengths of polymer within D'2 and D'7 do not agree within experimental error, despite being prepared under, as far as possible, identical conditions. The formation of the linear polymer is thus very sensitive to small changes in reaction conditions. The preparation route is subject to a large number of variables (4.7) and the linear polymer may be particularly sensitive to one or more of these. The sensitivity of polycondensation

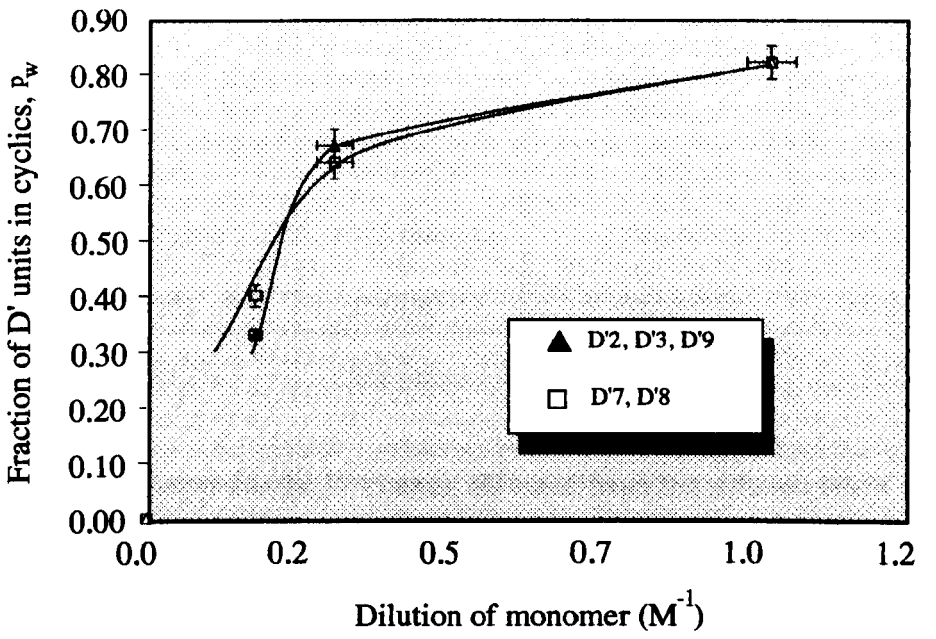

Figure 5.20. The fraction of cyclic D' units within the D' samples, plotted as a function of system dilution.

reactions to the catalytic environment has already been discussed (3.2.4), and as the control of the pH was fairly crude, with no controlled rate of addition being employed, it is likely that the resulting small variations in the pH - time profile may account for the observed differences in polymer structure. Assuming the cyclics do not significantly contribute to the broadness of the MMD of sample D'2 (Figure 5.21), a polydispersity of 2.53 indicates a broad distribution of species within the linear polymer. Conversely, the MMD of sample D'3 is very narrow, with a polydispersity of 1.22 (Table 6.6, Figure 5.20), as would be expected, considering the large proportion of low cyclic species. Comparison of the values of p_w obtained from the NMR results (Table 5.17) and the values obtained from the GPC is complicated by i) the process of alcohol exchange having occurred in these materials, as indicated by the two types of end group species (-24.60 and -26.53 ppm of Figure 5.4a), which, with reference to the D system spectral assignmemts (section 5.5.1), may be assigned to Si-OH and Si-OC_2H_5) [120, 121] and ii)

Sample	D_{av}	p_w	% cyclic tetramer	D_{neut} (M^{-1})
D'2	19±1	0.37±0.01	57±3	0.18±0.01
D'7	11±1	0.40±0.03	57±4	0.18±0.01
D'3	12±1	0.67±0.03	51±3	0.31±0.03
D'8	6±1	0.64±0.03	51±3	0.31±0.03
D'9	6±2	0.82±0.03	58±3	1.03±0.04

Table 5.17. Parameters for the D' system, obtained from the solution NMR results.

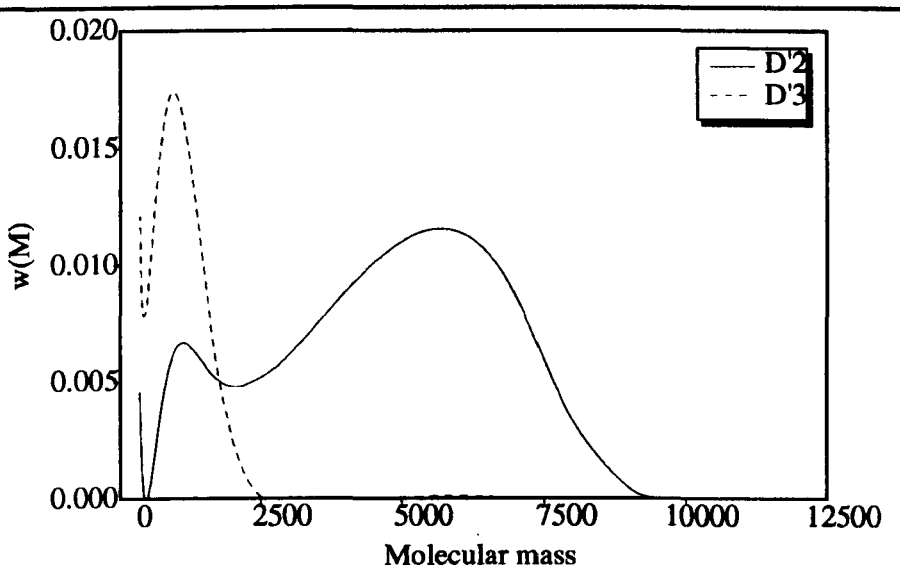

Figure 5.21. The MMD of samples D'2 and D'3, calculated for linear materials. Note, these MMDs were obtained from the equations of Appendix II and Figure II.1.

	D'2		D'3	
100% Si-OH	22 ± 1	(19 ± 1, 11 ± 1)	8 ± 1	(12 ± 1, 6 ± 1)
100% Si-OR	21 ± 1		7 ± 1	

Figures in parentheses are NMR values.

Table 5.18. The degree of polymerisation calculated from the GPC data of samples D'2 and D'3 and assuming 100% linear materials.

the presence of any cyclic material within the samples. The NMR average degree of polymerisation was calculated for D'2 and D'3 assuming 100% linear species and either 100% Si-OH or 100% Si-OC_2H_5 chain end occupancy. The results of this are presented in Table 5.18. As can be seen from Table 5.18, the type of end species attached to the linears does not have any significant effect upon the calculated species lengths outside the experimental error. The values are comparable to the NMR data and show similar trends but, as was discussed for the NMR data, DP_{av} is highly sensitive to preparation conditions.

The increase in p_w with dilution is seen to be consistent between samples prepared identically (see Figure 5.20), suggesting that the development of the cyclic is less sensitive than the linear polymer to the reaction conditions. This suggests that, as for the D system (5.5.1), the cyclics are preferentially formed in the first stage of the preparation. The values of p_w at high dilution appear to tend to those found for the D system. The levels of tetramer within these systems are independent of the system dilution, which is inconsistent with both the Jacobson - Stockmeyer theory [53], which predicts an increase in the population of the lower cyclics with increasing dilution, and with the results for the D system. The cyclic trimer is seen in the NMR spectra of sample D'5, (Table 5.8), prepared by maintaining the system temperature to below 5°C. This supports the suggestion that lack of trimer within samples prepared by the standard route is predominantly due to evaporative loss. The intensity of this resonance is much lower than that of the tetramer, even when taking into account the smaller number of units within the trimer compared with the tetramer. The low concentration of this species is probably due to the trimer being strained [48]. The lower temperature

preparation also resulted in a 15% higher than expected higher cyclic population (compared to trend observed in Figure 5.20) and a much reduced degree of polymerisation within the linear fraction (DP_{av} of 3.4±0.5). The increased cyclisation probably occurs during the extended reaction period at low pH (as a result of the required slow addition of the KOH solution to maintain the low temperature). The increased oligomerisation of the linear fraction is thus concomitant with a lower number of monomers available in the system.

Thermal treatment of sample D'5 at 150°C for 1 hr promotes a number of structural changes, as indicated in Table 5.8. The greatest loss was observed for the cyclic trimer, having been reduced to 30% of its original level. Losses are also observed for the whole of the cyclic component. These losses may be due to their evaporation, although increases are observed for both the bulk linear and the end group resonances, the largest gain being in the latter. This would suggest that the trimer has been ring opened by catalyst (base) residual in the system (see 3.2.5), thus increasing the linear component, and particularly, the oligomeric population.

The mass loss of a typical D' sample (D'9), when heated to a cure temperature of 200°C (Figure 5.10) of 43 wt% is only 66% of that for the equivalently prepared D sample (Figure 5.3) although this is still an unacceptably high value. Also, over the temperature interval 200 - 350°C, the percentage mass losses are 5±1 and 15±1 % for samples D'9 and D11 respectively. These differences may result from the development of an organic network through thermally induced cross - linking reactions involving the vinyl groups within the D' sample, which is not available within the D sample.

5.5.3 The D'D copolymer.

^{29}Si NMR may be used as a tool to determine microstructural details within copolymers [127]. In particular, a very useful parameter, the run number, is easily determined. This defines the average number of units of one type that run consecutively within the polymer and allows the degree of randomness of the structure to be assessed. To obtain this type of information, a number of requirements need to be met. Firstly, the exact composition of the polymer has to be known, and secondly, since the analysis entails a statistical study of the triads within the system, no degree of cyclisation can be tolerated. In the case of the DD' materials, the former is known, assuming that the initial precursor ratio reflects the ratio of the monomers in the final system. The latter though does not hold for these materials as the presence of cyclisation is clearly evident in their NMR spectra (Figure 5.12). The ordering within individual species may still be investigated, and a comparison between samples made. The chosen candidate for this study is the cyclic tetramer since this is clearly distinguished from other resonances and, being unstrained, should reflect the ordering of the system as a whole. Prior to such a study, a check should be made on the peak assignments made for the cyclic tetramer. Each spectrum of Figure 5.12 can be seen to consist of two subspectra, one for the D resonances and one for the D' resonances. From a purely statistical point of view, the sum of all the D intensities arising from one tetramer type (of the five presented in Table 5.12) must be related to the sum of D' intensities for the same species by the rules given in Table 5.19. It can be seen from Table 5.12 that, within the experimental error, these conditions are met and therefore the assignments of Table 5.11 and Figure 5.11 are justified.

Assuming that there is no preferred condensation between like or unlike species, the distribution of D and D' within each species would be random. Thus, based on a composition of 61D : 39D', the expected probabilities for the tetramer species may be calculated and are given in Table 5.12. Also given in Table 5.12 are the experimental intensities for both samples DD'1 and DD'2 and the ratio of these experimental intensities to those calculated for a random system are shown in Figure 5.22. From this it can be seen that neither shows a random distribution. DD'1 (solventless preparation) has an bias towards the D'D'D'D' cyclic and DD2' (4.0M preparation) has a more even distribution but shows a small bias towards DDDD and DDDD' species.

Although the lap shear tests were limited in number, due primarily to the difficulty in test sample preparation, a number of points can be made. The failure mechanism in all cases was cohesive failure of the sample material. A decrease in cohesive strength of the materials with an increase in vinyl content was observed (Table 5.13), although the sample set was small. This may be as a result of the increased organic cross - link density of the high vinyl sample reducing the chain flexibility.

Tetramer (in D subspectra)	Intensity	Tetramer (in D' subspectra)	Intensity
D'DDD	3	D'DDD	1
D'D'DD	2	D'D'DD	2
D'D'D'D	1	D'D'D'D	3

Table 5.19. The relationship between the intensities between the resonances within the D and D' subspectra for the tetrameric cyclic species.

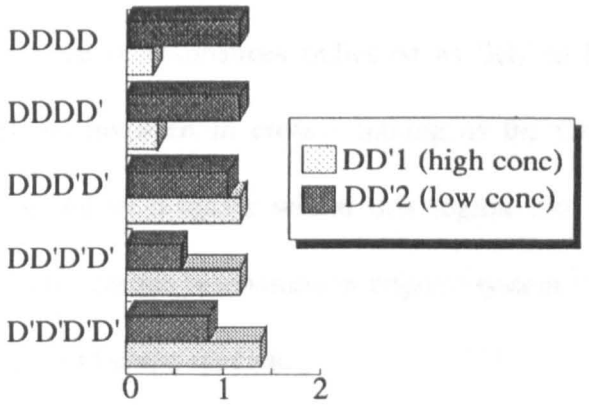

Figure 5.22. The ratio of the experimental intensities to those expected for a random distribution for D and D' units within the cyclic tetramer.

5.5.4 ^{13}C MAS NMR study of the D and D' systems.

The greater effectiveness of cross - polarisation (CP) over dipolar decoupling (DD) in obtaining a high resolution decoupled spectrum of heat cured polysiloxanes is demonstrated in Figure 5.13. The MAS DD spectrum of a 200°C / 8hr cured D' system (Figure 5.13b) is clearly no better resolved than the proton coupled spectrum (5.13a), obtained under otherwise identical conditions. It should be noted that the MAS DD spectrum was acquired using a larger number of pulses and, taking that into account, the signal to noise ratios (S/N) of the two are comparable. Using CP, a low noise, high resolution spectrum is obtained (Figure 5.13c) with line widths of the order of 90Hz (including 50Hz of applied line broadening - as was also applied to the previous two spectra). The efficiency of CP is fundamentally dependent upon the strength of the static dipolar interaction [135], which is greater for a rigid system than in more mobile elastomers and liquids. The high S/N observed in Figure 5.13c implies that the polymer systems investigated are indeed rigid, being below or very near to T_g and possessing a strong static component to the dipolar interaction. The narrow lines suggest that the

system is amorphous since any degree of crystallinity would result in a broadening of the resonances [136]. The group of resonances indicated as 'XL' in Figure 5.13c are thought to arise from carbons involved in cross - linking as the CH_3 and $CH{=}CH_2$ carbons would not be expected to resonate within this region (30 - 40 ppm). with reference to literature values for carbon resonances in organic system [137] these may be tentatively assigned as $-CH_2-$ mid chain species.

The CP spectrum of this sample is shown in more detail in Figure 5.14a. Three main resonance groups are observed, being 141.5±0.6 - 121.4±0.6 ppm, 42.8±0.6 - 33.7±0.6 ppm and 1.3±0.6 - 13.6±0.6 ppm. The first group, a doublet (124.7±0.6, 138.4±0.6 ppm) is assigned to the β and α carbons of the vinyl group ($Si\text{-}C^{\alpha}H{=}C^{\beta}H_2$) of the D' unit. These assignments are based on those reported by Schraml et al [138] for $((CH_3)_3SiO)_2(CH_3)Si(CH{=}CH_2)$ (see Figure 5.23), measured in 90% solution in C_6D_6. The triplet at mid frequencies (40.7±0.6, 37.5±0.6 and 35.0±0.6 ppm) are, as previously stated, assigned to cross - link carbons. The more intense of the two upfield resonances (-4.9±0.6 ppm) is assigned to the CH_3 group of the D' unit, but is more upfield (shielded) than the value of -0.2±0.3 reported by Schraml [138]. The lower intensity resonance at -5.9±0.6 ppm would not be expected in an uncured D' system since only one CH_3 environment would exist, it is thus proposed that this group is associated with the cross - linking. A significant difference is seen between the spectrum acquired using a 2ms contact time and that obtained using a 10ms contact time. In particular, the α carbon of the vinyl group and the CH_3 resonance are both observed to increase in intensity (as indicated in Figure 5.14). The former may be accounted for by the α carbon possessing fewer directly attached protons than the β

carbon and thus the rate of polarisation transfer for the latter is reduced. The lower polarisation rate of the methyl group, despite its three directly attached protons, is probably due to it being highly mobile, thus reducing the CP efficiency. The rapid polarisation transfer rate of the lower intensity CH_3 resonance (as inferred from its invariance to an increase in τ_c) suggests this to be less mobile than the slightly downfield CH_3. It is proposed that this resonance is a methyl group attached to a silicon, upon which the vinyl group has been reacted to form a cross - link.

Curing of the D' material at a higher temperature (220°C / 4hrs) results in a large increase in the intensity of the proposed cross - link resonance (Figure 5.18), and a concomitant decrease in the vinyl β (note peaks marked as SS on Figure 5.18 are spinning side bands, these being noticeable for unsaturated carbons as a result of their large chemical shift anisotropy [136]). The increase of the cross - link resonance is complemented by a growth of the upfield CH_3 resonance, which is commensurate with an increase in the number of D' units with reacted vinyl groups. The broadness of the cross - link resonance may be possibly due to a large number of resonances coalescing but may also be due to a few wide resonances, the breadth resulting from a lack of mobility, possibly even associated with a degree of crystallinity.

Spectra D'/3SS3 - D'/3SS6 were obtained at temperatures 295 - 400K using an identical pulse program to that employed for the previous spectrum. It is apparent from Figure 5.15 that the lineshape of the cross - link species is very little affected by an increase in temperature, suggesting that the species may be partially crystalline, since the line shape of resonances arising from an amorphous system would be expected to be greatly

influenced by temperature due to the sensitivity of the line width to molecular motion [100]. The vinyl resonances are very much affected by temperature, with the α carbon resonance halving in intensity (relative to the β carbon over the temperature range 295 - 353K. Thus the α carbon is much more sensitive to thermally activated molecular motion than the β carbon. This is unusual since both carbon atoms would be expected to have similar degrees of freedom. The insensitivity of the β carbon to temperature may be explained if the resonance is assumed to possess contributions from both mobile and immobile carbons. Schraml [138] suggests that $-CH_2-CH^*=C$ carbons resonate at a position very close to that of the β carbon of a vinyl group (see Figure 5.23). A proposed possible structure, resulting from a vinyl - vinyl interaction is given in Figure 5.23C. The α and β carbons of structure C would be expected to resonate at similar frequencies as 1' and 2' of structure B. The α carbon resonance for the cross - link structure may thus be within the broad group of resonances, indicated as XL of Figure 5.18. The β carbon of structure C could thus act as the immobile component of the =CH resonance of Figure 5.15. The trend reversal seen in the 400K spectrum may be due to the material having passed through T_g, with an associated higher cross - link mobility equalising the polarisation rates of the α carbon (vinyl) and the two β carbons (vinyl + cross - link). The upfield CH_3 resonance appears to increase in intensity with increasing temperature. This is probably due to an overall line narrowing as a result of heating of the shim coils.

Over the range of polarisation inversion times 20 - 700μs, all resonances are suppressed to some degree with the most marked supression being of the proposed cross - link species (see Figure 5.16). With reference to Wu and Zilm [107], it is inferred that these

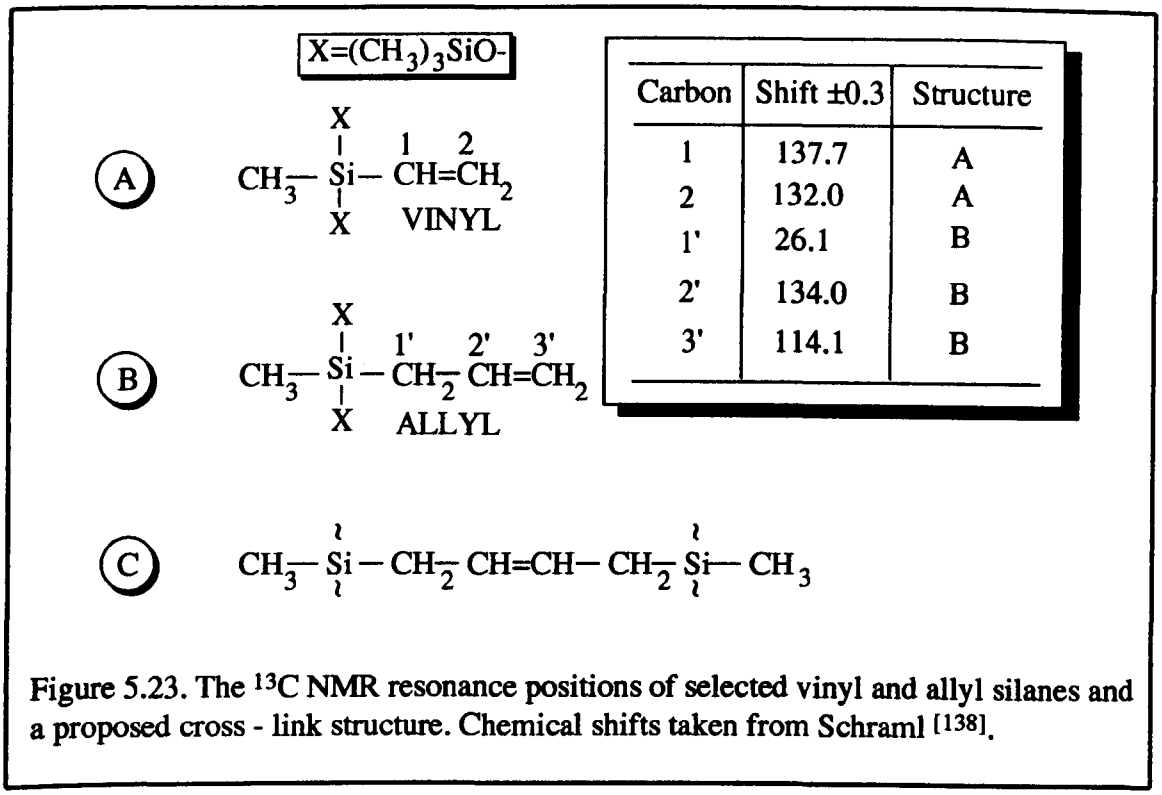

Carbon	Shift ±0.3	Structure
1	137.7	A
2	132.0	A
1'	26.1	B
2'	134.0	B
3'	114.1	B

Figure 5.23. The ^{13}C NMR resonance positions of selected vinyl and allyl silanes and a proposed cross - link structure. Chemical shifts taken from Schraml [138].

resonances are from $-CH_2-$ species, as was previously suggested. Suppression of the CH_3 resonances is much less pronounced, with a sizeable signal remaining after a 700μs polarisation inversion time. The resonance marked 'A' is a spinning sideband from unsaturated carbons. The small supression of the α carbon resonance is undestandable, this being a CH group, which , according to Wu and Zilm, requires substantially longer PI times before significant supression occurs. The absence of a marked suppression of the β carbon resonance suggests this to be largely of structure C of Figure 5.23.

Finally, comparison of the ^{13}C MAS CP NMR spectra of samples 100D/1 (200°C / 8hrs) and 100D/2(240°C / 4hrs) (Figure 5.18), indicates that a cross - linking mechanism also occurs within D systems, as evidenced by the growth of the low intensity resonance at 30 - 40 ppm (commensurate with $-CH_2-$ species).

CHAPTER 6: MONOFUNCTIONAL END - CAPPED POLYMERIC POLYSILOXANE MATERIALS - RESULTS AND DISCUSSION

6.1 Sample preparation

A summary of the samples prepared is given in Table 6.1. All the materials were prepared following the standard preparation route (4.7). The end blocking precursors were co - hydrolysed and co - condensed in situ with the chain forming precursors. The end - blocking precursors used were either chlorotrimethylsilane ($(CH_3)_3SiCl$ - CTMS) or allychloroldimethylsilane ($(CH_2{=}CHCH_2)(CH_3)_2SiCl$ - ACDMS). Both of these are, in the sense of their inorganic networking ability, monofunctional. ACDMS, possessing an unsaturated bond, offers the possibility of extending the organic network via suitable organic polymerisation reactions, as previously discussed (3.3). The reagents were hydrolysed with a stoichiometric volume of water and, as for the difunctional materials, reacted for ½ hr prior to neutralisation. It can be seen from Table 6.1 that both single component and copolymeric materials were prepared using DCDMS and DCMVS as difunctional chain formers. It should be noted that the samples listed in Table 6.1 are not the total sum of all the samples prepared and in many cases, multiple samples were prepared via an identical route but were employed in separate areas of the study. A note should also be made of the notation used in Table 6.1. M and M^A denote the use of CTMS and ACDMS respectively in the preparation, D and D' indicate the use of DCDMS and DCMVS as denoted in previous sections (5.1, 5.2). (Al_2O_3) and (Al) appended to the dielectric spectroscopy studies within Table 6.1 indicate the substrate material used in each study. As a preliminary study, it was important to identify the species formed in a co - polymerisation of the monomeric and difunctional units. For this ^{29}Si solution NMR was employed.

Sample	Composition (mol%)	Preparation Conditions	Reason for preparation
EB1	0.05M 99.95D	Standard route 5.6 M	Immersion bias testing Dielectric spectroscopy (Al_2O_3) Dielectric spectroscopy (Al)
EB2	0.5M 99.5D	Standard route 5.6 M	Dielectric spectroscopy (Al_2O_3) Dielectric spectroscopy (Al)
EB3	2M 98D	Standard route 5.6 M	$^{29}Si\ sol^n$ NMR Adhesion testing Dielectric spectroscopy (Al_2O_3) Dielectric spectroscopy (Al)
EB4	10M 90D	Standard route 5.6 M	$^{29}Si\ sol^n$ NMR Dielectric spectroscopy (Al_2O_3) Dielectric spectroscopy (Al)
EB5	50M 50D	Standard route 5.6 M	$^{29}Si\ sol^n$ NMR Dielectric spectroscopy (Al_2O_3)
EB6	$0.05M^A$ 99.95D	Standard route 5.6 M	Immersion bias testing Dielectric spectroscopy - (H_2O immersion)
EB7	$0.5M^A$ 99.5D	Standard route 5.6 M	Immersion bias testing Dielectric spectroscopy (Al) u.v curing trials
EB8	$0.5M^A$ 99.5D	Standard route 5.1 M	Immersion bias testing
EB9	$2M^A$ 98D	Standard route 5.6 M	Adhesion testing Immersion bias testing
EB10	$5M^A$95D	Standard route 5.6 M	Dielectric spectroscopy (Al)
EB11	$10M^A$90D	Standard route 5.6 M	Dielectric spectroscopy (Al)
EB12	2M D' 97D	Standard route 5.6 M	Adhesion testing Immersion bias testing Introduction of mercapto cross - linking species Dielectric spectroscopy (Al)
EB13	2M 5D' 93D	Standard route 5.6 M	Adhesion testing / dielectric
EB14	2M 25D' 73D	Standard route 5.6 M	Adhesion testing Immersion bias testing Dielectric spectroscopy (Al)
EB15	$0.5M^A$D' 98.5D	Standard route 5.6 M	Immersion bias testing

Table 6.1. The monofunctional end - capped, difunctional polysiloxane samples.

6.2 A ^{29}Si solution NMR study of the structure of monofunctional end - capped polymeric species from a co - polymerisation of CTMS and DCDMS.

Trimethylsiloxy ($(CH_3)_3SiO$-) terminated, polydimethylsiloxane materials (from here on referred to as x mol% TMSO t - PDMS, where x denotes the mol % of CTMS within the co - polymerisation) were prepared as above. This system was chosen for investigation since the spectra are uncomplicated by tacticity effects (Appendix I), thus allowing easier peak assignment.

Notes on the nomenclature used in the peak assignments: The linear species are denoted as MD_nM, (M=M, M^{OH}, M^{OR}), where M = $((CH_3)_3SiO$-), M^{OH} = $(CH_3)_2(OH)SiO$- and M^{OR} = $(CH_3)_2(OC_2H_5)SiO$-.

The D units of the linear species are identified by their position from the end unit, ie: M(D1)(D2)(D3)$\cdots$ etc, where M = $((CH_3)_3SiO$-), M^{OH} = $(CH_3)_2(OH)SiO$-, and M^{OR} = $(CH_3)_2(OC_2H_5)SiO$-.

All D units D(4+) are identified as D^*_{BL}, ie, 'bulk linear' units.

The ^{29}Si NMR spectra for samples EB3, EB4, EB5 (2, 10 and 50 mol% TMSO t - PDMS), are presented in Figure 6.1. Both M^{OH} and M^{OR} end groups are present in all three samples, with resonance positions as given in Table 6.2, and as indicated in Figure 6.1. As in section 5.4.1, it is difficult to identify which end group is which as a result of the closeness of the two resonances, their sensitivity to the environment [133] and the

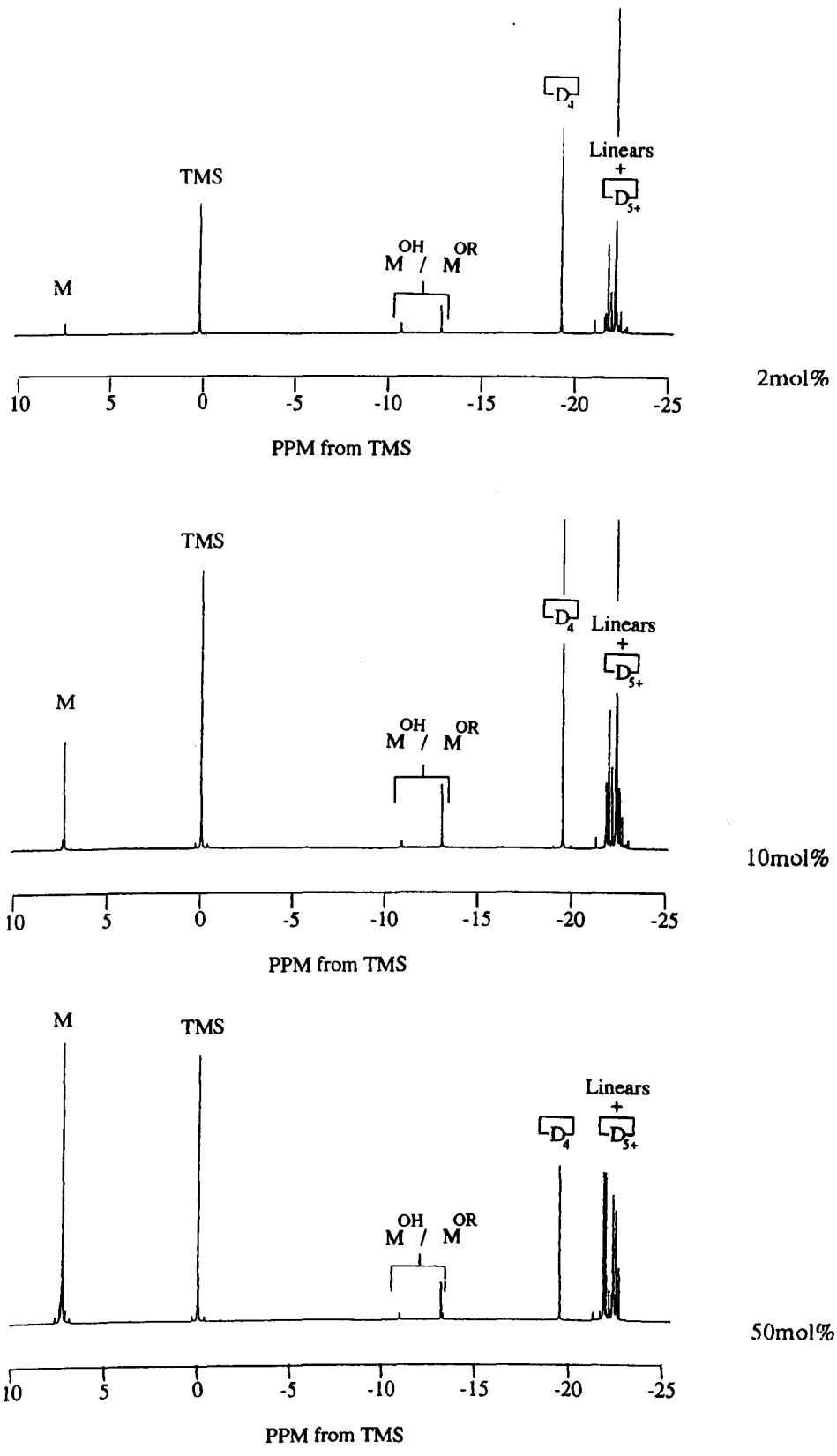

Figure 6.1. The ^{29}Si solution NMR spectra for samples a) EB3, b) EB4 and c) EB5 (2 mol%, 10 mol% and 50 mol% trimethylsiloxy end capped PDMS).

overlap between the literature values [131, 133, 134]. The M units are evident at 7.22±0.01 - 7.29±0.01 ppm (Table 6.2), these being close to those reported by Harris and Robins [133] of 7.22 ppm and 7.26 ppm (obtained for chains of DP_{av}= 26 and 64 respectively). The D resonance subspectra are complex, having resonances from both oligomeric and polymeric linears and from cyclics. Since three types of end group species are present in these materials, the diversity of linear species is possibly very broad. With reference to Burton et al [124], the cyclics up to the octomer level were identified as shown in Figure 6.2, and having intensities as given in Table 6.2. Cyclics above the nonomer are not easily identifiable as their reonance positions overlap with those of the linears [124]. Based upon the trend observed for the other cyclics, that of a decreasing population with increasing ring size, it is assumed that the higher cyclics are not present in any significant quantity. The bulk linear resonance, D_{BL}*was identified for all three samples (Figure 6.2, Table 6.3) using the value offered by Harris and Robins [133] and assuming that the position of this resonance is independent of the type of end species attached to the chains, as is supported by Harris and Robins [133]. The remaining unidentified resonances of Figure 6.2 originate from the oligomeric species MD_nM (n<4, M=M, M^{OH}, M^{OR}). Since it would be expected that the resonance position of the D units in oligomeric species would be sensitive to the type of M species attached to the chain ends (as inferred from Harris and Robins [133]), it is non - trivial to assign these resonances exactly. For the purposes of this study though, an exact assignment would be superfluous, only differentiation between linear and cyclic species is required. A summary of the resonance positions and intensities is given in Table 6.2. The M group subspectrum for sample EB3 (2mol% TMSO) is uncomplicated, with only one significant resonance at 7.22±0.01 ppm. For samples EB4 and EB5 (10 and 50 mol%

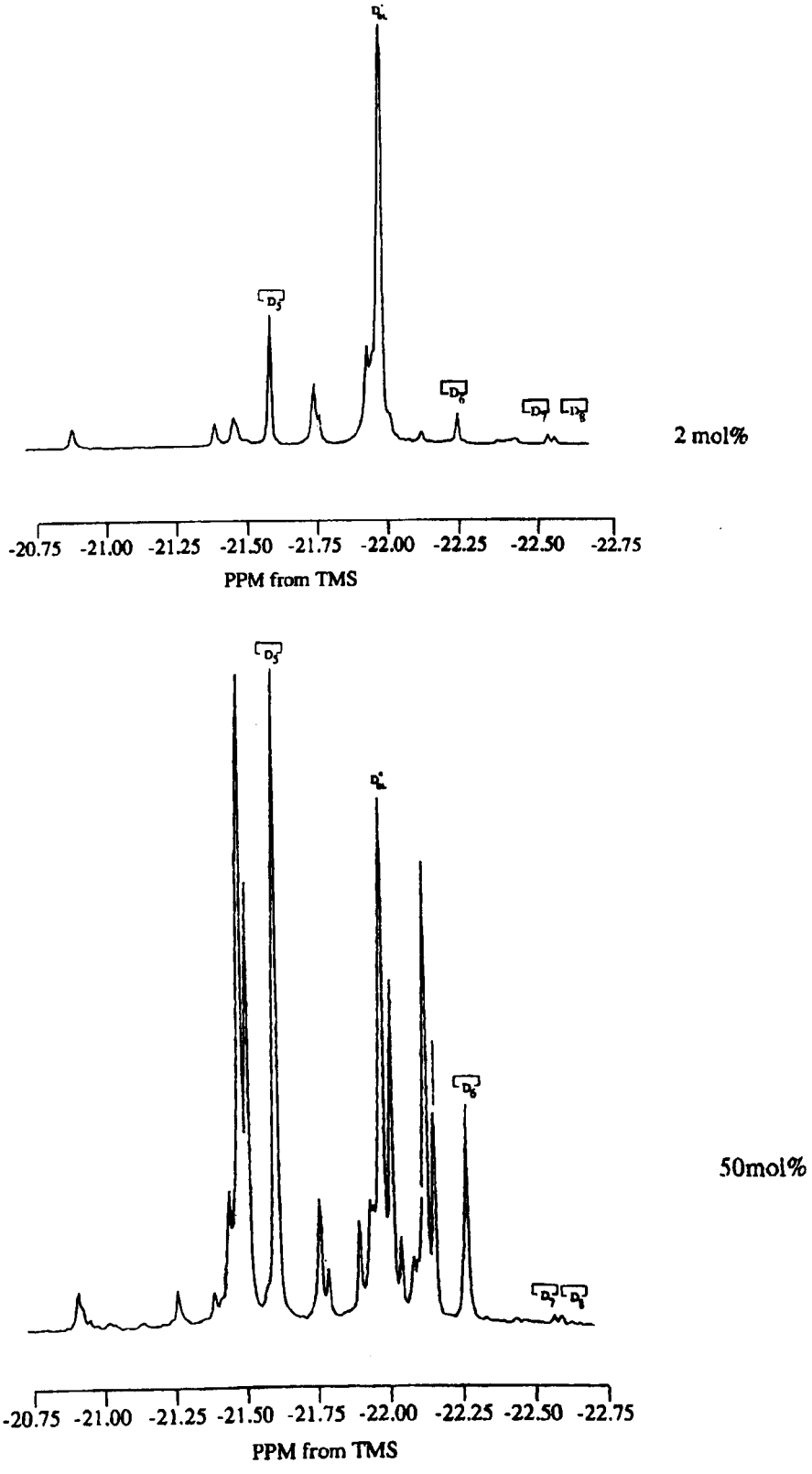

Figure 6.2. The D group ^{29}Si solution NMR subspectra for samples a) EB4 and b) EB5 (2 mol% and 50 mol% TMSO end capped polydimethylsiloxane).

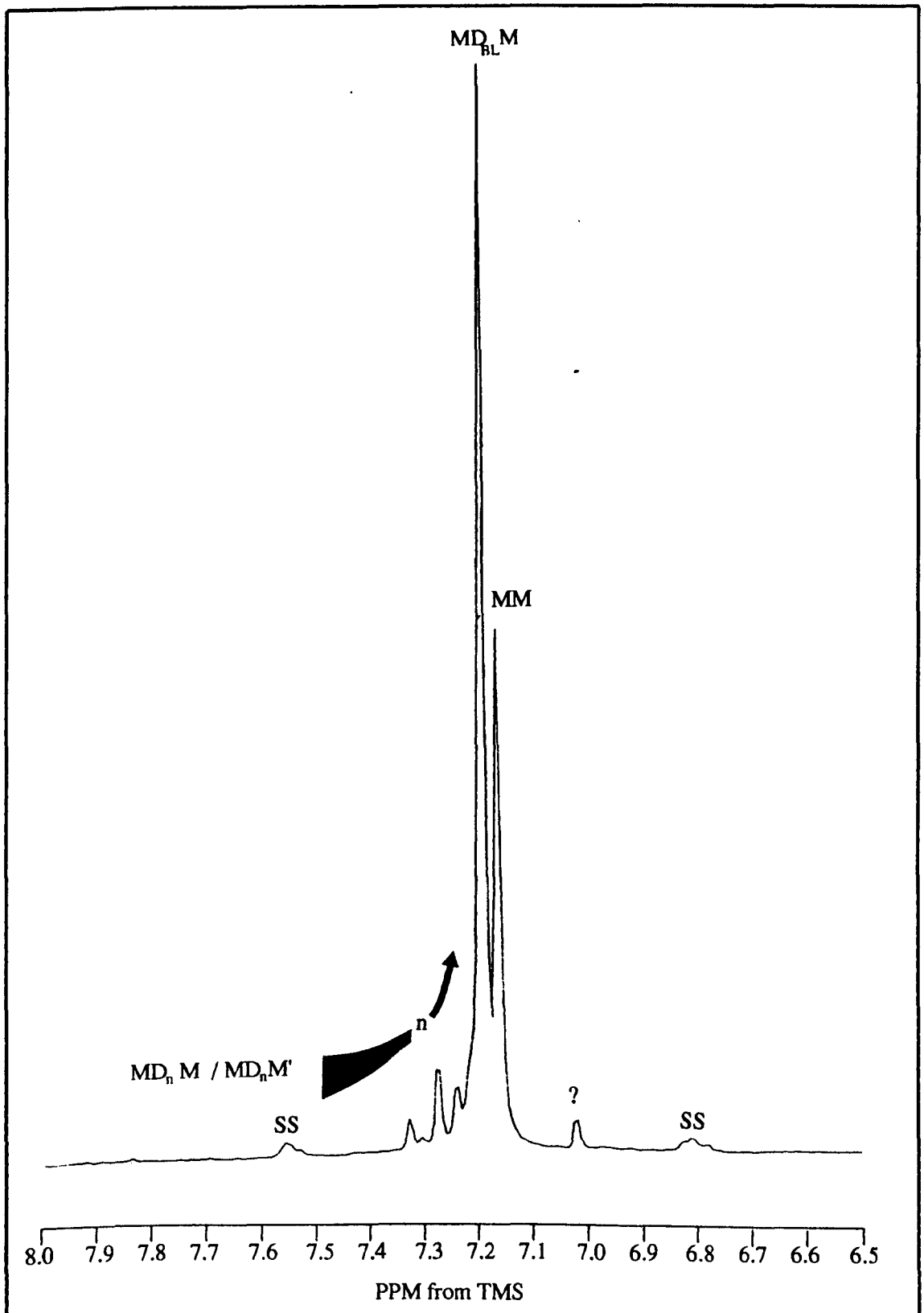

Figure 6.3. The M group ^{29}Si NMR subspectrum of sample EB5 (50 mol% trimethylsiloxy end capped polydimethylsiloxane).

Species	EB3 (2 mol% TMS) ppm ±0.01 / I % ±0.5	EB4 (10 mol% TMS) ppm ±0.01 / I % ±0.5	EB5 (50 mol% TMS) ppm ±0.01 / I % ±0.5
M	7.22 / 2.2	7.26 / 10.9	7.29 / 32.1
MM	- / -	7.18 / 12% of M	7.14 / 20% of M
M-MM	7.22 / 2.2	7.26 / 10.0	7.29 / 25.6
M^{OH}	-12.88 / 4.3	-12.91 / 4.3	-12.95 / 3.5
M^{OR}	-10.74 / 2.2	-10.78 / 1.1	-10.82 / 0.6
D^*_{BL}	-21.94 / 31±2	-21.96 / 28±2	-21.98 / 7.7
$\underline{D}_4$	-19.14 / 19.1	-19.17 / 19.6	-19.21 / 7.3
$\underline{D}_5$	-21.55 / 9.1	-21.58 / 7.6	-21.61 / 8.1
$\underline{D}_6$	-22.21 / 2.0	-22.24 / 3.8	-22.28 / 2.8
$\underline{D}_7$	-22.53 / 0.2	-22.55 / 0.2	- / 0.2
$\underline{D}_8$	-22.55 / 0.2	-22.58 / 0.2	- / 0.2
D_{other}	- / 29.5±0.9	- / 23±2	- / 38±2

Table 6.2. The ^{29}Si NMR shifts for samples EB3, EB4 and EB5, 2, 10 and 50 mol% TMSO t - PDMS. Intensities are calculated for a system with MM removed.

TMSO), the M subspectrum has more structure, displaying up to seven separately identifiable resonances. The largest of these (7.20±0.01 ppm, 7.19±0.01 ppm for EB4 and EB5 respectively) is from $\underline{M}D_{BL}$, ie for TMSO end groups attached to chains with a reasonably high degree of polymerisation. The other lower intensity resonances arise from M groups attached to oligomeric species. To evaluate the length of the linear species, removal of the MM resonance was necessary so as to only assess those linears with D units. Literature values for MM vary widely from 4.0 to 7.2 [129], with the actual position dependent upon the sample medium [133], although in moving through the series of species MD_nM, n=1 to 5, a gradual upfield shift occurs, with $\underline{M}D_{BL}$ being most upfield and having the highest intensity. Since the assignment of $\underline{M}D_{BL}$ is

reasonably confidently made, the resonance at 7.18±0.01 ppm and 7.14±0.01 ppm (10 mol% amd 50 mol% TMSO respectively) is most likely to arise from MM. The above assignments are presented in Figure 6.3, the ^{29}Si NMR M group subspectra for sample EB5 (50 mol% TMSO t - PDMS). Note that in Figure 6.3, 'SS' denotes spinning - sideband, these being congruent with the sample rotation rate of 30Hz. The resonance marked '?' is possibly that of MM^{OH} or MM^{OR}.

Using equation 25, the experimental average degree of polymerisation, DP_{av}, was calculated for samples EB3, EB4 and EB5 from the spectra of Figure 6.1, the results are given in Table 6.3. These calculations were performed with exclusion of the MM and cyclic resonances from the M group and D group subspectra respectively. From the results presented in Table 6.2, the fraction of D units within cyclic species, p_w, and the distribution of the D units within the cyclic component were calculated for the three samples, the results are given in Table 6.3. The NMR spectra of Figures 6.1, 6.2 and 6.3 will only be quantitative if the resonances are not saturated. Values of T_1 suggested by Marsmann [129] for polysiloxanes imply that the 12 second relaxation time employed in obtaining the above spectra is insufficient to obtain quantitative results. To assess the degree of saturation, ^{29}Si solution NMR spectra for a sample of 2 mol% TMSO - t PDMS were obtained using pulse repetition rates of 12 and 60 seconds. The intensities of the resonances within the two spectra were compared and the results are given in Table 6.4. From the results presented in Table 6.4 it can be seen that there are no significant differences between the two spectra, suggesting that the results presented in Table 6.3 are quantitative.

Sample	mol % TMS	TMS conc (Molar)	DP_{av}	p_w	$\lfloor D_4 \rfloor$ %	$\lfloor D_{5+} \rfloor$ %
EB3	2	0.11	16±1	0.36±0.04	62±3	38±2
EB4	10	0.58	9±1	0.31±0.04	62±2	38±2
EB5	50	3.70	5.1±0.5	0.19±0.04	39±1	62±3

Table 6.3. The experimental average degree of polymerisation, cyclic fraction and cyclic composition for the TMSO end - capped materials.

Species		12s pulse delay I ± 0.5	60s pulse delay I ± 0.5
M		2.2	2.0
M^{OH}		7.1	6.5
D^*_{BL}		45.0	45.8
$\lfloor D_4 \rfloor$		9.6	10.6
$\lfloor D_5 \rfloor$		3.0	4.0
$\lfloor D_6 \rfloor$		1.0	1.3
$\lfloor D_7 \rfloor$		0.5	0.5
$\lfloor D_8 \rfloor$		0.2	0.3
D_{other}	i	6.4	6.5
	ii	8.6	8.5
	iii	6.9	6.5
	iv	7.1	6.0
	v	1.7	1.5

Table 6.4. The intensity measurements for the spectra of a trimethylsiloxy end - capped PDMS, obtained using a 12s and a 60s pulse repetition rate. Resonances i - v are from oligomeric MD_nM species (n<4, M=M, M^{OH}).

6.3 Bonding results.

Limited adhesion testing to aluminium was performed using a simple lap shear test geometry (see 4.2.3.1). The test samples were all prepared from acetone cleaned aluminium substrate with a 50μm bond gap, supported by brass shim. The test procedure and results are given in Table 6.5.

Sample	Composition	Heat treatment	Result of adhesion test
EB4	2M 98D	150 / 1 + 250 / 3	• For all materials
EB9	2M^{A}98D	" "	- No full cure through material.
		150 / 1 + 250 / 22	
EB12	2M 1D' 97D	" 250 / 4	- Cohesively very weak
EB13	2M 5D' 93D	" "	- Some degree of edge bonding
EB14	2M 25D' 73D	" "	

Table 6.5. Materials, preparation and results of lap shear testing.

6.4 Immersion Bias Testing.

A selection of end - capped materials were tested using the immersion bias method (4.5.1). The samples prepared and the preparation and test conditions are given in Table 6.6. The test results are presented in Table 6.7.

Sample	Composition	Preparation °C / hrs	Test conditions
EB6	0.05M^{A}99.95D	150 / 1 + 250 / 3	10V dc, sample anode
EB7	0.5M^{A}99.5D	" "	" "
EB9 / 1	2.0M^{A}98D	" "	" "
EB9 / 2	" "	" "	" "
EB12 / 1	2.0M 1.0D' 97D	" "	" "
EB12 / 2	" "	" "	10V dc, sample cathode
EB14 / 1	2.0M 25.0D' 73D	" "	10V dc, sample anode
EB14 / 2	" "	" "	" "

Table 6.6. Composition and preparation conditions of immersion - bias samples.

Sample	I_i (A)	I_f (A)	I_f / I_i	t(hrs)
EB6	$(2.0\pm0.1)\times10^{-9}$	$(4.0\pm0.2)\times10^{-8}$	20±2	500
EB7	$(1.0\pm0.1)\times10^{-10}$	$(2\pm0.5)\times10^{-9}$	20±7	501.6
EB9 / 1	$(5\pm1)\times10^{-10}$	$(1.0\pm0.1)\times10^{-6}$	2000±600	278
EB9 / 2	$(5\pm1)\times10^{-10}$	$(5.0\pm0.2)\times10^{-8}$	100±24	240
EB12 / 1	$(2\pm0.2)\times10^{-9}$	$(2.8\pm0.1)\times10^{-8}$	14±2	500
EB12 / 2	$(7.0\pm0.1)\times10^{-9}$	$(4.0\pm0.2)\times10^{-8}$	5.7±0.4	500
EB14 / 1	$(2.0\pm0.1)\times10^{-9}$	$(5.4\pm0.1)\times10^{-7}$	270±2	44
EB14 / 2	$(2.8\pm0.1)\times10^{-8}$	$(4.0\pm0.1)\times10^{-6}$	143±9	52.66

Table 6.7. Immersion - bias results for end - capped materials.

6.5 Low frequency dielectric measurements of end - capped materials.

All samples were dispensed and cured onto aluminium, employing a nitrile 'o'ring retaining wall, and having gold sputtered electrodes (see 4.4.2.1). All measurements were performed using the HP192A low frequency impedance analyser with the HP16451B test fixture (4.2.2.4, 4.2.2.5). The samples prepared and the preparation conditions and test electrode employed, are given in Table 6.8. Samples EB1 / 1, EB2 / 1 and EB4 / 1 were measured using the spring loaded electrode (4.4.2.5, test method B). This was found to be unsuitable due to the low mechanical strength of the sample and the fragility of the Au sputtered electrodes. All subsequent measurements were thus made using the rigid metal electrode (4.4.2.5, test method C). The dielectric dispersion curves (dielectric permittivity vs frequency) of TMSO, ADMS end - capped PDMS siloxanes are presented in Figures 6.4, 6.5 respectively and those for TMSO end - capped PDMS - PMVS copolymers are given in Figure 6.6. The dielectric constant of samples EB6/1 and EB6/4, both 0.05 mol% ADMS end - capped PDMS, cured at 220°C and 250°C respectively, were measured as above and the results are presented in Figure 6.7. Samples EB6 / 2 and EB6 / 3, were again both 0.05 mol% ADMS end - capped PDMS and were both prepared for dielectric study at 220°C. The latter was immersed in distilled water at room temperature for a period of 7 days prior to measurement. After immersion, the sample was gently blown dry with compressed air so as to remove any excess surface moisture. The results are presented in Figure 6.8. The dielectric constant of samples bonded to alumina was also assessed but, due to the complex electrical path (two dielectrics in series), the testing was abandoned.

Sample	Cure conditions	Electrode
EB1 / 1 0.05M 99.95D	150 / 1 + 250 / 4	Spring loaded electrode
EB1 / 2 " "	" "	Rigid metal electrode
EB2 / 1 0.5M 99.5D	" "	Spring loaded electrode
EB2 / 2 " "	" "	Rigid metal electrode
EB4 / 1 10M 90D	" "	Spring loaded electrode
EB4 / 2 " "	" "	Rigid metal electrode
EB6 / 1 0.05M^{A} 99.95D	150 / 1 + 220 / 12	Rigid metal electrode
EB6 / 2 " "	" "	" "
EB6 / 3 " "	" "	" "
EB6 / 4 " "	150 / 1 + 250 / 12	" "
EB7 / 1 0.5M^{A} 99.5D	150 / 1 + 220 / 12	" "
EB7 / 2 " "	150 / 1 + 250 / 12	" "
EB10 / 1 5.0M^{A} 95D	150 / 1 + 220 / 12	" "
EB10 / 2 " "	150 / 1 + 250 / 12	" "
EB11 10M^{A} 90D	150 / 1 + 200 / 4	" "
EB12 2M 1D' 97D	150 / 1 + 220 / 3	" "
EB13 2M 5D' 93D	150 / 1 + 220 / 3	" "
EB14 2M 25D' 73D	150 / 1 + 190 / 2	" "

Table 6.8. The end - capped samples prepared for low frequency dielectric analysis - the preparation conditions and test electrode used.

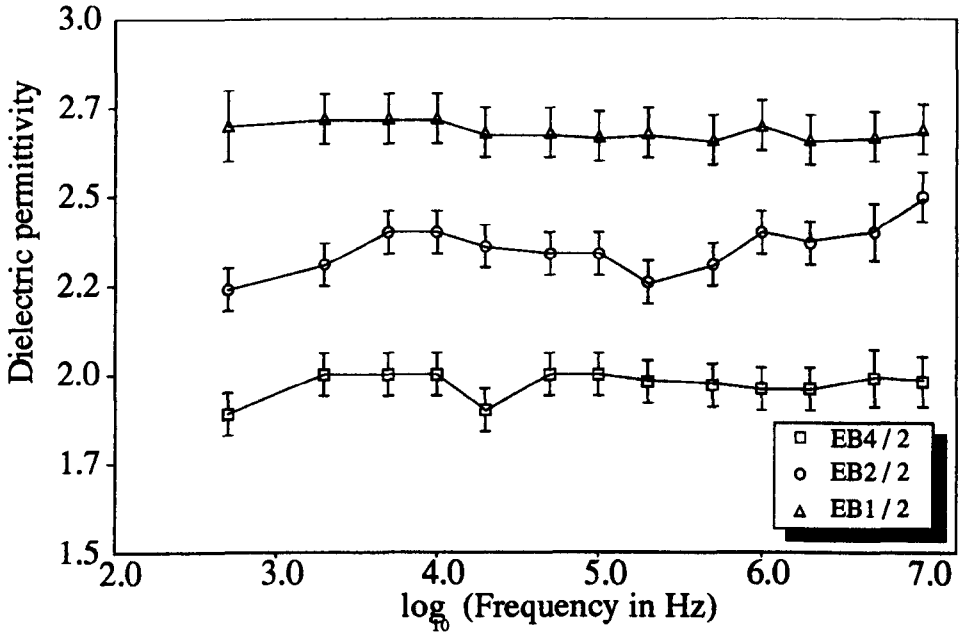

Figure 6.4.The dielectric dispersion curves for TMSO end - capped materials.

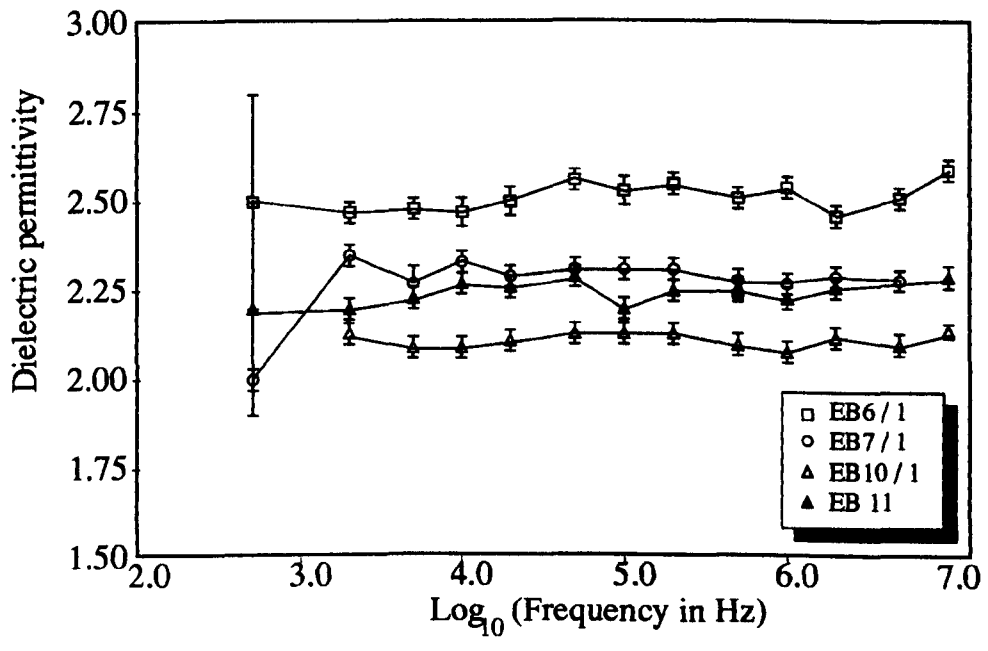

Figure 6.5. The dielectric dispersion curves for ADMS end capped materials.

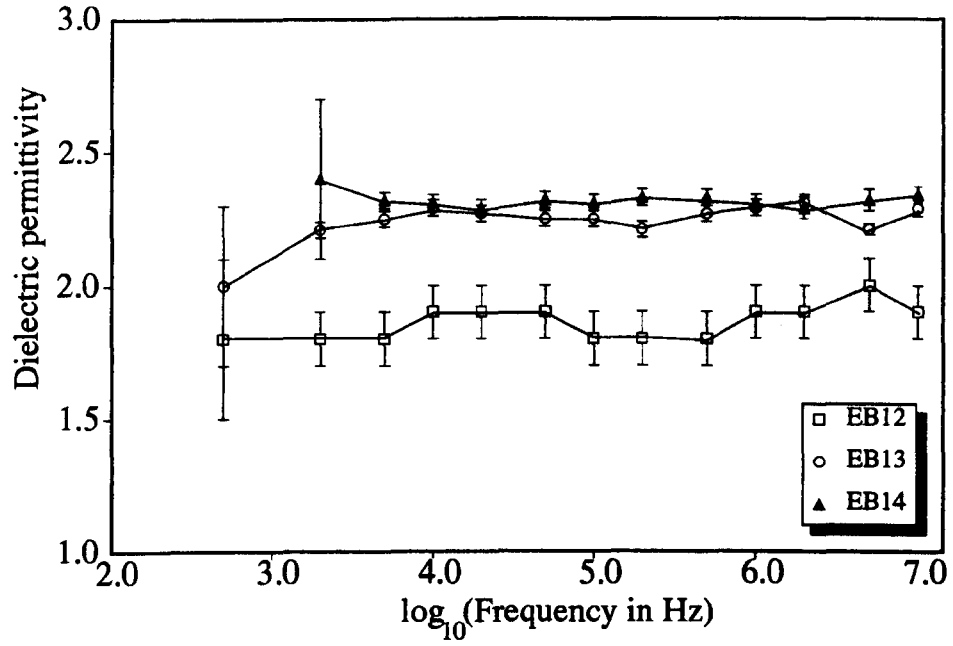

Figure 6.6. The dielectric dispersion curves for TMSO end capped PDMS - PMVS copolymers EB12, EB13 and EB14 (1, 5 and 25 mol% D').

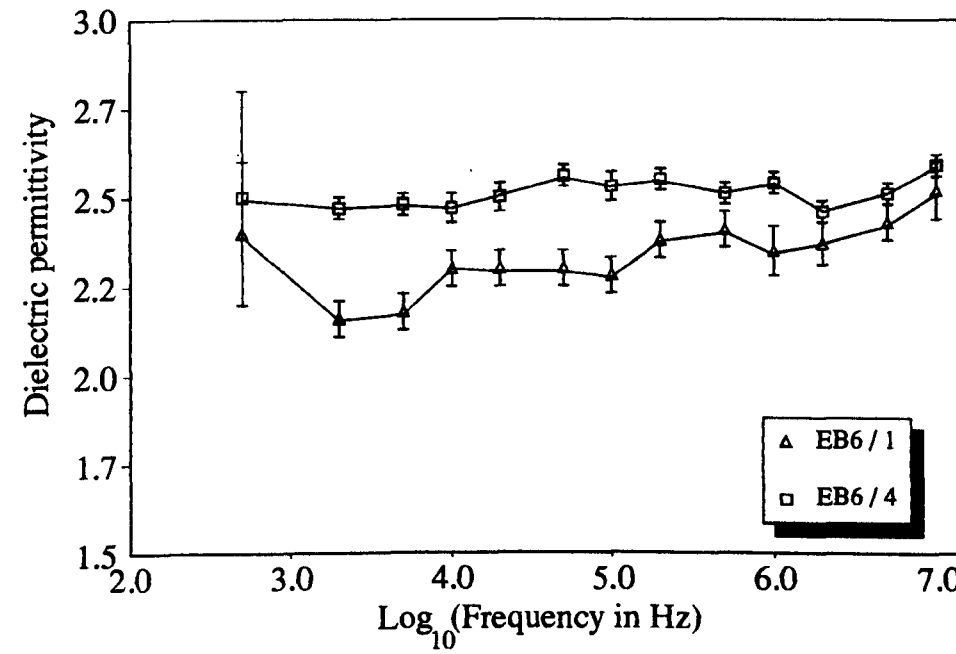

Figure 6.7. The dielectric dispersion curves for 0.05 mol% M^A end - capped PDMS materials, cured at 220°C (EB6/1) and 250°C (EB6/4).

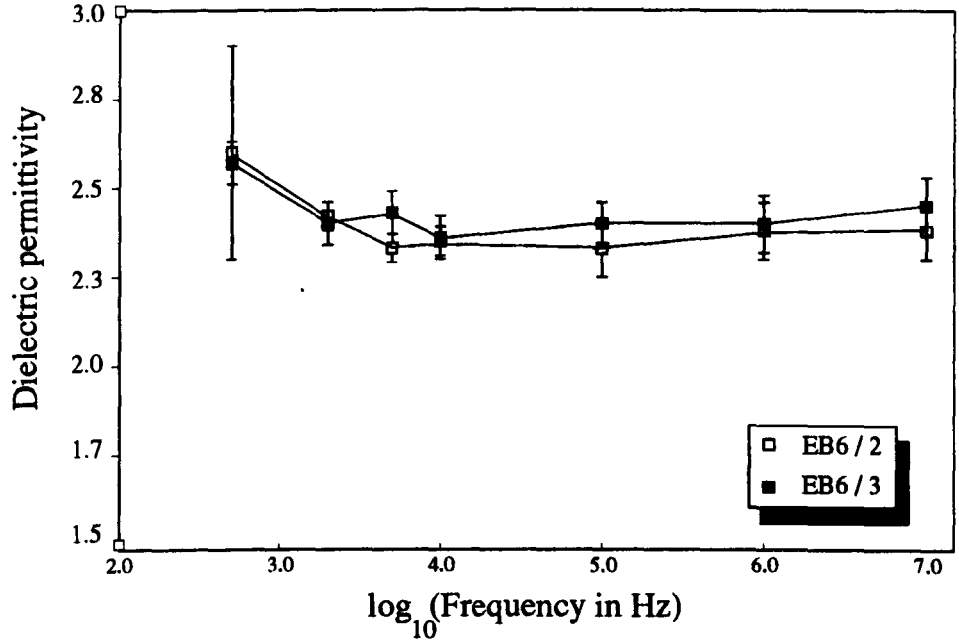

Figure 6.8. The dielectric dispersion curves for 0.05 mol% end - capped PDMS materials, cured at 220°C, with measurements taken both prior to (EB6 / 2) and after (EB6 / 3) a 7 day immersion in distilled H_2O.

6.6 Discussion

6.6.1 ^{29}Si NMR of trimethylsiloxane end - capped PDMS.

The copolymerisation of M and D units is seen to lead to the generation of a bimodal system, the components being MD_nM (linear species with M being either M, M^{OH} or M^{OR}) and cyclics. From Table 6.3 it is seen that the degree of polymerisation of the linear fraction decreases with an increasing M group concentration. This is evidenced in the NMR spectra by the relative growth of the oligomeric MD_nM resonances relative to the bulk chain D resonance, D^*_{BL} (cf. Figures 6.2a and 6.2b). Thus, as would be expected, an increase in the degree of substitution of M for D units yields a concomitant increase in the population of the oligomeric M end - blocked species. From Table 6.2,

it is noted that, within the limits of experimental error, the population of the M^{OH} species is independent of the level of M group substitution. This is somewhat surprising since, from a simple viewpoint, it would be thought that, with high levels of M group substitution, the silanol population would be depleted by the formation of MD_nM oligomers. The higher than expected levels of M^{OH} found in samples EB4 and EB5 may imply that the silanols are attached to a greater number of oligomeric materials than in sample EB3, possibly as a result of M group attachment to one of the chain ends reducing the probability of two silanols interacting and condensing. The cyclic population is seen to decrease with increasing M concentration, suggesting that fewer D units are available to cyclise as a result of chain termination by M groups.

The sum of the intensities for the D and M units within each sample's NMR spectrum (Figures 6.1a, b and c), assuming no losses from the system, would be expected to reflect the ratio of the initial precursor stoichiometry. The calculated and experimental ratios of D to M units within the three systems are given in Table 6.9. From this it can

Sample	M (predicted)	M (experimental)	D (predicted)	D(experimental)
EB3	2	3.0±0.3	98	97±2
EB4	10	9.5±0.3	90	90±2
EB5	50	33±3	50	66.7±0.8

Table 6.9. The calculated and experimental ^{29}Si solution NMR intensity ratios for the M and D units within samples EB3 (2mol% M) , EB4 (10mol% M) and EB5 (50mol%M).

be seen that the experimental ratios for the 2 and 10 mol% M systems are close to the calculated figures, whereas for the 50 mol% sample, the M resonance is 17% too low.

Since this system is known to have a large proportion of oligomeric MD_nM species, their evaporation is possibly the mechanism for the loss of the M species from the system. Also, the good correlation observed for the 2 and 10 mol% M systems implies that D_3 is not lost from these systems but is simply not produced under these conditions, due possibly to the associated strain. [48]

From an applicational point of view the system would be best prepared using a low M fraction since this would produce a material with a relatively low content of oligomeric species (both cyclics and linears). Such a material would thus have optimum thermal stability.

6.6.2. Immersion bias testing of end - blocked materials.

This test was employed as a material selection technique to identify poor materials at an early stage. Due to the limited number of platinum counter electrodes, all evaluations were limited to 500 hrs so as to allow testing of each type of material at least once. The sample set was thus limited to, at most, two evaluations of the same material being performed under identical conditions. A second measurement of a material was only made if the sample was seen to fail at an early stage. In these cases it was necessary to differentiate between material induced failure, ie poor hermeticity, and preparation induced failure, In the case of sample EB14 / 1 (2M, 25D', 73D copolymer), failure occurred after only 44 hrs. From Figure 6.9 it can be seen that the corrosion was limited to one point over the area of the sample. It was possible that this was due to a particulate or entrapped gas bubble within the sample affording an easy conduction path

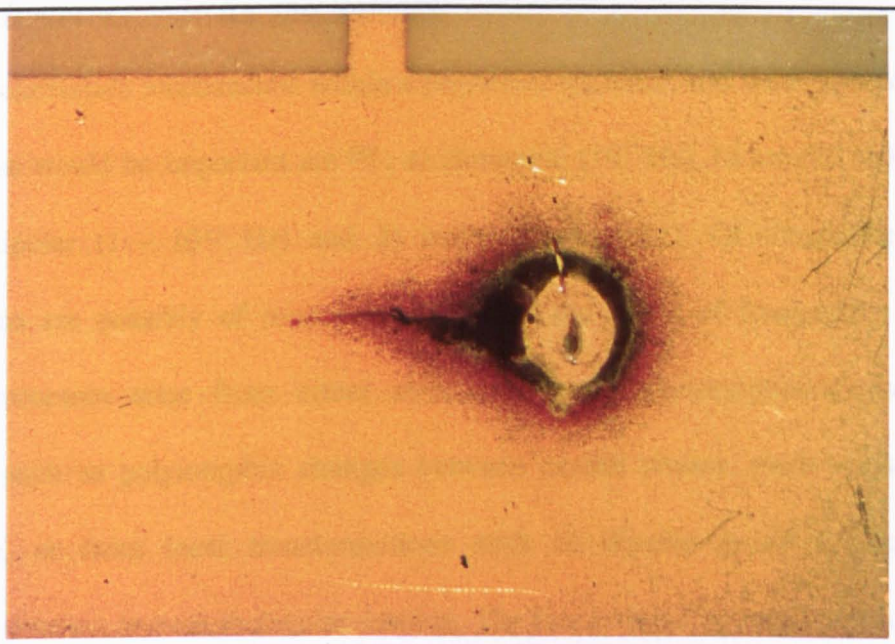

Figure 6.9. Sample EB14 / 1 (2M, 25D', 73D copolymer) after 44hrs immersion bias testing.

through the material. A repeat of this sample (EB14 / 2) under cleaner environmental conditions was found to fail after a similar time, thus suggesting that the material was hermetically poor. The point of failure seen for sample EB14 indicates that the dominant failure process occurs through the bulk of the material and not along the coating - substrate interface, although the nature of the interface is not clear as the coating is bonded to both the epoxy surround and the alumina. The low D' content copolymer (EB12 / 1 and EB12 / 2) was found to survive for 500+ hrs with only minimal change in leakage current over that period (with the sample as both cathode and anode). Thus it appears that a high vinyl content is deleterious to good hermeticity. The results for the M^A end - blocked materials (EB6, EB7, EB9) indicate that their hermeticity is degraded as the level of M^A is increased. This, and the observed loss of hermeticity with increased vinyl content, suggest that the hermetic properties are severely compromised with the introduction of unsaturated organic species into the systems.

6.6.3 Low frequency dielectric spectroscopy.

Possible polarisation mechanisms within a polymeric material, and the frequencies over which these would be important are [8] : a) electronic (10^{17}Hz), b) atomic (10^{11} - 10^{17} Hz), c) dipolar (1 - 10^{11} Hz) and d) interfacial (<1 Hz). Of these, the dipolar mechanisms are possibly of most relevance over the range of frequencies studied. Dipolar processes arise from either structural changes encompassing the whole structure, such as polymorphic changes between crystal phases, glass - viscoelastic transitions, or from local transformations such as dipolar group rotation, local segmental rotation or even molecular rotation. The former are only important for PDMS based systems at temperatures well below 0°C. At ambient temperatures, the local dipolar transformations will have the greatest impact upon the dielectric properties of such a material. The importance of each mechanism will depend upon the rigidity of each dipole. These materials do not possess strongly polar side groups, thus limiting the effect of dipolar group rotation on ε' and ε''. Local segmental motion will be limited by the local matrix and the degree to which the groups are constrained [135]. Interfacial polarisations are not important at frequencies above 1Hz except that, in the case of high dielectric inclusions such as H_2O ($\varepsilon' > 80$), Maxwell - Wagner type polarisations become important at frequencies up to 10^3 Hz [8].

From Figure 6.4 it is seen that ε' increases with an increase in the level of TMSO end - blocker. Materials with a high level of end - blocker contain a higher proportion of oligomeric linears (6.6.1). Being oligomeric, the linears are likely to be more mobile than the longer chain polymer, thus increasing ε'. As these materials are solid, some thermally activated mechanism must exist, whether it be simply chain entanglement or

a methyl - methyl interaction. It is possible that the oligomeric linears are short enough to become entrapped within the macrocyclic / polymeric linear network, and thus retain their flexibility. It can be seen from Figure 6.5 that ε' of ADMS end - capped materials decreases with increasing ADMS concentration, up to 5 mol% M^A. At 10 mol% M^A the trend is reversed and ε' is seen to increase. The decrease in ε' with increasing levels of M^A is possibly a result of the incorporation of $-(CH)_6-$ (CH_2CHCH_2 - CH_2CHCH_2 cross -linking), and $(CH_2)_4$ groups (CH_2CHCH_2 - CH_4 cross - linking) into the siloxane chain. These organics will alter the packing density of the material and also reduce the flexibility of the chains, the latter resulting in an increased rigidity and a lower ε'. Also, the incorporation of organic chains into the structure will result in a reduced molecular weight and an increased number of non - polar C-C bonds. In the limit of the high M^A concentration, the increased ε' is likely to be due to the high level of entrapped oligomer linears. The 0.05 mol% M^A material cured at 250°C has a higher ε' than the 220°C cured sample. This effect is possibly due to thermally induced damage of the allyl groups (and associated organic linkages) since both samples would be expected to have similar inorganic structures with similar flexibility. The good hermetic properties of the 0.05 mol% M^A material were evident from the immersion bias testing results (Table 6.7). This is complemented by the results of the dielectric measurements of samples EB6 / 1 and EB6 / 2 (Figure 6.8), with no significant difference observed between the two samples, despite the latter having been subjected to a 7 day immersion in distilled water. Comparison of values between the D'/D copolymers of Figure 6.6 suggest that increasing the vinyl content results in a concomitant increase in ε'. The higher vinyl content material would be expected to have a higher rigidity and possibly a lower packing density than the low vinyl content material, both of which would result in a

lower ε', which is contrary to what is observed. Under immersion bias testing, a high D' content has been shown to offer poor hermetic properties (6.6.1), suggesting that the structure is more open to water ingress, thus accounting for the observed increase in ε'.

7.1 Sample preparation

Two principal preparation strategies were investigated, those being a) addition of one precursor to a second, pre - hydrolysed, reactive monomer and subsequent condensation of the two, and b) cohydrolysis of two (or more) precursors.

7.1.1 Preparation method 'A':- reaction of pre-hydrolysed and unreacted precursors.

These preparations were investigated in an attempt to obtain systems with the trifunctional units (T) randomly distributed throughout the difunctional system. All systems of this type were prepared using either DCDMS or DCMVS (or both) as the chain extenders and trifunctional MTMOS as the inorganic chain cross - linking moiety. To minimise the degree of cyclisation, all precursors were solvated in dichloromethane (CH_2Cl_2, DCM) so as to encourage intra - inter catalysis [48] (3.2.4).

7.1.1.1 Pre - hydrolysis of trifunctional units (MTMOS).

The aim of this preparation was to prepare a pre - hydrolysed 'reservoir' of T groups to which, under suitable conditions, non - hydrolysed DCDMS monomer could be condensed. The preparation route employed is shown schematically in Figure 7.1. A small volume of HCl was added in the initial stage to catalyse the hydrolysis reaction. DMAP was added in the second stage to catalyse the heterocondensation reaction between Si-OH and Si-Cl [50] (see 3.2.3.2). Et_3N or pyridine (C_5H_5N) was used as a non - aqueous acid acceptor. Flushing with H_2O was necessary to remove the $Et_3N{\cdot}HCl$ or $C_5H_5N{\cdot}HCl$ from the solvent phase. During the initial stage, wherein the

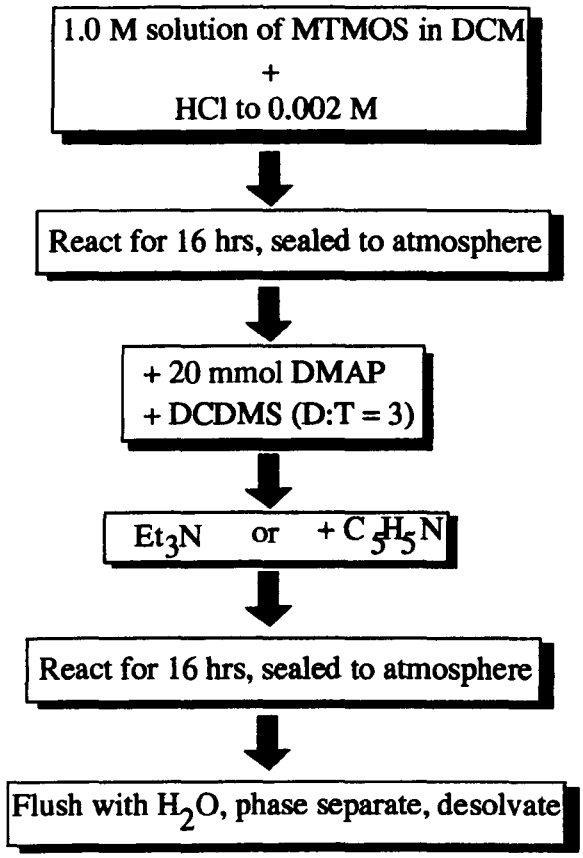

Figure 7.1. Preparation method 'A' - the preparation and reaction of pre - hydrolysed MTMOS with DCDMS.

MTMOS was hydrolysed, a white precipitate formed, indicating the self condensation between T group silanols. This preparation route was subsequently abandoned.

7.1.1.2 Pre - hydrolysis of difunctional units (DCDMS or DCMVS).

Two systems were investigated, a) 95D, 5T and b) 95D', 5T, and were prepared as in Figure 7.2. Both of the above preparations resulted in the development of a dark brown precipitate from which the siloxane was unrecoverable. It was assumed that the precipitate involved the triethylamine and thus this preparation was repeated using the

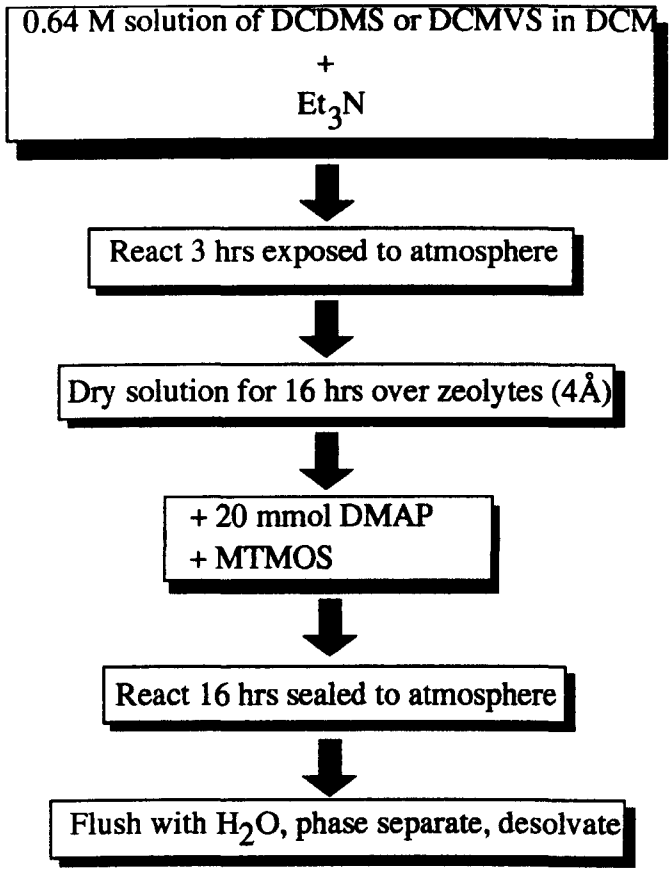

Figure 7.2. Preparation method 'A' - the preparation and reaction of pre - hydrolysed DCDMS with MTMOS.

preparation route given in Figure 7.2 with pyridine as acid acceptor and DCDMS as precursor, with a D : T ratio of 3 : 1. This preparation resulted in the development of a two phase material consisting of a white precipitate and a clear oil. These were assumed to be self - condensed MTMOS and PDMS respectively, indicating that the preparation route was not suitable for obtaining an homogeneous polymer.

A preparation route to dimethyldisiloxanediol ($HO\text{-}Si(CH_3)_2\text{-}O\text{-}Si(CH_3)_2\text{-}OH$) was suggested by Martin [136]. The suggested process was slightly modified (KOH solution added to neutralise HCl in place of NH_3), and is given in Figure 7.3. Substitution of the initial stage of the preparation outlined in Figure 7.2 with this process was investigated.

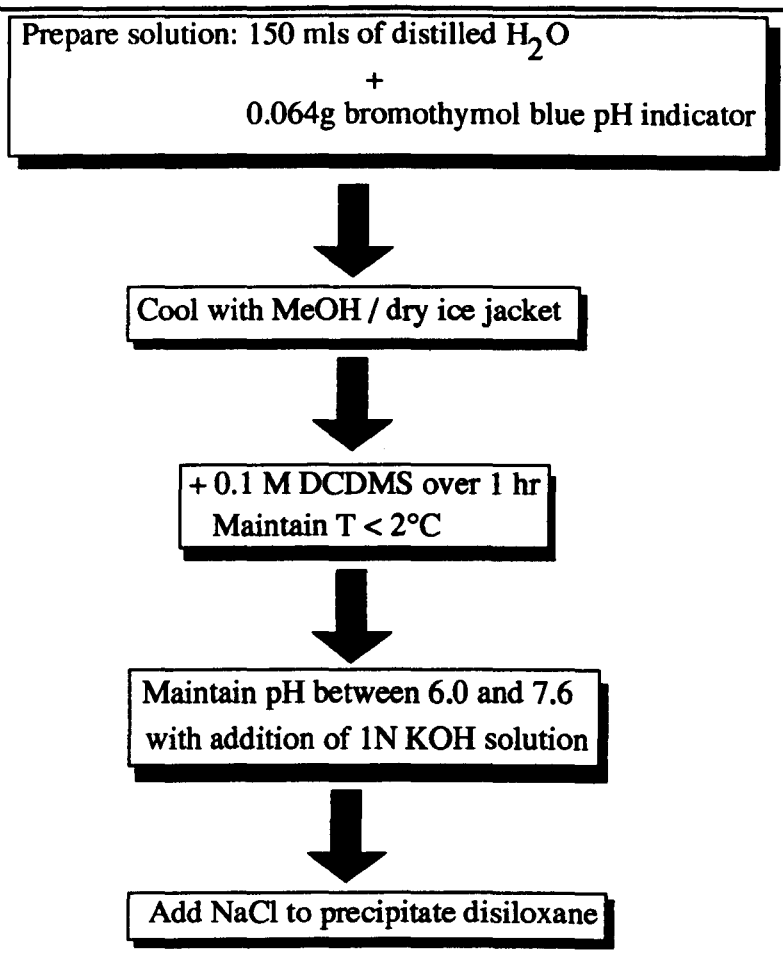

Figure 7.3 An adapted version of Martins' [136] route to disiloxanediol.

After addition of the DCDMS an oil formed that was immiscible with water and was assumed to be PDMS. This route was thus abandoned.

7.1.2 Preparation method 'B', the co - hydrolysis and co - condensation of difunctional and trifunctional monomers.

Directly co - condensed materials were prepared via two two different routes. The first route closely followed the standard route presented in 4.7, with addition of the silanes, as purchased, to DCM, to form a 2M solution, and their subsequent hydrolysis with a volume of water sufficient to just hydrolyse the silane. The reaction pH was maintained

approximately neutral with the addition of 1N aqueous KOH solution. The reactions were allowed to proceed for a period of between 2 and 18 hours prior to filtration, phase separation and desolvation (at STP). The second route had, in addition to, and, prior to, the above, a period wherein the silanes were heated together under nitrogen (in the required ratio), at temperatures near to or at the solution reflux temperature. A nitrogen atmosphere was employed as the silanes were heated at temperatures near to their flash point temperatures. A double walled condenser was employed to recondense any evaporates. This procedure is known to encourage exchange of the Cl and OCH_3 substituents between silane precursors [137]. Thus, such an exchange between the di- and tri - functional silanes was investigated as a means of reducing the differential in the reaction rates of the two monomers and thus preparing a more homogeneous material. The samples prepared via the above two processes are presented in Table 7.1.

7.2 Properties of some trifunctionally cross - linked materials

7.2.1 Sample viscosity.

The bulk viscosity of the materials prepared from both heated (HS) and non - heated (NHS) silanes were measured for a range of temperatures up to 120°C using the method outlined in 4.6. A number of materials had viscosities outside the range of measurement. The viscosities at 25°C are presented in Table 7.2 and the viscosity - temperature curves of a selection of suitable materials (both NHS and HS preparations) are given in Figure 7.4.

7.2.2 Coating properties.

Those materials with a suitable dispensing viscosity were applied to alumina

Sample	Preparation route	Composition	Reflux time (hrs) temperature (°C)	Hydrolysis / condensation time (hrs)
NHS1	A	2D8T	———	2
NHS2	"	DT **	———	"
NHS3	"	DT	———	"
NHS4	"	8D2T	———	"
NHS5	"	2D8D'	———	"
NHS6	"	D'T	———	"
NHS7	"	8D'2T	———	"
NHS8	"	$2D^{Ph}8T$	———	"
NHS9	"	$D^{Ph}T$	———	"
NHS10	"	$8D^{Ph}2T$	———	"
HS1	B	DT	104 / 2	18
HS2	"	2D'8T	94 / 2	2
HS3	"	D'T	93 / 3	"
HS4	"	$2D^{Ph}8T$	105 / 2	"
HS5	"	$D^{Ph}T$	100 / 2	"

** diethoxydimethylsilane (DEODMS) used as difunctional precursor

Table 7.1. Trifunctionally cross - linked polysiloxane materials, prepared from non heated silanes (NHS) and heated silanes (HS).

Sample	Composition	Viscosity Pa.s	Sample	Composition	Viscosity Pa.s
NHS1	2D8T	$> 1.6\times10^3$ Solid	———	———	———
NHS5	2D'8T	$> 1.6\times10^3$ Solid	HS2	2D'8T	7.44±0.08
NHS8	$2D^{Ph}8T$	$> 1.6\times10^3$ Solid	HS4	$2D^{Ph}8T$	$> 1.6\times10^3$
NHS2	$DT^{(DEODMS)}$	$> 1.6\times10^3$ Solid	———	———	———
NHS3	DT	8.00±0.08	———	———	———
NHS5	D'T	$> 1.6\times10^3$ Solid	HS3	D'T	< 0.08
NHS9	$D^{Ph}T$	$> 1.6\times10^3$ Liquid	HS5	$D^{Ph}T$	26.0±0.3
NHS4	8D2T	< 0.08	———	———	———
NHS7	8D'2T	40.0±0.3	———	———	———
NHS10	$8D^{Ph}2T$	500±2	———	———	———

Table 7.2. The room temperature viscosities of the trifunctionally cross - linked polysiloxanes, measured at 25°C.

hermeticity test substrates (4.5.1, Figure 4.25). All samples were heated in air at 200°C for a period of 4 hours. The results of the coating trials are given in Table 7.3. Materials that appeared to offer flaw free coatings were evaluated under humidity - bias

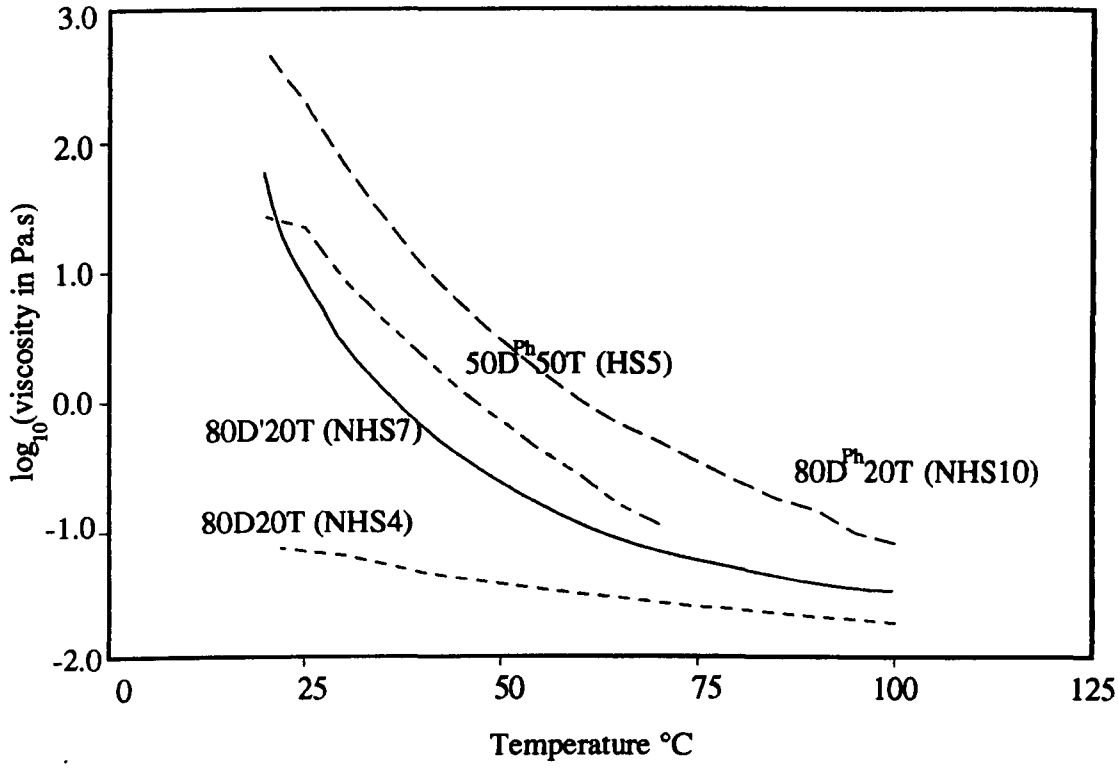

Figure 7.4. Viscosity - temperature curves for a number of trifunctionally cross - linked polysiloxanes.

Sample	Composition	Coating appearance	Humidity - bias test result
NHS3	DT	Irregular, cracked	———
NHS4	8D 2T	Smooth, transparent	Failed after 4.9 hrs due to cracking
NHS7	8D'2T	Irregular, cracked	———
NHS9	$D^{Ph}T$	Smooth, transparent, Cracked upon cooling	———
NHS10	$8D^{Ph}2T$	Smooth, transparent	No fail 310+ hrs
HS2	2D'8T	Irregular, cracked	———
HS3	D'T	Smooth, transparent	Failed after 18 hrs due to cracking
HS5	$D^{Ph}T$	Smooth, transparent	No fail 310+ hrs

Table 7.3. The results of the coating trials and immersion - bias evaluation of a selection of trifunctionally -cross - linked materials.

test conditions (anodic sample) (4.5.1), the results of which are also presented in Table 7.3.

7.3 Tetrafunctionally cross - linked materials.

A system was required that could be used to investigate the relationship between the properties of a material and the conditions under which it was prepared. A tetrafunctionally cross - linked D^{Ph} / D' copolymer material suggested by Schmidt and Wolter [117] was selected for this purpose since it also possessed properties well suited to dielectric applications (low dielectric permittivity, low dielectric loss, immersion resistance and good adhesion to aluminium).

7.3.1 Sample preparation.

All samples were prepared with the composition 32.5 D^{Ph}, 65 D', 2.5 Q, and were all prepared via the standard preparation route (4.7). The precursors employed were DCMVS, DCDPS (dichlorodiphenylsilane) (for the difunctional units) and tetraethoxysilane (TEOS) for the tetrafunctional cross - linking moieties. Two samples were prepared, with the temperature during the preparation maintained at 0°C (PREP0) and 75°C (PREP75). During the 3 hr reaction period, the pH of the systems was maintained at 8 - 9 with the addition of 1N KOH H_2O / EtOH solution. Three other samples were prepared under conditions of pH1 (PREP1), pH9 (PREP9) and pH14 (PREP14). No heating or cooling of the samples was applied during these reactions.

7.3.2 Analysis of PREP0 and PREP75.

The two materials were considerably different in appearance. PREP0 was visually clear

and transparent whereas PREP75 contained a white precipitate. Using the viscometer system 2 (see 4.6), the viscosities of these samples were measured whilst they were heated under simulated cure conditions (200°C in air), the results of which are presented in Figure 7.5. Transmission IR spectra of PREP0 and PREP75 were recorded and can be seen in Figure 7.6 . The spectra are seen to be very similar, but an extra

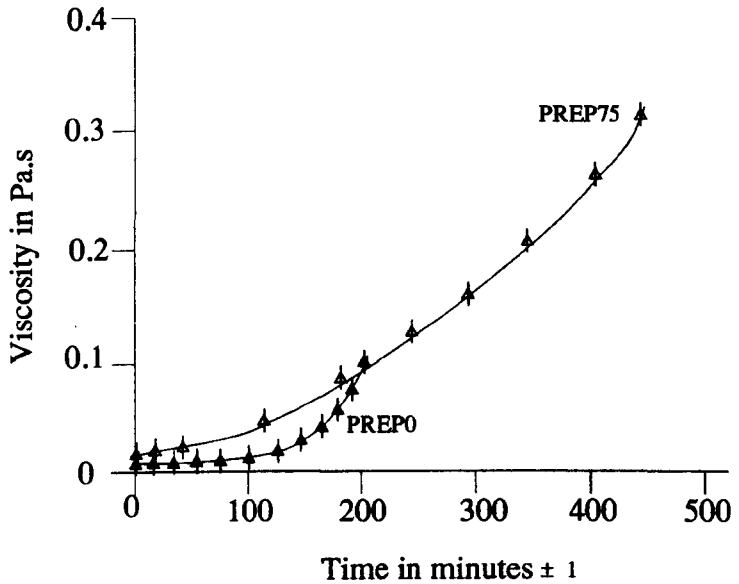

Figure 7.5. The viscosity (@200°C) for tetrafunctionally cross - linked D^{Ph} / D' copolymers prepared at 0°C (PREP0) and 75°C (PREP75) when heated at 200°C in air.

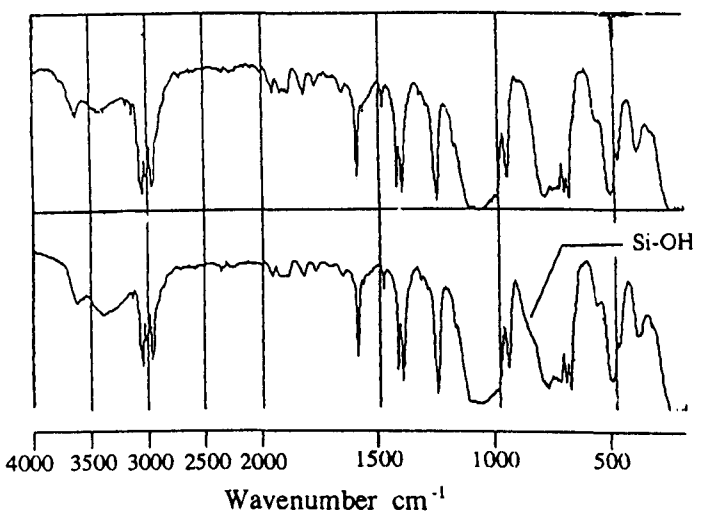

Figure 7.6. The transmission IR spectra for samples PREP0 and PREP75 (tetrafunctionally cross - linked D^{Ph}/D' copolymers prepared at 0° and 75°C.

absorption is evident at 860cm^{-1} for PREP0, this being congruent with that of a Si-OH absorption [138]. Heating sample PREP0 at temperatures up to 100°C resulted in a a complete removal of the absorption.

7.3.3 Analysis of PREP1, PREP9 and PREP14.

With an increase in the preparation pH there was observed a decrease in the amount of white precipitate that was produced. PREP14 was devoid of any precipitate and was visually transparent and clear. The results of viscosity measurements, taken whilst exposed to simulated cure conditions of 200°C, are given in Figure 7.7.

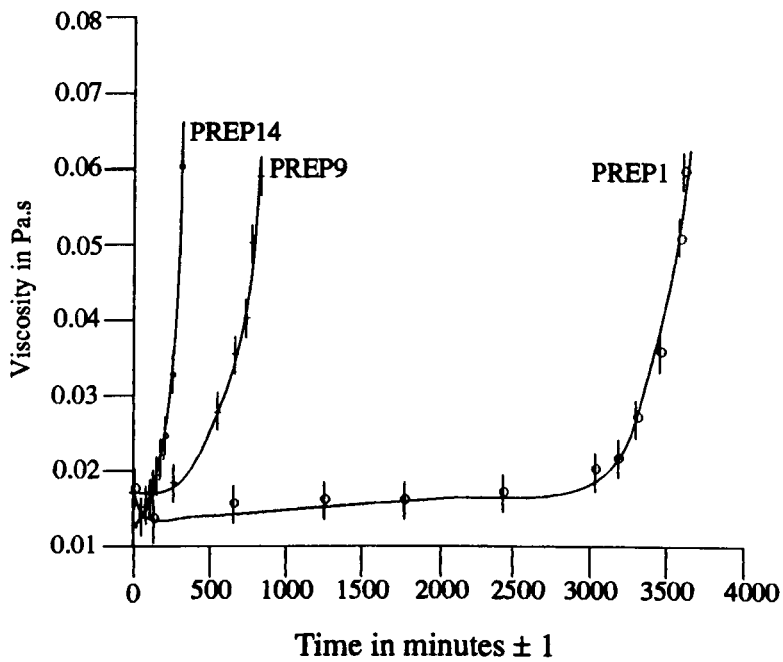

Figure 7.7. The viscosity (@200°C) for tetrafunctionally cross - linked D^{Ph} / D' copolymers prepared at pH1 (PREP1), pH9 (PREP9) and pH14 (PREP14) when heated at 200°C in air.

7.4 Discussion

7.4.1 The pre - hydrolysis of trifunctional units.

From the literature [40], the conditions of low pH and low H_2O / Si-X ratio would be expected to encourage hydrolysis and discourage condensation reactions, so as to create

an abundance of hydrolysed monomer. Despite these conditions being maintained (addition of HCl and hydrolysis with under - stoichiometric H_2O), a rapid development of a white precipitate was observed, implying that condensation was occurring at a significant rate very shortly after the precursors were added to the system. The precipitate was most likely to have formed via a reaction - limited, cluster - cluster aggregation (RLCA) growth mechanism[139], which would be the dominant process under these conditions. The development of stable oligomeric silanols under these conditions is thus unlikely. The ratio of H_2O / Si-X would not be expected to have prevented or delayed the aggregation, only to have reduced the degree of branching to some extent [40]. Reaction under higher pH was not attempted as under these conditions the dominant growth mechanism is nucleation and growth, combined with a high depolymerisation rate, leading to the development of large smooth Stöber type particles [40].

7.4.2 The pre - hydrolysis of difunctional units.

The development of the white precipitate only occurred after the addition of the H_2O, 16 hours after the MTMOS and DMAP were added to the system, suggesting that a heterocondensation, alcohol forming reaction between the T and D units was very limited, despite this being the favourable reaction under the conditions (anhydrous, DMAP catalyst). It is inferred from these results that the difunctional system was already highly condensed prior to the addition of the MTMOS, emphasising the susceptibility of the D units to condensation. Even when prepared under the very closely controlled conditions employed by Martin [136] (Figure 7.3), the production of PDMS oil was unavoidable.

7.4.3 The co- hydrolysis of di - and tri - functional silanes.

It can be seen from Table 7.2 that the viscosities of materials prepared from heated silanes are always considerably lower than those of materials prepared from the equivalent non - heated silanes. This may be either a structural rearrangement of the di - and tri - functional units within the materials or due to a change in the ratio of the two different moieties. The latter is unlikely since a change in the system stoichiometry during the heating stage could only occur by differential evaporation. The boiling points of the relevant silanes are given in Table 7.4, and from this it can be seen that the Bpts of DCMVS and MTMOS are reasonably close, which, when considering the relatively low heating temperature of 93 - 94 °C (Table 7.4) and the use of a double walled condenser, makes it improbable that differential evaporation would have occurred at a high enough rate to result in the large viscosity differences observed between samples NHS5 and HS2 and between NHS6 and HS3 (Table 7.2). This suggests that a structural rearrangement of the systems has occurred. Since the expected effect of heating the silanes was to obtain an exchange of Cl and OCH_3 units between them, it appears that the rates of reaction of the difunctional and trifunctional silanes have been equalised, resulting in the development of a more homogenous material.

Silane	Bpt °C @ 760mmHg
DCMVS	70.3
DCDPS	305.2
MTMOS	103 - 103.5

Table 7.4. The Bpt of some common silanes.

The structures of these systems are not fully characterised but the utility of using this preparation technique is that it permits a higher loading of inorganic cross - linking moiety to be incorporated into the system whilst maintaining the viscosity within a

useable region. Whether or not a higher inorganic cross - link density is a benefit or not will now be discussed in relation to their observed mechanical and hermetic properties. It is obvious from Table 7.2 that, to obtain a material prepared directly via the co - hydrolysis and co - condensation of non - heated precursors, the level of T group substitution must be generally in the region of 20%. Values higher than this elevate the material viscosity to unuseable levels. Obviously, substitutions of 50% and higher are possible when employing heated silanes. It was hoped that the higher levels of T substitution possible with this technique would improve the viscosity - temperature behaviour of the materials but it can be seen from Figure 7.4 that the loss of viscosity with temperature for the 50% T containing sample ($D^{Ph}T$, HS5) mirrors that of the equivalent sample containing 20% T ($8D^{Ph}2T$ NHS10), the extra T groups do not, to any significant extent, control the viscosity of the sample. The dominant controlling factor is thus the distribution of the species within the polymer, but considerable sensitivity to the type of organics present is also observed, with D^{Ph} units having the greatest influence. The coating properties of these materials are not, on the whole, promising (see Table 7.3). A large variability in the morphology of the coatings was observed, with a number of coatings, from both heated and non - heated silanes, developing a highly irregular surface, as indicated in Figure 7.8, although none of the materials containing D^{Ph} exhibited this effect. Those materials having the best coating properties were, in general, heated silanes, containing D^{Ph} units. Those samples containing D and D' units, from which smooth transparent coatings were obtained (NHS4, HS3), were found to crack at an early stage of the immersion testing. The materials offering the best performance were NHS10 ($8D^{Ph}2T$) and HS5 ($5D^{Ph}5T$), both of which survived 300+ hrs under immersion test conditions.

Figure 7.8. Coatings of 50D50T (NHS3) and 20D'80T (HS2), demonstrating the highly uneven surface morphology obtained after a 200°C cure in air.

7.4.4 The co - hydrolysis of di - and tetra - functional silanes.

The nature of the white precipitate formed in PREP75 was assumed to be self condensed TEOS. Its lack of development in PREP0, and the existence of Si-OH groups in this material, suggest that the conditions under which PREP0 was prepared do not favour condensation. Since, under these conditions (moderately high pH, high H_2O / Si-X ratio), hydrolysis would be expected to be complete [40], it is proposed that the homocondensation between silanols is retarded at reduced temperature. This is contrary to that expected for methyl substituted silane diols whose homocondensation has been shown to be slightly exothermic [140] but the thermodynamics of homocondensation between silanols with other functionalities and organic substituents has not been addressed and may well be different to those of the basic methylsilanols. When heated at 200°C, both PREP0 and PREP75 show an increase in viscosity with time (Figure 7.5) suggesting thermal activation of an organic cross - linking reaction. The curves given in Figure 7.5 have two important characteristics, firstly, PREP75 has a higher initial viscosity, and secondly, the rate of increase in viscosity of PREP0 is higher than that of PREP75. From the conclusions made in 7.4.3, it may be inferred that the higher initial viscosity of PREP75 is due to the ordering of the D^{Ph} units within the sample, with these possibly being less ordered than in PREP0. The increased rate of cure observed for PREP0 may be due to a steric effect. If it is assumed that the D^{Ph} units are more randomly arranged through the structure then so too will be the D' units. Once a vinyl group has reacted, it is unlikely that a neighbouring group would also react since the mobility of the chain at that point would be reduced by the organic linkage to another siloxane chain, thus reducing its interaction with other groups. A chain with a random distribution of D' units would thus be expected to have a higher

percentage of reacted D' units than one with a blocky structure.

Preparation of a system at low pH results in the generation of a phase separated system, evident on a macroscopic scale by the precipitation of the self - condensed TEOS. This suggests that the rate of reaction of moieties of different functionality are different under these conditions, with the difunctional species preferentially condensing with themselves, the TEOS thus self - condensing at a later time, forming the precipitate via a RLCA growth mechanism [139]. Thus, at high pH it can be argued that the rates of reaction of the different precursors are equalised, so that all three are incorporated into the structure, thus forming an homogeneous system. It may also be proposed that, under conditions of high pH and a high H_2O / Si-X ratio, the favoured growth mechanism would be nucleation and growth [40]. Thus, assuming the reaction rates of the moieties not to be equal, the self condensation of the TEOS would lead to the generation of smooth silica particles that are prevented from gelling via mutual electostatic repulsion[40] . The system would thus evolve to be phase separated, but on a smaller scale to that prepared at low pH. An argument against this is that these systems were prepared with up to 50% of the H_2O having been replaced by EtOH. This has been shown [40] to severely limit the rate of the dissolution reaction. Since dissolution is of utmost importance to the nucleation and growth process, under these conditions the growth mechanism would be similar to RLCA, with a random and not blocky distribution of difunctional and trifunctional units maintaining the homogeneity. A similar trend is observed for the rate of cure at 200°C for these samples as for PREP0 and PREP75, with the more homogeneous system (PREP14) curing fastest, and the least homogeneous system (PREP1) curing the slowest (see Figure 7.7).

CHAPTER 8: FULL INTERPENETRATING POLYMER NETWORK-RESULTS AND DISCUSSION.

8.1 Development of preparation techniques.

As discussed in 3.4, interpenetrating networks (IPNs) are systems employing at least two polymer networks (a network is defined as a system of linear chains cross - linked with multifunctional units). It has been shown [88] that in an interpenetrating system composed of two networks, one of long chains and one of short chains, the mechanical properties of such a network are governed by those of the long chain network, and hence are mechanically more favourable (low Young's modulus, greater flexibility). It was the aim of this study to develop an IPN material based on a long - short chain system, with the long and short chains being chemically different. All materials prepared are termed **full IPNs** since they are developed from the full interpenetration of two inorganic networks, with the structure of the system not simply relying on the physical mixing of two different polymers or upon the infiltration of one polymer into the network of a second. The next section introduces the preparation techniques used to develop the long and short chain polymers (LCPs and SCPs).

8.1.1 The development of the short chain polymer (SCP).

D^{Ph} species were chosen as a component of the SCP so as to afford the material good hermetic properties. All SCP systems thus employed D and / or D^{Ph} units in various ratios. To obtain an oligomeric population it was decided to prepare the systems under reasonably dilute conditions (0.5M initial precursor concentration). Under these conditions though, preparation in toluene would have produced a large degree of cyclisation (5.1.4.1), thus all samples were prepared in dichloromethane (DCM) so as

to encourage intra - inter catalysis [48] (3.2.4) and discourage cyclisation. A number of samples were prepared as part of the preparation route development process. These may be placed into three groups: i) those prepared via the standard preparation route (4.7) with cohydrolysis and cocondensation of precursors and employing aqueous KOH solution as acid acceptor, ii) as above but employing pyridine in place of KOH and iii) as above but employing a controlled addition of one component to a solution of the other. These three routes are shown schematically in Figure 8.1. A summary of the samples prepared and the reaction conditions used is given in Table 8.1. The samples were end - blocked by the addition of excess bistrimethysilylacetamide (BSA - a silylating agent) so as to obtain stable systems suitable for analysis.The results of the

Sample	Composition	Neutralisation	(H_2O:SiX)		Time to end - blocking (hrs)
			Pre KOH	Post KOH	
Route i					
PREPA	DCDPS	20N KOH to pH9 over ½hr	1	7.5	3
PREPB	DCDPS / DCDMS	" " "	1	7.5	11
PREPC	DCDPS / DEODMS	" " "	1	7.5	3
PREPD	DCDPS	20N KOH to pH14 over ½hr	1	8.9	3
Route ii					
PREPE	DCDPS / DEODMS	C_5H_5N in stoich ratio to SiX	1		30
PREPF	"	" "	"		55
Route iii					
PREPG	20 DCDPS / 80 DCDMS	" "	0.69		1
PREPH	"	" "	"		2
PREPI	"	" "	"		4
PREPJ	"	" "	"		16
PREPK	"	" "	"		55

Table 8.1. The short chain polymers prepared via the three routes of Figure 8.1.

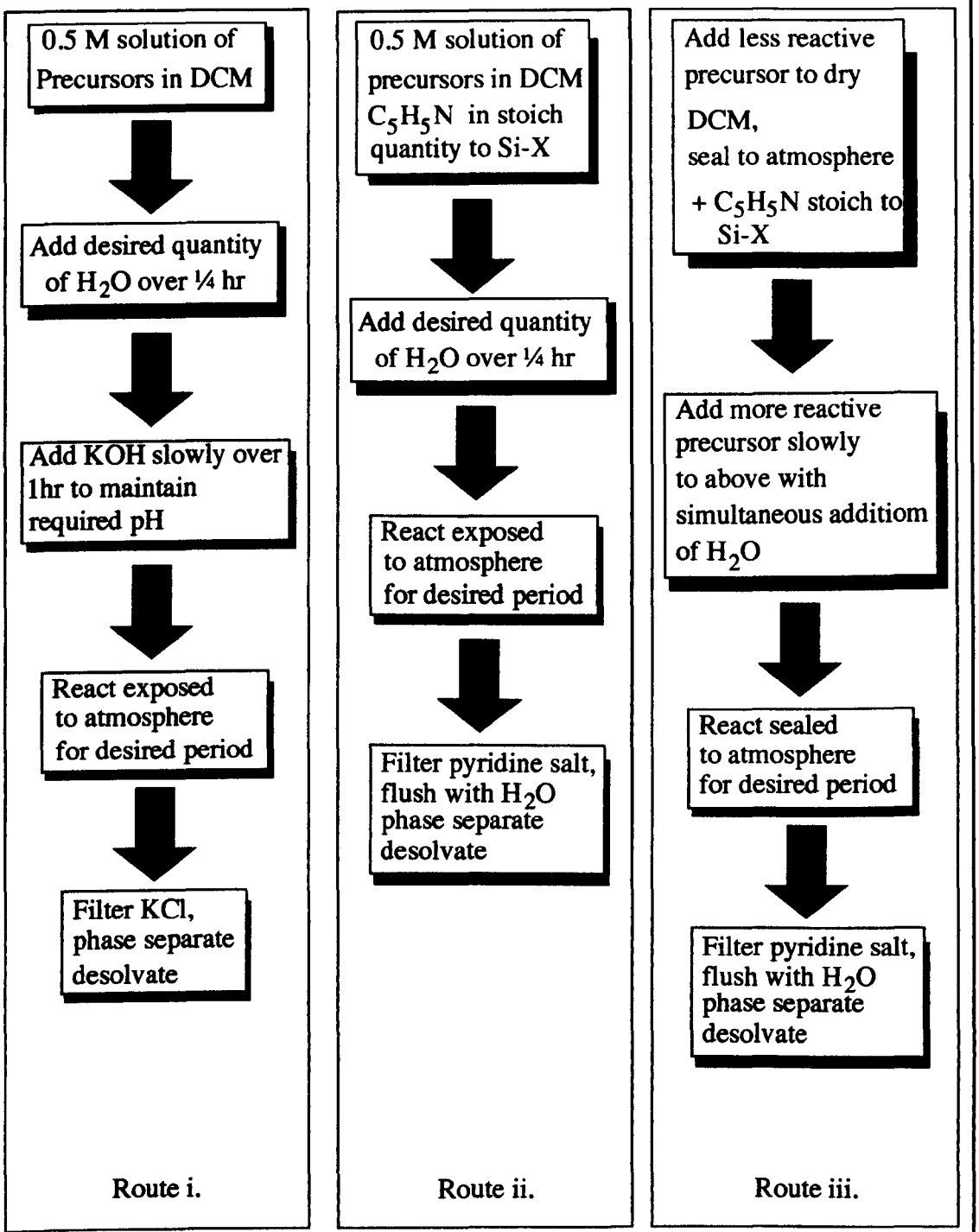

Figure 8.1. The three preparation routes investigated for the preparation of the SCP materials.

preparations of Table 8.1 are given in Table 8.2. For those samples in which two phases were prepared (a white precipitate and an oil), the phases were separated via filtration

Sample	Prior to desolvation	After desolvation
PREPA	Homogeneous	Biphasic - white ppt clear oil
PREPB	White suspension	Biphasic - white ppt clear oil
PREPC	Homogeneous	———
PREPD	Homogeneous	Biphasic - white ppt clear oil
PREPE - F	Homogeneous	———
PREPG - K	Homogeneous	———

Table 8.2. The results of the SCP preparations of Table 8.1.

and the solid precipitate was flushed with MeOH to remove any remaining oil. All materials were analysed using IR spectroscopy (4.1.2) (TR - IR / transmission IR where appropriate) and GPC (4.1.3). The TR - IR spectrum of a typical sample of the insoluble precipitate is shown in Figure 8.2 and the transmission IR of a typical soluble sample is given in Figure 8.3. The GPC chromatographs (insoluble + soluble, solvated in THF) of samples PREPA, B and D are all very similar (see Figure 8.4a for an example chromatograph), whereas that of the insoluble phase of PREPC has a tail to high mass (Figure 8.4b). The preparation route employed to prepare PREPE and PREPF produced material without a white precipitate. The GPC chromatographs of these samples are presented in Figure 8.5. The preparations PREPG-K utilised a slightly altered preparation route (see Figure 8.1) so as to create reaction conditions consistent with a more homogeneous reaction. The model samples prepared (stabilised with BSA after a range of reaction periods) were investigated using GPC, the chromatographs are presented in Figure 8.6.

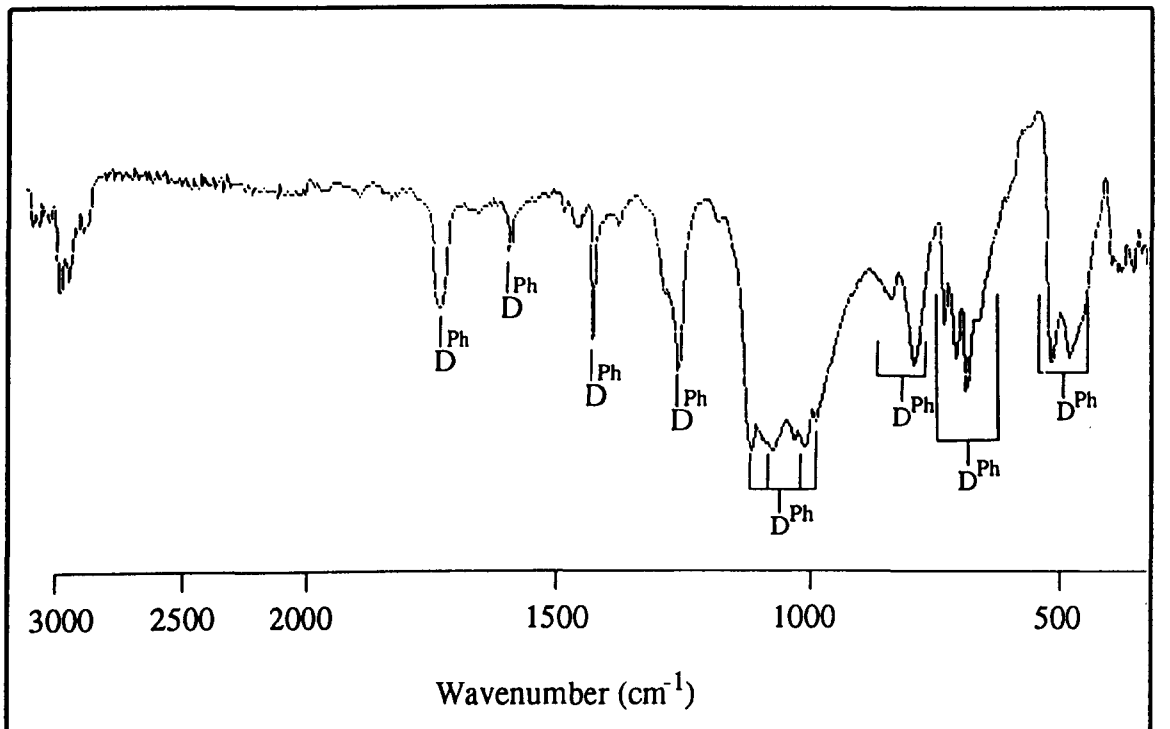

Figure 8.2. The TR - IR spectrum of the white precipitate formed in samples PREPA - D.

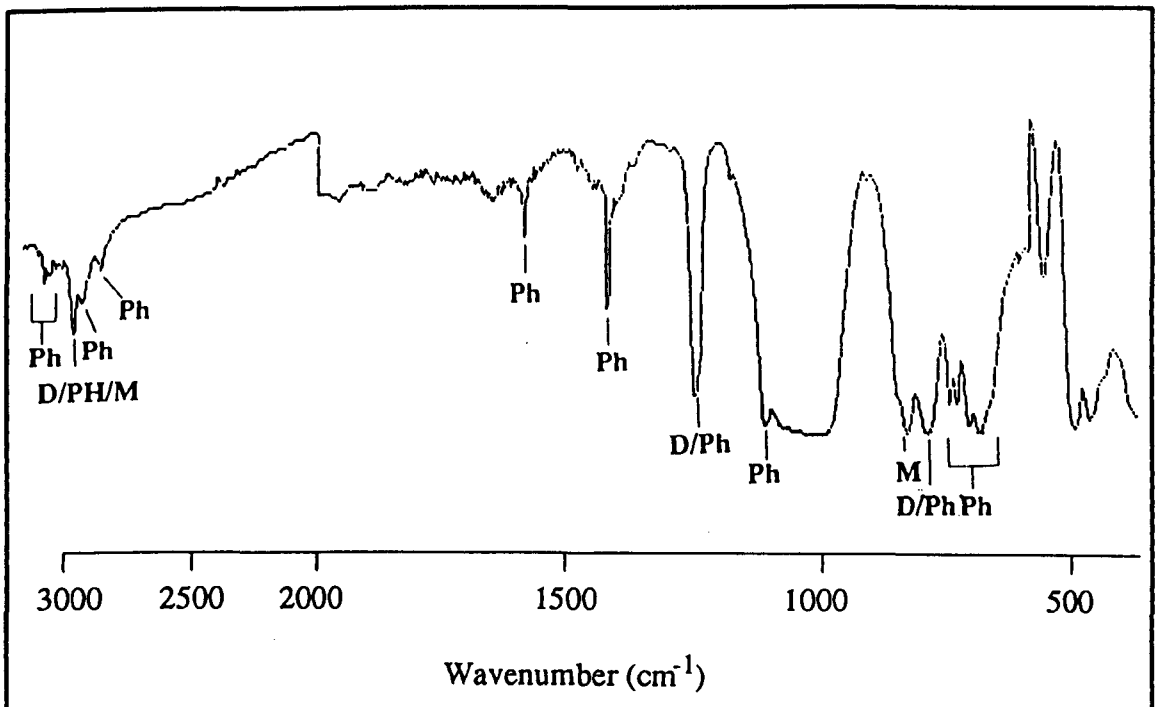

Figure 8.3. A typical transmission IR spectrum for the liquid phases of samples PREPA-D.

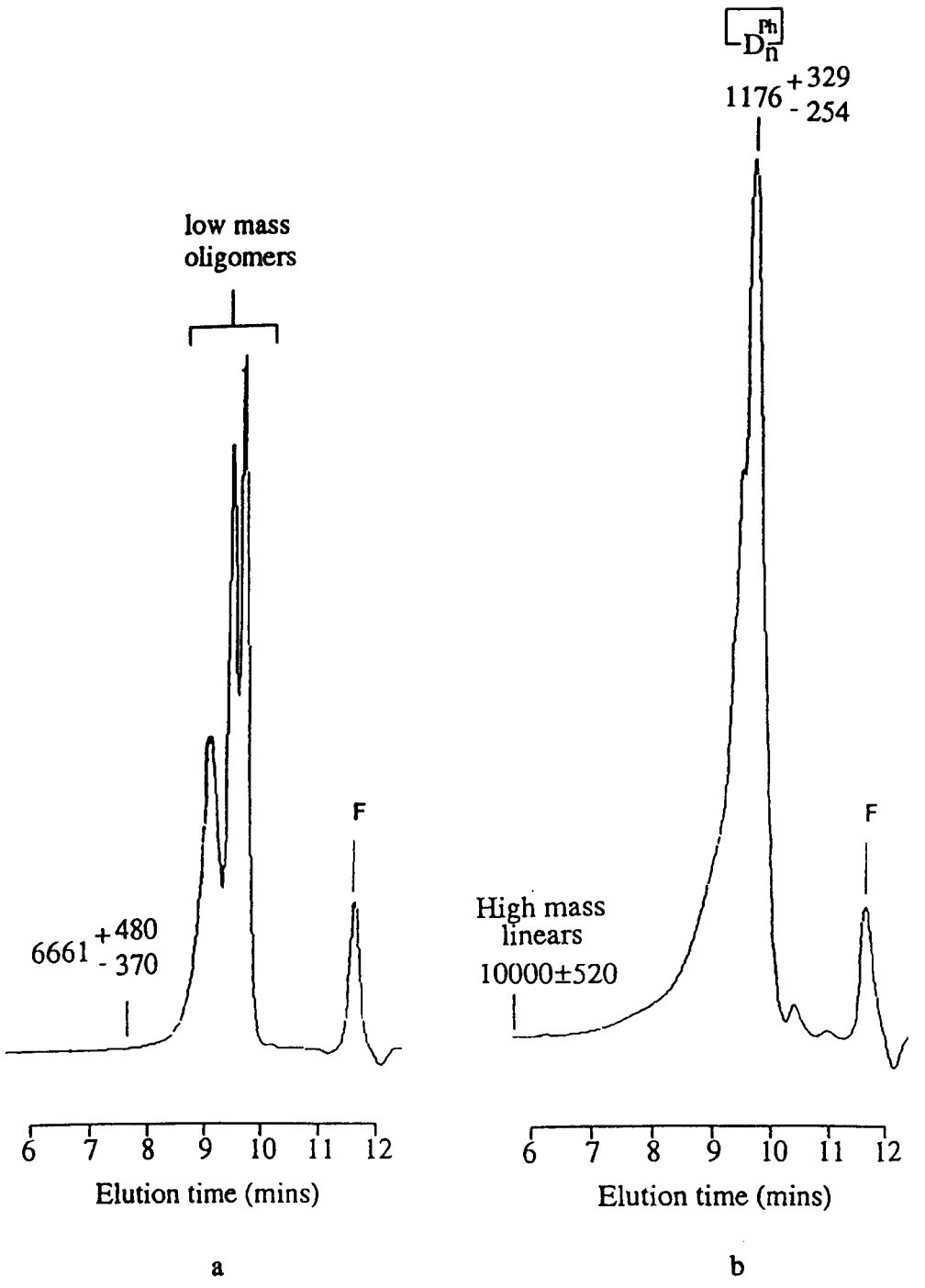

Figures 8.4. a) A GPC chromatograph typical of samples PREPA, B and D, b) the GPC chromatograph of the insoluable phase of sample C.

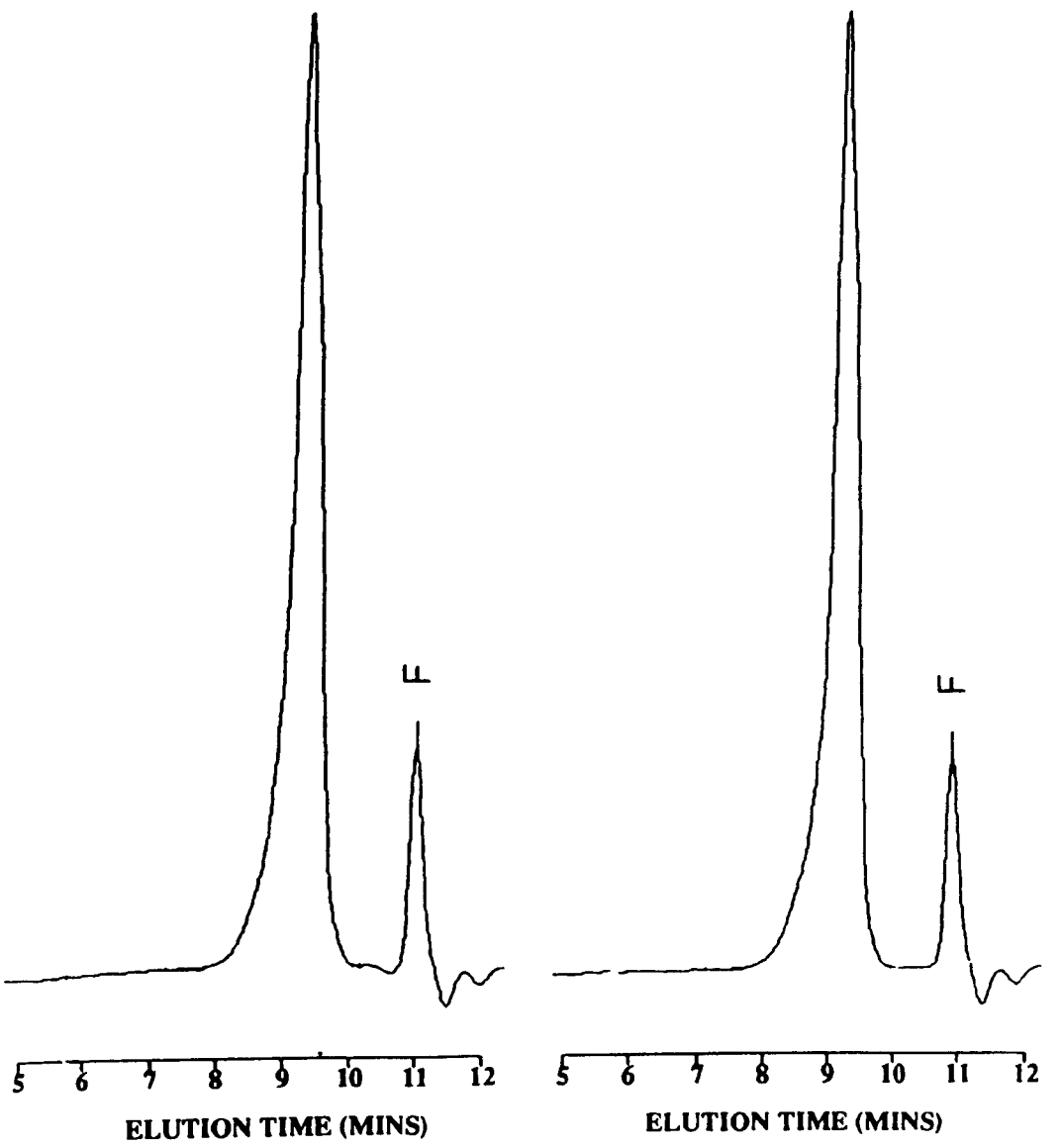

30 55

Figure 8.5. The GPC chromatographs of samples PREPE (30hrs) and PREPF (55hrs).

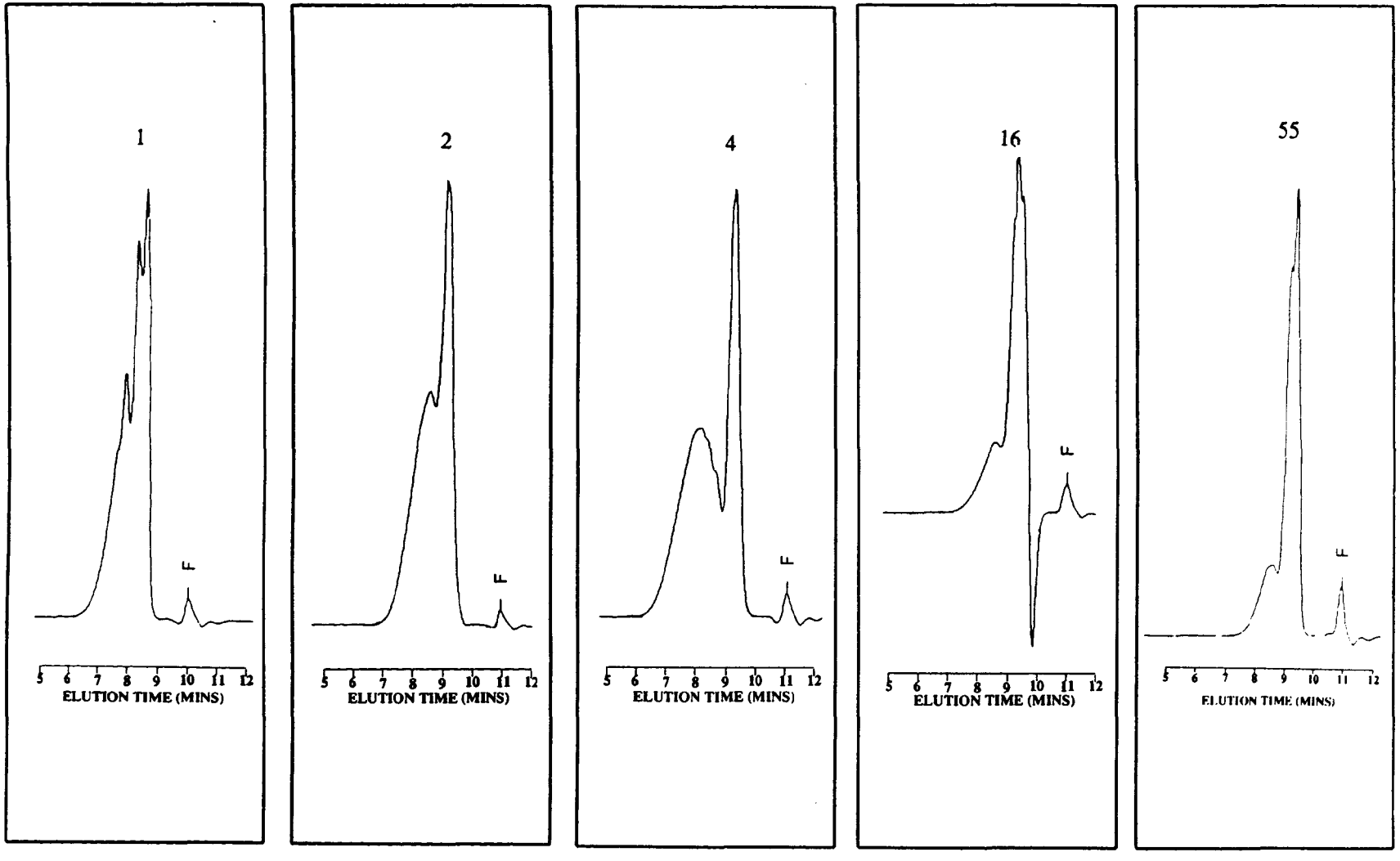

Figure 8.6. The GPC chromatographs of samples PREPG - K, stabilised after variousreaction periods.

8.1.1.2 Discussion of the preparation of the SCP systems.

Samples A, B and D all formed, to some degree, a white precipitate, with the highest levels being found in PREPA and PREPB. From the TR - IR spectrum of the precipitate (Figure 8.2), the lack of M and D resonances suggest it to be composed of D^{Ph} cyclics (these being white solids at room temperature [36] and insoluble in MeOH). PREPD, prepared under conditions of high pH and high H_2O : Si-X ratio, was expected to prepare the most homogeneous system since, under these conditions, the dissolution rate is high, the condensation rate low and hydrolysis is complete. In fact, this preparation route did result in a lower level of insoluble D^{Ph} material than for PREPA and PREPB but the level was still 5wt %, which is unacceptable. Thus, direct addition of the chlorosilane (DCDPS and / or DCDMS) to DCM, and their hydrolysis under alkaline conditions (controlled by the addition of aqueous KOH solution) is not a suitable preparation route to an homogeneous short chain polymer of the composition D^{Ph} or D^{Ph} / D.

PREPC, which utilised DEODMS (difunctional alkoxy precursor) again developed a white precipitate. As can be seen from the GPC of this precipitate (Figure 8.4b), it exhibits a more significant population of higher mass species. The TR - IR spectrum of this precipitate (not given), exhibits resonances from M, D and D^{Ph} units, suggesting that the tail to high mass results from polymeric material with a high DP_{av}. Due to both the inhomogeneity of the material and the development of the higher polymer, the preparation route is also considered unsuitable for the preparation of SCP.

The preparation route employed to prepare PREPE and PREPF produced an apparently

homogeneous material without a precipitate. The reaction times employed were rather long (30 and 55 hrs) as it was thought that the precursors employed (DCDPS and DCDEOS) would have slow reaction rates. The GPC analysis of these materials (Figure 8.5) indicates that they possess a smooth population distribution. It is also seen from Figure 8.5 that there is no significant difference between the two samples. This may indicate that either the system is highly cyclised (and thus, in the absence of dissolution reactions, the population distribution is invariant with time) or that an equilibrium has been reached both between the linear and cyclic components and between the species within each component.

To assess which of the above is the more likely, the preparations PREPG - K were investigated. All the chromatographs of the samples prepared via route iii (Figure 8.1) are common in that they all demonstrate two main peaks. The narrow peak at high elution times is indicative of low mass oligomers and can be seen to be composed of a number of discrete peaks, each one corresponding to a particular oligomer. The broader peak, extending to shorter elution times, results from higher mass species. In all samples, the low mass peaks are very similar and are little affected by the reaction time. On the other hand, the higher mass feature varies considerably with reaction time. In general, for increasing reaction periods up to 4 hours, both the maximum mass of the species present, M_{max}, and the mass corresponding to the most abundant species, M_{abu}, are observed to increase, as illustrated in Table 8.3 (where masses are calculated using the calibration curve for the linear species (Appendix II Fig II.2). At some time between 4 and 16 hours, the whole peak is seen to shift to lower mass, a trend which continues with even longer reaction periods. Since these preparations were not performed under

Sample	Reaction period (hrs)	M_{max}	M_{abu}
PREPG	1	3236^{+654}_{-275}	———
PREPH	2	5688^{+1073}_{-902}	1026^{+237}_{-192}
PREPI	4	10000^{+1749}_{-1489}	924^{+216}_{-125}
PREPJ	16	3236^{+654}_{-275}	528^{+128}_{-106}
PREPK	55	2891^{+598}_{-492}	492^{+122}_{-98}

Table 8.3. Mass calculations obtained from the GPC of samples PREPG - K, prepared via route iii.

conditions thought to encourage dismutation / dissolution reactions (such as high pH), it is not possible that processes leading to a lowering of the size of the species are operative within these systems. It is thought that the observed decrease in species size occurs as a result of cyclisation since the mass of a cyclic species, as obtained from GPC, is lower than that of an equivalent linear (see Figure II.2), cyclisation would result in a shift in the peak to lower mass. The loss of the highest mass species would suggest that even these, given a long enough reaction period, are susceptible to cyclisation. It would thus be very likely that samples PREPE - F would have a large cyclic content, thus accounting for the observed insensitivity to reaction time.

8.1.2 The development of the long chain polymer (LCP).

The aim of the LCP preparation was to develop a system based on a D / D' copolymer, having a mass distribution with a large population of high mass species. A wide range of preparation routes were investigated. These could be classified as either being neutralised using an aqueous KOH solution (type I) or using a non - aqueous acid

acceptor such as pyridine or ethylacetate (type II).

8.1.2. Type I preparations.

All type I preparations were made by addition of the chlorosilane precursors to DCM (the order of addition being a variable between samples). The systems were reacted for a desired period, during which the pH was maintained at 8 - 9 via the addition of 20N KOH solution. Two variations on the preparation were investigated i) addition of both precursors to the DCM and their subsequent cohydrolysis and cocondensation (Figure 8.7a) and ii) controlled addition of a solution of one precursor in DCM to a solution of the other precursor in DCM (Figure 8.7b). A summary of the samples prepared, and the reaction conditions employed, are given in Table 8.4. After the reaction period, the

Sample	Route (see Fig 94)	Composition	H_2O : Si-X		Reaction period (hrs)
			Pre KOH	Post KOH	
LCP1/A	A	20D' / 80D	1	3.8	0.5
LCP2/A	B	20DCMVS 'A' 80DCDMS 'B'	1	3.8	24
LCP2/B	B	80DCDMS 'B' 20DCMVS 'A'	1	3.8	24

Table 8.4. The LCP samples prepared via the type I preparations of Figure 8.7.

systems were inorganically cross - linked with 20 mol% (relative to difunctional precursors) methyltrimethoxysilane (MTMOS). Sample LCP1/A, formed a biphasic system with the development of a white solid, insoluble in DCM, and a clear oil. IR spectroscopy was performed on each phase and the resonances were identified by comparison to spectra of siloxanes of known composition. The TR - IR and

transmission IR spectra of the insoluble and soluble phases respectively are presented in Figure 8.8, which also serves to illustrate the specificity of the D, D' and T absorptions.

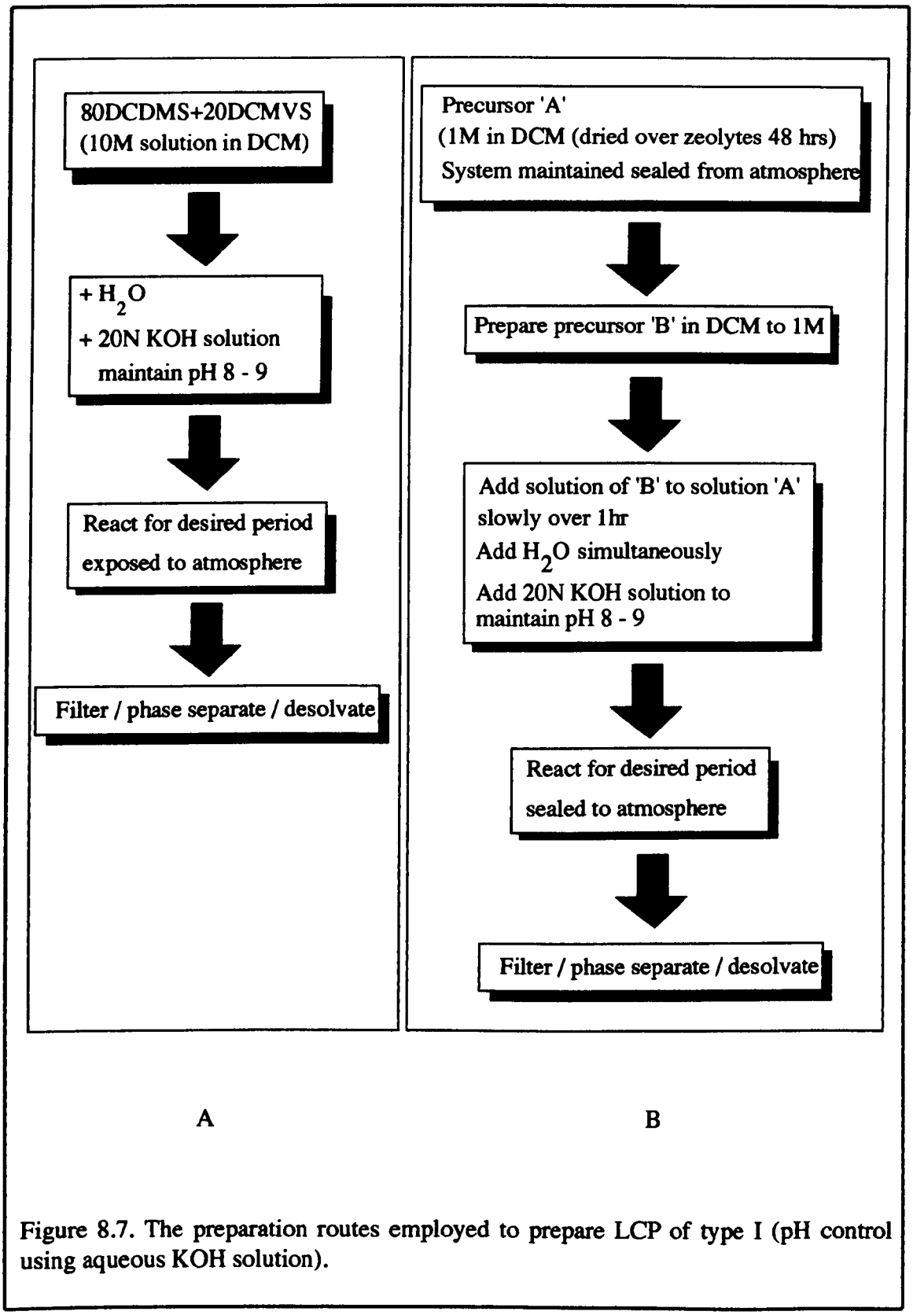

Figure 8.7. The preparation routes employed to prepare LCP of type I (pH control using aqueous KOH solution).

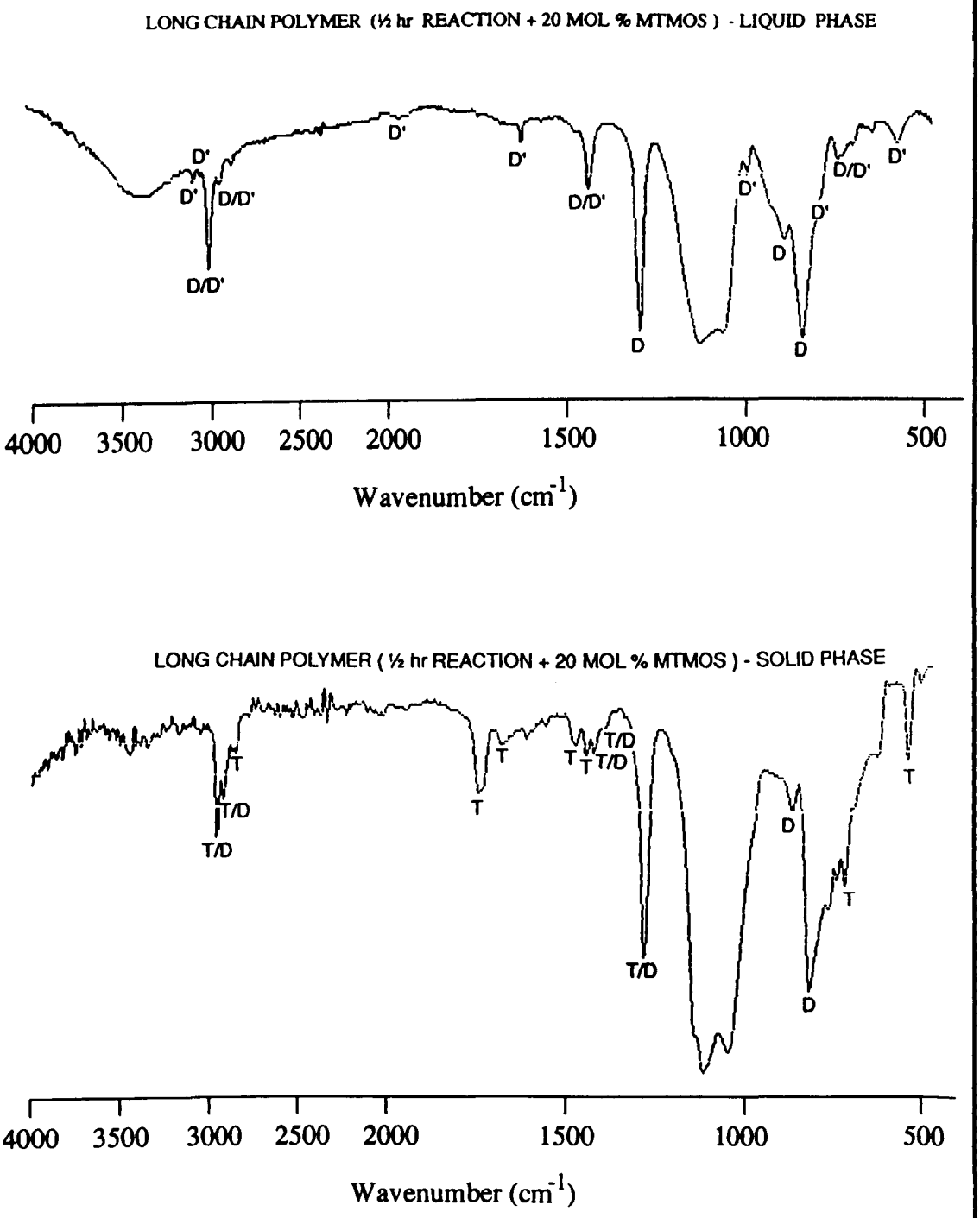

Figure 8.8. Transmission and TR - IR spectra of the soluble and insoluble phases of samples LCP1/A, prepared via prep route 'type I - A' (see Figure 8.7).

Both samples prepared using method B resulted in the development of phase separated materials, with an insoluble white phase and a soluble clear oil. IR spectroscopy of both phases of each sample was performed and the spectra were characterised using the same method as for LCP1/A. The spectra are not presented here, only the results of the analysis, which are presented in Table 8.5.

Sample	Phase	Composition
LCP2/A	Soluble	D / D'
	Insoluble	T / D (minor)
LCP2/B	Soluble	D / D'
	Insoluble	T / D(minor)

Table 8.5. The species present in the soluble and insoluble phases of the LCP2 materials as inferred from an IR spectroscopy analysis.

8.1.2.2 Type II preparations.

All samples prepared via this route can be categorised into one of two principal groups, these being; i) Addition of both precursors to the acid acceptor (sealed under dry N_2), and their subsequent co - hydrolysis and co - condensation, ii) controlled addition of one precursor to a solution of the other in DCM / acid acceptor (over 1hr), sealed under N_2. These routes are shown schematically in Figure 8.9. All samples were prepared using a H_2O : Si-X ratio of 0.28 and DMAP was used as a heterofunctional condensation catalyst [48] in a number of samples. The systems were reacted, sealed to the atmosphere, for a period of 24 hrs. After the reaction period the materials were prepared for analysis by chain end termination with the addition of excess BSA (to prepare systems stable to further condensation). A number of preparations were

investigated for each route. The reaction conditions employed for each preparation are summarised in Table 8.6. All samples prepared were single phase, oily materials. The molecular size distribution were investigated using GPC. GPC chromatographs of these samples are presented in Figures 8.10 (LCP3, LCP3MOD, LCPMOD / 1 and 8.11(LCP4, LCP4MOD and LCP5). Transmission IR spectra of all samples were also obtained and indicated that all three unit types (D, D' and M) were incorporated into each material, with no significant difference in the absorption intensities between samples.

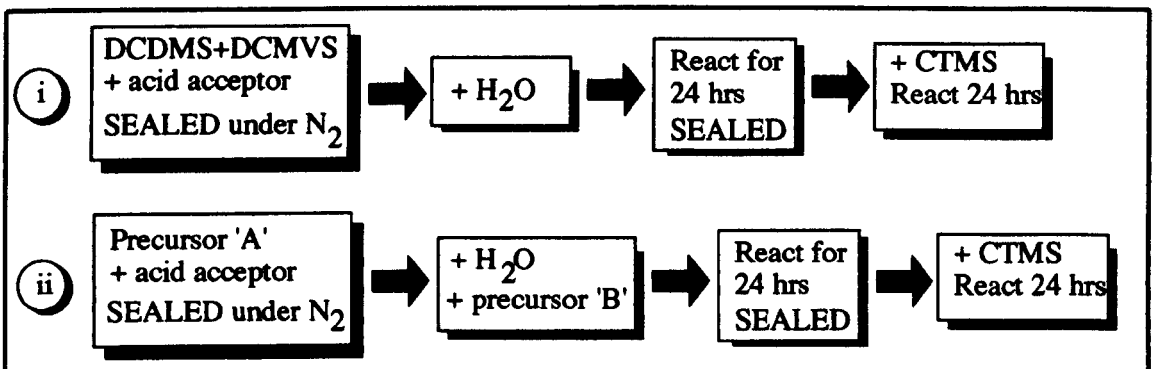

Figure 8.9. The two principal routes employed to prepare the type II long chain polymer materials.

Sample	Route*	Acid acceptor	Precursors	Catalyst
LCP3	i	C_5H_5N	DCDMS+DCMVS	✗
LCP3MOD	i	Et_3N **	DCDMS+DCMVS	✔
LCP3MOD/1	i	Et_3N	DCDMS+DCMVS	✗
LCP4	ii	C_5H_5N	DCDMS 'B'+DCMVS 'A'	✗
LCP4MOD	ii	C_5H_5N	DCDMS 'B'+DCMVS 'A'	✔
LCP5	ii	C_5H_5N	DCDMS 'A'+DCMVS 'B'	✗

* Refer to Figure 8.9 for route. ** Et_3N = triethylamine

Table 8.6. Long chain polymer samples prepared and reaction conditions used.

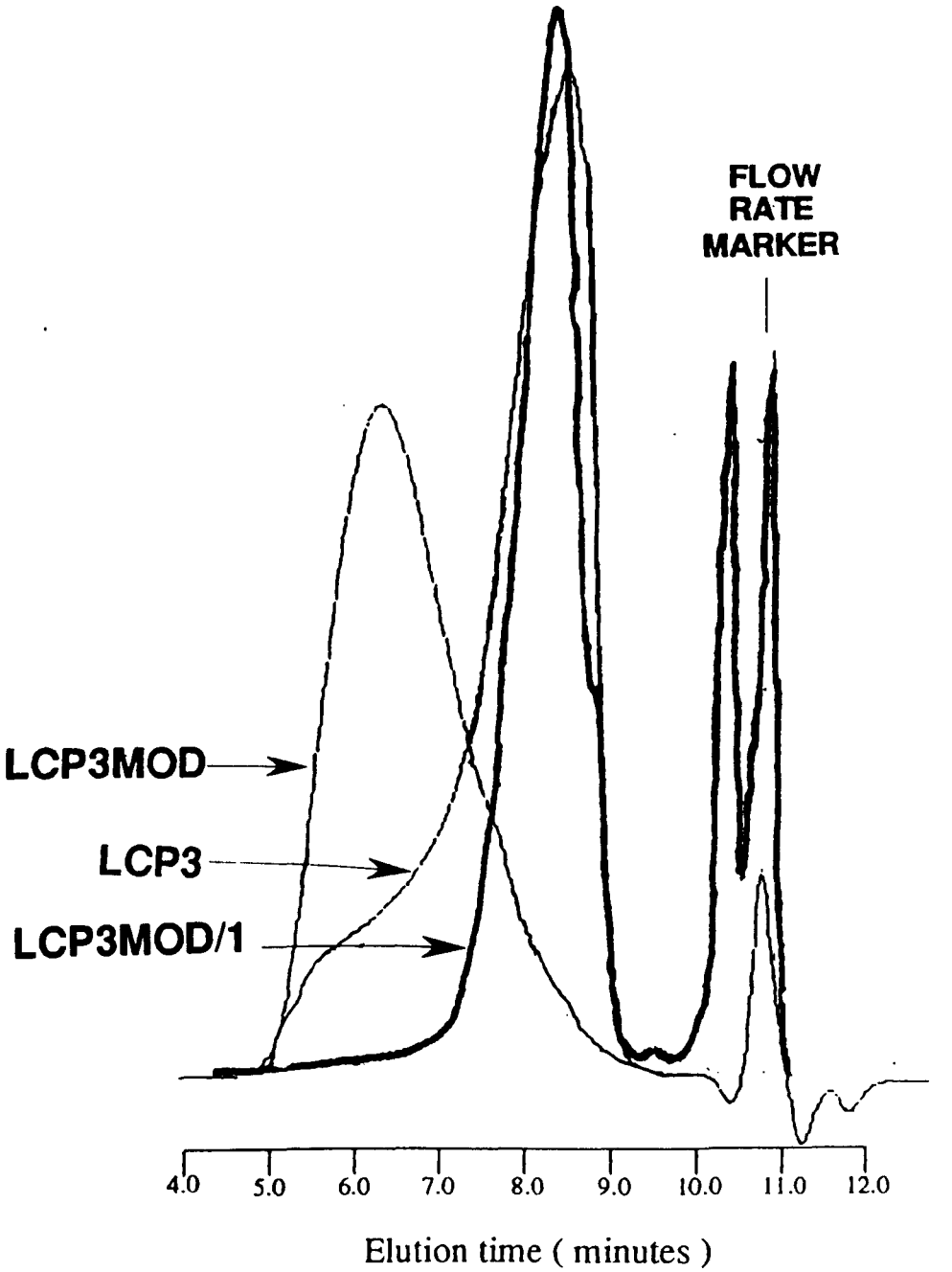

Figure 8.10. GPC chromatographs of samples LCP3, LCP3MOD and LCP3MOD/1.

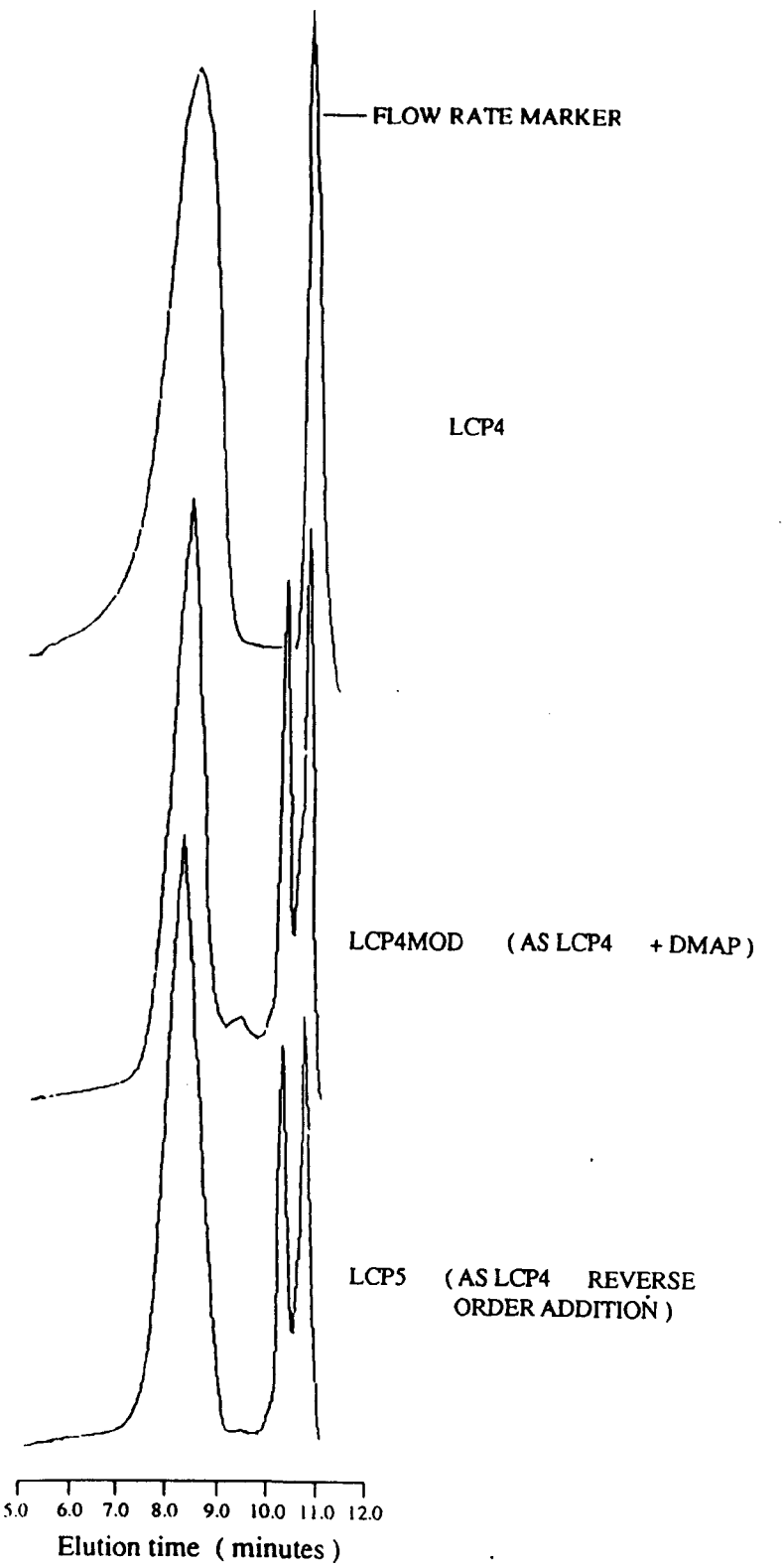

Figure 8.11. The GPC chromatographs of samples LCP4, LCP4MOD and LCP5.

Preparation using a non - aqueous acid acceptor offered more promising results than the aqueous neutralisation route, with all the samples being single phase (from visual inspection). Two figures of merit for the preparations are the mass corresponding to the most abundant species, M_{abu}, and the highest mass species that are present within the population, M_{max}. It is evident from the GPC chromatographs that the highest mass species for all the samples are above the high mass limit of the column used and thus were eluted after that point.Mabu values were obtained from the GPC chromatographs of the samples (Figures 8.10 and 8.11) and are given in Table 8.7 and were calculated assuming the species to be linear. Although all samples do possess very high mass species, only sample LCP3MOD has a significantly high proportion of high mass species (see Table 8.7 and Figure 8.10). This sample was prepared using simultaneous addition of precursors and a triethylamine acid acceptor in conjunction with a DMAP catalyst. In comparison to this, sample LCP3, prepared using pyridine as acid acceptor and without the presence of DMAP catalyst, has the majority of species at low mass, although it does still have a reasonably high proportion of high mass species (see Figure 8.10). It was not clear whether the large increase in molecular mass seen for LCP3MOD was as a result of action of the DMAP or whether the Et_3N has strong catalytic properties of its own. This would not be expected since the catalytic constant of Et_3N for the heterofunctional condensation between Si-Cl and Si-OH in model oligosiloxanes has been reported to be only $1.8x10^{-4}$ that of DMAP [50]. To ascertain the extent, if any, of the catalytic effect of the Et_3N, sample LCP3MOD/1 was prepared. This was prepared as for LCP3MOD but with the exclusion of the DMAP. The result of the GPC of the above indicates that the material has very few components at high mass (Figure 8.10, Table 8.7). This proves conclusively that the high degree of

Sample	M_{abu}
LCP3	339^{+88}_{-70}
LCP3MOD	$(3.2^{+0.6}_{-0.5})x10^3$
LCP3MOD/1	494^{+122}_{-98}
LCP4	434^{+110}_{-87}
LCP4MOD	434^{+110}_{-87}
LCP5	403^{+100}_{-75}

Table 8.7. The mass corresponding to the most abundant species within each LCP prepared via a non - aqueous neutralisation route.

polymerisation is predominantly due to the DMAP. It should be noted that comparison between the chromatograph of LCP3 (pyridine only) with that of LCP3MOD/1 (triethylamine only) (Figure 8.10) indicates that the synthesis of higher molecular weight species is catalysed to a higher degree by pyridine than it is with triethylamine. Since the latter is the stronger base but the weaker nucleophile, the nucleophilic action of the catalyst is reinforced. This is congruent with the work of Rubinsztajn et al [50]. The GPC chromatographs of samples LCP4, LCP4MOD and LCP5 (Figure 8.11), prepared by sequential addition of precursors, indicate that no high mass species are produced under these conditions, a result that is independent of the order of precursor addition, of acid acceptor type and of catalyst. The latter is most surprising given its observed effect on accelerating the polymerisation of the LCP3 systems. Thus, in conclusion, the route LCP3MOD affords the optimum route to the preparation of homogenous long chain polymer.

8.1.3 Preparation of the IPN from the SCP and LCP.

All short chain polymers were prepared using route iii (Figure 8.1), employing a $20D^{Ph}80D$ composition and a reaction period of 3hrs (chosen on the indication that this period does not result in a high degree of cyclisation (8.1.1.2)). The long chain polymers were prepared using the LCP3MOD route, as this offers a high proportion of high mass species within an homogeneous material (Figure 8.10, Table 8.7).

Networking of the materials was achieved using MTMOS, with employment of DMAP during its reaction with the hydroxy - end - blocked linear copolymers. A range of materials were prepared and their compositions are given in Table 8.8. Included in Table 8.8 are the levels of inorganic cross - linking employed, given in mol% relative to the respective linear precursors. The preparation of the full IPN is indicated schematically in Figure 8.12.

Sample	LCP Composition	SCP Composition	Mol% MTMOS Networker in: SCP	LCP	Ratio LCP : SCP
1	1MV4DM	1DP4DM	10	10	1:1
2	" "	" "	50	50	"
3	1MV1DM	" "	10	"	"
4	9MV1DM	" "	"	"	"
5	1MV1DM *	" "	"	"	"
6	1MV4DM	" "	10	10	4:1
7	" "	" "	"	"	1:4

MV = DCMVS DM= DCDMS DP=DCDPS
*= Anionically polymerised LCP

Table 8.8. Composition of IPN materials prepared.

8.1.4 IPN material analysis - results.

For all measurements discussed below, the samples were cured to an elastomeric state using a temperature excursion of 200°C for a period of 16hrs in air. Samples 1 - 5 were prepared for Young's modulus determination using the method discussed in 4.2.1. The Young's moduli of the materials, Y, were calculated from the linear part of the stress - strain data. Also obtained were the maximum percentage extensions prior to rupture, defined as $(\Delta l/lo)x100$, where Δl is the sample extension and lo is the original sample

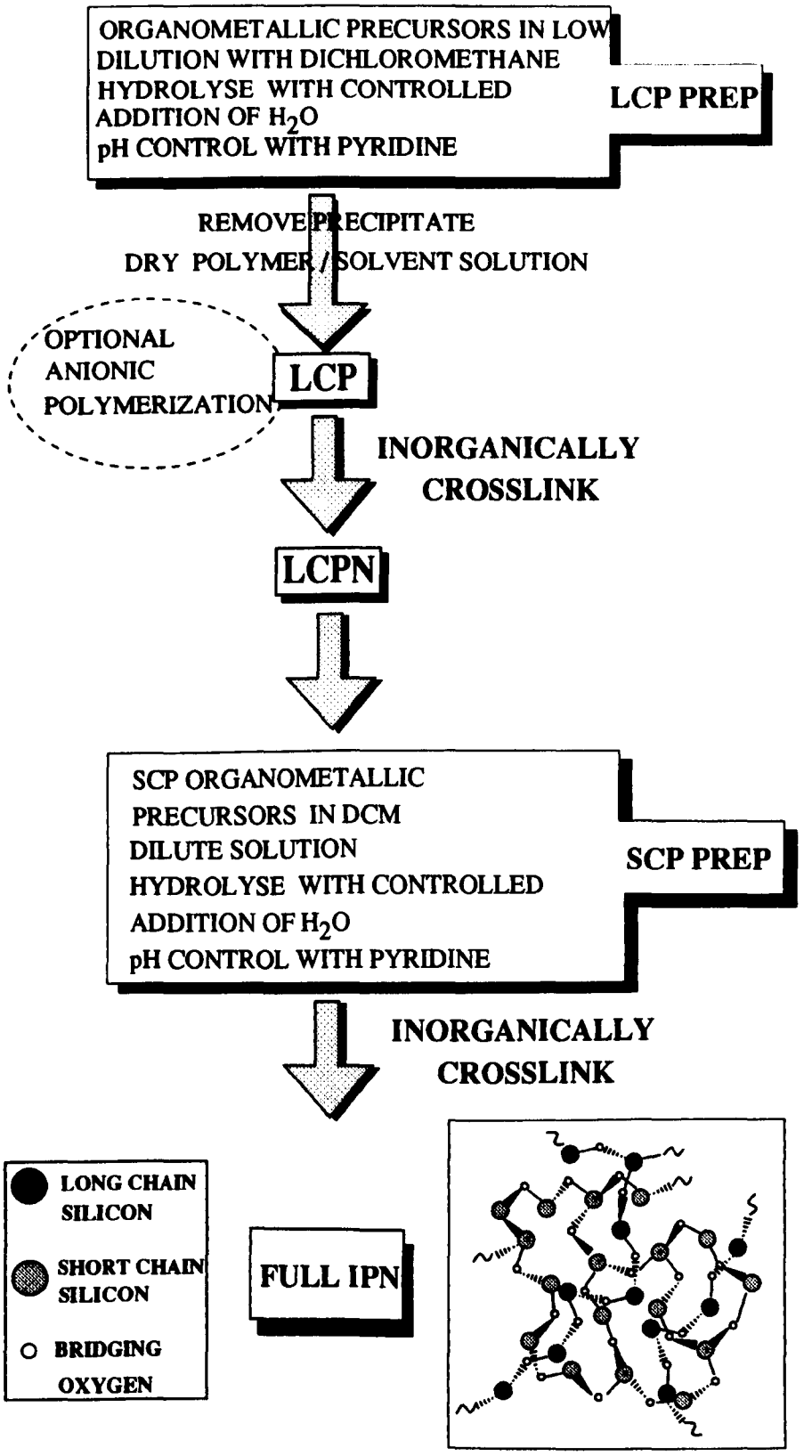

Figure 8.12. A Schematic representation of the preparation of IPN materials.

length. These results are given in Table 8.9. Samples 1 - 4 were prepared for low frequency dielectric analysis using the method discussed in 4.4.2.2. Dielectric measurements were made using the fabricated test fixture (4.4.2.6). The results of these measurements are presented in Table 8.10. Finally, cured, samples of materials 1 - 4 were assessed for thermal stability using thermo gravimetry (4.3.1), being subjected to 250°C in air for a period of 1000 minutes. The resulting percentage mass losses are given in Table 8.11. The thermal expansion coefficients of samples 1 - 4 were measured using a Netzsch 402E dilatometer (4.2.3). The expansion results are presented in Table 8.12 along with the calculated contraction expected for each material when cooling from a cure temperature of 200°C to RT.

Sample	Y (MPa)	Δl/lo x100 (%)
1	0.0288±0.004	43
2	0.64±0.01	15
3	0.54±0.01	8
4	16.6±0.3	2.9
5	0.51±0.03	10.1

Table 8.9. Experimental Youngs moduli and maximum percentage extensions

Sample	ε_r / *tanδ*	
	1MHz	10MHz
1	3.36±0.06 *0.0010±0.005*	3.57±0.06 *0.0073±0.0008*
2	3.4±0.2 *0.0370±0.0002*	—— ——
3	3.9±0.1 *0.0110±0.0001*	3.9±0.1 *0.0020±0.001*
4	—— *0.0194±0.0008*	3.71±0.01 ——

Table 8.10. Low frequency dielectric constants and *dielectric loss* of IPNs

Sample	Percentage mass loss
1	3.85
2	3.15
3	5.10
4	5.57

Table 8.11. Percentage mass loss of IPN samples heated at 300°C for 1000 minutes

Sample	$\alpha_{50\text{-}200}$ (MK^{-1})	Contraction $\%_{200\text{-}20°C}$
1	371±6	6.8±0.1
2	566±3	10.18±0.05
3	540±41	9.7±0.7
4	252±3	4.54±0.05

Table 8.12. Experimental TCE values and calculated percentage contractions

Samples 1,2,6 and 7 were prepared for THB testing as outlined in 4.5.2. Samples were prepared onto a number of different substrates, namely polyimide (PI) (see 2.3.3), cyanate ester and alumina. The samples prepared, the conditions employed for their preparation, and the coating thicknesses are summarised in Table 47. The cure conditions employed were those that offered an optimum level of cure without incurring heat damage to the sample. The surface insulation resistance (SIR) of the test samples (the resistance measured between the two interdigitated patterns (Figure 4.27) was calculated for each sample with the exception of sample CE2, which was found to have a short circuit (surface resistance <200Ω). Initial measurements were made at RT /

Sample	IPN*	Substrate	Cure conditions	Coat thickness (mm)
PI1	1	Polyimide	200 / 72	0.27±0.02
PI2	1	"	" "	0.25±0.03
PI3	2	"	240 / 16	0.37±0.03
PI4	2	"	" "	0.47±0.03
PI5	6	"	200 / 96	0.51±0.05
PI6	6	"	" "	0.63±0.05
PI7	7	"	" "	1.07±0.07
PI8	7	"	" "	0.88±0.04
CE1	2	Cyanate ester	240 / 16	0.36±0.02
CE2	2	"	" "	0.53±0.03
CE3	1	"	200 / 72	0.35±0.07
CE4	1	"	" "	0.50±0.02
CE5	6	"	200 / 96	0.47±0.01
CE6	6	"	" "	0.72±0.02
CE7	7	"	" "	1.041±0.009
CE8	7	"	" "	0.51±0.01
AL1	6	Alumina	200 / 72	0.26±0.01
AL2	6	"	" "	0.33±0.01

* See Table 8.8 for sample compositions.

Table 8.13. The samples prepared for temperature - humidity - bias testing.

Sample	Meander	Surface insulation resistance (Ω)										RT / 50%
		At 25°C	At 85°C	At 85 / 85	24hrs	48hrs	135hrs	250hrs	500hrs	750hrs	1000hrs	1000hrs
PI1	fine	2.5E11	4.00E9	7.50E8	1.85E8	2.25E8	4.00E8	6.00E8	3.30E8	1.50E8	1.60E8	8.50E10
PI2	coarse	1.55E11	5.00E9	1.00E9	1.00E9	1.30E9	1.50E9	2.00E9	1.00E9	6.50E8	5.00E8	1.67E11
PI3	fine	1.00E12	9.90E8	4.00E6	1.50E6	2.4E7	7.50E7	9.00E7	3.20E7	7.00E6	9.00E6	5.00E5
PI4	coarse	2.0E11	1.99E8	1.50E7	1.20E6	2.4E7	8.50E7	1.50E8	5.00E7	1.20E5	7.50E4	6.30E4
PI5	fine	3.33E11	2.00E10	2.50E10	2.90E10	5.00E11	7.50E10	1.00E10	1.00E11	4.00E10	5.00E9	2.50E10
PI6	coarse	2.00E11	2.50E10	2.50E8	1.60E9	1.85E9	3.00E9	3.00E9	1.50E9	6.50E8	5.00E8	2.00E11
PI7	fine	1.67E11	9.99E8	9.50E7	1.25E8	1.70E8	3.50E8	5.00E8	2.40E8	1.00E8	1.35E8	7.50E10
PI8	coarse	1.00E12	5.00E10	4.00E8	9.90E8	1.70E9	5.00E9	3.30E9	1.60E9	4.00E8	4.90E8	5.00E11
CE1	fine	1.4E11	1.20E9	2.50E8	1.10E8	1.25E8	2.50E8	4.20E8	2.00E8	9.90E7	1.00E8	3.25E10
CE2	coarse	1.55E11	1.20E9	2.50E8	3.30E8	2.40E8	5.00E8	7.50E8	3.30E8	1.60E8	1.50E8	1.67E10
CE4	coarse	2.50E11	5.20E9	3.30E8	7.50E8	6.50E8	1.30E9	1.50E9	7.50E8	2.50E8	2.30E8	9.95E10
CE5	fine	1.00E11	8.00E9	2.50E8	9.90E8	7.50E8	9.50E8	1.00E9	5.00E8	2.30E8	2.50E8	5.00E11
CE6	coarse	2.50E11	2.00E9	1.85E8	2.50E8	4.00E8	9.50E8	1.20E9	8.00E8	3.30E8	3.30E8	1.67E10
CE7	fine	2.50E11	3.30E9	1.85E9	9.90E8	6.00E8	9.50E8	1.00E9	5.00E8	2.30E8	2.00E8	1.50E11
CE8	coarse	2.50E11	1.60E9	3.30E8	1.90E8	3.30E8	5.00E8	6.00E8	5.00E8	2.30E8	2.50E8	7.50E10
AL1	fine	1.20E11	1.20E9	9.90E7	1.90E8	3.30E8	7.50E8	7.50E8	4.00E8	7.50E8	8.00E8	3.90E10
AL2	coarse	1.20E11	3.30E8	1.66E8	1.35E8	2.00E8	5.00E8	6.00E8	3.30E8	1.75E8	3.50E8	4.50E10

Table 8.14. The surface insulation resistances of IPN coated test substrates, measured over a 1000hr 85 / 85 THB test.

50%RH, 85°C / 50%RH and then at 85°C /85%RH for a range of times up to 1000hrs. The results of this study are presented in Table 8.14.

8.1.5 IPN material analysis - discussion.

8.1.5.1 Low frequency dielectric spectroscopy.

The dielectric constant is fairly similar for all materials and does not vary by more than 7% over the frequency range 1 - 10MHz (see Table 8.10). The samples containing a higher vinyl content have a slightly higher ε', as was found for the monofunctional end capped materials of 6.6.3. It was concluded previously that the high vinyl content materials have a more open structure and are thus more open to moisture ingress (6.6.3), thus resulting in a higher ε'.

8.1.5.2 Thermo gravimetric analysis.

Since the TGA samples were precured prior to analysis, solvent loss is not a possible mass loss mechanism. Also, at 250°C, inorganic depolymerisation is not expected, and therefore the observed mass loss is either due to the reaction / degradation of the organic groupings or to the removal of low mass cyclic species. The high vinyl content samples (3 and 4) exhibit a higher degree of mass loss than samples 1 and 2 (Table 8.11), suggesting that the vinyl groups are involved in the mass loss process. It is probable that at 250°C, cleavage of the Si-$CHCH_2$ bond occurs and thus loss of vinyl groups could account for some of the mass loss. Post TGA examination of the high vinyl content samples indicated that some further curing had taken place, as evidenced by their increased brittleness. Such curing reactions may thus also contribute to the mass loss but only CH_3 - CH_3 interactions would result in a mass loss.

8.1.5.3 Mechanical properties.

The mechanical properties of a material containing both inorganic and organic cross - links will be determined by the competition between the increase in stiffness associated with the higher levels of inorganic networking and the lower levels of organic cross - linking that are achievable as a result of the decreased chain mobility. Standard heat treatment of sample 2 (200°C / 16hrs) afforded a cure of the material to a solid, indicating that the development of the organic cross - linkages does not appear to be significantly hindered by the higher level of networking. Comparison between samples 1 and 2 indicates that an increase in the level of networking of both the SCP and LCP is accompanied by an increase in Y and a decrease in the maximum allowable extension (Table 8.9). This is also observed in samples with a high SCP cross - link density and a low level of LCP networking (cf samples 1 and 3), thus suggesting that the system does not demonstrate the SCP independent behaviour seen by Hamurcu[88]. It is well known that, for low elongation, Y is directly proportional to the cross - link density [139]. This suggests that the development of thermally induced organic cross - links, most likely involving the vinyl groups of the LCP, reduces the effective length between junction points within the LCP and thus compromises its flexibility. This effect is demonstrated when comparison between samples 3 and 4 is made (Table 8.9). Both these materials would be expected to possess similar levels of inorganic cross - linking but sample 4 will contain a higher proportion of organic cross - links due to its higher vinyl content. This is reflected in the observed high value of Y and poor extensibility. This is further supported when comparison between samples prepared using an anionically polymerised LCP (sample 5) and a non polymerised LCP (sample 3) is made. The mechanical properties of 3 and 5 are very similar, suggesting that the nature of the LCP

is similar in both materials, ie, that the average segmental length between junctions has been equalised by the generation of organic cross - links. Despite the levels of inorganic networking being very different between the two LCPs, the cured materials have similar properties, thus demonstrating the dominance of the organic cross - linking over the inorganic networking in determining the mechanical properties of the system. Comparison of the calculated contraction values given in Table 8.12 with the experimental maximum extensions (Table 8.9) indicate that in samples 2 - 4, the percentage contraction exceeds the allowable extension. The values calculated for the contraction on cooling are those that would be experienced by a completely unrestrained material. In practice, the material would be constrained, particularly at the substrate - encapsulant interface. At this interface, the TCE difference between the two materials will always be large due to the high TCE of the IPN (Table 8.12). The mismatch will induce a shear force across the interface which may induce the encapsulant to crack or the substate - interface bond to be ruptured. Sample cracking was observed for a number of the THB test samples (PI4, 7, 8, CE8 and AL1), a typical example is shown in Figure 8.13. It will be necessary to reduce the occurrence of such sample failures. It has been shown that polymerisation of the LCP is not on its own a means of achieving this but it requires a revision of its composition. Thermally inert organics (methyl, trifluoropropyl etc) will be employed in the LCP and thermally active organics (vinyl, allyl, epoxy) will be reserved for the SCP.

8.1.5.4 Hermetic properties.

With the exception of sample CE3, all samples had SIRs between $1x10^{11}$ and $1x10^{12}\ \Omega$ (Table 8.14). At 85°C / ambient RH, the SIR dropped to values between $2x10^{8}$ and

$5x10^{10}\Omega$. Throughout the exposure to 85°C / 85%RH, the SIRs were seen to decrease with time. After 1000hrs (test end), the SIR of all samples was below $5x10^{9}\Omega$, with the lowest value being observed for PI3 and PI4 ($9x10^{6}\Omega$ and $7.5x10^{4}\Omega$ respectively). The IPN applied to PI3 and PI4 was also applied to CE1 and CE2 to a similar thickness (Table 8.13) which were not subject to as great a drop in SIR as the former two. The polyimide board for samples PI3 and PI4 was darkened prior to THB testing and became delaminated during the test. This suggests that the higher cure temperature of 240°C necessary to cure IPN2 is too near the T_g of the PI substrate, resulting in board deterioration, thus giving unrepresentative results. Cracking was observed on PI4 prior to testing, which may have allowed moisture to ingress. Upon returning the samples to RT / ambient RH, all SIRs returned to above $1.67x10^{10}\Omega$, again with the exception of PI3 and PI4 ($5x10^{5}\Omega$ and $6.3x10^{4}\Omega$ respectively). Of the samples on PI board, only PI3 and PI4 had evidence of dendritic growth (Figures 8.14a and 8.14b). Both samples also exhibited discolouration of the tracks. All samples on cyanate ester board (except CE3) survived the full 1000hrs without any visible signs of dendritic growth. The short circuit of CE3 may be a result of the cure temperature of 200°C being 20°C above the T_g of CE, resulting in board deterioration. Discolouration of the Ag tracks was present for AL6 (Figure 8.15a) and dendritic growth was observed on AL5 (Figure 8.15b). The latter may be due to moisture ingress through the crack in the coating. It is thought that the discolouration of the tracks in AL6 occurred by ingress of moisture and contaminants either along the coating - substrate interface or through the thick film metallisation, which is known to be porous since the discolouration appears to be a continuation of that observed on the exposed track and pads outside of the coating (Figure 8.16).

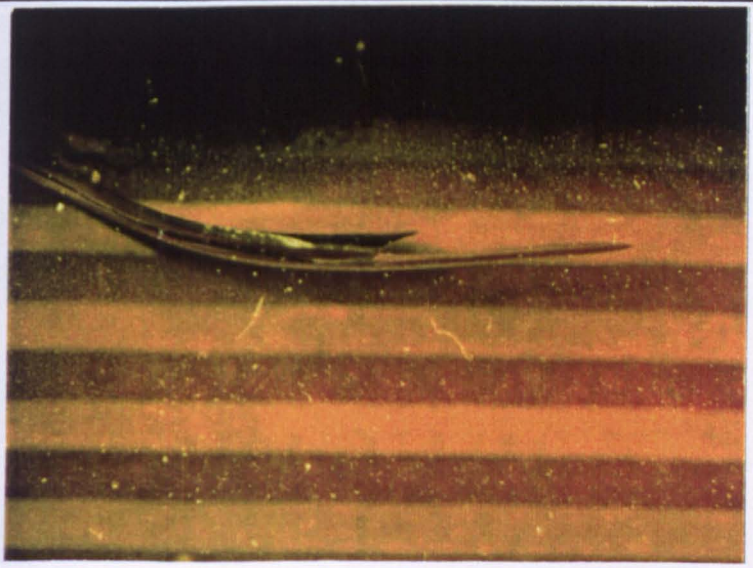

x 15

Figure 8.13. A typical crack in IPN coating (THB test sample CE8).

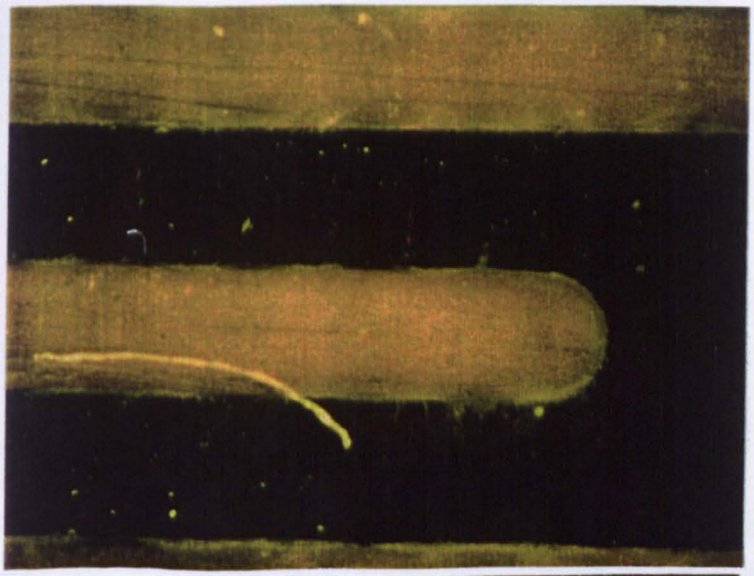

x 25 A

B

x 25

Figure 8.14. Dendritic growth on samples a) PI3 and b) PI4 (copper metallisation).

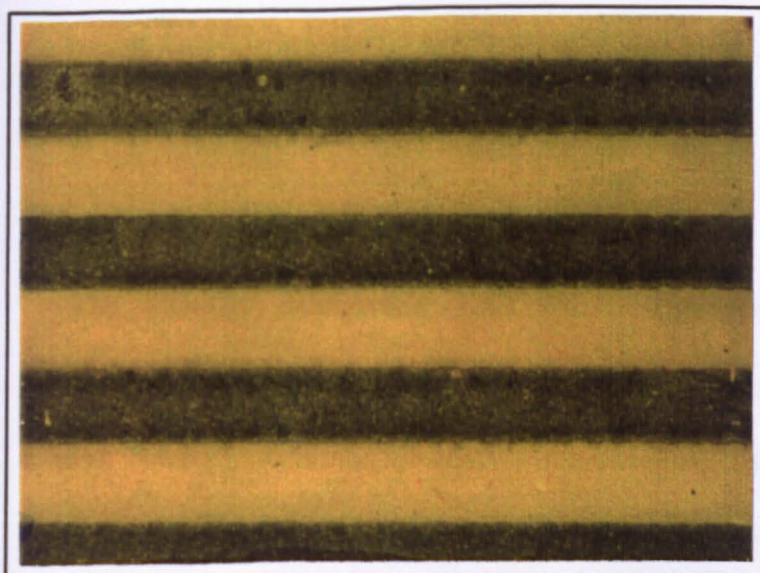

x 10

A

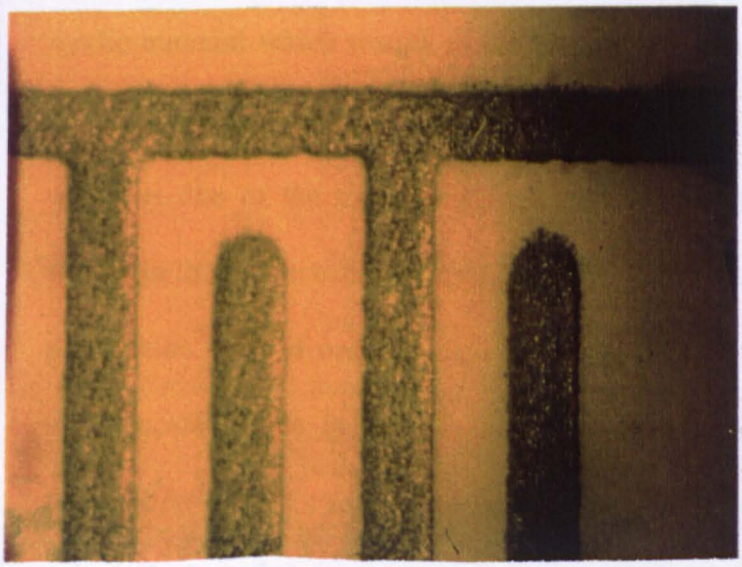

B

x 25

Figure 8.15 a) discolouration of Ag track (AL6) and b) dendritic growth on AL5.

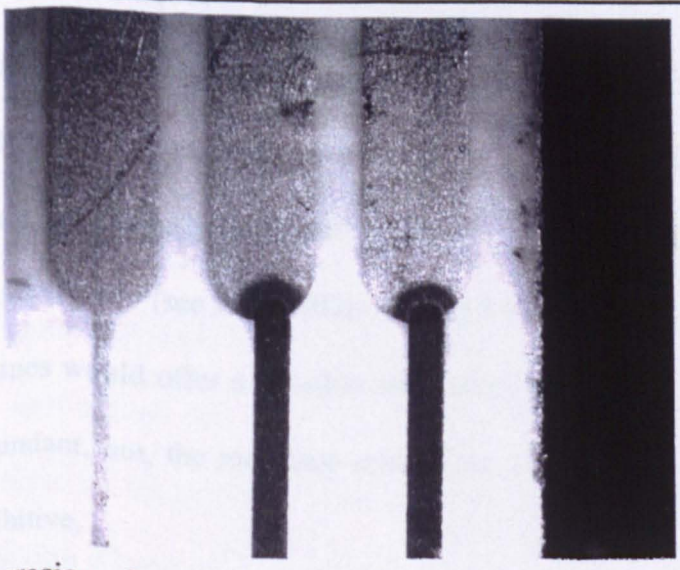

Figure 8.16. Corrosion of exposed Ag metallisation and pads.

9.1 SUMMARY

9.1.1 Difunctional systems.

The standard application route (4.7), characterised by the cohydrolysis and cocondensation of chlorosilanes, with system neutralisation by aqueous KOH solution, has been shown to be unsuitable for the preparation of difunctional systems from chlorosilanes (5.1 and 5.2), principally as a result of the generation of a high level of cyclic material which results in the materials possessing very poor thermal properties. Under these preparation conditions, the cyclisation is most sensitive at low system dilutions due to the associated high pH, and as such, even solventless preparation results in the production of a significant cyclic component. Employment of the standard preparation route is only feasible at precursor dilutions below 0.1 M, although this is impracticable since the KOH solution results in a dilution in excess of this. The preparation of low cyclic content, highly polymerised difunctional systems by direct cohydrolysis and cocondensation of chlorosilanes would most likely be achieved by employment of a non aqueous acid accepting group such as pyridine or triethylamine, thus preventing excessively low pH levels being created. The use of pyridine has been shown (8.1.2.2) to allow preparation of linear systems with a much increased degree of polymerisation, particularly with the inclusion of a heterofunctional condensation catalyst such as DMAP (see LCP3MOD, Figure 8.10). Substitution of the chlorosilanes by alkoxysilanes would offer a sensible alternative, making the requirement of an acid acceptor redundant, but, the increased cost of the alkoxysilanes over the chlorosilanes may be prohibitive.

9.1.1.1 ^{13}C CP / CPPI MAS NMR study of thermally activated cross - linking within a D' and D system.

Evidence for a thermally activated cross - linking process was given by ^{13}C CP MAS NMR of a polymethylvinylsiloxane, thermally cured at 220°C. The line shape of the cross - link resonances was not found to be a strong function of temperature over the range 295 - 400K, implying a degree of crystallinity within the material. CPPI NMR suggested the cross - link carbons to be methylene ($-CH_2-$). It was concluded that vinyl - vinyl cross - linking was significant, and for this a $-Si-CH_2-CH=CH-CH_2-Si-$ cross - link was postulated. Evidence was also found for the development of methyl - methyl cross - linking within a polydimethylsiloxane system.

9.1.2. Monofunctional end - capped linear materials.

As was observed for the reaction of difunctional silanes, the copolymerisation of M and D units leads to the generation of a bimodal system consisting of a linear and a cyclic component. Despite the use of high end - blocker levels (50 mol%), cyclisation was at a level comparable to that observed in the difunctional systems. An increase in the substitution of M for D results in a decrease in the average degree of polymerisation of the linear fraction due to the creation of MD_nM oligomers. In fact, these are produced to such an extent that the stoichiometry of the system is altered by evaporative loss of such oligomers from the system. The degree of cyclisation was found to decrease with increasing M group substitution although the benefits of a low cyclic content material are possibly outweighed by the deleterious effects of the associated increased oligomeric component. In particular, the thermal stability of the system may be severely degraded by having a large oligomer population as this may lead to mass loss occurring

thus limiting their use to lower temperature applications. The dielectric properties of the siloxanes are also sensitive to the level of end group substitution. This is particularly apparent for the trimethylsiloxy end - capped materials where an increase in M group substitution results in a concomitant increase in ε', and is possibly associated with the mobility of the oligomers within the network. This effect is less apparent for M^A substitution since the reactive end groups are available for cross - linking, thus reducing the oligomeric component of the system. In fact, a decrease in ε' is observed for M^A substitution up to 5 mol% and is possibly as a result of the decrease in the packing density of the system due to the introduction of four and six membered organic cross - links. Unfortunately, it is observed that a high vinyl or allyl content is deleterious to good hermeticity, possibly as a result of the more open structure.

9.1.3. Tri - and tetrafunctionally cross - linked materials.

The initial section of Chapter 7 was aimed at developing a preparation route that would encourage the development of trifunctionally cross - linked systems with an homogenous distribution of di - and trifunctional units throughout the network. The pre - hydrolysis of one monomer, its addition to the other, and their reaction together under conditions favouring heterocondensation (DMAP catalyst, non aqueous acid acceptor) was investigated (see 7.1.1 for details of the preparation routes employed). All preparations resulted in the development of biphasic systems, which was independent of the order in which the precursors were hydrolysed. More favourable results were achieved with the cohydrolysis and cocondensation of both precursors under standard preparation conditions (7.1.2), with the preparation of macroscopically homogeneous

materials. Heating of the silane precursors under reflux prior to reaction was seen to result in a lower viscosity for a system prepared with heated silanes compared to a system of similar composition prepared with non - heated silanes. Since it is known that heating of silanes under these conditions may result in hydrolysable group exchange between precursors [137], it was inferred that this had occurred, thus equalising the reaction rates of the precursors. The more homogeneous materials were preparable with useable viscosities for trifunctional group substitutions up to 50%, this being 30% higher than those allowable in a similar non - heated silane system. From this, and further viscosity measurements, it was concluded that the viscosity of the systems was predominantly controlled by the distribution of the species within the system and was particularly sensitive to the type of organic grouping pendent to the silicons, with the more bulky phenyl group dramatically increasing the system viscosity. The incorporation of high levels of T groups into the systems was not found to be of benefit in maintaining the system viscosity at elevated temperature as was hoped. Despite this, these materials show promise as encapsulation materials, displaying an easily controllable dispensing viscosity and good hermetic properties (particularly those with a high proportion of T units and diphenyl organic modification).

A number of preparation - structure relationships were investigated for the incorporation of tetrafunctional groups into a difunctional D^{Ph} / D' copolymer under standard preparation conditions. Preparations at 0 and 75°C produced quite dissimilar materials with preparation at higher temperature producing an inhomogeneous system whereas, that prepared at low temperature resulted in an homogeneous system. The inhomogeneity in the former was observed to compromise the curing properties of the

system, with an apparent reduced D' reactivity and a resulting increase in cure period. This was concluded to be due to the inhomogeneous nature of the system creating blocks of D' units, with the reactivity (to forming an organic cross - link) of each unit in a block, sensitive to the mobility of the polymer chain in that region, which is itself dependent upon the extent of organic cross - linking that has already occurred. Thus, if one D' has already cross - linked, it will be less probable that neighbouring D' units will react. It was concluded that, for a standard preparation at room temperature, the relative rates of reaction of the di - and tetrafunctional precursors was dependent upon the system pH, with their equalisation at elevated pH. This was inferred from the observed differences in system homogeneity, with the degree of phase separation being a decreasing function of pH. Again, minimum cure periods were required for the homogeneous material (high pH preparation).

9.1.4. IPN materials.

Chapter 8 outlined the development of suitable processes for the preparation of short and long chain polymers from which the IPN materials were constructed. The aim of this process was to develop systems with a minimal degree of cyclisation whilst maintaining a significant differential in the degree of polymerisation between the short and long chain systems.

Both single component (D^{Ph}) and two component (D^{Ph} / D) SCP systems were prepared using a standard preparation, with acid neutralisation achieved via aqueous KOH solution. This was found to be unsuitable for the preparation of an homogeneous polymer due to a high level of cyclisation within the D^{Ph} system, this being independent

of the rate of reaction of the D precursor. Employment of a non aqueous acid acceptor (C_5H_5N) (Routes i and ii, Table 8.1) was found to offer single phase materials. Route iii (Table 8.1) was chosen for preparation of all subsequent SCP systems. A reaction period of 3hrs was employed so as to minimise the degree of cyclisation, as this was found to be significant after 4hrs reaction period.

LCP systems were D' / D copolymers prepared from DCDMS and DCMVS. As for the SCP system, all preparations employing aqueous KOH, regardless of the order of hydrolysis of the precursors, resulted in phase separated materials. An optimum high mass population was obtained with use of pyridine as acid acceptor, in conjunction with DMAP which proved to be a very efficient polymerisation catalyst for this system, although it was found to be ineffective in systems where a sequential addition of precursors was employed. Further chain extension was successfully achieved by anionic polymerisation with KOH as catalyst and diglyme as promoter.

IPN materials were successfully prepared from the growth of the short chain polymer within the trifunctionally cross - linked long chain polymer network and its subsequent trifunctional cross - linking to form two independent, inseparable networks. The mechanical properties of these materials were found to be dependent upon the level of networking of both the SCP and the LCP, with higher levels of networking resulting in materials with higher Young's moduli and lower maximum extensions. The mechanical properties were found to be independent of the degree of polymerisation of the LCP, suggesting that the vinyl cross - linking within the LCP was dominating the mechanical properties of the system. Due to the high TCE of these materials, and the low maximum

allowable elongations, cracking of coatings prepared from the IPNs was a problem. A revision of the composition of the IPN may be required so as to enhance the properties of the LCP's inherent flexibility. A range of IPN materials were evaluated under 85°C / 85% RH THB test conditions with the majority of the samples affording protection over the entire 1000hrs testing period. No failures resulting from sample limitations were seen, failures that did occur were most likely due to degradation of the substrate due to exposure of temperatures in excess of the materials T_g, and, where discolouration of the metallisation occurred, this was thought to result from moisture ingress through the metallisation.

9.2 CONCLUSIONS.

For all difunctional systems, the standard preparation route (direct hydrolysis and condensation of chlorosilanes and neutralisation with KOH aqueous solution) encourages cyclisation and phase separation (within copolymer systems), and is thus not applicable for the preparation of homogeneous linear systems. Such systems were suitably prepared by employment of a Lewis base such as pyridine or thiethylamine in stoichometric quantity to Si-Cl.

A reduction of the degree of cyclisation is achievable with the cohydrolysis and cocondensation of mono and difunctional silanes. High levels of end blocker with unreactive organic groups (such as methyl) are to be avoided as the population of MD_nM oligomers becomes significant, these being deleterious to the materials dieletric and thermal properties. Higher levels of monofunctional groups with reactive organics (allyl, vinyl etc) may be achievable without degradation of the materials properties.

Where precursors with widely varying reactivities are employed, homogeneous polymers may be prepared by heating the precursors together under reflux prior to their hydrolysis and condensation.

The properties of inorganically cross - linked materials are determined by the distribution of the cross - links throughout the network. System homogeneity for tetrafunctionally cross - linked D^{Ph} / D' copolymers was optimised for preparation at high pH and low temperature.

Transferal of the long standing organic chemical synthesis of IPNs to inorganic siloxane systems has been demonstrated by development of IPN materials from the sequential formation of long and short chain polymer networks. Initial hermetic testing of these indicated that they possess very promising hermetic properties. Further development is required to optimise their mechanical properties.

9.3 FUTURE WORK.

Of all the systems studied, the IPN materials have the ability to offer the widest range of properties and, in view of the parallel organic technology, the possibility exists for combining properties that would be incompatible with each other were they to be achieved simply by use of copolymers. Thus, any future work must be directed towards investigation of these systems. Important areas of development are:

i) In the short term, the current IPN compositions should be modified so as to maintain the flexibility of the LCP. Promising materials should be subject to more extensive

environmental testing with larger sample sets. Novel organic moieties such as methacrylate and epoxy may be introduced to the current IPN systems to develop lower temperature curing materials so as to extend the range of substrate materials available for encapsulation.

ii) Further characterisation of the LCP and SCP is required. Qualitative knowledge of parameters such as chain end group density, average degree of polymerisation and levels of cyclisation would in turn allow the networks to be more fully characterised, permitting fundamental network - property relationships to be determined. Only when the networks are fully characterised can the effect that the organics have on the properties of the IPNs be understood.

Appendix I- tacticity effects.

Tacticity effects arise due to interactions between a difunctional siloxy unit ($-R_1R_2SiO-$) and its neighbouring units, where one or both of the neighbouring units are ssymetrical (R_1 is different to R_2). Typically, in the materials studied here, this would occur between a D' ($(CH_3)(CHCH_2)SiO-$) unit and a D ($(CH_3)_2SiO-$) or D' unit. The result of such an interaction is a splitting of the resonance of the unit under consideration, with the number and intensity of the splittings being dependent upon the type and spatial orientation of the neighbouring units. No interaction will be observed for a symmetrical difunctional unit surrounded by symmetrical difunctional units on both sides, and a maximum number of splittings will be observed for an asymetrical difunctional unit surrounded by two other assymetrical difunctional units, assuming all possible spatial orientations are allowed. A typical splitting is shown schematically in Figure I.1.

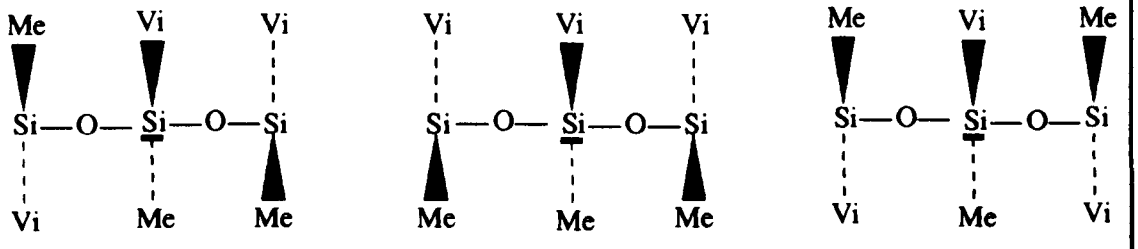

Figure I.1. Tacticity effects between D' ($(CH_3(CHCH_2)SiO-$) units.

Further splitting may also be observed at the pentad level, where the unit at the centre of the pentad is influenced by the orientation of its next nearest neighbours.

Appendix II- GPC calibration.

After addition of a guard column to the GPC apparatus, a system calibration was performed using four linear trimethylsiloxy end - capped siloxanes of known mass. Three of these were obtained from ABCR with m_n of 770, 5970 and 17250 and the fourth was hexamethyldisiloxane (M_n = 162.4), obtained from Aldrich Chem Co. The calibration plot obtained is presented in Figure II.1, with the curve fitted to a 3rd order polynomial since this offered a better fit than a linear fit. It was found that the high mass standard was too high for the column used and was immediately eluted. Figure II.1 and the associated equation was used to obtain all mass parameters for samples in Chapter 5.

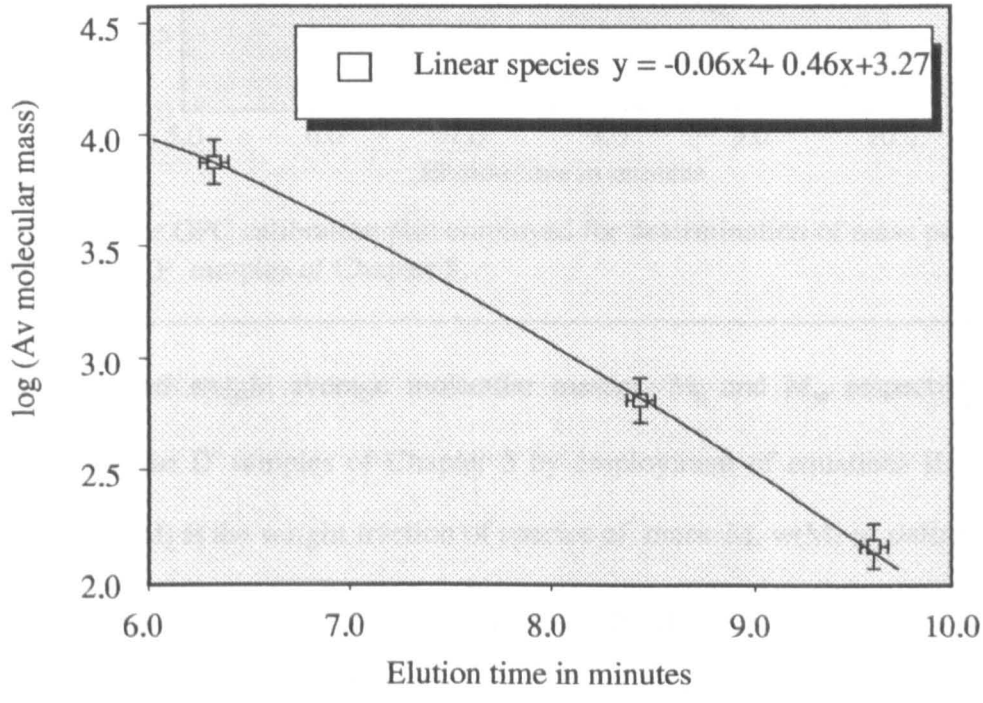

Figure II.1. The initial GPC calibration plot employed for determination of mass parameters of difunctional materials in Chapter 5.

During the course of the study it was necessary to recalibrate the GPC system after replacement of the guard column. The 770, 5979 and 17250 mass standards were

employed for the linear calibration and octaphenyltetrasiloxane (M_n= 793) was used to obtain a cyclic calibration. The calibration curve for cyclic species is known to have the same gradient as that of the linear calibration curve [139] and thus the linear curve was linearly fitted, as given in Figure II.2.

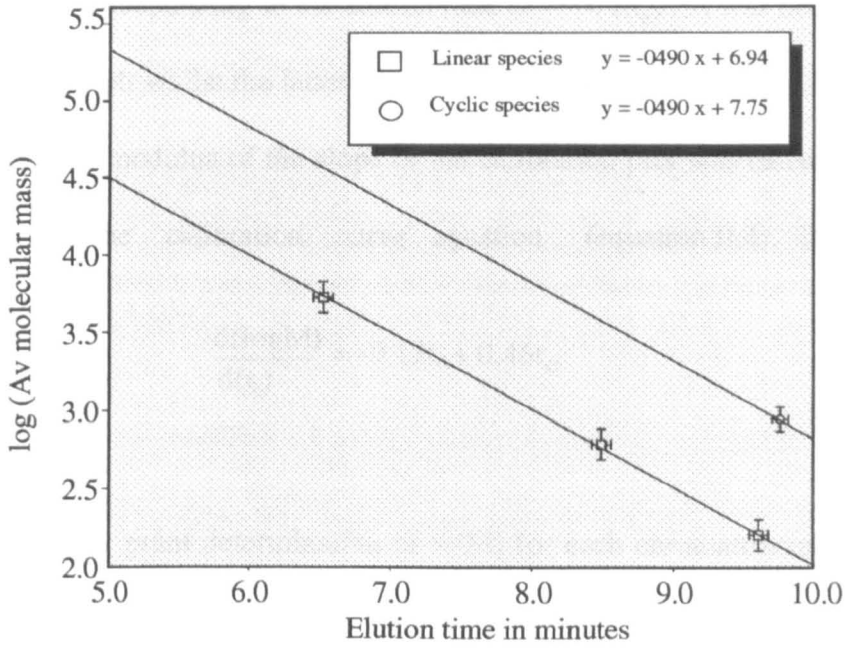

Figure II.2. The GPC calibration plot employed for determination of mass parameters of SCP and LCP samples of Chapter 8.

The number and weight average molecular masses, M_n and M_w respectively, were calculated for the D' samples of Chapter 5 by employment of equations II.1 and II.2 [140], where w(M) is the weight fraction of species of mass M. w(M) is defined as the

$$\overline{M}_n = 1 / \int_0^\infty w(M)(1/M)dM \qquad \text{(II.1.)}$$

$$\overline{M}_w = \int_0^\infty w(M)MdM \qquad \text{(II.2.)}$$

number of species having a mass M over the total number of species within the system. This value is obtained from the GPC calibration curve by application of equation II.3,

$$w(M) = \frac{f(t_e)}{A} (1/2.303) \left|S(t_e)\right| (1/M(t_e)) \qquad \text{(II.3.)}$$

where t_e is the elution time, $f(t_e)$ is the detector response, A is the area of the chromatograph, $|\ S(t_e))\ |$ is the modulus of the slope of the calibration plot and $M(t_e)$ is the value of M corresponding to the elution time te [140]. $f(t_e)$ / A was obtained from the GPC chromatograph whilst the latter two terms were obtained from the calibration plot (Figure II.1). The modulus of the slope of the calibration plot was calculated using the differential of the calibration curve equation (equation II.4). This treatment

$$\frac{d(\log M)}{d(t_e)} = -0.12t_e + 0.46t_e \qquad \text{(II.4.)}$$

allowed a point by point determination of w(M) for each chromatograph. Substitution of w(M) into equations II.1 and II.2 yielded M_n and M_w.

Publications

(i) Refereed Journals

Published Conference Proceedings.

Polysiloxane Interpenetrating Networks for Electronic Device Encapsulation,

Gibbons, G. J., Holland, D.

Special volume of the J. Sol - Gel. Sci. Tech containing the Proceedings of the 8th International Workshop on Glasses and Ceramics From Gels, held in Faro, on September 18 - 22, 1995.

(ii) Conference Presentations

8th International Workshop on Glasses and Ceramics From Gels (Faro, Portugal), September 18 - 22, 1995

Polysiloxane Interpenetrating Networks for Electronic Device Encapsulation,

Gibbons, G. J., Holland, D.

(Poster)

REFERENCES

1. Rymaszewski, E. J., and Tummala, R. R., " Microelectronics packaging - an overview" in Microelectronics Packaging Handbook, Van Nostrand Reinhold, New York, p33, 1989

2. Pienemaa, S., " Encapsulation of chip on board packages", Eureka EU462/315, p2

3. Bartholmew, P. M., " The application of glob top materials to chip on board components - a review", TWI company internal report TWI 77263/1/94, Jan 94, p1

4. Pienemaa, S., " Encapsulation of chip on board packages", Eureka EU462/315, p1

5. Bartholmew, P. M., " Review of hermetic sealing techniques ", company internal report, Eureka EU462/ PTG/TWI/304, p1

6. Kumar, A. H., and Ozmat, B., " Package sealing and encapsulation", in Microelectronics Packaging Handbook, Van Nostrand Reinhold, New York, pp 727 - 777, 1989

7. Dexter, A. J., Goldman, L. S., Howard, R. T., " Package reliability", in Microelectr - onics Packaging Handbook, Van Nostrand Reinhold, New York, p 254, 1989

8. Harrop, P. J., " Dielectrics", Butterworth & Co, London, p6, 1972

9. Davidson, E. E., Katopis, G. A., " Signal distribution", in Microelectronics Packaging Handbook, Van Nostrand Reinhold, New York, pp 126 - 163, 1989

10. Wong, C. P., " Integrated circuit device encapsulation" in " Polymers for Electronic Applications", Ed Lai, J. H., CRC Press, Boca Raton, Florida, USA, pp 63 - 92, 1989

11. Robock, P. V., and Nguyen, L. T., " Plastic packaging", in Microelectronics Packaging Handbook, Van Nostrand Reinhold, New York, pp 523 - 672, 1989

12. Kuwata, K., etal., " Low - Stress resin encapsulants for semiconductor devices", Trans. IEEE Components, Hybrids and Mfg Tech., CHMT - 8 (4), Dec 1985

13. Saunders, K. J,, Organic Polymer Chemistry, Chapman and Hall, London, p299, 1973

14. Belton, D. J., " The effect of post mould curing upon the microstructure of epoxy moulding compounds", Trans. IEEE Components, Hybrids and Mfg Tech., CHMT 10(2) pp 358 - 363, Sept 1989

15. Wong, C. P., "Understanding the use of silicone gels for non-hermetic plastic packaging", Trans. IEEE Components, Hybrids and Mfg Tech., CHMT - 12(4), pp 421 - 425, Dec 1989

16. Robock, P. V., and Nguyen, L. T., " Plastic packaging", in Microelectronics Packaging Handbook, Van Nostrand Reinhold, New York, p563, 1989

17. Edwards, D. R., "Shear stress evaluation of plastic packageing", Trans. IEEE Components, Hybrids and Mfg Tech., CHMT - 12 (4), p 618, Dec 1987

18. Thomas, R. E., " Stress induced deformation of aluminium metallization in plastic moulded semiconductor devices", Trans. IEEE Components, Hybrids and Mfg Tech., CHMT - 8 (4), p427, Dec 1985

19 Sullivan, T., et al., " Photoelastic and numerical investigation of thermally induced restrained shrinkage stresses in plastics", Trans. IEEE Components, Hybrids and Mfg Tech., CHMT - 11 (4), Dec 1988

20. Otsaka, K., " A new sealing mechanism for high reliability encapsulation",

Trans. IEEE Components, Hybrids and Mfg Tech., CHMT - 7 (3), pp 249 - 256, Sep 1984

21. Sasaki, S., " Development of mini plastic IC packaging for DIP soldering", Proc 34th Electronic Components conf, pp 383 - 387, 1984

22. Electro - Lite Product Data Sheet ELC 2060 - A & 2060 - AG

23. Otsuka, K., et al., " The mechanisms that provide corrosion protection for silicone gel encapsulated chips", Trans. IEEE Components, Hybrids and Mfg Tech., CHMT - 12 (4), pp 666 - 668, 1987

24. Mancke, R. G., " A moisture protection screening test for hybrid circuit encapsulation", Trans. IEEE Components, Hybrids and Mfg Tech., CHMT - 4, pp482 - 498, 1981

25. White, M. L., "Encapsulation of integrated circuits", Proc IEEE - 57 (9), pp 1610 - 1615, 1989

26. Lin, W. A., "Encapsulant for nonhermetic multichip packaging applications", Trans. IEEE Components, Hybrids and Mfg Tech., CHMT - 15 (4), pp 510 - 518, 1992

27. Wong, C. P., "Alcohol modified RTV silicone encapsulation for integrated circuit device packaging", Trans. IEEE Components, Hybrids and Mfg Tech., CHMT - 6 (4), pp 485 - 493, 1983

28. Larson, G. L., "An introduction to silicones", Petrarch Systems p89

29. Balde, J., " The effectiveness of silicone gels for corrosion prevention of silicon circuits: the final report of the IEEE computer society computer packaging committee special task force", Trans. IEEE Components, Hybrids and Mfg Tech.,

CHMT - 14 (2), p 352, 1991

30. Saunders, K. J., Organic Polymer Chemistry, Chapman & Hall, London, pp 191 - 223, 1988

31. Jenson, R. J and Lai, J. H., " Polyimides: chemistry, Processing, and Application For Microelectronics" in, Polymers for electronic applications, Ed Lai, J. H., CRC Press, Boca Raton, Florida, USA, pp 33 - 61, 1989

32. Burack, J., J et al., " Enhanced moisture protection of electronic devices by ultra - thin polyimide films", Trans. IEEE Components, Hybrids and Mfg Tech., CHMT 13 (1), 1990

33. Saunders, K. J., Organic Polymer Chemistry, Chapman & Hall, London, pp 266 - 277, 1988

34. Pauling, L., The Nature of the Chemical Bond, Cornell University Press, Ithaca (NY), 3rd Ed, 1960

35. Thompson, R., J. Chem. Soc., p1908, 1953

36. Noll, W., "The polymeric organosiloxanes", in Chemistry and technology of Silicones, Academic Press Inc, San Diego, California, pp 246 - 331, 1968

37. Pauling, L., J. Physic. Chem., **56**, p361, 1952

38. Noll, W., "Preparation of polyorganosiloxanes", in Chemistry and technology of Silicones, Academic Press Inc, San Diego, California, pp191 - 246, 1968

39. Noll, W., "Monomeric organosilicon compounds R_nSiX_{4-n}", in Chemistry and Technology of Silicones", Academic Press Inc, San Diego, California, pp67 - 123, 1968

40.Brinker, C. J.," Hydrolysis and condensation of silicates: effects on structure", J. Non- Cryst. Solids **100**, pp31 - 50, 1988

41. Aelion, R., et al., J. Amer. Chem. Soc, **72** p5705, 1950

42. Vorankov, M., Mileshkevich, V. P., and Yuzhelevski, Y. A., The Siloxane Bond, Consultants Bureau, New York, 1978

43. Pohl, E.R., and Osterholtz, F. D., Polym. Sci. Technology, **27**, Plenum, New York, pp157 - 170, 1985

44. Keefer, K. D., Better Ceramics Through Chemistry, Eds Brinker. C. J., Clark. D., and Ulrich. D. R., Elservier North - Holland, New York, pp59 - 70. 1984

45. McNeil, K. J., et al., J. Am. Chem. Soc, **102**, p1859, 1980

46. Swain, G. C., et al., J. Am. Chem. Soc, **11**, p965, 1949

47. Schmidt, H., Scholze, H., and Kaiser, A., J. Non-Cryst. Solids, **48**, pp65 - 77, 1982

48. Chojnowski, J., " Polymerization" , in Siloxane Polymers, Ellis Horwood - PTR Prentice Hall, New Jersey, pp1-62, 1993

49. Soloman, M. M., Tyler, L. J., J. Amer. Chem. Soc, **76**, p1030, 1964

50. Rubinsztajn, S., Cypryk, M., and Chojnowski, J., J. Organometal. Chem, **367**, pp27 - 37, 1989

51. Cypryk, M., Rubinsztajn, S., Chojnowski, J., J. Organometal. Chem, **377**, pp197 - 203, 1989

52. Flory, P. J., Chem. Rev, **39**, pp137 - 197, 1946

53. Jacobson, H., Stockmeyer, W. H., J. Chem. Phys, **18**, 12, pp1600 - 1607, 1950

54. Davies, M. M., Trans. Faraday. Soc, **34**, p410, 1938

55. Soloman, G., Trans. Faraday. Soc, **32**, p153, 1936

56. Wright, P. V., Beevers, M. S., "Preparation of cyclic siloxanes", in Cyclic Polymers, Semlyen, J. A.. Ed., Elsevier Applied Science, London, pp85 - 133, 1986

57. West, R., J. Am. Chem. Soc, **81**, 6145, 1959

58. Patnode, W., and Wilcock, D. F,. J. Amer. Chem. Soc., **68**, p358, 1946

59. Chojnowski, J., Wilczek, L., Makromol. Chem, **180**, p117, 1979

60. Andrianov, K. A., and Yakushkina, S. E., Vysokomol. Soed, **1**, p613, 1959

61. Parkins, A. W., Poller, R. C., An Introduction to Organometallic Chemistry, Macmillian Publishers plc, London, pp100 - 101, 1986

62. Solomons, T. W. G., Fundamentals of Organic Chemistry 4th Edition, John wiley and sons, New York, pp260 - 262, 1994

63. Thomas, D. R., Siloxane Polymers, Ellis Horwood - PTR Prentice Hall, New Jersey, pp567 - 614, 1993

64. Odian, G., Principles of Polymerization, Wiley and Sons, New York, p233, 1991

65. Bobear., W. J, Rubber. Chem. Technol, **40**, p1560, 1967

66. Bork, P. G., and Rousch, G. W., Vulcanisation of Elastomers, Reinhold, NewYork, p369, 1964

67. Burrows, S. E., PhD Thesis, Warwick University, to be published.

68. Utracki, L. A., and Weiss, R. A., (Eds), Multiphase Polymers: Blends and Ionomers, American Chemical Society, Washington, USA, 1989

69. Quirk, R. P., Kinning, D. J., and Fetters, L. J., Comprehensive Polymer Science, Aggarwal, S. L (Ed), 7, pp1 - 22, 1989

70. Goodman, I., "Heterochain block copolymers", in Comprehensive Polymer Science, Eastmond, G. C., Ledwith, A., Russo, S., Sigwalt, P., (Eds), Pergaman Press, Oxford, UK , vol6, pp364 - 403, 1989

71. Schue, F., Copolymers by transformation reactions, ibid pp359 - 369, 1989

72. Rempp, P. F, Lutz, P. J., Synthesis of graft copolymers, ibid pp403 - 423, 1989

73. Sperling, L. H., Interpenetrating networks, ibid pp423 - 437,1989

74. Siegfried, D. L., et al., J. Polym. Sci, Polymer. Phys. Ed, **16**, p583, 1978

75. Millar, J. R., J. Chem. Soc, p1311, 1960

76. Thiele, J. L., and Cohen., R. E., Polym. Eng. Sci, **19**, p284, 1979

77. Arkles, B., Chemtech, **13**, American Chemical Society, pp542 - 555, 1983

78 Tunney, S. E., Fitzgerald, J. J., Proceedings - International Conference on Polyimides, Oct - Nov 1991, No 4, p1

79. Kole, S., et al., J. Applied. Polym. Sci, **48**, 3, p529 - 545, 1993

80. McGarey, B., et al., British Polymer Journal, **21**, 3, pp227 - 232, 1989

81. He, X. W., et al., Polymer, **30**, 2, pp364 - 368, 1989

82. Frisch, H. L., et al., J. Polym. Sci, PartA: Polym Chem, **26**, 9, pp2589 - 2596, 1988

83. Novak, B. M., Macromol, **24**, 19, pp5481 - 5483, 1991

84. Dillon, M. E., Proc. ACS Division of polymeric materials: science and engineering 1990

85. Ryntz, R. A., et al., J. Coatings. Technology, **64**, 813, pp83 - 89, 1992

86. Zhou, P., et al., J. Polym. Sci, PartA: Polymer Chemistry, **31**, 10, pp2481 - 2491, 1993

87. Nishi, S., et al., Polymer preprints, Presented at New Orleans Louisianna Meeting, 1988

88. Hamurcu, E. E., and Baysal, B. M., Polymer, **34**, 24, pp5163 - 5167, 1993

89. Kang, Y. S., et al., J. Applied. Polym. Sci, **53**, 3, pp317 - 323, 1994

90. Harris, R. K., Nuclear Magnetic Resonance Spectroscopy, A Physiochemical View, Longman Scientific and Technical, Harlow, UK, John Wiley & Sons, New York, pp1 - 35, 1992

91. Purcell, E. M., and Torrey, H. C. and Pound, R. V., Phys. Rev, **69**, p37, 1946

92. Bloch, F., Hansen, W. W., and Packard, M. E., Phys. Rev, **69**, p127, 1946

93. Marsmann, H., "^{29}Si NMR spectroscopic results", in NMR, Basic Principles and Progress 17, Eds., Diehl, P., Fluck, E., Kosfeld, R., Springer Verlag, Berlin, p67, 1981

94. Harris, R. K., Nuclear Magnetic Resonance Spectroscopy, A Physiochemical View, Longman Scientific and Technical, Harlow, UK, John Wiley & Sons, NewYork, pp232 - 234

95. Fennel, J. W., and Klinowski, J., Fundamentals of NMR, Longman Scientific and Technical, Harlow, UK, pp159 - 160, 1993

96. Harris, R. K., Nuclear Magnetic Resonance Spectroscopy, A Physiochemical View, Longman Scientific and Technical, Harlow, UK, John Wiley & Sons, New York, pp96 - 119, 1989

97. Marsmann, H., "^{29}Si NMR spectroscopic results", in NMR, Basic Principles and Progress 17, Eds., Diehl, P., Fluck, E., Kosfeld, R., Springer Verlag, Berlin, p112 - 120, 1981

98. Kalnowski, H. O., Berger, S., and Braun, S., Carbon - 13 NMR Spectroscopy, John Wiley and Sons, New York, pp49 - 51, 1984

99. Harris, R. K., Nuclear Magnetic Resonance Spectroscopy, A Physiochemical View, Longman Scientific and Technical, Harlow, UK, John Wiley & Sons, New York, pp144 - 164

100. Komoroski, R. A., "High resolution NMR of glassy amorphous polymers", in High Resolution NMR Spectroscopy of Synthetic Polymers in Bulk, vol7, Komoroski, R. A., (Ed), VCH Publishers, Florida, pp19 - 62, 1986

101. Herbert, I. R., and Clague, A. D. H., Detailed structural analysis of polysiloxane antifoam agents using carbon - 13 and silicon - 29 NMR spectroscopy., Macromolecules, **22**, pp 3267 - 3275, 1989

102. Morris, G. A., and Freeman, R., J. Magn. Reson, **29**, p433, 1978

103. Alla, M, Lippmaa, E., Chem. Phys. Lett., **37**, p260, 1976

104. Sangill, R,. et al., "Optimised spectral editing of ^{13}C MAS NMR spectra of rigid solids using cross - polarization methods"., J. Mag. reson., A **107**, 67 - 78, 1994

105. Pines, A., Gibby, M. G., Waugh, J. S., J. Chem. Phys, **59**, p569, 1973

106. Nielsen, N. C., et al., J. Magn. Reson., **79**, p554, 1988

107. Wu, X., Zilm, K. W., J. Magn. reson., A **102**, p205, 1993

108. Carleton, A. S., "Physical constants of fluoropolymers"., in Polymer Handbook, Wiley and sons Inc, USA, 1989

109. British standards., BS 5350: Part C5., Bond strength in longitudinal shear., 1976

110. British standards., BS 5350: Part C3., Bond strength in direct tension, 1989

111. Harrop, P. J., Dielectrics, Butterworth and Co Ltd, London, pp1 - 15, 1972

112. Hewlett Packard 4192A LF Impedance Analyser Operation and Service Manual, Chapter 3., Operation., pp1 - 64

113. Hewlett Packard 16451B Dielectric Test Fixture Operation Manual, Chapter 3., Fixturing and Cabling., pp1 - 10

114. Needes, C. R. S., and Button, D. P., "Reliability testing of thick film multilayer materials"., IEEE, pp505 - 511, 1985

115. Hillman, A. W., Knight, E., Watts, J. D., "Humidity testing of silicone glob top materials"., BNR internal report, IR/ 1994/1653

116. Hillman, A. W., "A humidity test of some ormocer materials"., BNR internal

report, MEC/1995/****/6132

117. Schmidt, H., and Wolter, H., "Organically modified ceramics and their applications"., J. Non-Cryst. Sol., **121**, pp428 - 435, 1990

118. Semylen, J. A., and Wright, P. V., Polymer, **10**, p543, 1969

119. Harris, R. K., and Kimber, B. J., "End - groups and tacticity in polymeric silicones detected by ^{29}Si nuclear magnetic resonance"., J. Chem. Soc., Chem. Comm., pp 559 - 561, 1974

120. Newmark, R. A., Copley, B. C., Macromolecules, **17**, pp1973 - 1980, 1984

121. Engelhardt, G., Jancke, Magi, M., Pehk, T., Lippmaa, E., J. Organometal. chem., **28**, p293, 1971

122. Soucek, J., Engelhardt, G., Stránsky, K., Schraml, J., Coll. Czech. Chem. Comm., **41**, p234, 1976

123. Herbert, I. R., Clague, A. D. H., Macromolecules, **22**, pp3267 - 3275, 1989

124. Burton, D. J., Harris, R. K., Dodgson, K., Pellow, C. J., Semlyen, J. A., Polymer Communications., **24**, pp278 - 280, 1983

125. Levy, G. C., Nuclear Magnetic Resonance Spectroscopy of Nuclei Other Than Protons, Wiley Interscience, NY, p255, 1974

126. Williams, E. A., Cargioli, J. D., Ann. Rep. NMR. Spectroscopy., **9**, p256, 1979

127. Kennan, J. J., "Siloxane copolymers" , in Siloxane Polymers, Ellis Horwood - PTR Prentice Hall, New Jersey, pp72 - 134, 1993

128. Harris, R. K., Kimber, B. J., Wood, M. D., J. Organometal. Chem., **116**, pp291 - 298, 1976

129. Marsmann, H., "^{29}Si NMR spectroscopic results"., in NMR, Basic Principles and Progress 17, Eds., Diehl, P., Fluck, E., Kosfeld, R., Springer Verlag, Berlin, pp147-231, 1981

130. Scott, W., "Equilibria between linear and cyclic polymers"., J. Amer. Chem. Soc., **68**, pp2294 - 2295, 1946

131. LaRochelle, R. W., and Cargioli, J. D., and Williams, E. A., Macromolecules, **9**, p85, 1976

132. Solomons, T. W. G., Fundamentals of Organic Chemistry, 4th Edition, John Wiley and sons, New York, pp384 - 432, 1994

133. Harris, R. K., Robins, M. L., Polymer, **19**, pp1123 - 1132, 1978

134. Horn, H. G., Marsmann, H. C., Makromol. Chem., **162**, p225, 1972

135. Komoroski, R. A., "High resolution NMR of glassy amorphous polymers"., in High Resolution NMR Spectroscopy of Synthetic Polymers in Bulk, vol 7, Komoroski, R. A., (Ed), VCH Publishers, Florida, pp121- 155, 1986

136. Komoroski, R. A., "High Resolution NMR of glassy amorphous polymers", in High Resolution NMR Spectroscopy of Synthetic Polymers in Bulk, vol 7, Komoroski, R. A., (Ed), VCH Publishers, Florida, pp63 - 119, 1986

137. Levy, G. C., Lichter, R. L., Nelson, G. L., Carbon -13 Nuclear Magnetic Resonance Spectroscopy, 2nd Edition, John Wiley & Sons, New York, pp50 - 63, 1980.

138. Schraml, J., et al., Coll. Czec. Chem. Comm., **42**, pp306 -317, 1977

139. Phillips, H. B., and Boyd, P. J., The Science of Polymer Molecules, Cambridge University Press, Cambridge, p290, 1993

(ACDMS)	Allylchlorodimethylsilane
(ADMS)	Allyldimethylsiloxy
(BSA)	Bis - trimethylsilylacetamide
(COB)	Chip - On - Board
(CP)	Cross - Polarisation
(CPD)	Cross - Polarisation - Depolarisation
(CPPI)	Cross - Polarisation - Polarisation - Inversion
(CTMS)	Chlorotrimethylsilane
(D)	$-OSi(CH_3)_2-$
(D')	$-O(CH_3)Si(CHCH_2)-$
(D^{Ph})	$-O(CH_3)Si(C_6H_5)-$
(DCM)	Dichloromethane
(DD)	Dipolar Decoupling
(DGEBA)	Diglycidylethers of Bisphenol - A
(DCDMS)	Dichlorodimethylsilane
(DCMVS)	Dichloromethylvinylsilane
(DCDPS)	Dichlorodiphenylsilane
(DEODMS)	Diethoxydimethylsilane
(Diglyme)	2 - methoxymethylether
(DMAP)	4 - Dimethylaminopyridine
(DP_{av})	Average Degree of Polymerisation
(DSC)	Differential Scanning calorimetry
(DTA)	Differential Thermal Analysis
(DTG)	Differential Thermogravimetry
(DUT)	Device Under Test
(ET_3N)	Triethylamine
(FID)	Free Induction Decay
(FT NMR)	Fourier Transform Nuclear Magnetic Resonance
(GPC)	Gel Permeation Chromatography
(g - s - g)	Ground - signal - ground
(HEB)	Hydroxy End Blocked
(HS)	Heated silane
(I/O)	Input / Output
(IC)	Integrated Circuit
(ISP)	Integral Substrate Package
(IPN)	Interpenetrating Network
(J - S Theory)	Jacobson - Stockmeyer Theory
(LB)	Langmuir - Blodgett
(LCP)	Long Chain Polymer
(M)	$-O_{½}Si(CH_3)_3$
(M^A)	$-O_{½}(CH_3)_2Si(CH_2CH=CH_2)$
(MAS)	Magic Angle Spinning
(MCM)	Multi - Chip - Module
(MCM - L)	Laminated Substrate Multi - Chip - Module

(MMD)	Molecular Mass distribution
(M^{OH})	$-O_{½}(CH_3)_2SiOH$
(M^{OR})	$-O_{½}(CH_3)_2SiOR$
(MTMOS)	Methyltrimethoxysilane
(NHS)	Non - heated silane
(NOE)	Nuclear Overhauser Enhancement
(NMR)	Nuclear Magnetic resonance
(PA - I)	Poly(amide - imide)
(Parylene ©)	Poly - p - Xylene
(PCB)	Printed Circuit Board
(PDMS)	Polydimethylsiloxane
(PE)	Polyethylene
(PED)	Plastic - Encapsulated - Package
(PI)	Polyimide
(PMMA)	Polymethylmethyacrylate
(PPTTA)	Pentathirtoltetraacrylate
(PTH)	Plated Through Hole
(PTMSP)	Poly (1 - trimethylsilyl - 1 - propyne)
(PWB)	Printed Wire Board
(RLCA)	Reaction - Limited, - Cluster - Cluster - Aggregation
(RME)	Rigid Metal Electrode
(RT)	Room Temperature
(RTV)	Room Temperature Vulcanising
(SCP)	Short Chain Polymer
(SCPa)	Single Chip Package
(SLE)	Spring Loaded Electrode
(SIR)	Surface Insulation Resistance
(SR)	Signal Reference
(SMT)	Surface Mount Technology
(SiOH)	Silanol
(SR)	Signal Reference
(SS)	Spinning Sideband
(TCE)	Temperature Coefficient of Expansion
(TEOS)	Tetraethoxysilane
(TGA)	Thermogravimetric analysis
(THB)	Temperature - Humidity - Bias
(TMS)	Tetramethylsilane
(TMSO)	Trimethylsiloxy
(ULSI)	Ultra - Large - Scale - Integration